Universidad Autónoma de Madrid

Facultad de Ciencias

Departamento de Biología Molecular

P. falciparum humanized mouse model: Characterization and further studies for antimalarial drug development

Un modelo de ratón humanizado para *P. falciparum*: Caracterización y estudios adicionales para el desarrollo de fármacos antimaláricos

SARA VIERA MORILLA

Madrid 2017

Universidad Autónoma de Madrid

Facultad de Ciencias

Departamento de Biología Molecular

Un modelo de ratón humanizado para *P. falciparum*: Caracterización y estudios adicionales para el desarrollo de fármacos antimaláricos

Memoria presentada por:

Sara Viera Morilla

Para optar al grado de:

DOCTORA EN BIOLOGÍA

Trabajo realizado bajo la dirección de:

Dra. María José Lafuente Monasterio

María José Lafuente Monasterio Doctora en Ciencias Químicas por la Universidad Autónoma de Madrid e Investigadora y responsable del Grupo de Eficacia Terapéutica de la DPU de Malaria,

INFORMA:

Que el trabajo titulado "*P. falciparum* humanized mouse model: Characterization and further studies for antimalarial drug development " constituye la Memoria que presenta Sara Viera Morilla para optar al grado de Doctora. Esta tesis doctoral se ha realizado bajo mi dirección en la DPU de Malaria en el Grupo de Eficacia Terapéutica en el Centro de Diseases of Developing World de GlaxoSmithKline (GSK DDW).

Y para que conste firmo el presente informe a 28 de Febrero de 2017

Fdo. María José Lafuente Monasterio

A todos los que creyeron en mí.

為せば成る
為さねば成らぬ何事も
成らぬは人の為さぬなりけり

Si lo intentas, puede que tengas éxito
Si no lo intentas, no tendrás éxito. Esta es la única verdad
No tener éxito es el resultado de no intentarlo

Uesugi Youzan

Agradecimientos:

La realización de este trabajo me ha supuesto un reto personal que me ha llevado más años de los que en un principio había planeado, sin embargo no me arrepiento de haber tomado este camino ya que he aprendido mucho durante todo el proceso.

La culminación de este proyecto ha sido posible gracias al apoyo de mucha gente, de lo cual me siento agradecida, y algo que he aprendido durante este largo camino es que si quieres algo, no tienes que tener miedo a intentarlo, hazlo, luego pensarás en cómo hacerlo y cómo afrontar los problemas que te vayan surgiendo. No hay que rendirse antes de comenzar.

Este trabajo no hubiera sido posible sin la ayuda de todas mis compañeras de trabajo, gracias por haberme ayudado en los interminables muestreos y horas de citometría. Gracias a Vanessa por ser mi compañera de fatigas y por darme su apoyo en estos larguísimos 12 años trabajando codo con codo. A Noemi por tu sinceridad y aliento en las horas bajas. A Helen por ser como es, acompañándome y, dejándome espacio cuando era necesario. A Lorena por ser el aire fresco que necesitaba en un determinado momento. A Javi, por ser una más y ser mi "nakama" cuando nadie más me entendía. A Carmen por darme el último empujón y aliento que necesitaba para acabar. A Fini por su bondad y hermosas palabras de ánimo. A Alba por todos sus consejos y por aguantarme en la recta final. A la otra Noemi por ser mi consejera y ayudarme a no desviarme del camino. Gracias a todas por todo el tiempo que me habéis dedicado y por soportarme cuando tenía un mal día.

Gracias a mi jefa y directora Mariajo por adoptarme y creer en mí cuando había sido derrotada y abandonada. Sin su paciencia y aliento esta tesis no hubiera sido posible. Gracias por recorrer este camino conmigo y enseñarme tantas cosas en tan poco tiempo, y lo que nos queda…

A mi tutor Manuel y a Mada por tener tanta paciencia conmigo y ayudarme en todo lo que necesitaba todos estos años.

A mi familia por estar siempre ahí. A mis padres por hacerme como soy con mis defectos y virtudes, por apoyarme en las sombras y por darme aliento cuando me hacía falta oxígeno. Gracias a mi madre por enseñarme tantas cosas y por esperar siempre lo mejor de mí. Gracias a mi padre por ser mi compañero biólogo y ayudarme a mejorar. A mi hermano Aarón, por ser mi compi de juegos en la infancia, mi compañero de fatigas en la universidad, por entenderme, apoyarme incondicionalmente y por ser mi amigo cuando más me hacía falta. A mi tía Isabel por ser mi segunda madre y confidente. A mis primos Fran y Cristian por querer verme convertida en doctora, vuestras ganas de verme presentar la tesis me dieron el último empujón que necesitaba.

Gracias a mi compañero de viaje en esta vida, Fran, por quererme como soy y aguantarme, por estar a mi lado en los buenos y en los malos momentos, por regañarme cuando fue necesario y darme luz cuando todo se había vuelto oscuro, no podía haber elegido mejor compañero. A mi familia política, por acogerme en tierras extrañas haciéndome sentir una más de la familia y animarme siempre que fue necesario.

A todos mis amigos que están cuando los necesito, en especial a mi amiga Mari, uno de mis pilares en esta vida, tu ausencia me ha dejado un gran vacío, allá donde estés perdóname por darme cuenta tan tarde de lo fundamental que has sido en mi vida.

Y a todos los que han contribuido de manera consciente o inconsciente a hacerme crecer como persona y como científica.

Gracias también a todas las ratonas que han sido parte fundamental de este trabajo, sin vosotras este trabajo no hubiera sido posible.

A todos vosotros, GRACIAS.

Sara

Table of contents

Abreviations List

β2: NODscid *β2 microglobulin*$^{-/-}$

IL2: NODscidIL2Rγ^{null}

NOG: NOD.Cg-*Prkdc*^{scid} *Il2rg*^{tm1Sug}/JicTac

Rag2IL2: Rag2$^{-/-}$ IL2 rg $^{-/-}$, H-2kb+

FRG: FRG® KO

NRG: NOD-Rag1^{null} IL2rγ^{null}

IL: Interleukine

i.p.: Intraperitoneal

i.v.: Intravenous

RBC: Red blood cell

hRBC: Human red blood cell

hEry: Human erythrocytes

mEry: Mouse erythrocytes

SAV: Streptavidine

PE: Phycoerythrine

PerCP: Peridinin Chlorophyll Protein Complex

APC: Allophycocyanin

MCV: Mean Corpurscular volume

GSK: GlaxoSmithKline

Pf: Plasmodium falciparum

Hu: Humanized

FBS: Fetal bovine serum

ihE: Infected human erythrocytes

PBS: Phosphate buffer solution

AUC: Area under the curve

ASA: Acetyl salicylic acid

NSAID: Non-steroideal anti inflammatory

NK: Natural killer

INFγ: Gamma interferon

TNFα: Tumor necrosis alpha

MCP-1: Monocyte chemotactic protein

CBA: Cytometric bead assay

SMFA: Standard membrane feeding assay

Summary

Malaria is caused by the asexual stages of human parasites of the genus *Plasmodium*. Among the five species pathogenic for humans, *P. falciparum* is accountable for more than 500.000 deaths per year in Africa. The emergence of resitances to the actual treatments have made the development of new antimalarial medicines a key part of the global strategy for malaria eradication.

P. falciparum infects almost exclusively human erythrocytes. In order to study the human malaria disease, a mouse model for *P. falciparum* infection has been developed. This model consist in the xenotransplant of human blood to immunodeficient mice that lacks T, B and NK cells (NODscidIL2Rγ^{null}), by the daily intraperitoneal injections of human erythrocytes.

A detailed study of this xenotransplant have been addressed in the present work. A robust and reprocible growth of *P. falciparum* has been obtained in engrafted mice. The erythrocytic cycle length determined in the *P. falciparum* mouse model is smilar to the reported in the human host (48±1 hours). It has also been demostrated that the transmission to the mosquito host is also possible, confirming the presence of fertile sexual stages in the animal model. Three different phases have been identified in the *P. falciparum* humanized mouse model: engraftment with human erytrhocytes, *P. falciparum* infection and growth, and anaemia phase provoked by the massive clearance of infected and uninfected human erythrocytes. Throughout the phases, different inflammatory cytokines have been observed to be secreted, besides the model have been developed in immunodeficient mice. Some of the cytokines explored have shown a similar secretion pattern to the one observed for the human host.

The high reproducibility of the model makes suitable the use of the *P. falciparum* humanized mouse model as a drug discovery tool to test the efficacy of new antimalarial drugs in the preclinical phases of the drug development process. In this context, the *P. falciparum* mouse model have been used to achieve the efficacy parametres of new antimalarial drugs, so as the phenotypical characteristics of the effect of the treatment on the parasite to discriminate different mechanism of action.

All the similiarities found between the mouse model and the human infection, support that the *P. falciparum* humanized mouse model can be a good surrogate of the natural *P. falciparum* infection and a unvaluable tool for the drug development to assess the malaria eradication.

Resumen

La malaria está causada por los estadíos asexuales de los parásitos humanos del género *Plasmodium*. Entre las cinco especies patógenas para humanos, *P. falciparum* es el responsable de más de medio millón de muertes al año en África. La aparición de resistencias a los tratamientos actuales ha hecho que el desarrollo de nuevos fármacos antimaláricos sea crucial para la estrategia global de la erradicación de la malaria.

P. falciparum infecta casi exclusivamente a eritrocitos humanos. Para poder estudiar la malaria human, un modelo murino de la infección de *P. falciparum* ha sido desarrollado. Este modelo está basado en el xenotransplante de sangre humana a ratones inmunodeficientes que carecen de células T, B y NK (NODscidIL2Rγ^{null}), mediante la inyección diaria de eritrocitos humanos.

Un estudio detallado de este xenotransplante ha sido realizado en este trabajo. Se ha conseguido un crecimiento robusto y reproducible de *P. falciparum* en los ratones xenotransplantados. La duración del ciclo eritrocítico de *P. falciparum* determinado en el modelo murino de *P. falciparum* es similar al reportado en el hospedador humano (48±1 horas). También se ha demostrado la transmisión al hospedador invertebrado (mosquito), confirmando la presencia de estadíos sexuales fértiles en el modelo animal. Además, se han identificado 3 fases diferentes en el modelo murino; quimerización con eritrocitos humanos, infección y crecimiento de *P. falciparum* y la fase de anemia provocada por la eliminación masiva de eritrocitos infectados y no infectados. Durante las distintas fases del modelo, diferentes citoquinas inflamatorias son secretadas y cuantificadas, a pesar de que el modelo se desarrolla en ratones inmuodeficientes. Algunas de las citoquinas observadas han mostrado un patrón de secreción similar al observado en el hospedador humano.

La alta reproducibilidad del modelo hace posible su uso como una herramienta para probar nuevos fármacos antimaláricos en las fases preclínicas del desarrollo farmacéutico. En este contexto, el modelo murino de *P. falciparum* ha sido usado para obtener parámetros de eficacia de nuevos fármacos antimaláricos, además de las características fenotípicas del efecto del tratamiento en el parásito para poder discriminar diferentes mecanismos de acción.

Todas las similaridades encontradas entre el modelo murino y la infección humana, respaldan el hecho de que el modelo de ratón humanizado puede ser un buen sustituto de la infección natural de *P. falciparum* y una herramienta esencial para el desarrollo de nuevos fármacos en la consecución de la erradicación de la malaria.

Introduction

Malaria: The problem

Malaria is one of the most deadliest disease in the world, with a high rate of mortality. Although malaria was prevalent throughout most of the world, currently is endemic of sub-tropical regions in the Asian, African and American continents (figure 1). However, malaria remains to be a disease of global health importance with 3.3 billion people at risk in more than 100 countries. Actually, it is estimated that anually there are 200 million cases and around 600.000 deaths [155]. The more susceptible population to suffer from malaria are pregnant women and children under 5 years old.

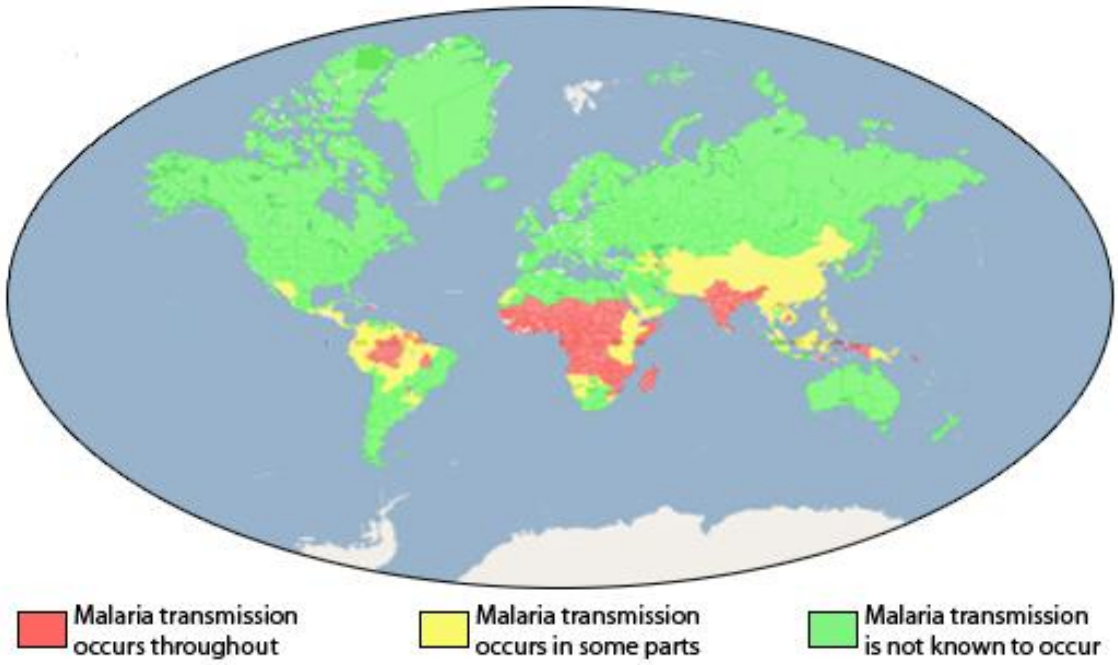

Figure 1. Malaria global distribution (source CDC). In red is indicated high risk of malaria transmission, in yellow medium risk and in green are zones in which malaria is not transmited or reported.

Around 50% of the worldwide population lives in areas with risk of malaria transmission. However, the continent which is more punished with this disease is Africa, in which the 90% of malaria cases are reported. Malaria is usually a serious disease in developing countries where the resources are limited, the access to medicines is complicated and other serious diseases are common.

Malaria is caused by the unicellular obligate intracellular protozoan parasite of the genus *Plasmodium*. There are more than 100 kinds of *Plasmodium* that can infect many animal species such as reptiles, birds and various mammals. Among these species, four can cause malaria in human beings: *P. falciparum*, *P. vivax*, *P. malariae* and *P. ovale*. In addition,

studies in Southeast Asia have shown that *P. knowlesi*, a malaria parasite that typically involves monkeys as the natural reservoir, can also infects humans [126].

Malaria due to *P. vivax*, *P. ovale* and *P. malariae* is less severe than that experienced by *P. falciparum* infections, these three species are accountable of less than 10% of the worldwide malaria cases [155]. However, *P. falciparum* is responsible of the 90% of the malaria cases and cause te 99% of deaths associated with this disease.

The *P. falciparum* pathophysiological sympthoms ranges from asymptomatic infections to the usual malarial symptoms: fever, chills, sweating, headaches and muscle aches. However, in a subpopulation of the cases, malaria results in severe life-threatening complications such as hypoglycemia, metabolic, acidosis, cerebral malaria, severe malarial anaemia and respiratory distress. Most of the reported cases of severe malaria include malarial anaemia and cerebral malaria are typically displayed in children. However, adults are more likely to present jaundice, renal failure and respiratory distress due to pulmunary edema [153]. For this reason, most of the efforts in drug discovery programs are focused on the treatment of *Pf* sympthoms.

The lack of control of the regimen doses in addition to a delay in the diagnosis of the disease, have accelerated the emergence of resistances to the current available drugs. The development of new antimalarial medicines and vaccines is a key part of the global strategy for malaria eradication.

The two most widely used antimalarial drugs chloroquine and sulfadoxine-pyrimethamine are failing at an accelerating rate in most malaria-endemic regions. Actually, chloroquine resistance has spread and contributes to the increase in the malaria-associated mortality. Sulfadoxine-pyrimethamine resistance is also leading to unaceptable levels of therapeutic failure in many areas in Asia, South America and Africa (figure 2).

The Artemisinin-based combinations therapies are recommended as first-line treatment for malaria, and its implimentation has contributed significantly to reduce the malaria burden in many endemic countries and countering resistance to key antimalarial medicines [155]. However, the emergence of resistance to artemisinin based treatments have been a drawback in the fight against malaria [106].

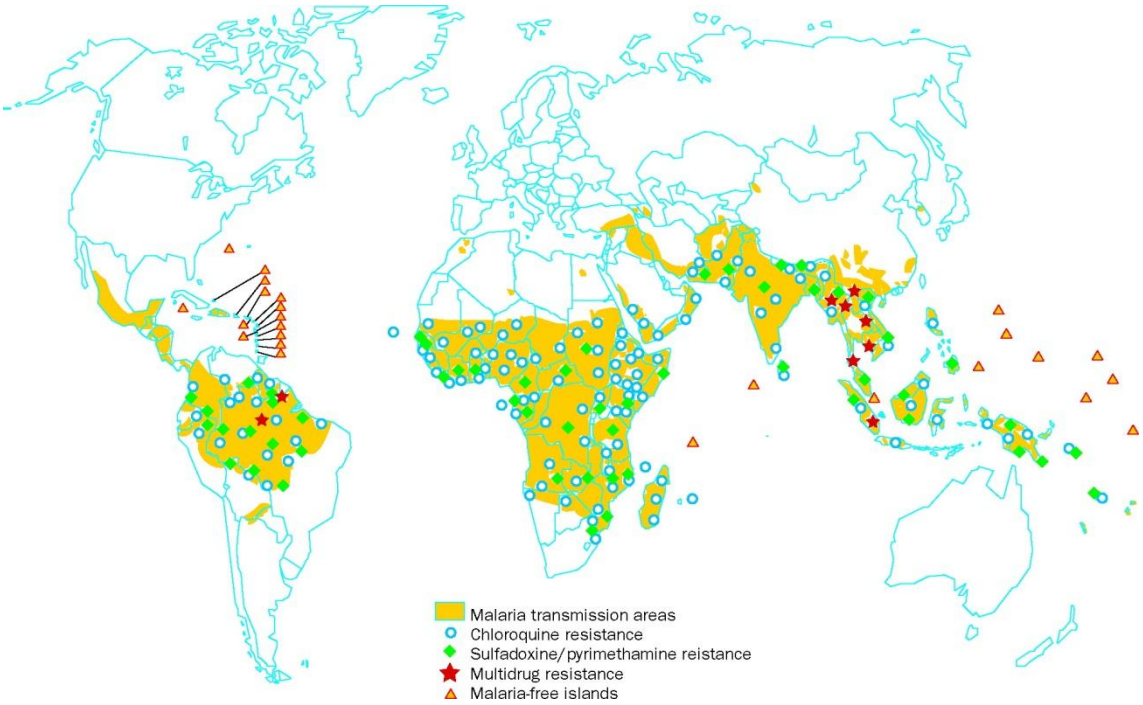

Figure 2. The emergence of malaria resistances to chloroquine (blue circle), sulfadoxine-pyrimethamine (green diamond) and other treatments (red star) in Malaria transmission areas (yellow). Orange triangles indicate free malaria island in malaria endemic regions [157].

The development of new antimalarial drugs has become a new priority to achieve the goal of malaria eradication and elimination by 2030, due to the most advanced vaccine, the RTS,S, have shown only around 50% of efficacy in children under 2 years old [142]. New antimalarial drugs must meet the requirements of rapid efficacy, minimal toxicity, and above all a low cost to reach the real affected countries in the poorest regions of the world. The eradication programme includes the development of new antimalarial vaccines.

Plasmodium life cycle

The protozoa from the *Plasmodium* genus show a complex life cycle where they present different hosts and phenotypic characteristics throughout their cycle (figure 3).

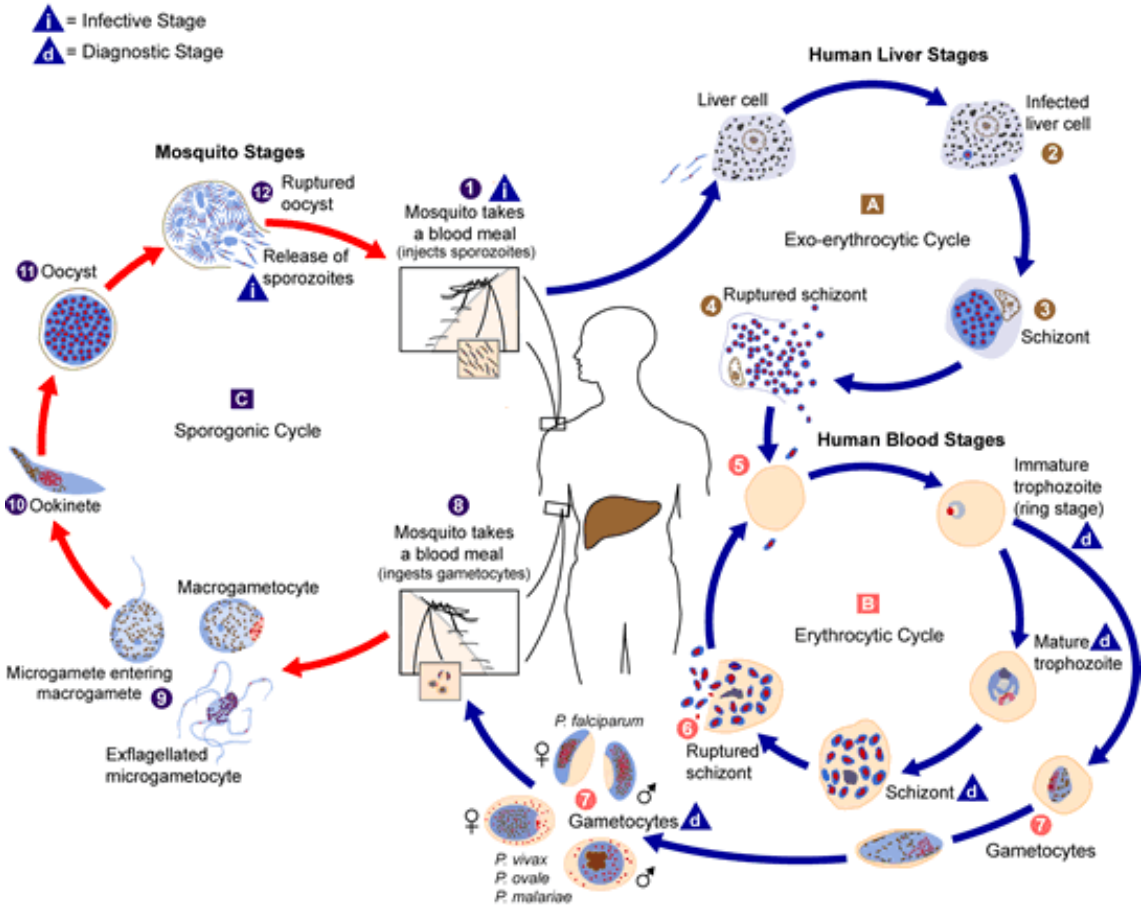

Figure 3. Plasmodium life cycle in the human host and mosquito(source CDC). A) Exoerythrocytic cycle, where the mosquito release sporozoites that invade hepatic cells and develop to schizont, which release thousands of merozoites; B) Erythrocytic cycle, where the merozoites released by the hepatic schizont invade RBCs and form a ring that then mature to trophozoite and posterior schizont that release more merozoites ready to invade new RBCs, some merozoites that invade RBCs are able to develop to the sexual stages of the parasite, the gametocytes; C) Sporogonic cycle, where the gametocytes develop to female and male gametes after the uptake by the mosquito, inside the mosquito midgut takes place the fecundation of the female gamete by the male gamete, and the zygote and posterior ookinete is formed, the ookinete develop to a oocyst that forms thousands of sporozoites, which after the release migrate to the salivary glands and are ready to be introduced to a new human host.

The main mode of transmission of the disease is by bites from infected female *Anopheles* mosquitoes that have previously had a blood meal from an individual infected with malaria. Less common routes of transmission are via infected blood transfusion, transplantation, infected needles and from mother to her fetus during pregnancy.

In order to complete the life cycle, *Plasmodium* needs two hosts: the mosquito and the mammal host. In the mosquito the sexual reproduction of the parasite takes place and it is the vector for the transmission of the disease. In the mammalian host takes place the asexual reproduction of the parasite and this phase of the cycle is the responsible of the pathophysiology associated to the malaria disease [151].

The human infection begins when an infected female *Anopheles* mosquito bites a person and injects salive containing sporozoites, the invasive crescent-shaped form, into the dermis. These sporozoites enter into the blood circulation directly or through the lymphatic system. Sporozoites find their way through the blood circulation to their first target, the liver. The sporozoites enter the liver cells (hepatocytes), where it is formed a parasitophorous vacuole that includes the parasite and it is separated from the host cell cytoplasma [120]. Inside the hepatocyte the parasite starts dividing leading to a new cell type, the schizont. Each schizont gives birth to thousands of merozoites that are packed into vesicules (merosomes). The infected hepatocyte is lysed and the merosomes that contain the merozoites are released to the blood stream [140].

This phase, denominated exoerythrocytic cycle or exoerythrocytic schizogony has a length that range from 5 to 15 days depending on the *Plasmodium* specie [151]. The exoerythrocytic phase is not pathogenic and do not produce symptoms or signs of the disease. It is worth mentioning that, concerning *P. vivax* and *P. ovale*, sporozoites may not follow the reproduction step and stay dormant, in a parasite form known as hypnozoite, in the liver. They may be activated after a long time leading to relapses entering the blood stream (as merozoites) after weeks, months or even years [56].

Once the merosomes are outside the hepatocyte, they head to the pulmonary capilars, where within 48-72 hours the contained merozoites are released. These merozoites are directed to their second target, the red blood cells, this mark the beginning of the erythrocytic phase [14].

The blood stage merozoite is the smallest cell within the *Plasmodium* cycle, and one of the smallest eukaryotic cells known (≈1-2 μm). The merozoite has the convenient organelle repertoire of eukaryotic cells with the cytoeskeletal architecture of an apicoplexan cell, the phylum to which malaria parasite belong. This includes an apical complex of secretory organelles (micronemes, rhoptries and dense granules), mitocondrion, nucleus and relict plastid, apicoplast [18].

The erythrocyte invasion process by the merozoite is very fast (within 30 seconds), and takes place through several sucessive steps. Initial interaction involves a recognition between the merozoite and erythrocyte, followed by a reorientation that places the parasite appex abutting the host cell membrane and provoking a deformation of the erythrocyte surface. After a brief pause and major deformation of the erythrocyte membrane, the parasite enters and the erythrocyte membrane return to its normal shape within 10 minutes (figure 4). During the internalization, the parasite forms a new parasitophorous vacuole that isolate the parasite from the erythrocyte cytoplasm. The internalized parasite, now refered as a ring, undergoes a rapid and dramatic changes after this process [52].

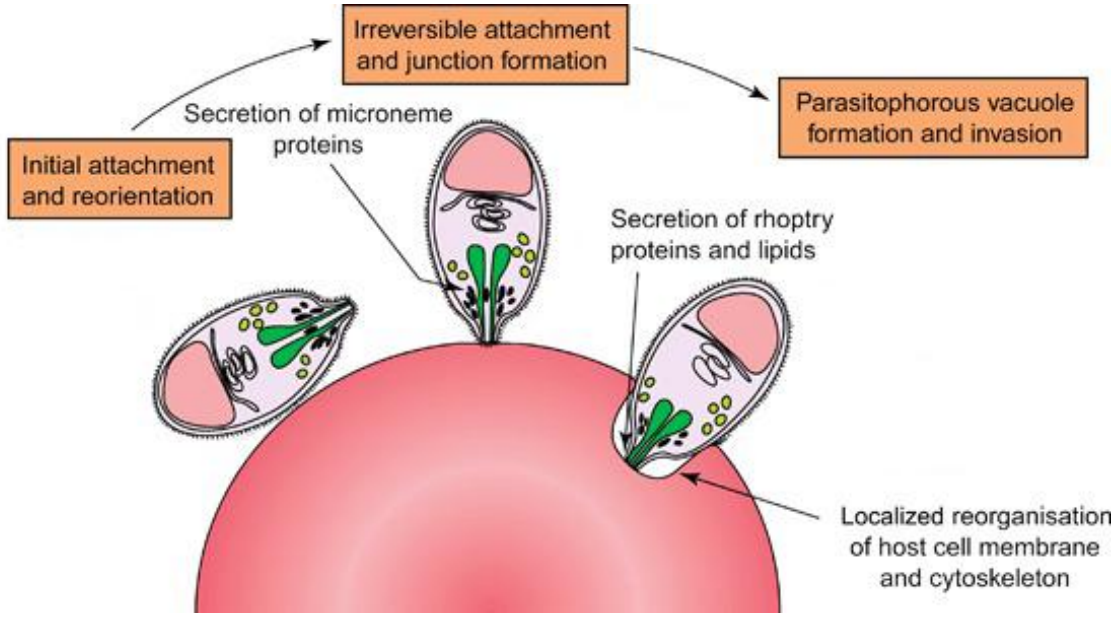

Figure 4. Invasion of a RBC by a P. falciparum merozoite (adapted from [68]). Invasion is a complex multi-stage process. Initial attachment can occur with the merozoite in any orientation and involves low-affinity interactions. Subsequent interactions are facilitated by proteins that are initially hidden within the apical organelles and are secreted only shortly prior to or at the time of attachment.

Typically, ring morphology is thin discoidal flat-shaped and has a thick rim of cytoplasm housing the major organelles, while the centre of the disc is thin and contains few structures. Parasite begins to feed on the surrounding RBC haemoglobin and enlarges until occupy almost all the RBC, originating a new form metabolically very active, the trophozoite. This trophozoite continues the digestion of the RBC haemoglobin. The haemoglobin degradation is a nutritional resource for the parasite. As a result of the catabolitic process, it is generated cytotoxic wastes, as the haeme group in the form of

protoporphyrin α. The parasite has developed an strategy to avoid the toxic effects of this metabolite, in the cytoplasm takes place the polymerization of the haeme group generating inhert brown crystals known as hemozoine, that accumulates within the digestive vacuole throughout the erythrocytic phases to avoid the toxicity [49]. However , the globin group, from the haemoglobin digestion, is used as a source of aminoacids for the reproduction.

The next cellular stage is the schizont. Technically speaking a schizont is an intracellular parasite that is undergoing or has undergone repetitive nuclear divisions. However, the synthesis of some of the molecules needed for the parasite multiplication, including DNA is known to start in the trophozoite stage. Conversely, ingestion of RBC cytosol lasts until late in the schizont period. The nucleus divides about four times to produce about 16 nuclei. Nuclear division is accompanied by numerous cytoplasmic changes that prefigure merozoite formation. Then, a constriction ring separates each merozoite from the residual body of the schizont, and the merozoites cluster within the parasitophorous vacuole. Finally, the parasitophorous vacuole membrane and RBC membrane are breached and the new merozoites, released to the blood stream, are ready to find and invade new RBCs [151] (figure 5). This erythrocytic cycle is denominated erythrocytic schizogony and is when parasitemia occurs and clinical manifestations appear. The liver phase occurs only once, while the erythrocytic phases undergoes multiple cycles, the merozoites release after each cycle and created the febrile waves in patients.

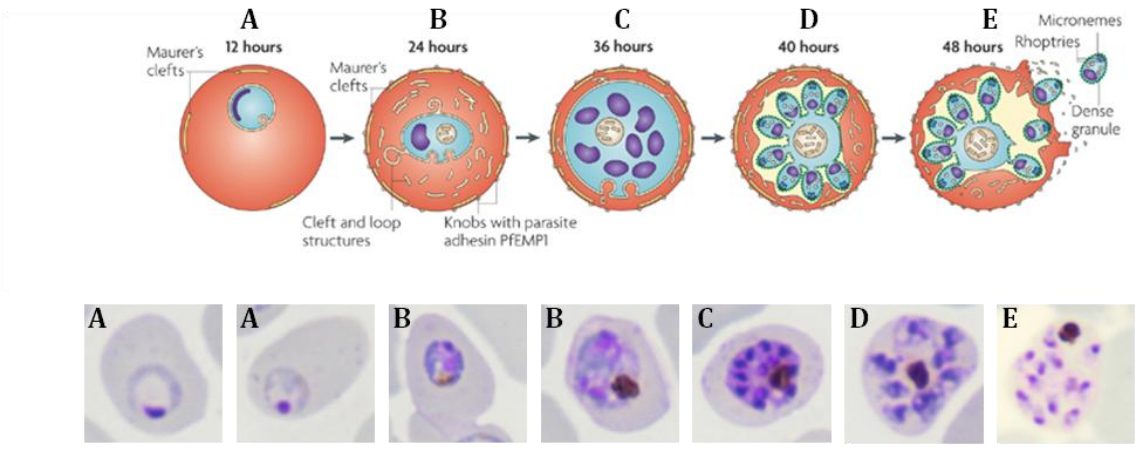

Figure 5. Erythrocytic stages of Plasmodium falciparum parasite (adapted from [86]). After the invasion of the RBC by the merozoite, this develop to a ring stage (A), later to trophoite stage (B) and finally to schizont stage (C), where new merozites are formed and assembled (D). The new merozoites are released to the blood stream after RBC and parasitophorous membrane rupture (E).

Although most of the merozoites that invade the erythrocytic cells develop an asexual cycle, a small fraction can differentiate into male and female gametocyte inside the human host. These gametocytes are a non pathogenic form of the parasite, and this process is known as gametocytogenesis (figure 6). There are five different stages of gametocytes depending on the grade of maturation, the stage V is the final stage and the only one able to reproduce. This process is a crutial step in the *Plasmodium* life cycle, as it is required for parasite transmission from the human host to the mosquito and thus for the subsequent infection of other humans. The commitment to sexual development occurs at some point before schizogony, as all merozoites within a mature schizont will either differentiate into gametocytes or continue asexual development. However, the mechanisms involved are currently unclear [2, 33].

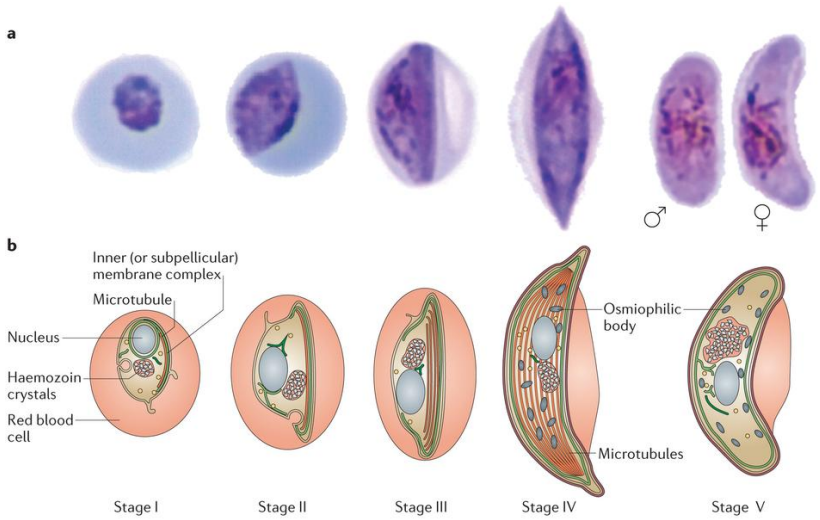

Figure 6. Plasmodium falciparum gametocytes development (adapted from [66]). Gametocytes development is divided in five morphologically distint stages shown as Giemsa photographs a) and schematics b). Stage I gametocytes are very similar to trophozoites, stage II begin to elongate and acquire a D-shape, stage III elongate further and ends become rounded, stage IV continues to elongate but ends are now pointed, and stage V acquire crescent shape, at this stage female gametocytes are more elongated and thicker than male.

When a female *Anopheles* mosquito bites an infected person, it takes up these gametocytes with the blood meal. Following ingestion by the mosquito, gametocytes experience a drop in temperature, a change in pH and exposure to xanturenic acid, which together trigger their maturation from gametocyte in stage V into gametes in the mosquito midgut. Female stage V gametocytes transform to macrogamete and male stage V gametocytes rapidly undergo three rounds of DNA replication to form an octoploid nucleus, followed by the

assembly of eight flagella to produce microgametes, this process is known as gametogenesis (figure 7).

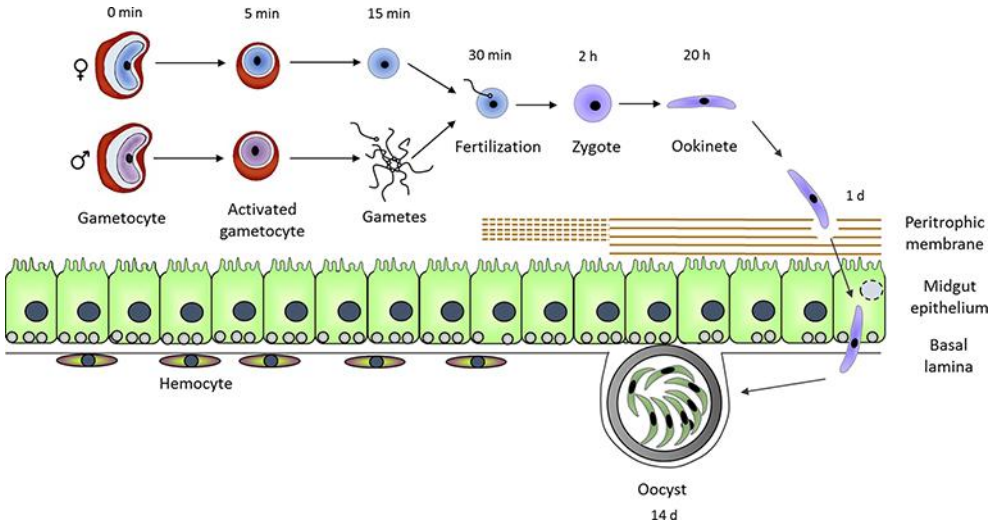

Figure 7. Development of malaria parasite in the mosquito midgut (adapted from [102]). Stage V gametocytes activate in the mosquito midgut to form gametes, then fertilization occurs and the ookinete is formed. This penetrates the midgut epithelium and develop an oocyst which forms thousands of sporozoites that are released and migrate to the salivary glands waiting for the next mosquito bite to infect a new host.

This transformation occurs in less than 20 minutes. Then, haploid gametes fuse with female macrogamete to form a diploid zygote. The zygote, after the fusion of nuclei and fertilization, becomes a ookinete. The ookinete, then penetrates the midgut wall of the mosquito where it encysts and form and an oocyst. Inside the oocyst, the ookinete nucleus divides to produce thousands of sporozoites. This is the end fo the sporogonic cycle (figure 7) which lasts from 8 to 15 days , depending on the Plasmodium specie [135].

Finally, the oocyst ruptures and the sporozoites are released inside the mosquito cavity and actively migrate through the haemocoel to the salivary glands, where they reside until the mosquito takes a blood meal, which simultaneously delivers sporozoites to the next human host.

The complexity of *Plasmodium* life cycle has made the eradication strategy difficult. Drug discovery efforts usually focus on the erythrocytic phase, but the development of new tools have made possible the search of drugs that are effective in other phases of the parasite life cycle in the last years.

Mouse models for drug discovery

An animal model for a human disease is by no means attempting to reproduce the human disease with all its complexities in an animal but rather to model specific aspects of a disease. When adequately designed and conducted, animal models can give invaluable information to our knowledge of biology and medicine, including the discovery and development of new drugs. The selection of a validated and predictive animal model is essential to address the clinical question.

To fight Malaria, new drugs are needed. Ideally, new drugs for *P. falciparum* malaria should be efficacious against drug-resistance strains, provide a cure in a resonable time, have appropiate formulations for oral use and be affordable as the target population lives in developing countries with few resources.

Most antimalarial drugs that are now in use were not developed on the basis of rationally identified targest, but following the identification of antimalarial activity of natural products, for example quinine and artemisinin. Recently, an improved understanding of the biochemistry of the malaria parasite and the description of the entire *P. falciparum* genome sequence has identified many potential targets for new drugs and helped to know more about the mode of action of older drugs.

Targets that are shared between the parasite and human host offer opportunities for chemotherapy if structural differences can be found. Alternatively, targets can be selected from enzymes or pathways that are present in the malaria parasite but absent from humans. A reverse drug discovery approach can also be used to elucidate the nature of previously unidentified target of older antimalarial drugs as a basis for new drug discovery development.

Modern drug discovery can be structured as a series of sequential steps in which the properties of drugs as potential medicines are investigated. The drug discovery process is typically divided in four stages: hit to lead, lead optimization, preclinical development and clinical development (figure 8) [64]. At each step, compounds are evaluatted in different assays to understand risk and assess efficacy, toxicity, DMPK (drug metabolism and pharmacokinetics) and physicochemical properties as indicators of their potential as future drug molecules. The progression from one stage of drug discovery to the next indicates that drugs has no evident issues or the risks identified can be managed at a later stage in the development process.

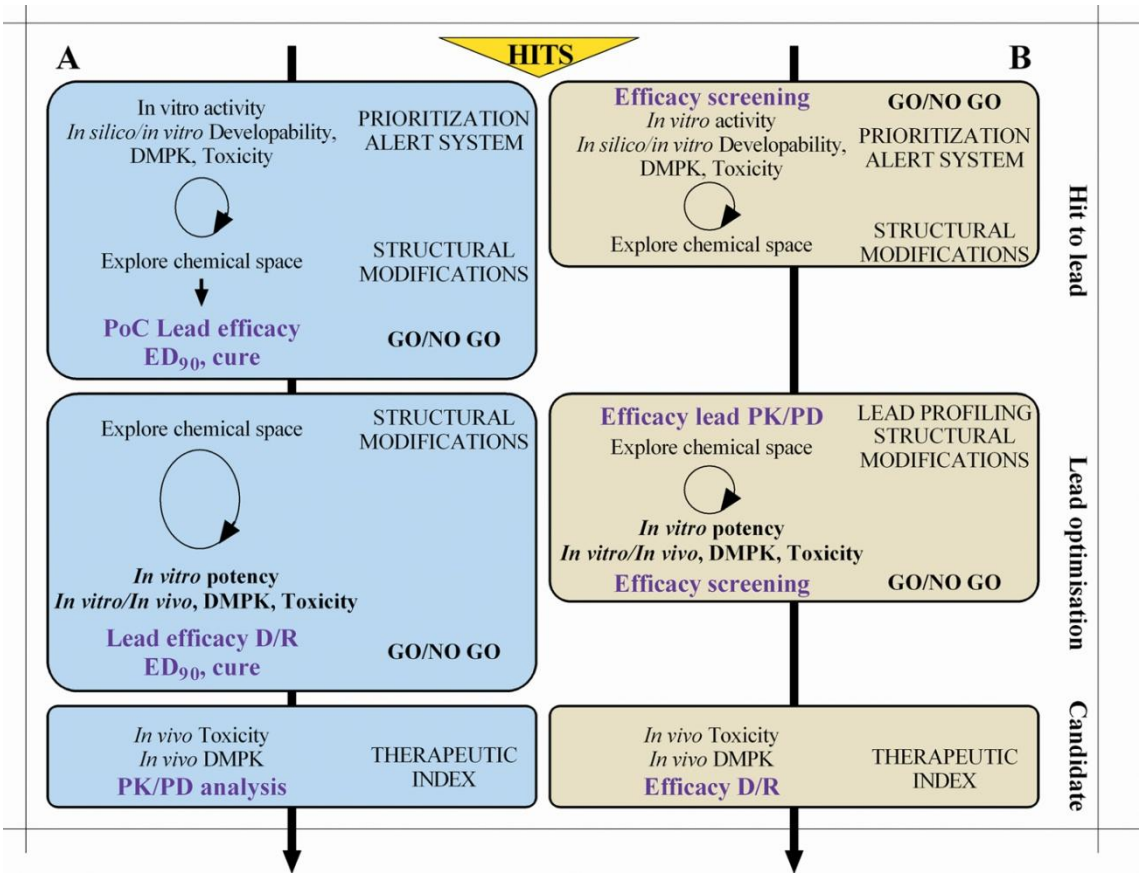

Figure 8. Two strategies of critical pathways in the drug development progress. (A) Efficacy evaluation is performed at the end of each progression step. This strategy of evaluation is followed by most current drug discovery programmes. In general, efficacy evaluation relies on relatively large experiments (dose–response, abbreviated as D/R, >10 mice per compound) designed to estimate the potency of compounds. The compounds tested are generally selected after extensive filtering using in silico/in vitro filtering; (B) Efficacy is performed at the beginning of each evaluation step. Efficacy evaluation relies on screening format assays involving small number of mice per compound (≤3 per compound) aiming at detecting improvement or not over a reference compound of the series. In this strategy all in silico, in vitro and in vivo data are integrated in decision-making on compounds at early stage.

The hits are usually selected based on the activity shown *in vitro* against an essential target of *Plasmodium* or the whole parasite itself. The sources of hits are usually high-throughput molecular or phenotypic screenings, depending whether the objective is to inhibit a specific molecular target or the intact parasite/host cell.

In vitro screens for compound activity are based on the ability to culture *P. falciparum* in human erythrocytes. Detailed standardized protocols for culturing *P. falciparum* and

assaying susceptibility to antimalarial compounds are available worldwide [88, 130]. This protocol describes the measurement of the uptake of ^{3}H-hypoxanthine (which is taken up by the parasite for DNA synthesis) to determine the level of *P. falciparum* growth inhibition. Usually, parasites are cultured in the presence of different concentrations of test compounds. IC_{50} values can be determined by linear regression analysis on the linear segment of the dose-response curves.

Although ^{3}H-hypoxanthine incorporation is the most commonly used method to assay antimalarial activity *in vitro*, it is costly and generate radioactive waste. Flow cytometry can also be used to test candidate antimalarial compounds, and takes advantage of the fact that human erythrocytes lack DNA [79]. In this assay, parasite killing kinetics can be determined by culturing unlabelled erythrocytes with *P. falciparum* in the presence of antimalarial drugs for 24 or 48 hours. After removing the drug, samples were added to pre-labelled erythrocytes with intracellular dye to allow their subsequent identification. The ability of viable parasites to re-establish infection in labelled erythrocytes can be detected by two-colour flow cytometry after tagging parasite DNA. This simply assay provides quite high-throughput but requires expensive equipment.

The demonstration of efficacy *in vivo* of the hits detected *in vitro* is a major goal of the initial stages of the drug discovery process. *In vivo* evaluation typically begins with the use of rodent parasites. Of these, *P. berghei*, *P. yoelii*, *P. chabaudi* and *P. vinckei* have been used extensively in drug discovery and early development. These animal models remain a standard part of the drug discovery and development pathway. Individual species and strains have been well characterized including duration of cycle, time of schizogony, synchronicity, drug sensitivity and reticulocytes preference [115, 129, 148].

The most widely used initial tests, which uses mainly *P. berghei*, is the Thompson survival assay and the Peters´ 4-day test [114, 143]. The Thompson´s assay requires relatively large numbers of animals and/or long observation time. However, in the Peters´4-day test the efficacy of four daily doses of compounds is measured by comparison of blood parasitemia (on day four after infection) and mouse survival time in treated and untreated mice. Rodent infection is initiated by needle passage from an infected to a naïve rodent via intravenous or intraperitoneal route using a small inoculum (10^{6}-10^{7} infected erythrocytes). Compounds can be administered by several routes including intraperitoneal, intravenous or oral. The administration of compounds starts from one to three hours after infection, when parasite is still below to the limit of detection of microscopy or flow cytometry.

Recently an *in vivo* screening approach has been assessed as a strategy to rapidly identify starting points for drug discovery projects in early stages of drug development [65]. The screening assay used a *P. berghei* murine model of malaria infection based on parametres of human disease, for example, parasitemia in the peripheral blood of patients at the point of hospital admission and the parasite reductionn rate (PRR), defined as the ratio of the baseline parasite count to that following treatment. Infection is assessed by intravenous route from an infected mouse with a small inoculum (10^7 infected parasite). However, compound administration starts two days after the infection, and the treatement length is only two days, with one daily dose of compound administered by oral route in a unique dose of 50 mg/kg (figure 9).

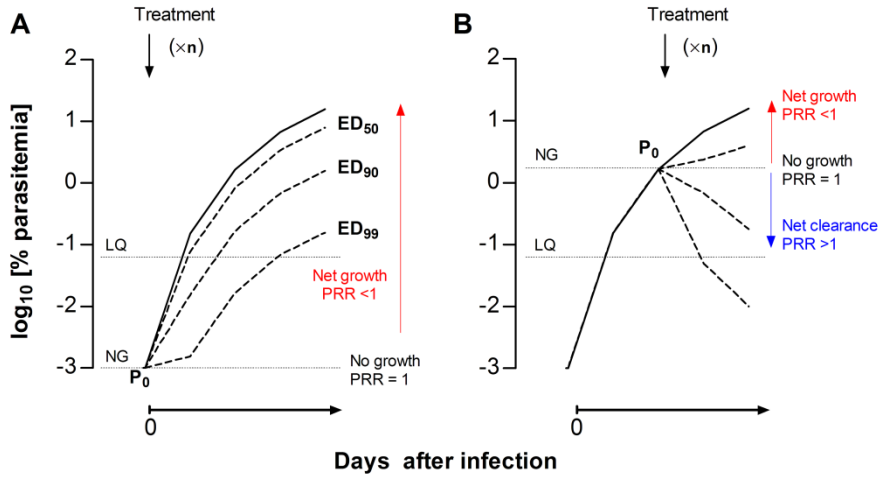

Figure 9. Comparison of the theoretical growth curves of Plasmodium berghei upon intravenous infection at day 0 under (A) a Peters' 4-day test-type or (B) the in vivo screening assay format for the evaluation of the antimalarial efficacy of drugs. The solid curves represent the growth of parasites treated with vehicle. The dotted lines represent the growth of parasites under arbitrary treatments (×n, denotes arbitrary number of drug dosages) leading to ED_{50}, ED_{90} and ED_{99}, respectively. The parasitemia that marks the limit between net growth and net clearance of the parasite circulating in peripheral blood is denoted as the NG line. The limit of quantification of parasitemia is denoted as the LQ line. PRR is the parasite reduction ratio, the ratio of the baseline parasite count to that following treatment.

Compounds identified as active in the *in vivo* assays can subsequently be progressed through several secondary tests. In the dose ranging full 4-day test, compounds are tested at a minimum of four different doses to determine ED_{50} and ED_{90} values (doses that clear 50% or 90% of parasite, respectively). The parametres of efficacy are essentially measurement of the potency that is, the miligrame per kilograme of body weight necessary to achieve a specific biological endpoint. Results are expressed as the rapidity of

onset of activity (dissapearance of parasitemia) and time to onset of recrudescence (increase of parasitemia).

When using rodent parasites, several variables need to be considered. Rodent plasmodia can differ significantly in their degree of infection, lethality and synchronicity. In addition, rodent malaria species can also differe significantly in sensitivity to certain classes of compounds. The choice of model may depend on the genetic similarity at the level of the molecular target. For example, *P. yoelii* was chosen to test 4-(1H) pyridones because the high sequence homology with *P. falciparum* for the target cytochrome bc_1, which is a key protein in the mithocondrial respiratory chain [158]. In other cases, the choice is guided by empirical considerations based on the relative sensitivity of each model to the drugs tested. Thus, pentamidine and diamidines have been tested in the *P. vinckei* model because *P. berghei* is almost insensitive to these drugs [5].

It is important to note that the drug sensitivity of a given rodent malaria does not always mirror that of *P. falciparum* and can limit the types of researching that can be performed. A differential susceptibility to the drug between the human pathogen *in vitro* and the rodent surrogate *in vivo* is inferred in these situations. In these cases evaluating the efficacy of drugs in non-human primates or humanized mouse models is the only realistic alternative. Primate models have provided a final confirmation of the choice of a drug candidate. Infections with certain strains of *P. falciparum* has been well characterized in both Aotus and Samiri monkeys [139]. However, these hosts are mostly used in projects seeking drugs for radical cure, and their use is not widely extensed due to ethical issues.

By contrast, *P. falciparum* mouse model offers a practical alternative that has been exploited by several drug discovery projects. For example, the poor activity of some triazolpyrimidines against *P. berghei* dihydroorotate dehydrogenase compare to the P. *falciparum* enzyme prompted researchers to use the *Pf* humanized mouse model to measure efficacy *in vivo* [40]. Noteworthy, an increasing number of projects employ the *Pf* mouse model at some point during the lead optimization process irrespective to the difference in susceptibility between *P. falciparum* and *P. berghei* [28, 39, 63, 90, 103].

Humanized Mouse Models for Malaria

The humanized mouse models are crutial in infectious diseases caused by specific human pathogens. Malarial parasites have a complex life cycle, and are highly host cell specific. *P. falciparum* infects almost excusively human cells with the expection of new world monkeys of the genus Aotus and Samiri. Blood stage parasites are responsible for all sympthoms of malaria infection. Therefore, a small animal model for *P. falciparum* blood

stages would enhance understanding of disease pathophysiology, and is critical for modelling the complete life cycle in small animals and without the ethics problems that entails the use of non-human primates.

The development of a small animal model for the blood stages of *P. falciparum* was preceded by the discovery of mice with spontanenous immune deficiencies, which allow for the engraftment with human cells. The severe combined immunodeficiency (scid) mouse harbouring a point mutation in the Prkdc kinase ($Prkdc^{SCID}$), which interferes with the development of functional B and T lymphocytes, accepts xenogenic grafts of hRBCs and was used to establish *P. falciparum* blood stage infection for up to 2 weeks in the 90s [146]. This model established the starting point for the development of a reliable humanized mouse model for human malaria. Nevertheless, the initial studies included difficulties in obtaining high levels of hRBC chimerism, as well as, the rapid clearance of parasite-infected hRBC by the mouse. Some of these problems have been analyzed and are mainly due to substantial innate responses still present in immunodeficent mice [8]. Macrophages and NK cells are responsible for the clearance of the parasite infected and uninfected hRBCs. Additional mutations in mice were explored to increase the immunodeficience to reduce the innate immune response present in *scid* mice.

The non-obese diabetic (NOD) mouse dramatically reduced the clearance of human haematopoietic cells, in part because of a polymorphism in the signal regulator protein alpha (SIRPα) gene that enhances binding to human CD47 and diminishes macrophage phagocytosis [105]. Natural killer cells also have reduced activity in NOD mice because of a defect in the NKG2D receptor [109]. These properties have made the NOD background prefered for the development of models that uses xenotransplantation of haematopoietic cells.

Targeted gene deletions have also contributed to the immunocompromised status that is required for the development of humanized mouse models. The recombination activation gene 1 or 2 (Rag1 or Rag2) is responsible for V(D)J recombination, and thus its elimination in mice lend to lack of B and T cells [38]. Similarly, deleting the IL-2 receptor gamma chain (IL2Rγ) depletes the common receptor of IL-2, IL-4, IL-7, IL-9, IL-15 and IL-21 cytokines, eliminating functional T cells and NK cells. In addition, homozygosity for the β2 microglobulin (β2m) allele results in the absence of MHC class I expression, loss of $CD8^+$ T cells and NK cell activity. Crosses between these mice have resulted in the NODscid mouse, the IL2 mouse (NODscidIL2Rγ^{null}), the β2 mouse (NODscid$\beta2m^{-/-}$), the NOG mouse

(NODscidIL2Rγ^{truncated}), the Rag2 IL2 mouse (NODRag2IL2Rγ^{null}) and the NRG (NODRag1IL2Rγ^{null}), each of will be used in this work (figure 10).

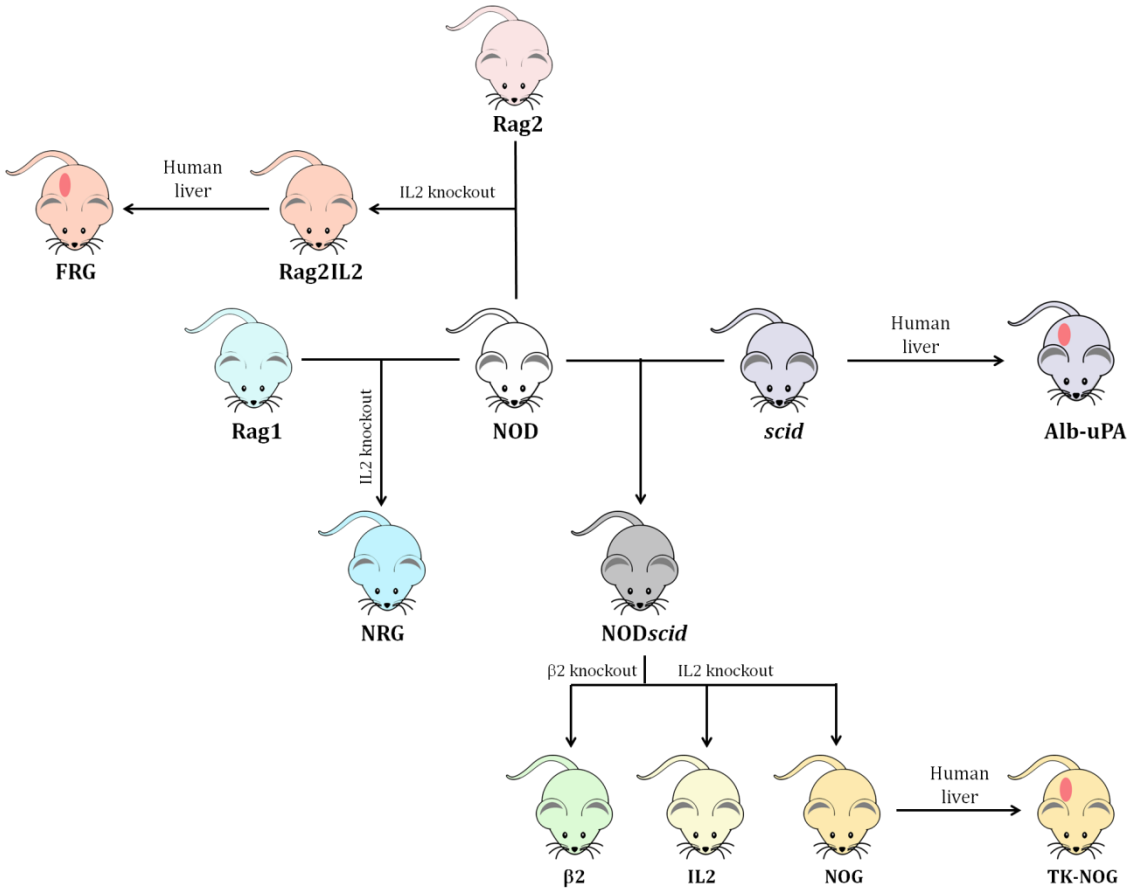

Figure 10. The origin of the different immunodeficent strains used for the generation of humanized mouse models. The parental mice strains NOD, scid, Rag1 and Rag2 can be used for the generation of mice with more immunodeficiencies (NODscid). The knock out of different genes, as the β2 and IL2 can increase the immuodeficiency level generating new mice strains (β2, IL2, NOG, NRG, Rag2IL2) . The scid, NOG and Rag2IL2 strains can be used to generate new mouse strains able to support the xenotransplant of human hepatocytes.

Liver stages

The development of a robust humanized model for the hepatic stage of *Plasmodium* depends on the transplantation of functional human hepatocytes into mice. These models are based on procedures that kill murine hepatocytes followed by transplantation of human hepatocytes. There are three major murine models of liver transplantation: i) scid mice transgenic for urokinase–type plasminogen activator under the albumin promoter (Alb-uPA) [91]; ii) fumaryl acetoacetate hydrolase-deficient (FAH-deficient) Rag2$^{-/-}$ IL2Rγ^{null} mice (FRG) [11]; iii) mice that express the HSVtk transgene under the albumin promoter onto the NOG background (TK-NOG) [53].

Hepatotoxicity in Alb-uPA mice is caused by the overexpression of urokinase-type plasminogen activator, which cleaves plasminogen to form the activate enzyme plasmin. These mice can be engrafted with human hepatocytes from day 7 after birth, and the degree of engraftment that can achieved is up to 99%. However, Alb-uPA mice are prone to haemorrhagic complications and difficult to breed due to homozygous transgenic mice are infertile. Though, successful infections of humanized mice with *P. falciparum* sporozoites have been described [93].

Conversely, the deficiency of FAH (an enzyme which is essential for tyrosine catabolism) in FRG mice leads to liver failure by accumulation of toxic metabolites. The cytotoxic effects are avoided by continuos treatment of mice with 2-(2-nitro-4-trifluoromethylbenzyol)-cyclohexane-1.3-dione (NTBC), an inhibitor of tyrosine catabolism upstream of FAH. Upon withadrawal of NTBC and subsequent progressive liver injury, FRG mice can be transplanted with human hepatocytes at any age. Although the engraftment achieved is more variable than Alb-uPA mice (between 3% and 97%), the FRG mice have been used for a succesful complete infection with *P. falciparum* and *P. vivax* sporozoites, culminated with the release of exoerythrocytic merozoites that are able to invade hRBC and initiate a sustainable asexual erythrocytic replication *in vitro* in the case of *P. falciparum* [94, 147].

In the case of TK-NOG mouse strain, the loss of endogenous hepatocytes is inducible by a brief exposure to a non-toxic dose of gancyclovir, a method that is rapid and temporally restricted, and routinely leads to a subtantial human hepatocytes repopulation (60-80%). A double engraftment of TK-NOG mice with human hepatocytes and hRBCs has been successfully described and these mice were receptive to infection and maturation by sporozoites from two species that infect human, *P. falciparum* and *P. ovale* [136].

Erythrocytic stages

The availability of *scid* mice led to the first attempt in establishing a humanized mouse model for erythrocytic stages of *P. falciparum*. The control of innate immunity is crutial to achieve a high degree of reproducibility in etyrhocytic *P. falciparum* humanized models. This innate immunity has been controled by using cases immunomodulatory treatments *in vivo* [7, 13, 98] and/or by selection of immunodeficent mouse strains having impaired immunity [5, 63].

Different immunomodulatory treatments have been used to inhibit the activity and reduce the number of phagocytes in tissues of mice used for *P. falciparum* infection. The most commonly used method is the injection of clodronate encapsulated liposomes (lip-clod).

The treatment of humanized mice with lip-clod regimes prior to the injection of human erythrocytes in the retro orbital senus, allow the growth of previously cultured strains and clinical isolates of *P. falciparum* in different murine backgrounds after intraperitoneal infection. However, the reproducibility of the infections and the parasite growth were low despite the immunosupression treatment [13, 98, 100]. An improvement in the immunomodulatory treatment with the addition of a monoclonal antibody NIMP-R14, that blocks the polymorphonuclear leukocytes, the change of the mouse strain background, the refinement in the techniques of hRBCs injection (addition of human serum), and the infection protocol, intravenous injection instead of intraperitoneal, lead to a increase in the parasite burden and the reproducibility of *P. falciparum* infections [7, 8].

On the other hand, the use of mice with NODscid background with impaired phagocytic activity, has allowed the development of models that do not require immunomodulatory treatments. Two major differences in this improved mouse model could account for the success: the selection of the mouse background and the *in vivo* selection of a *P. falciparum* strain that was adapted to replicate within the mouse. In this model, NODscidβ2m$^{-/-}$ were used. The daily intraperitoneal injections of hRBCs, at a 50% hematocrit with 25% of 3.1 mM Hypoxanthine and 25% Human serum, was able to obtain a hRBC chimerism up to 99%. Then, the parasite adaptation to grow in mice was performed by intravenous injection with parasite-infected erythrocytes, which reduced to below detectable parasitemia, but then parasite emerged and established a productive infection 2-3 weeks later. Adapted parasites were further transmitted and expanded *in vivo* and reproducible growth of the isolate was observed in all mice tested (figure 10). The significant improvement of *P. falciparum* blood stage replication allowed the experimental testing of antimalarials *in vivo* in a dose-response assay [5].

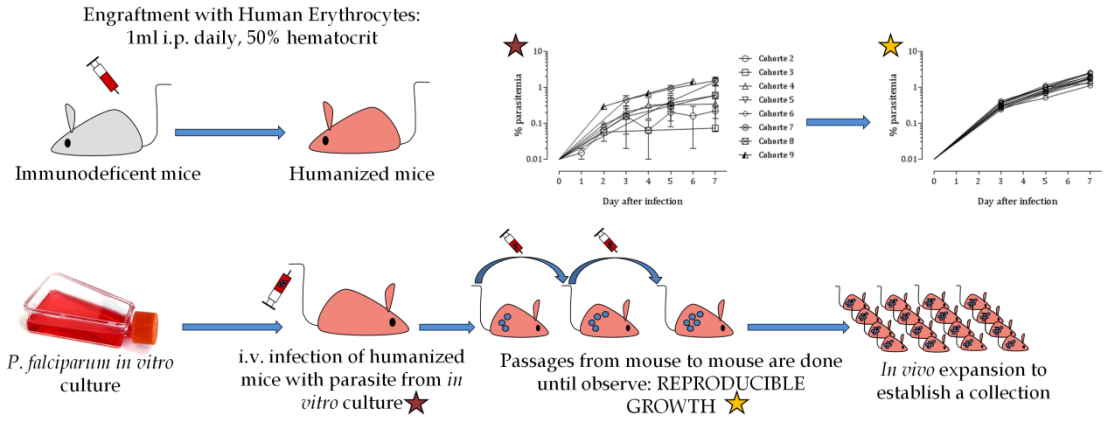

Figure 10. Schematic representation of the in vivo adaptation protocol for P. falciparum strains in humanized mice. First immunodeficent mice are injected daily with hRBCs in a

50% hematocrit suspension. Then, humanized mice are infected with P. falciparum infected erythrocytes from in vitro culture. Passages are done from mice to mice until obtain a reproducible growth in all mice. Finally, the strain is adapted and freezed to establish a stock collection.

However, the β2 mouse strain retains residula NK cell activity as well as other innate immune functions and shows a high incidence of early thymic limphomas, which dramatically diminish their life span, a do not allow to perfom long lasting experiments. A new mouse strain was then selected to overcome these issues, the NODscidIL2Rγ^{null} strain [63], several improvements were achieved that have been described in this work.

The humanized models of *P. falciparum* asexual erythrocytic stages without immunomodulatory treatment have been validated to evaluate the efficacy of new antimalarials by measuring dose-response relationships for drugs. However, to the date there are no reports describing assays to test the ability of compounds to block transmission of *P. falciparum* gametocytes from humanized mice to mosquitoes, even though the presence and transmission of mature gametocytes in humanized mouse models with immunosupression treatment has been documented [7, 97]. By contrary, until the date neither evidencies of gametocytes production nor transmission to mosquitoes have been described for the non-myelodepleted *P. falciparum* mouse model.

Although the use of IL2 mice for erythrocytic stages of *P. falciparum* has been transformational in malaria drug discovery, little is known about the mechanisms that govern the xenotransplant of hEry. Those mechanisms have been elucidated in this experimental work, so as the relevance of the model when used in the drug discovery field and the analysis of the potential of the *P. falciparum* humanized model to be used as a powerful tool to elucidate different aspects of the biology of the malaria disease.

Materials and Methods

Mice

Female NODscid *β2 microglobulin*$^{-/-}$ mice (NOD.Cg-*Prkdc*^{scid} *B2m*^{tm1Unc}/J), abbreviated *β2,* deficient for the β2-microglobulin, are class I deficient, B and T cell deficient, C-5 deficient (*Hc*^{0}), and have low NK cells. They were obtained from Charles River Laboratories (L´Arbresle, France).

Female NODscidIL2Rγ^{null} mice (NOD.Cg-Prkdc^{scid} IL2rg^{tm1Wjl}/SzJ), abbreviated IL2, deficient for the γ chain of the IL-2 receptor. As a result, these mice lack mature T cells, B cells, or functional NK cells, and are deficient in cytokine signaling. These mice were raised and maintained in the Charles River Laboratories. IL2 mice were also obtained from Taconic (NOD.Cg-*Prkdc*^{scid} *Il2rg*^{tm1Sug}/JicTac) (Albany, NY, USA) these mice were abbreviated NOG.

Rag2$^{-/-}$ IL2 rg $^{-/-}$, H-2kb+ mice (B10;B6-*Rag2*^{tm1Fwa} *Il2rg*^{tm1Wjl}), abbreviated Rag2IL2 lack functional receptors for many cytokines, including: IL-2, IL-4, IL-7, IL-9, IL-15 and IL-21. As a consequence lymphocyte development is greatly compromised. The double knockout mice lack T, B and NK cells. These mice were obtained from Taconic (Albany New York, USA).

FRG® KO mice (Fah-/- Nod/Scid), abbreviated FRG, has a controllable lethal liver disease, which permits a highly efficent repopulation with human hepatocytes. This strain has multiple mutations that induce liver disease, T and B cells deficiency and defects in macrophage regulation and NK activity. These mice were obtained from Yecuris Inc. (Portland, Oregon, USA)

NOD-Rag1^{null} IL2rγ^{null} mice (NOD.Cg-*Rag1*^{tm1Mom} *Il2rg*^{tm1Wjl}/SzJ), abbreviated NRG, deficient for the γ chain of the IL-2 receptor, lack mature T cells, B cells, or functional NK cells and show more resistance to radiation than the IL2 mice. These mice were obtained from the Jackson Laboratories (Bar Harbour, Maine, USA).

Pathogen-free CD1 (Hsd:ICR) were obtained from Harlan Interfauna Iberica (Barcelona, Spain).

Animal research was performed in the Laboratory Animal Science acredited by AAALAC (Association for Assessment and Accreditation of Laboratory Animal Care) at the Diseases of Developing World (DDW), GlaxoSmithKline, sited in Tres Cantos (Madrid).

Immunodeficient mice were maintained in ventilated racks and cages, and were provided with autoclaved tap water and γ–irradiated pelleted diet *ad-libitum*.

All the experiments were ethically reviewed and approved by the DDW Ethical Committee on Animal Research and were conducted according to National legislation, European Directive 2010/63/EU and GlaxoSmithKline policy on the Care, Welfare and Treatment of Laboratory animals. IACUC numbers for studies are PROEX 110/14 and PROEX 110/17.

Parasite

Different *Plasmodium falciparum* strains were used along this study: $3D7^{0087/N9}$, $V1/S^{0176/N10}$, $NF54^{0230/N3}$, $K1^{0275/N3}$, $FCR3^{0325/N2}$, $D10^{0325/N2}$ and $\Delta D10^{0325/N3}$ for the infection of immunodeficent mice. These *P. falciparum* strains were adapted by the Therapeutic Efficacy Group (Malaria DPU-DDW Tres Cantos) to grow *in vivo* in non-myelodepleted immunodeficent mice engrafted with human erythrocytes [5, 63]. Mice were injected by intravenous route with $20x10^6$ parasitized erythrocytes in a final volume of 0.3 ml. *P. falciparum* strains were mantained by weekly passages from infected mice to engrafted mice with this quantity of inoculum. Original *P. falciparum* strains were obtained from MR4, accurate descriptions of the genetic background of these strains can be obtained at http://www.beiresources.org.

P. falciparum thawing

Cryopreserved parasites kept at -150ºC were thawed immediately by plunging the cryovials in a water bath at 37ºC for a few minutes and transfering whole vial content to a 50 ml sterile tube. Then, slowly add 1 volume (0.2 ml) of 12% NaCl solution dropwise via a 1 ml syringe attached to a 21G needle to 5 volumes (1 ml) of thawed sample and agitate continuosly. Next, slowly 10 ml of 1.6% NaCl solution is added for each ml of thawed sample shaking gently and continuosly to allow to mix both solutions. Finally, 10 ml of NaCl 0,9% and glucose 0,2% solution is added for each ml of thawed sample, while shaking gently and continuously the tube.

Solution obtained is centrifuged for 5 minutes at 520 g, at room temperature, high acceleration speed and medium deceleration speed. Then, supernatant is removed, and the pellet is resuspended with 10 ml of RPMI, by adding the solution drop by drop and shaking gently. Solution obtained is centrifuged 5 minutes at 520 rpm, room temperature, high acceleration speed and medium deceleration speed. Finally, supernatant is removed but leaving at least 100 µl of RPMI to keep the sample hydrated. Parasite thawed is kept at room temperature until its inoculation.

Reagents

Soluble Hypoxanthine 50X (Ref. 41065012), Dulbecco´s PBS (Ref. 14190250), and RPMI 1640 (Ref. 31870074) were purchased from Gibco (Paisley, U.K.). Hepes Buffer 1M (Ref.

H0887), human serum AB+ (Ref. H4522), 5(6)-carboxyfluorescein diacetate N-succinimidyl ester (CFSE) (Ref. 21888), DMSO (Ref. D2650), Hypoxanthine (Ref. H9377), ribonuclease A (Ref. R6513), fetal bovine serum (Ref. F6178), bovine serum albumin (Ref. A2153), ethylenediaminetetraacetic acid (EDTA) disodium salt solution (Ref. E1161), Triton X-100 (Ref. 93443), Lidocaine hydrochloride monohydrate (Ref. L5647), Tripan Blue (Ref. T8154), PKH26 kit (Ref. PKH26GL), glutaraldehyde 25% (Ref. G5882), D-glucose (Ref. G8270), $NaHCO_3$ (Ref. S5761) and NaCl (Ref. S7653) from Sigma-Aldrich (St. Louis, MO, USA). SYTO-16 (Ref. S7578) and YOYO-1 (Ref. Y3601) were from Molecular Probes (Leiden, The Netherlands). Biotin-X-NHS (Ref. 203188) and DMF (Ref. 103053) were obtained from Calbiochem (La Jolla, CA, USA). Giemsa staining solution (Ref. 1.09204.0100) was from Merck & Co., Inc. (Whitehouse Station, NJ, USA). TruCount™ tubes (Ref. 340334) were obtained from Becton Dickinson (Franklin Lakes, NJ, USA).

Antibodies

TER119-PE (Ref. 553673), CD45-PerCP (Ref. 557235), Streptavidin-PE (Ref. 554061), Rat anti-mouse CD45-APC (Ref. 9864), rat anti-mouse GR1-PerCP (Ref. 552093), rat anti-mouse F4/80-PE (Ref. 565410) were acquired from Pharmingen (San Diego, CA, USA).

Human blood

Incomplete donations or erythrocytes concentrates of malaria–negative donors were used, they were generously provided by the Spanish Red Cross Blood Bank in Madrid, Spain. Blood was stored at 4ºC and in the dark until its use.

Erythrocytes concentrates were washed twice with washing buffer (RPMI 1640 containing 25 mM Hepes Buffer and 0.1 mM hypoxanthine) at 860 g during 10 minutes at room temperature. Buffy coat was removed by aspiration, and erythrocytes were resuspended at 50% hematocrit (RPMI 1640, 25% inactivated human AB serum, 3.1 mM hypoxanthine). Finally, blood suspension was warmed at 37ºC for 10 minutes prior to intraperitoneal injection to immunodeficient mice.

The human biological samples were sourced ethically and their research use was in accordance with the terms of the informed consents.

Murine blood

Murine blood was obtained from IL2 donor mice. According with the standard procedures approved by DDW Ethical Committee on Animal Research, mice were euthanized with CO_2. Then, blood was collected by heart puncture using a heparinized 2 ml syringe with 25G needle. Blood was used within the 2 hours after extraction.

Mosquitoes

A colony of *Anopheles stephensi* mosquitoes was breeded in DDW Insectary facilities (Tres Cantos, Spain). Mosquitoes colony were mantained in climate controlled chambers at 27.5±1ºC: 10D photoperiod and 75±5% relative humidity (Panasonic MLR 352PE). Adults were kept in insect rearing cages (30x30x30 cm; Bugdorm®), and had *ad libitum* access to water solution containing 10% glucose + 1% Karo syrup until its use. Mosquitoes selected for experimentation were female from 3 to 5 days old. Female mosquitoes were selected and transferred to containers (30 mosquitoes each) and put in starvation at least 12 hours before the experimentation process.

Containers used for mosquitoes transfer were cylindrical and had a hole in the middle of the wall (covered with double elastic material) to introduce mosquitoes with an aspirator. The top of the cylindrical cup was covered with a double mesh to avoid mosquitoes escape.

Erythrocytes biotinylation

Biotinylation of intact mammalian red blood cells was performed by attachment to the amino groups by means of biotin N-hydrosuccinimide ester (biotin-X-NHS). Different concentrations of biotin-X-NHS were tested (100, 30 and 5 μg/ml) for the setting up of the erythrocytes biotin labeling protocol. 1 ml of erythrocytes was incubated for 15 or 30 minutes in the dark at room temperature. The concentration of 30 ug/ml incubated for 30 minutes was chosen as the most suitable condition for erythrocytes labeling which provides a clear discrimination between positive and negative cells measured by flow cytometry in terms of fluorescence intensity values.

For optimal labeling efficiency, 2 ml of human or mouse blood were washed twice with 10 ml of 0.9% saline solution and centrifuged at 860g for 10 minutes. Erythrocytes were labeled with biotin-X-NHS diluted in DMF (30 μl of DMF per every milligram of Biotin-X-NHS weighted). For every milliliter of washed erythrocytes it was used 1.5 ml of the Biotin-X-NHS solution adjusted at 30 μg/ml in saline solution. Erythrocytes were incubated with the biotin solution during 30 minutes in the dark at room temperature. Then, labeled erythrocytes were washed 4 times with saline solution, centrifuged at 650g during 5 minutes to remove the excess of biotin. Blood pellet obtained after centrifugation was resuspended in 0.3 ml of saline solution and injected to IL2 mice (10^9 of labeled erythrocytes by i.v. route per mouse).

5(6)-carboxyfluorescein diacetate N-succinimidyl ester (CFSE) erythrocytes labeling

Different concentrations of CFSE were used for erythrocytes labeling (2000, 500, 150, 50 and 10 μg/ml). 1 ml of erythrocytes were incubated at 15 or 30 minutes in the dark at room temperature. The concentration of 50 μg/ml and an incubation time of 30 minutes was set up as the most appropriated protocol for erythrocytes labeling, determined by flow cytometry as the condition with the higher difference in mean fluorescence intensity rate between positive and negative populations.

For the labeling protocol, 2 ml of human or mouse blood erythrocytes were washed twice with 0.9% saline solution, centrifuged at 860g during 10 minutes. 1 ml of washed erythrocytes were labeled with 1.5 ml of a 50 μg/ml CFSE saline solution dissolved in DMSO (30 μl of DMSO per every milligram of CFSE weighted). Erythrocytes were incubated with the CFSE solution during 30 minutes in the dark at room temperature. Then, labeled erythrocytes were washed 4 times with 0.9% saline solution, centrifuged at 650g during 5 minutes to eliminate the excess of CFSE. Finally, buffy coat was removed and blood pellet was resuspended in 0.3 ml of saline solution and injected to IL2 mice by *i.v.* route (10^9 of labeled erythrocytes per mouse).

Magnetic Separation

Sincronization of P. falciparum 3D7$^{0087/N9}$

Malaria parasite generates free haem upon catabolism of host haemoglobin during their intraerythrocytic growth cycle. The free haem molecules are polymerized into the biomineral beta-haematin (haemozoin). Haemozoin crystals are paramagnetic, and this property can be exploited for the purification of late stage parasites as the contain larger haemozoin crystals than early stage parasites and uninfected cells. Positive selection of trophozoites and schizonts from IL2 infected mice was performed using an AutoMACS cell separator (Miltenyi Biotec, Auburn, CA, USA).

Blood from mice infected with *P. falciparum* was collected by heart puncture into 15 ml conical tubes containing PBS supplemented with 1% Fetal Bovine Serum (FBS) to reach 5% hematocrit. The protocol was optimized for a cell number of $6x10^8$ parasitized erythrocytes using the separation program “depl025” on the AutoMACS cell separator. Positive fraction collected in port “pos1” (late stage parasites was centrifuged at 650 g for 5 minutes, buffy coat was removed and cellular pellet was resuspended in the residual liquid. Then, $100x10^6$ mature parasites were injected *i.v.* into engrafted IL2 mice. Samples

of 2 µl of peripheral blood were taken at different time points (Times: 0, 7, 14, 21, 28, 35, 42, 49, 56, 63, 70, 72, 96 and 120 hours after infection) for flow cytometry staining (TER119-PE/YOYO-1 protocol). In addition, 2 µl of mice blood was collected to do a blood smear for Giemsa staining.

Giemsa staining

Giemsa solution was prepared at 10% in buffered water, smears were stained during 20 minutes, dried and analyzed using light microscopy.

Erythrophagocytosis assay

Removal of senescent, damaged or diseased erythrocytes from the circulation *in vivo* occurs by a process known as erythrophagocytosis which takes place mainly in the spleen by macrophages, but also in the liver and the bone marrow. Assays for the assessment of *in vivo* and *in vitro* erythrophagocytosis have been used through this study.

In vivo

In order to address the *in vivo* erythrophagocytosis, spleens from IL2 mice were obtained at different time points. CD1 mice were used as positive control for the erythropagocytosis of human erythrocytes.

1 ml of human blood was labelled with CFSE (as previously described) and was injected by *i.v.* route in CD1 mice and IL2 mice in different phases of the model: engrafted, infected and in anaemia. Mice were euthanized with CO_2 at different time points and spleens were removed and processed.

Following sacrifice of each mouse, spleens were removed and placed into individual 15 ml conical tubes containing ice-cold RPMI. Spleen cells were obtained by homogenizing the organs. For the processing spleen organs were placed into a pot with a 200 mm pore diameter mesh on a petri dish containing ice-cold washing buffer (PBS + 10% FBS). All the process was done on ice to stop phagocytosis. Spleens received several transversal cuts to break the capsule and to allow the release of the spleen cells. Then, spleens were hit smothly on the pot with a 5 ml syringe piston and washing buffer were added drop by drop to allow the filtering of the cells through the 200 mm mesh to the petri dish. After the release of all the cells, they were transferred to a 15 ml conical tube and centrifuged during 5 minutes at 4ºC and at 360 g. The supernatant was removed and pellet resuspended, in 1 ml of distilled water and the tubes were shacked to allow the lysis of the erythrocytes present in the pellet. To stop the lysis, 12 ml of ice cold washing buffer was added and the tubes were mantained in ice for 2 minutes to favor the erythrocytes

membrane debris go to the bottom. The supernatant, avoiding the membrane debris, was transferred to another 15 ml conical tube, centrifuged 5 minutes at 4ºC and 360 g. The process was repeated for eliminating membrane debris, and finally cells were resuspended in 5 ml of washing buffer.

For staining procedure, cells concentration was adjusted to $2x10^6$ cells per mililiter using a Neubauer chamber, and a 1/10 dilution of Trypan Blue in 0.9% saline solution to discard dead cells. Aproximately $6x10^5$ cells were put in each well for staining and flow cytometry analysis.

In vitro

To study the *in vitro* erythrophagocytosis, cells from the peritoneum cavity of naïve IL2 mice were obtained.

Removal of peritoneum cells

According with the standard procedures approved by the ethical committee in GSK facilities, mice were euthanized with CO_2. Then, 5 ml of ice-cold PBS (with 2 mM EDTA) was injected into the peritoneal cavity using a 26G needle attached to a 2 ml syringe. The needle was slowly pushed into the peritoneum cavity being careful to not puncture any organs. After injection, the peritoneum was gently massaged during 2 minutes to dislodge any attached cells to the abdominal wall into the PBS solution. Then, a 25G needle, bevel up, attached to a 2 ml syringe was inserted in the peritoneum and the fluid was collected while moving the tip of the needle gently to avoid clogging by the fat tissue or other organs. As much fluid as possible is collected, and cell suspension is collected in a 15 ml conical tube kept on ice until use.

In vitro culture of peritoneum cells

Cells obtained from the peritoneum were centrifuged during 5 minutes at 4ºC and 360 g. Pellet was resuspended in 1.5 ml of 0.9% saline solution and 500 µl of the cell suspension was transferred to a well of a 6 well culture plate. Culture plate was coated with 2 ml of culture medium (RPMI + 10 mM Glutamine + 2% FBS) per well.

Erythrophagocytosis assay

After overnight incubation, the culture medium was removed and wells were washed 4 times using 1 ml of RPMI per well at room temperature. In each washing step, the plate was shaked slightly to allow the resuspension of cells that did not adhere to the plate. Then, 1 ml of RPMI was added to each well and the plate was observed under the microscope to check that macrophages were adhered. Finally, non-attached cells

resuspended in RPMI were removed and 2 ml of culture medium (RPMI + 10 mM Glutamine + 2% FBS) was added to each well.

To study the erythrophagocytosis *in vitro*, human erythrocytes were labelled using the membrane marker PKH26 dye (PKH26 Red Fluorescent Cell Linker Kit). Briefly, 500 µl of human erythrocytes (aproximately $3000x10^6$ of cells) were put in 1.5 ml of RPMI and were washed to remove the proteins from the preservation medium (included in the kit). Cells were centrifuged at room temperature during 5 minutes at 400 g. Washing step was repeated once. Then, supernatant was removed and human erythrocytes were divided in two parts each containing equal volume of packed erythrocytes and distributed in 15 ml conical tubes. Next, 1 ml of the diluent C from the kit was added to resuspend the pellet of cells. At the same time, PKH26 was prepared in diluent C at a concentration of 8 µM. Then, 1 ml of the PHK26 dilution was added to each tube and mixed with the erythrocytes and incubated during 3 minutes and 30 seconds at room temperature. Finally, the reaction was stopped by adding 2 ml of human serum and incubated during 1 minute at room temperature. Then, 4 ml of RPMI was added to the erythrocytes and were centrifuged during 10 minutes at room temperature at 400 g. Supernatant was removed and cells were put in a new 15 ml conical tube. Then, 10 ml of RPMI containing 10% of human serum was added and erythrocytes were centrifuged three times during 10 minutes, at room temperature at 400 g, and resuspended in 10 ml of RPMI containing 10% human serum.

Erythrocytes labelling was confirmed by flow cytometry after fixation with 10 µl of 0.25% glutaraldehyde.

In the 6-well culture plate, 50 µl of PKH26 labelled erythrocytes were added to one well (erythrophagocytosis). 50 µl of non-labelled erythrocytes were added to another well and (erythrophagocytosis negative control). The plate was shaked to allow an uniform distribution of the erythrocytes. Then, 150 µl of human serum was added to each well and the plate was incubated at least 2 hours in a ventilated incubator (37ºC and 5% CO_2).

After the incubation, erythrocytes that had not been phagocytosed by macrophages were eliminated with 4 washes steps with 1 ml of RPMI at room temperature. Erythrocytes binded to macrophages membrane but not internalized were lysed by adding 500 µl of a hypotonic buffer (155 mM NH_4Cl; 5.7 mM K_2HPO_4; 0.1 mM EDTA) and incubating 5 minutes. Lysis was stopped by the addition of 2 ml of PBS. Then, the plate was washed 3 times with 1 ml RPMI.

After the washing steps, macrophages were detached from the bottom of the well of the 6-well plate by the addition of 1 ml of lidocaine solution (4 mg/ml of lidocaine in PBS; 5 mM EDTA; 5% Ethanol). Macrophages were incubated 15 minutes on ice with constant and gentle pipetting. Then, macrophages were put in a 15 ml conical tube and were centrifuged 5 minutes at 4ªC and 400 g. The supernatant was removed and pellet was resuspended in the remaining liquid. Half of the volume was used for flow cytometry analysis.

Quantification of cells: Flow Cytometry method with Trucount™ tubes

For the measurement of cells concentration it was needed 30 µl of the sample resuspended in 300 µl of saline solution in TruCount™ tubes (these tubes contain a known number of fluorescent beads). Sample acquisition was done in FACSCalibur (two lasers: 488 nm and 640 nm) and LSRII (three laser: 488 nm, 640 nm and 355 nm) flow cytometers. At least 3000 events in beads region were acquired. Acquired samples were analyzed using the CellQuest Pro or FACSDiva program (Becton Dickinson), and the following equation was applied to obtain the absolute count of cells of interest in the sample:

Cells of interest/ml = (NCA/NBA) x (Beads/ml $_{\text{of acquisition tubes}}$)

NCA = Number of cells of interest acquired
NBA = Number of beads acquired
Beads = Number of fluorescent beads that contains the TruCount™ tube used.

The real concentration of cells of interest was calculated by multiplying the cells of interest concentration by the dilution factor used.

Flow cytometry

Calculation of the percentage of human erythrocytes in mice peripheral blood

2 µl of blood from the lateral tail vein of mice was collected in 0.1 ml of 0.9% saline solution containing 5 µM of SYTO-16 and 10 µg/ml of the mAb TER119-PE. Samples were incubated during 20 minutes in the dark at room temperature. Then, samples were fixed by adding 10 µl of 0.25% GTA during 6 minutes at 4ºC and in the dark. 30 µl of the sample were put in cytometry tubes containing 300 µl of saline solution, or in TruCount™ tubes when it was needed to determine the concentration of human erythrocytes per microlitre

of sample. Samples were acquired in FACSCalibur or LSRII flow cytometers by using the acquisition programs CellQuest or FACSDiva, respectively.

During acquisition, the percentage of human erythrocytes was considered those events included in the TER119-PE negative region related to the total cells region previously selected in a dot plot of 180º dispersed light (forward scatter-FSC) opposite to 90º dispersed light (side scatter-SSC). The percentage of murine erythrocytes was calculated as the TER119-PE positive events in a FL1/FL2 dot plot. Compensation of TER119-PE emission in FL-1 was done to precisely establish the region of murine erythrocytes. This region must be determined by comparison of blood samples from non-chimeric and chimeric IL2 mice by increasing compensation of TER119-PE emission in FL-1 until obtaining a defined region for mouse erythrocytes.

Calculation of the percentage of parasitemia of the human parasite P. falciparum in IL2 mice peripheral blood

2 µl of mice peripheral blood from the lateral tail vein was collected and stained in the same conditions described in the previous section. Then, 30 µl of samples were put in 300 µl of saline solution in cytometry or TruCount™ tubes. Samples were acquired in FACSCalibur of LSRII flow cytometers.

During acquisition, the percentage of infected human erythrocytes was considered those events negative for the mAb TER119-PE but positive for the DNA dye SYTO-16 related to the total cells region previously selected in a dot plot of 180º dispersed light (forward scatter-FSC) opposite to 90º dispersed light (side scatter-SSC). The percentage of infected erythrocytes was calculated as the SYTO-16 positive/TER119-PE negative events in a FL1/FL2 dot plot. Erythrocytes and leukocytes were gated in logarithmic forward/side dot plots. Green and red fluorescence were detected in the corresponding FL-1 and FL-2 photomultipliers through 530/30 or 585/42 band pass filter, respectively. The mean fluorescence channels in FL-1 and FL-2 were adjusted to equal values in the first decade of intensity in bivariate logarithmic scale dot plots with non-infected erythrocytes. Leukocytes were excluded during analysis in SSC/FL-1 dot plots because they show much amount of nucleic acids than infected erythrocytes.

Compensation of SYTO-16 emission in FL-2 and TER119-PE in FL-1 was achieved to set up accurately the region of infected events. This region must be defined by comparison of blood samples from uninfected-chimeric and infected-chimeric IL2 mice by increasing compensation of SYTO-16 emission in FL-2 until obtaining a defined region for infected events. Data analysis was performed by using the CellQuest Pro or FACSDiva software.

Detection of biotinylated erythrocytes in mice peripheral blood

2 µl of mice peripheral blood from the lateral tail vein was collected in 0.1 ml of 0.9% saline solution containing 0.5 µg/ml of Streptavidine-PE (SAV-PE). Samples were incubated during 20 minutes in the dark at room temperature. Then, samples were fixed by adding 10 µl of 0.25% GTA in saline solution and incubated 6 minutes in the dark at 4ºC. Finally, 30 µl of the samples were put in 300 µl of saline solution in TruCount™ tubes and at least 3000 events were acquired in "beads" region in the FACSCalibur flow cytometer. During acquisition, the percentage of biotinylated erythrocytes was considered those events included in the SAV-PE positive region related to the total cells region previously selected in a dot plot of 180º dispersed light (forward scatter-FSC) opposite to 90º dispersed light (side scatter-SSC). Data was analyzed by using the CellQuest Pro software. Acquisition with TruCount™ tubes was performed for the calculation of the concentration of biotinylated erythrocytes per microliter of blood.

Detection of CFSE-stained erythrocytes in mice peripheral blood

2 µl of blood from the lateral tail vein of mice was collected in 0.1 ml of 0.9% saline solution containing 10 µg/ml of the mAb CD45-PerCP. Samples were incubated in the dark at room temperature. Then, samples were fixed by adding 10 µl of 0.25% GTA in saline solution and were incubated 6 minutes in the dark at 4ºC. For the flow cytometry acquisition 30 µl of samples were put in 300 µl of saline solution in TruCount™ tubes. At least 3000 events in the region named "beads" were acquired in the FACSCalibur flow cytometer. During acquisition, the percentage of CFSE erythrocytes was considered those events included in the CFSE positive region related to the total cells region previously selected in a dot plot of 180º dispersed light (forward scatter-FSC) opposite to 90º dispersed light (side scatter-SSC). Data was analyzed by using the CellQuest Pro software. Acquisition with TruCount™ tubes was performed for the calculation of the concentration of biotinylated erythrocytes per microliter of blood.

Staining of P. falciparum infected erythrocytes using YOYO-1

To detect the parasitized human erythrocytes in mice peripheral blood using YOYO-1, a modification of the staining protocol for murine parasites was done. Briefly, 2 µl of blood from the lateral tail vein of IL2 infected mice was collected into 0.1 ml of saline solution containing 10 µg/ml mAb TER119-PE, in V-bottomed 96-well plates. Samples were incubated 20 minutes in the dark at room temperature. Then, cells were washed with saline solution and cellular pellets were resuspended with 0.2 ml of 0.025% (v/v) glutaraldehyde in saline solution with 1 mM EDTA to fix the cells for at least 16 hours at 4ºC in dark. Before staining, 40-50 µl of fixed cells were put into another clean V-bottomed

96-well plate and YOYO-1 staining was performed as described for murine parasites. Samples were acquired in FACScalibur flow cytometer. Erythrocytes and leukocytes were gated in logarithmic forward/side dot plots. The mean fluorescence channels in FL-1 and FL-2 were adjusted to equal values in the first decade of intensity in bivariate logarithmic scale dot plots with non-infected human erythrocytes. Leukocytes were excluded during analysis in SSC/FL-1 dot plots because they show much higher amount of nucleic acids than parasitized erythrocytes. The voltage photomultipliers was set up using non infected blood from control mice stained with TER119-PE and YOYO-1 as described above. Samples were analyzed using CellQuest-Pro software (BD), and compensation of YOYO-1 emission was achieved as described for the SYTO-16/TER119-PE staining.

Study of in vivo erythrophagocytosis

For the flow cytometry analysis, $6x10^5$ cells from spleen were put in each well. Cells were washed with ice cold PBS (5 minutes, 4ºC and 360 g). Pellet was resuspendended in 35 µl of staining medium (PBS + 2% FCS + 0.1 % Sodium Azide) + 10 µl rat serum, and incubated 15 minutes in the dark at 4ºC. Then, add 5 µl of the monoclonal antibodies previously prepared at 100 µg/ml (CD45-APC, GR1-PerCP or F4/80-PE), and incubate 30 minutes in the dark at 4ºC. Finally, wash twice by adding 150 µl ice cold PBS (5 minutes, 4ºC and 360 g). Resuspend the pellet in 200 µl of 1% Paraformaldehyde solution and store at 4ºC until acquisition. All the staining procedure was done on ice.

Samples were acquired using a LSRII Flow cytometer and FACSDiva software. During acquisition, leukocytes were considered those events included in the CD45-APC positive region related to the total cells region previously selected in a dot plot in a linear scale of 180º dispersed light (forward-FSC) opposite to 90º dispersed light (side-SSC). The erythrophagocytosis was considered those events double positive for CD45-APC and CFSE (FL1 detector) in a FL1/FL4 dot plot. No compensation was needed to estabish the erythrophagocytosis population. To identify the type of leukocyte that was involved in the erythrophagocytosis each monoclonal antibody used in each detector (F4/80 in FL2 or GR1 in FL3) was ploted with the FL1 detector (CFSE).

Study of in vitro erythrophagocytosis

For the flow cytometry analysis, half of the cells obtained from mice peritoneum cavity and incubated with PKH26 labelled human erythrocytes (see *in vitro* erythrophagocytosis section), were put in a well of a 96 wells plate in 100 µl of 0.9% saline solution The plate was centrifuged 5 minutes at 4ªC and 400 g. The supernatant was removed and cells were resuspended in 45 µl of saline solution + 5 µl of rat anti-mouse CD45-APC monoclonal

antibody (prepared at 100 μg/ml). Cells were incubated with monoclonal antibody during 20 minutes at 4ºC. Then, cells were washed to eliminate the excess of antibody and resuspended in 200 μl of 1% Paraformaldehyde solution and store at 4ºC until acquisition.

Samples were acquired using a LSRII Flow cytometer and FACSDiva software. During acquisition, leukocytes were considered those events included in the CD45-APC positive region related to the total cells region previously selected in a dot plot in a linear scale of 180º dispersed light (forward-FSC) opposite to 90º dispersed light (side-SSC). The erythrophagocytosis was considered those events double positive for CD45-APC and PKH26 (FL2 detector) in a FL2/FL4 dot plot. No compensation was needed to estabish the erythrophagocytosis population.

Measurement of inflammation cytokines

Mouse inflammation cytokines IL-6, IL-10, MCP-1, IFN-γ, TNF and IL-12p70 were quantified in IL2 mice using the CBA kit from Becton Dickinson (Ref. 552364). Briefly, 50 μl of mice plasma was mixed with 50 μl of the mixed Capture Beads, which contained capture beads for each cytokine to be detected and was prepared following the manufacturer´s instructions. Then, 50 μl of the Mouse Inflammation PE detection reagent was added to the samples and were incubated 2 hours in the dark at room temperature.

For the quantification of the cytokines a standard curve was done by serial 1:2 dilutions of the Inflammation Standards using the assay diluent provided in the kit.

Samples were acquired in a FACSCalibur flow cytometer. The setup process before sample acquisition was performed following manufacter´s instructions. Samples were acquired at medium speed and at least 8000 events in stopping gate. Cytokines were detected in a FL2/FL3 dot plot. The intensity of fluorescence in the FL2 detector indicates the quantity of each cytokine present in mice plasma, while the FL3 detector identify each cytokine depending on the fluorescence intensity of the capture beads provided in the kit. Once acquired, samples were analyzed using the FCAP Array™ software (Becton Dickinson).

Measurement of erythrocytes half life and distribution volume

Labelled erythrocytes with Biotin or CFSE were injected in IL2 mice by *i.v.* route ($1x10^9$ labelled erythrocytes). Then, samples of mice peripheral blood were taken at different time points and were stained with SAV-PE or CD45-PerCP (as described before). Samples for quantification of labelled erythrocytes were taken in regular periods of time until labelled erythrocytes were undetectable by flow cytometry.

To determine the volume of distribution (abbreviated Vd) and erythrocytes half life ($t_{1/2}$), a monocompartimental kinetic model was applied. The monocompartment model represents the simplest mathematical model of pharmacokinetics and was suitable for this study. Erythrocytes do not leave the blood stream except transiently during passage through hepatic sinuses and the interstitium in the splenic follicles. The delivery of erythrocytes after *i.v.* injection is fast and uniform.

The volume of distribution in given by the following equation.

$$\mathbf{V_d = C_i/Y}$$

V_d = Distribution volume.

C_i = Initial labelled erythrocytes concentration.

Y = Erythrocyte concentration at time t.

For the calculation of the biological half life ($t_{1/2}$) of erythrocytes, the formula used depends on the clearance kinetics showed by injected erythrocytes.

When the concentration of labeled erythrocytes decreases with the time in an exponential way, erythrocytes clearance fit to a one-phase exponential decay function. In this case, the formulas applied to do the calculations are the following one:

$$\mathbf{Y = a_0 \times e^{-kt} + c}$$

Y = Erythrocytes concentration at time t.

a_0 = Labelled erythrocytes concentration at time 0.

k = Clearance constant.

t = Time.

c = Constant (limit of detection of the quantification method).

$$\mathbf{t_{1/2} = 0.693/k}$$

$t_{1/2}$ = Half life of labelled erythrocytes.

k = Clearance constant.

If the erythrocytes clearance fit to a lineal regression function, distribution volume and half life were calculated using the following formulas:

$$\mathbf{Y = b + mt}$$

Y = Labelled erythrocytes concentration at time t.

b = Labelled erythrocytes concentration at time 0.

m = Slope.

t = time.

The formula applied for the calculation of the distribution volume was the same that in the case of one-phase exponential decay.

$t_{1/2}$ = -b/2m

$t_{1/2}$ = Half life of labelled erythrocytes.

b = Labelled erythrocytes concentration at time 0.

m = Slope.

Compound formulation

Formulations can profundly impact drug release, absorption and metabolism, which influence the resulting pharmacokinetic profile and the associated pharmacodynamic response. Physicochemical properties of compounds determine the vehicle formulations. Compounds were orally administered and most of them were formulated three days prior to the administration.

Atovaquone, GSK932121, Proguanil, Sulfadoxine and Lumefantrine were prepared in 1% Methylcellulose; Primaquine, Chloroquine, Amodiaquine and Quinine were dissolved in 0.9% saline solution; Mefloquine was prepared in a distilled water solution containing 0.2% Methylcellulose and 0.4% Tween-80; Pyrimethamine formulation was prepared using a dionised water solution with 0.5% Hydroxypropylethyl cellulose, 0.4% Tween-80 and 0.5% benzyl alcohol; Dihydroartemisinin was formulated in 5% DMSO and 20% Captisol distilled water solution; Piperaquine was dissolved in MiliQ water and Artesunate was daily prepared in a MiliQ water solution containing 3% Tween-80 and 7% Ethanol and pH 7. All compounds were administered orally at a dose volume of 20 ml/kg, except Artesunate and Dihydroartemisinin that were administered at 10 ml/kg. Compounds were obtained from the GSK Compound Management Database.

Pharmacokinetics analysis

After oral dosing, blood samples (20 µl) were collected from the lateral tail vein of mice at different time points, 0.5, 2, 4, 6, 8 and 23 hours post dosing. All the blood samples were diluted in 20 µl of MiliQ water and stored at -80ºC until analysis.

Mice blood samples were analyzed for each compound after protein precipitation and liquid/liquid extraction, the samples were assayed by LC/MS using ESI in Q1 M+1 mode conditions by selected inon monitoring in an API 2000 mass spectrometer (Applied Biosystems Sciex, Foster City, CA) coupled to a HPLC chromatograph (Agilent HP1100 Series , Agilent Technologies Spain). Quantification was conducted by comparison to

calibration curves. Blood concentrations versus time data were analyzed by non-compartemental analysis (NCA) methods using WinNonlin® Professional Version 6.3 (Pharsight Corporation, Mountain View, CA) and GraphPad Prism 6.0 (GraphPad Software).

Gametocyte production

P. falciparum NF54 asexual-stage culture was performed as described by Trager and Jensen [145]. Cultures synchronized at the ring stage were used to start gametocyte cultures (day 0) at 1% parasitemia and 4% hematocrit in 200 mL final volume. Complete culture medium (RPMI 1640 supplemented with 25 mM HEPES, 50 µg/ml hypoxanthine, 2 g/liter $NaHCO_3$ and 10% pooled human male type A+ serum) was totally replaced daily for 14 days without fresh erythrocyte addition. To ensure a stable temperature at 37°C, which is crucial for gametocyte production and maturation, pre-warmed medium and a slide warmer were used. Sexual-stage development was monitored microscopically by Giemsa-stained thin blood smears, at day 7 asexual stages and stage I to III gametocytes were detected and at day 14 mostly gametocytes present were at stage IV and V.

Exflagellation assay

Engrafted IL2 mice were infected with *Plasmodium falciparum* NF54 strains. Parasite strains were thawed using the thawing method set up for humanized mice blood (described above). $20x10^6$ infected erythrocytes were injected i.v. in IL2 chimeric mice. Thawing was done two weeks before mosquito feeding. At least 1 *in vivo* passage of *P. falciparum* erythrocytic stages was done from infected mice to engrafted mice by i.v. route with $20x10^6$ infected erythrocytes. From day 3 until day 30 after infection with the *P. falciparum* strain, daily samples from peripheral blood of *P. falciparum* NF54 infected mice were taken. 2 µl of blood was put in a 0.5 ml eppendorf containing 10 µl of ookynete medium (RPMI medium containing hypoxanthine, bicarbonate and xanthurenic acid), after 10 minutes of incubation in the dark at room temperature, exflagellation is checked under a light microscope using the 100X objective. When exflagellation occurs, the movement of the male gamete is easily detected.

Mice anesthesia

Anesthetic procedure is performed only by trained personnel. Mice are anesthetized with 150 µl of a solution of Ketamine/Xylazine (80 mg/kg and 15 mg/kg, respectively) by intraperitoneal route. These mice are injected intraperitoneal with 3 mg/kg Midazolam 15 minutes before injecting anesthetics to induce a deep sedation state that lasts at least 40 minutes. A tear solution is applied to mice eyes to avoid dryness during the anesthesia.

Mice are covered with a thermal blanket to avoid the loss of temperature during mosquitoes feeding.

Mosquitoes feeding assay

Female mosquitoes of Day 3 to 5 days old are put in starvation at least 12 hours before the feeding. Then, mice ventral zone is exposed to the mesh of the mosquitoes´ containers for the feeding. Mosquitoes are fed with anesthetized mice during 20 minutes in a dark chamber at 26.5±1ºC of temperature. After feeding, mosquitoes are put in an incubator (12 hours of dark/light cycle, 26.5±1ºC and 75-80% humidity) and each mouse returned to its cage unde red warm light until their recovery from anesthesia.

Mosquitoes are fed with soaked cotton with 10% glucose and 1% Karo syrup, which is put in the top of the mesh and is changed every day until the mosquitoes dissection takes place. Mosquitoes are not manipulated during the 7 days of incubation.

Mosquitoes dissection

At day 7 or 10 after mosquitoes were fed with mice, mosquitoes´ containers were taken out from the incubator and put in a CO_2 chamber, with the CO_2 flux at maximum level, during 1 minute to induce an anesthesia. Then, mosquitoes´ cups were taken out from the chamber. After checking that all mosquitoes were down in the bottom of the container and that there were no mosquitoes in the hole of the container, ethanol 70% is poured through the hole until all mosquitoes were immersed. After 1 minute, the mesh of the container was cut with a scalpel and the mosquitoes were taken out one by one using entomological forceps for catching the mosquitoes by the proboscis. Quickly, mosquitoes were transferred to a petri dish on humidified paper filter. Then, mosquitoes´ heads were cut off with the scalpel. Mosquitoes bodies were transferred to another petri dish with filter paper soaked in distilled water. Finally, the petri dish was sealed with parafilm and it was placed into the fridge at 4ªC until dissection.

Midguts were obtained from mosquitoes under a stereo microsope. Mosquitoes bodies were removed from the fridge and put in a drop of PBS 1X on a slide. Under the scope vision mosquitoes were dissected by holding firmly the mosquito by the thorax with one forceps and by the terminalia (approximately the 7th segment) with a second pair of forceps. Then, gently the terminalia was pulled away from the abdomen. The midgut should be detached to the final abdomen, and the ovaries should stay in the abdomen. To obtain the midgut, the last abdominal segment and the malpigian tubules were removed by entomological forceps.

Picture from Anopheles method MR4

Oocyst count

Anopheles stephensi midguts containing *P. falciparum* oocysts were stained with 0.1% mercurochrome solution for 15 minutes and then were placed separately in the wells of a 12-well glass slide containing one drop of mercurochrome solution. The slide is covered with a cover slip and midguts can be observed under the microscope using the 10X objective which allows the oocysts count.

Statistics

Sample sizes for comparative experiments were calculated to detect a decrease of 50% in the mean of control group. Typically, the level of Type I error α was set at 0.05, meaning that we are 95% confident and a power of 80% (Type II error β at 0.2). For the comparison of the kinetics curves, the area under the curve (AUC) was calculated to take into account the temporal dimension of data. The variables weight, percentage of chimerism in pheripheral blood and the percentage of parasitemia against time ($AUC_{0\rightarrow t}$) followed a normal distribution. The comparision among the averages of each experimental group was analyzed using Student´s *t* test, an Analysis of Variances (ANOVA) followed by post hoc test such as Dunnett´s, Tukey´s or Games-Howell´s post test, depending on the experiment. The homogeneity of the variance was calculated with the Levene´s test. The variability of the data was expressed as the standard deviation (SD) or as the standard error mean (SEM). The statistical analysis was performed using the GraphPad 6.0 software for Windows. Probability values larger than 0.05 were considered non-significant.

Results

Characterization of the GSK*Pf*Hu mouse model

Engraftment of immunodeficent IL2 mice with human eythrocytes

P. falciparum parasite infects almost exclusively human erythrocytes. The most successful method for generating a human erythroid chimeric mouse is through regular infusions of humans red blood cells. Immunodeficent mice have emerged as an enabling technology for studying human malaria. In the non-myelodepleted model with β2 mice previously described [5], the engraftment of mice was achieved by the daily intraperitoneal injections of 1 ml of human erythrocytes at 50% hematocrit (RPMI 1640, 25% decomplemented AB human serum, 3.1 mM hypoxanthine). The β2 mouse strain retains residuel NK cells activity and shows a high incidence of developing early thymic lymphomas, which dramatically diminish their life span. These characteristics are a serious problem for adressing long term studies. However, the generation of a new immunodeficent mice which overcome the β2 deficiencies, open an new possibility for the improvement of the GSK*Pf*Hu mouse model.

The ability of IL2 mice to be engrafted with human red blood cells was compared with the β2 mice for the improvement of the murine model of *P. falciparum* malaria. Both mice strains received daily intraperitoneal injections of 1 ml of human blood at 50% hematocrit. As shown in figure 11 the kinetics of engraftment of IL2 mice fit to a one-phase exponential association function (R^2=0.92), the time of engraftment required to obtain at least 40-50% of human erythrocytes in mice peripheral blood was 6.8 ± 0.1 days (n=80 mice). These data were similar to that found in the engraftment of β2 (R^2=0.76), the time of engraftment needed to obtain 40-50% of human erythrocytes in mice peripheral blood was 6.9 ± 0.4 days (n=142 mice), also shown in figure 11.

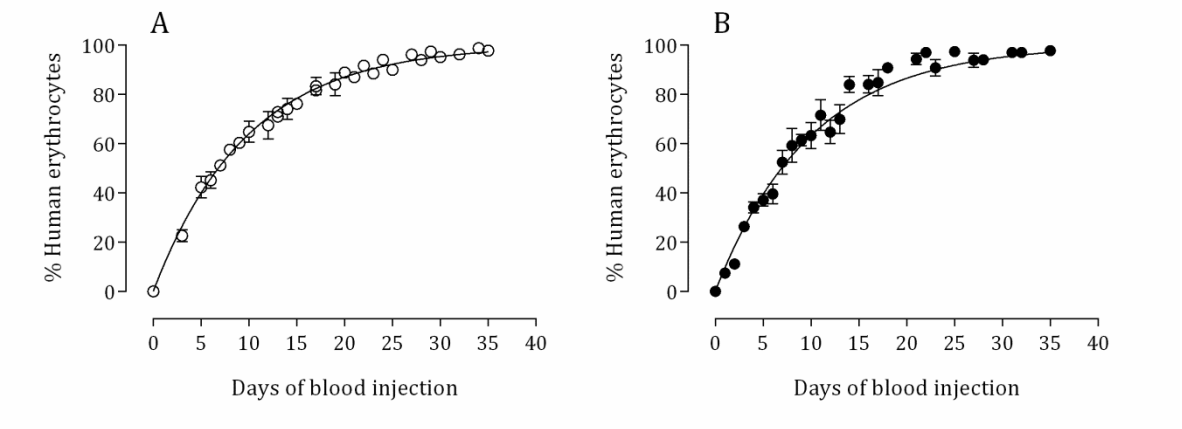

Figure 11. Comparison of engraftment kinetics of human erythrocytes in IL2 and β2 mice (A and B, repectively). The percentage of human erythrocytes was calculated by flow cytometry as TER119-PE- events. Data are the mean percentage ± standard error of the mean of 142 β2 mice and 80 IL2 mice. Only errors bars that extend beyond the symbols are shown.

Consequently, the IL2 mice can be engrafted with human erythrocytes by intraperitoneal daily injections of 1 ml of human erythrocytes (50% hematocrit). Nevertheless, to reach a 50% of human erythrocytes in mice peripheral blood it was needed around 10 days of daily blood injections, which means around 5 ml of human erythrocytes per mouse to be engrafted.

Infection of engrafted IL2 mice with the human parasite P. falciparum 3D7 strain

The susceptibility of the IL2 mice engrafted with human erythrocytes to infection by competent *P. falciparum* 3D7 was also compared to the β2 mice, which was shown to support blood-stage infection of *P. falciparum* but at low levels, less than 2% [5]. Two cohorts of engrafted IL2 or β2 mice (10 mice/cohort) were infected intravenously with $20x10^6$ parasitized erythrocytes obtained from donors mice infected with a *P. falciparum* 3D7 strain, adapted to grow *in vivo* in engrafted mice [5]. Mice were infected after 10 days of receiving daily intraperitoneal injections of human blood (50% hematocrit).

Parasite growth in both mice strains was monitored during 52 days. The parasite growth peak was obtained around day 7 after parasite infection, in IL2 mice this peak was around 12-14% of parasitemia, which means 10-fold higher than that found in β2 mice (figure 12).

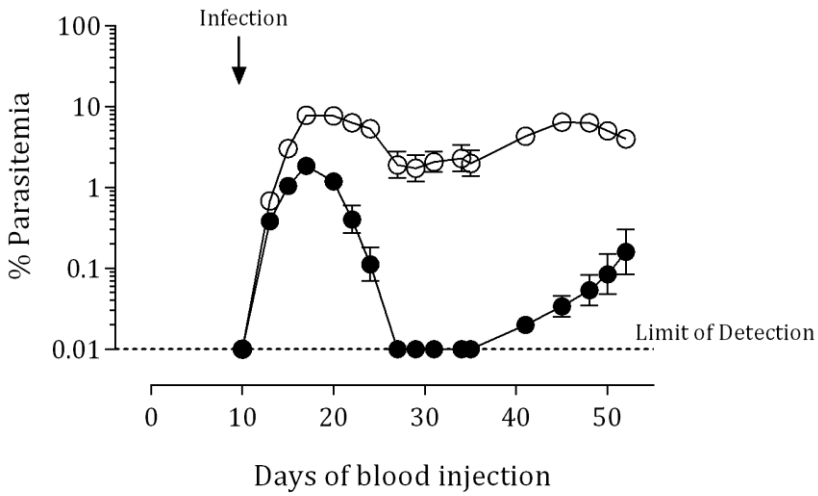

Figure 12. Parasite growth after infection by i.v. with 20x10⁶ infected hE with P. falciparum (Pf3D7$^{0087/N9}$ strain) in IL2 (open circles) and β2 (close circles) mice. All mice were injected i.p. with hE daily from day 0 to day 52. Data are the mean ± standard error mean of five mice per data point. Only errors bars that extend beyond the symbols are shown. The percentage of parasitemia was calculated by flow cytometry as SYTO-16⁺ and TER119-PE⁻ population.

Murine and human erythrocytes dynamics were also studied during the parasite growth. The erythrocytes dynamics were similar in engrafted IL2 and β2 mice, as shown in figure 13A and 13B. Both mice strains showed a selective clearance of human erythrocytes after the parasite reach the maximum peak of parasitemia. Concurrent to this human erythrocytes clearance, an increase in the percentage of murine erythrocytes was observed. During the clearance of human erythrocytes, parasite cannot be detected by flow cytometry (limit of detection of the technique 0.01%) in β2 mice, while in IL2 mice, parasite growth can be detected in spite of a reduction in the percentage of human erythrocytes.

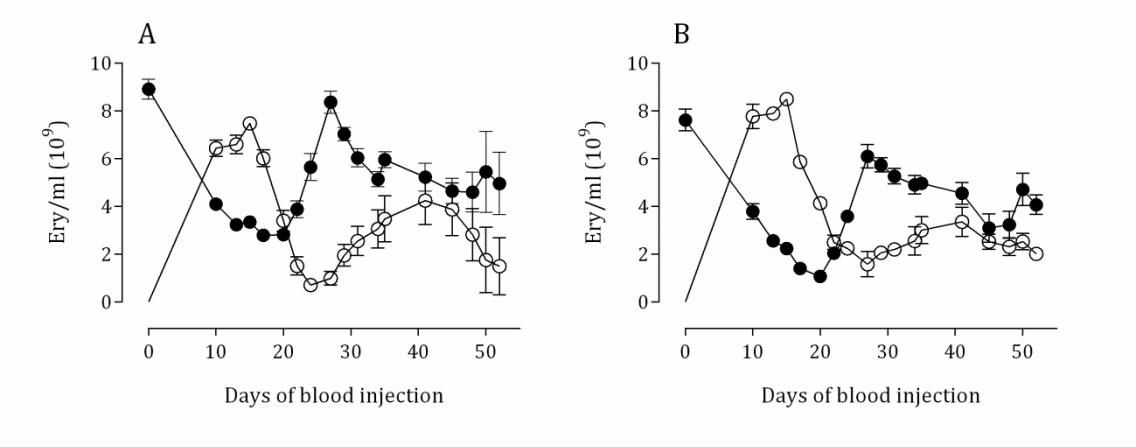

Figure 13. Dynamics of mouse (close circle) and human erythrocytes (open circle) from day 0 to day 52 of β2 (A) and IL2 (B) mice. Mice received daily i.p. injection of hE throughout the experiment and were infected by i.v. route, at day 10 of blood injection, with 20x10⁶ infected hE. Data are the mean ± standard error mean of five mice per data point. Only errors bars that extend beyond the symbols are shown. The quantification of mouse (TER119-PE⁺ events) and human erythrocytes (TER119-PE⁻ events) was done by flow cytometry, using Trucount™ tubes.

These results indicate that the IL2 mice strain was more susceptible to infection by the *P. falciparum* competent strain than β2 mice. In addition, the results suggest that the massive

destruction of human erythrocytes was provoked by the *P. falciparum* infection that is probably triggering a massive immune response in the immunodeficent mice. We have denominated this phase of the parasite growth as anaemia phase.

At this point, the *P. falciparum* murine model developed in this work with the IL2 mice receive the name of GSK*Pf*Hu mouse model and can be divided in three different phases: i) Engraftment, in which IL2 mice were injected i.p. daily with 1 ml of human erythrocytes (50% hematocrit), ii) Infection, were the parasite grows exponentially, and iii) Anaemia, in this phase there was a massive destruction of human erythrocytes as the parasite growth decreases 10-fold compared with the peak of parasitemia reached at day 17.

P. falciparum lyfe cycle in IL2 mice

Once the susceptibility of the IL2 mice strain to the *P. falciparum* (Pf3D7$^{0087/N9}$) infection has been tested, the erythrocytic parasite life cycle was studied in these mice. Within the parasite life cycle a parasite goes through several phases of development after the infectionof a red blood cell. The first phase is the ring stage, in which the parasite begins to metabolize hemoglobin. The next phase is the trophozoite stage, during which the parasite metabolized most of the hemoglobin, gets larger, and prepares to produce more parasites. Finally, the parasite divides asexually to form a multinucleated schizont. At the end of the cycle, the red blood cell bursts open and the parasites are dispersed to infect more red blood cells.

The *P. falciparum* parasite growth in the mouse model is asynchronous in which all the stages mentioned before are present at the same time. To study the length of the parasite life cycle, first this parasite has to be synchronized to start the infection from the same parasite stage and do the follow up at different time points. To attempt this issue, the parasite was synchronized in mature stages (late throphozoites and schizonts) by magnetic separation, mature stages were observed to have a shorter synchronic window than young stages (data not shown). Then, 100x10^6 infected erythrocytes in mature stages were injected by i.v. route to engrafted IL2 mice and parasite growth was monitored by flow cytometry and microscopy.

The parasite growth by flow cytometry was assessed using the TER119-PE/YOYO-1 staining method (see Material and Methods). The YOYO-1 DNA staining was selected for this study instead of SYTO-16, because YOYO-1 is performed with fixed cells and the staining procedure can be done within two weeks. On the contrary, SYTO-16 staining has to be performed at the moment with life cells. For logistic reasons, some samples points were during the night, YOYO-1 was the best option for this type of experiment.

The flow cytometry strategy used for the analysis of the different development stages of the *P. falciparum* parasite is shown in figure 14. The DNA quantity of young stages of parasite (rings and young trophozoites), is less than in mature stages (late throphozoites and schizonts). For this reason, young stages of parasite stay in a low YOYO-1 fluorescence intensity. In the process of maturation, the parasite structure acquires complexity and the DNA quantity increases, for this reason mature stages of parasite express high YOYO-1 fluorescence and autofluorescence measured in TER119-PE axis (corresponding to FL-2 photomultiplier) [148].

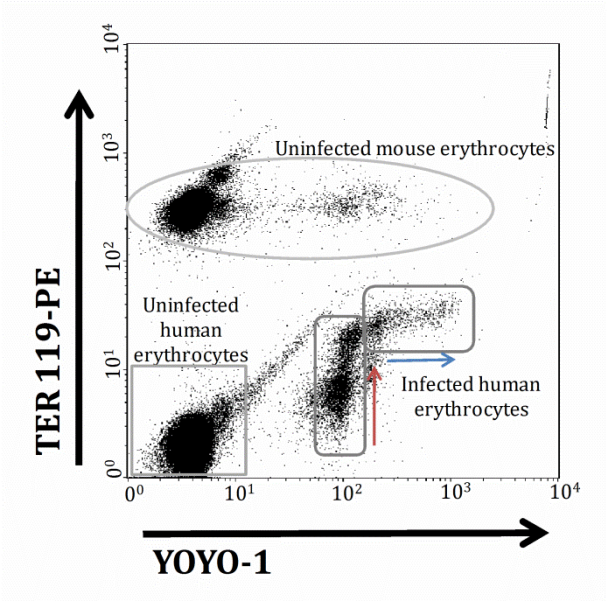

Figure 14. Flow cytometry analysis of peripheral blood samples from IL2 mice infected with P. falciparum. Red arrow mean mature stages and blue arrow mean young stages. The Dot plot shows two types of erythrocytes: mouse and human. Only human erythrocytes are infected.

To study the whole erythrocytic cycle of *P. falciparum,* samples from infected mice were obtained at different time points (every 7 hours) during 72 hours after infection with mature stages. The most representative dot plots graphs for one parasite cycle from flow cytometry analysis and microscopy images are shown in figure 15. The study of these images reveals that from 42 to 49 hours after the infection with mature stages, infected mice show *de novo* mature stages in their peripheral blood. In addition, young stages of parasite were the longer parasitic phase in the erythrocytic life cycle. These young stages remain in peripheral blood from 7 hours to 35 hours after infection, which means 28 hours of parasite development from young rings to late trophozoites. Therefore, the parasite only needs 14 hours for the maturation from late trophozoites to schizonts and

for the invasion of new erythrocytes generating new young rings. Of note, parasite synchronizity was mantained within the 72 hours.

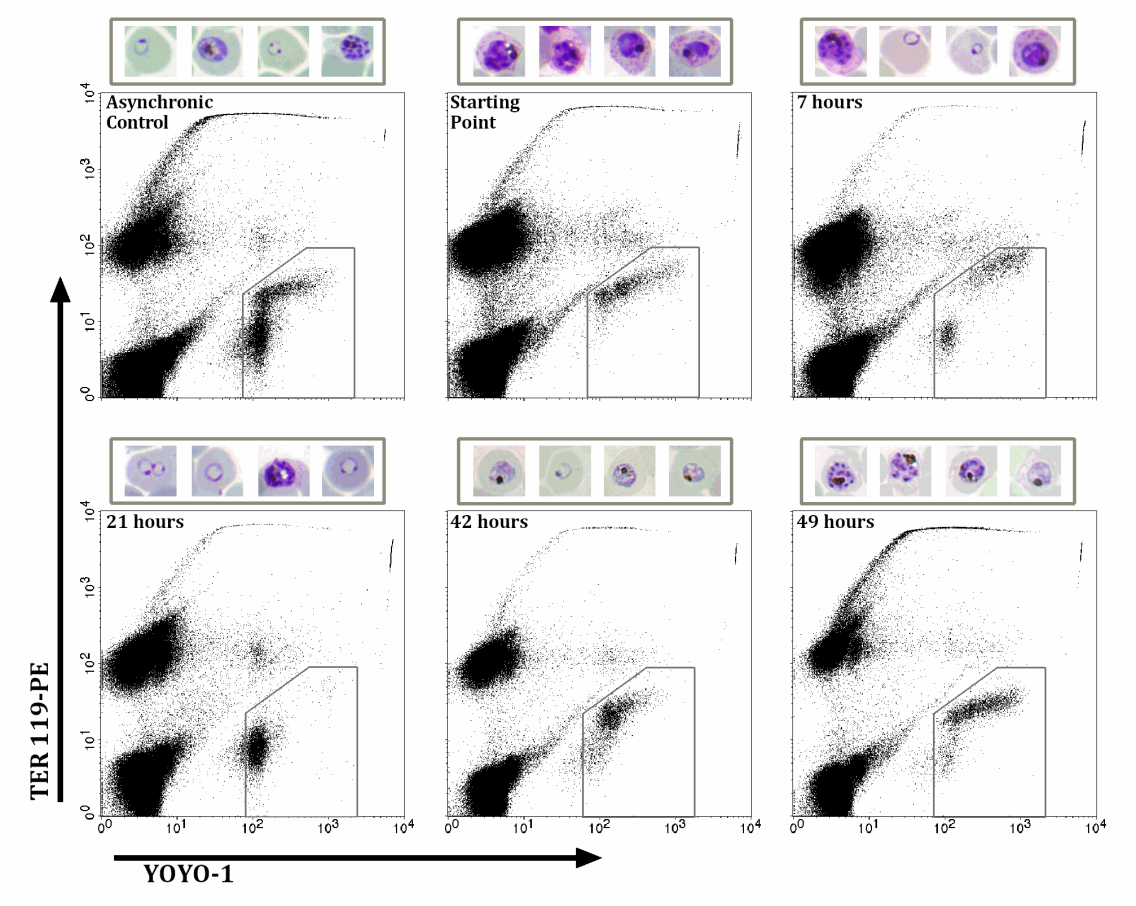

Figure 15. P. falciparum erythrocytic life cycle after infection with mature stages. Dot plots show IL2 infected mouse (one representative mouse) peripheral blood stained with TER119-PE and YOYO-1 at different timepoints (Time 0, 7, 21, 42 and 49 hours after infection). Microscopy photographies are examples of parasites found in Giemsa smears analysis of the same mouse and at the same timepoint than the dot plots.

In conclusion, these results reveal that the *P. falciparum* Pf3D7$^{0087/N9}$ strain shows an erythrocytic life cycle of 49 hours in IL2 engrafted mice. The length of the blood-stage life cycle was similar to that found in the natural *P. falciparum* infection in human beings.

Study of erythrokinetics of human and mouse eythrocytes in the GSKPfHu mouse model

The GSK*Pf*Hu mouse model has been developed as a chimera in which human erythrocytes can replace totally the host erythrocytes (it can be obtained engraftment of 98%), this means that human erythrocytes are acepted by the mouse host and are used as own. At this point, it is important to understand the process of the engrafment and the absence or

presence of rejection of the xenotransplant with human erythrocytes during the engraftment phase. In addition, it is also interesting to know the dynamics of erythrocytes during the infection and during the anaemia phase, where human erythrocytes are massively cleared.

To study the human and mouse erythrokinetics in the GSK*Pf*Hu mouse model. Erythrocytes were labelled using CFSE or Biotin to grant the detection of the erythrocytes in mice peripheral blood. Human and mouse erythrocytes were labelled using both dyes interchangeably. Then, labelled human and mouse erythrocytes were injected by i.v. route in IL2 mice in the different phases of the murine model: i) engraftment, ii) infection and iii) anaemia. In addition, labelled erythrocytes were also injected by i.v. route in naïve IL2 mice to study the erythrokinetics.

After the i.v. injection of 1500x10^6 labelled erythrocytes, samples of mice peripheral blood were taken at different timepoints until labelled erythrocytes were undetetectable. The detection of labelled erythrocytes was achieved by flow cytometry as shown in figure 16. The quantification of tagged erythrocytes in each phase of the murine model was calculated using the TruCount™ tubes formula.

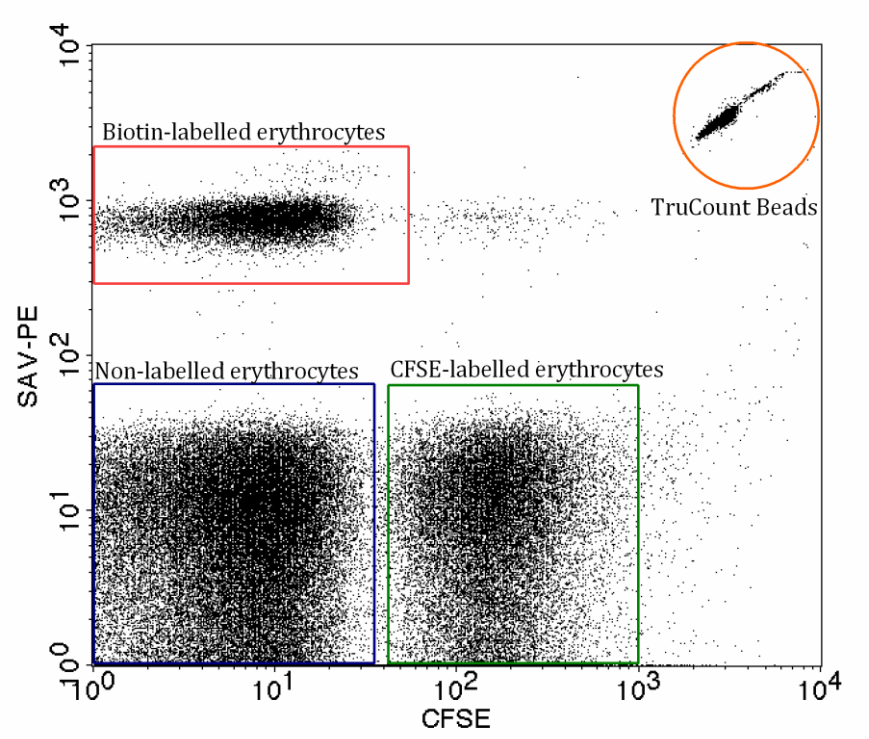

Figure 16. Flow cytometry dot plot of labelled erythrocytes detection in mice peripheral blood. Red rectangle includes erythrocytes marked with Biotin and stained with SAV-PE. Green square contains erythrocytes tagged with CFSE. Blue square harbours non-labelled

erythrocytes. Orange region includes the fluorescence beads from the Trucount™ tubes used for the quantification of the erythrocytes.

Kinetics of human and mouse erythrocytes obtained in naïve mice were different. The kinetic of hE in naïve mice fit to a one-phase exponential decay function (R^2=0.90), as shown in figure 17A. As a result, clearance of human erythrocytes was very fast, they were completely eliminated in less than 48 hours. These human erythrocytes showed a half life of 5.42 ± 1.98 hours (n=5) in naïve mice peripheral blood. Conversely, mouse erythrocytes kinetic adjust to a lineal regression function (R^2=0.77), as shown in figure 17B. Half life calculated for mouse erythrocytes in naïve mice was 363.59 ± 27.83 hours (n=5). These results of mouse erythrocytes half life are included in the normal values obtained for healthy mice (from 12 to 24 days), these data confirms that the labelling method do not affect the erythrocytes morphology and phisiology.

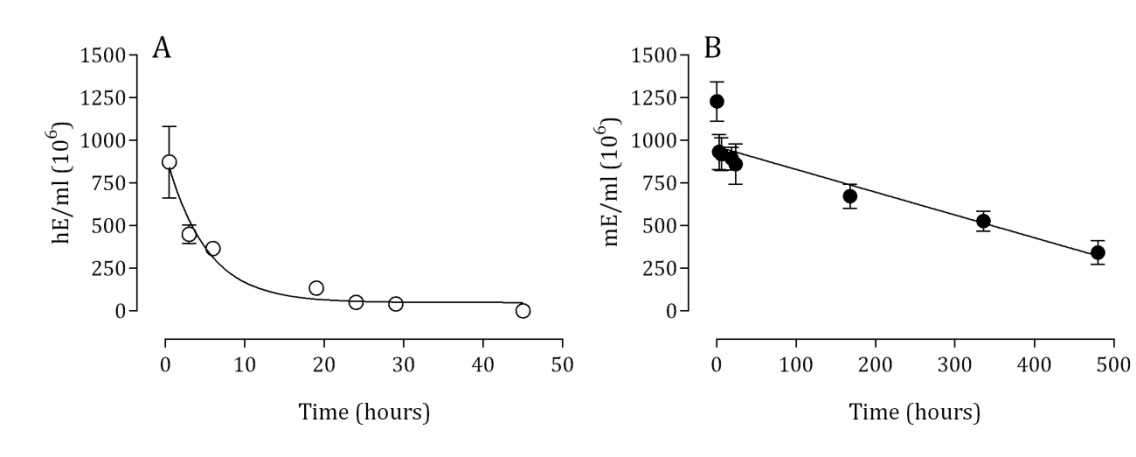

Figure 17. Kinetics of human and mouse erythrocytes (A and B, respectively) in naïve IL2 mice. Data are the mean ± SD of five mice per data point. Only errors bars that extend beyond the symbols are shown. Note that the X axis are different in each graph. The quantification of human and mouse erythrocytes was done by flow cytometry, using Trucount™ tubes.

Significantly, the kinetics of clearance for both human and mouse erythrocytes during engraftment phase fit to a lineal regression function (R^2=0.89 for hE and R^2=0.95 for mE), as shown in figure 18A and 18B, respectively. Labelled erythrocytes were injected at day 13 after starting engraftment of IL2 with daily i.p. injections of 1 ml of human blood (50% hematocrit), to ensure a stable engrafment of hEry in which more than 50% of hEry are present in mice peripheral blood. The calculated half life for human erythrocytes in peripheral blood of engrafted IL2 mice was considerably largest (253.56 ± 3.02 hours, n=5) when compared to that found in naïve mice. At the same time, half life of mouse

erythrocytes suffered a light decrease and was similar to human erythrocytes half life, 258.96 ± 4.74 hours (n=5).

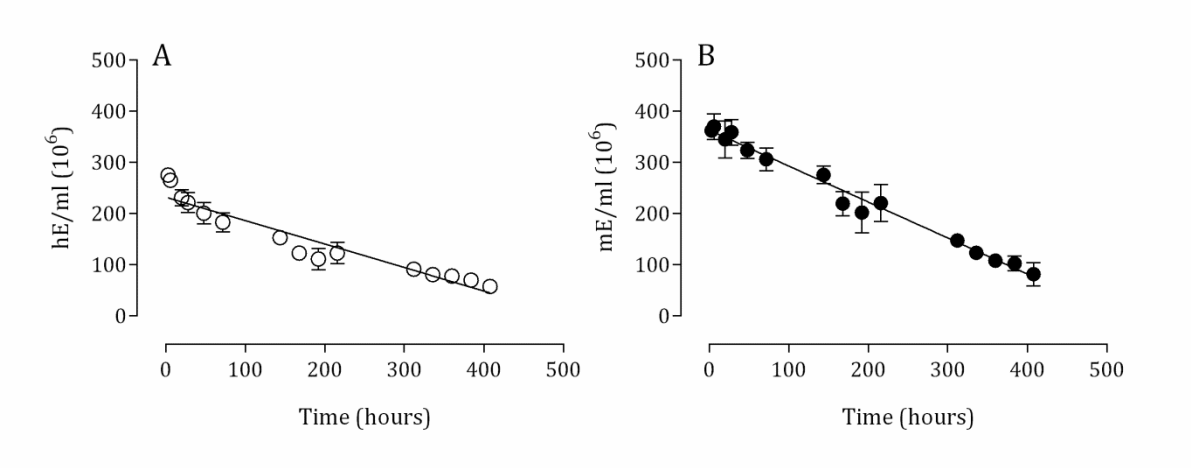

Figure 18. Kinetics of human and mouse erythrocytes (A and B, respectively) in engrafted IL2 mice. Data are the mean ± SD of five mice per data point. Only errors bars that extend beyond the symbols are shown. The quantification of human and mouse erythrocytes was done by flow cytometry, using Trucount™ tubes.

To study the kinetics of human and mouse erythrocytes during the infection phase, at day 1 after infection (day of infection: day 0) infected mice were injected by i.v. route with labelled erythrocytes. In this phase, human and mouse erythrocytes kinetics continued to fit a lineal regression function (R^2=0.77 and R^2=0.52, respectively), as shown in figure 19A and 19B. Although, half life of both types of erythrocytes decreased to 174.71 ± 15.83 hours (n=4) for mouse erythrocytes and 131.21 ± 4.92 hours (n=4) for human erythrocytes.

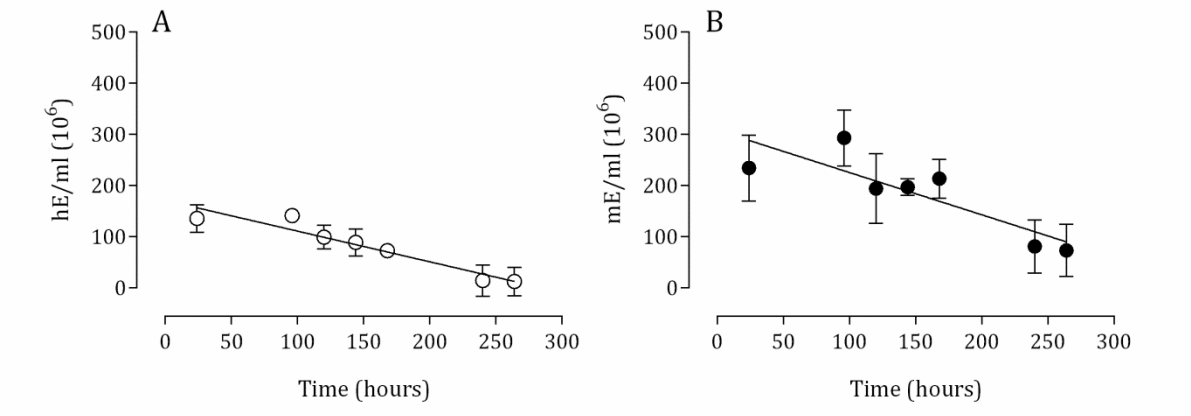

Figure 19. Kinetics of human and mouse erythrocytes (A and B, respectively) in infected IL2 mice at day 1 after infection with P. falciparum. Data are the mean ± SD of five mice per data

point. Only errors bars that extend beyond the symbols are shown. The quantification of human and mouse erythrocytes was done by flow cytometry, using Trucount™ tubes.

However, the observed hEry kinetics after 1 day post-infection was probably understimated due to a low number of labelled erythrocytes detected. For this reason, human erythrocytes kinetic was studied in mice at day 3 after infection and this kinetic fit to a one-phase exponential decay function (R^2=0.87), as shown in figure 20. At this point, half life of human erythrocytes is also similar to that found for mouse erythrocytes during the infection (at day 1 post-infection), 173.4 (n=5). These results suggests that massive clearance of human erythrocytes is not occuring at low parasitemias (around 0.5% at day 3 after infection).

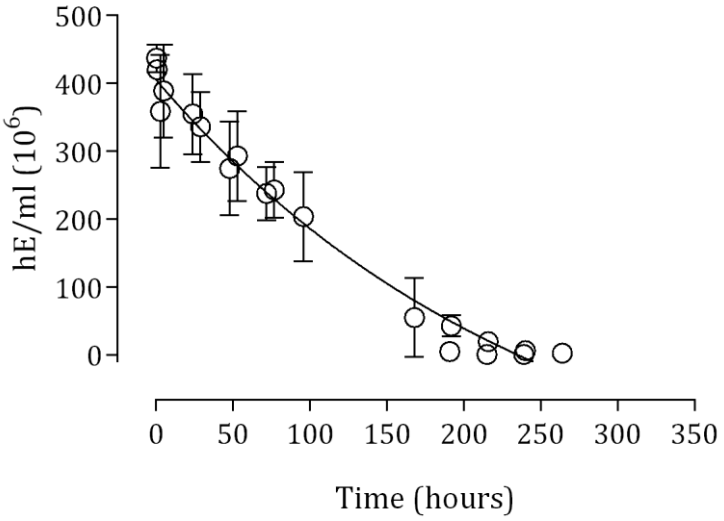

Figure 20. Kinetics of human erythrocytes in infected IL2 mice, labelled erythrocytes were injected at day 3 after infection with P. falciparum. Data are the mean ± SD (n=35, not all the mice have the same data point). Only errors bars that extend beyond the symbols are shown. The quantification of human was done by flow cytometry, using Trucount™ tubes.

When the anaemia phase was reached at day 12 after infection, kinetic of human erythrocytes clearance fits to a one-phase exponential decay function (R^2=0.79) as shown in figure 21A. In addition, half life of human erythrocytes was similar to that found in naïve mice, 11.86 ± 7.4 hours (n=5). However, kinetic of mouse erythrocytes continues to fit to a lineal regression function (R^2=0.35), although the adjust of the function was not good (figure 21B). Half life of mouse erythrocytes calculated in anaemia phase was 146.62 ± 28 (n=5).

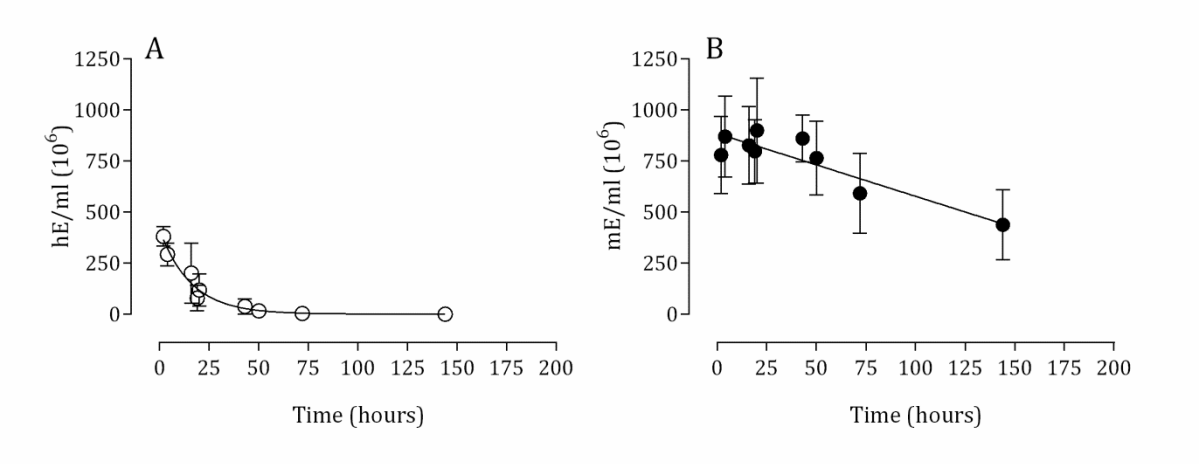

Figure 21. Kinetics of human and mouse erythrocytes (A and B, respectively) in anaemia phase of infected IL2 mice, labelled erythrocytes were injected at day 12 after infection with P. falciparum. Data are the mean ± SD of five mice per data point. Only errors bars that extend beyond the symbols are shown. The quantification of human and mouse erythrocytes was done by flow cytometry, using Trucount™ tubes.

These results reaveal that the dynamics of human and mouse erythrocytes in the GSK*Pf*Hu mouse model is very complex (figure 22). Mouse erythrocytes were eliminated following a lineal regression function in all the phases, but the rate of clearance of these erythrocytes depends on the phase of the model. Nevertheless, both the kinetics and the rate of clearance of human erythrocytes depend critically on the phase of the GSK*Pf*Hu mouse model.

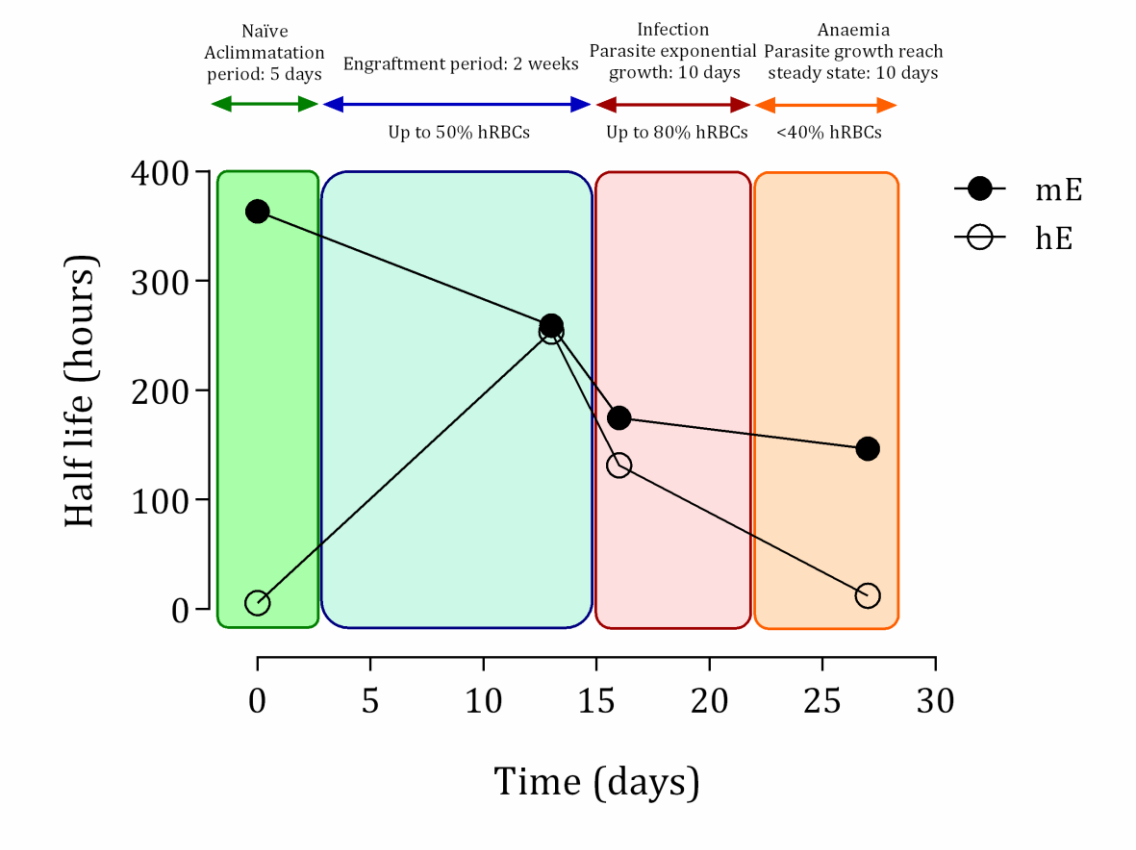

Figure 22. Half life of human and mouse erythroyctes (open and close circles, respectively) in all the phases of the GSKPfHu mouse model: i) naïve (green), ii) engraftment (blue), iii) infection (pink) and iv) anaemia (orange).

During the anaemia phase, a massive clearance of hEry takes place, a further analysis is done to understand this phenomeno. At day 27 after infection the quantification of parasites in peripheral blood are around 147000 parasites per milliliter of blood. The parasite cycle takes 48 hours from the ring stage (young) to the schizont stage (mature), for instance parasite multiplies every 48 hours. In addition, the 3D7 strain used in these experiments has an average of 12 merozoites per schizont, so in theory each parasite is able to infect 12 human erythrocytes every 48 hours. Therefore, around $1.7x10^6$ of human erythrocytes per milliliter (147000 parasites x 12 merozoites) are infected within 48 hours in mice peripheral blood. Nevertheless, at the beginning of the anaemia phase around $331x10^6$ labelled-human erythrocytes per milliliter are quantified. However, 48 hours later, only $4x10^6$ of these human erythrocytes are quantified. Hence, more than $327x10^6$ human erythrocytes (only labeled erythrocytes were quantified) have been cleared in 48 hours, much more than the parasite is able to destroy in its growth ($1.7x10^6$ hEry per milliliter). To summarize, 191 uninfected hEry are destroyed per each human erythrocyte consumed by the parasite.

In conclusion, there were two phases of the GSK*Pf*Hu mouse model in which the rate of clearance of human erythrocytes was very high: i) naïve (and first days of engraftment), and ii) anaemia phase. These phases can be susceptible for improvement in terms of human blood consumption, and further studies for the refinement in the use of the blood have been done. In addition, massive clearance of hEry during anaemia phase cannot be explained by parasite growth, the majority of hEry cleared are uninfected erythrocytes.

Measurement of volume of distribution in the GSKPfHu mouse model

The distrution volume is not defined as a physical volume, but a dilution space. It is one of the pharmacological parameter calculated for a drug that gives an idea of the distribution in the body of the drug after intravenous injection, if it is retained in the tissues or not. Regarding the GSK*Pf*Hu mouse model, the "drug" intravenously administered is red blood cells and the distribution is the blood system without any tissue retention. For instance, in this case the volume of distribution calculated is the same as the circulation blood volume of the mice in which labelled red blood cells are injected. The importance of this parameter to be calculated in the GSK*Pf*Hu mouse model is to study if all the phases of the model are based in a policytemic state.

The distribution volume was measured in the different phases of the GSK*Pf*Hu mouse model: i) engraftment, ii) infection, and iii) anaemia. Also, naïve mice distribution volume was studied and used as control mice to establish the basal distribution volume.

Human and mouse erythrocytes were labelled with Biotin or CFSE and were injected by i.v. route at the different phases of the model. Then, samples of mice peripheral blood were taken at different timepoints for the detection and quantificatin of labelled erythrocytes by flow cytometry. Distribution volume was calculated using the formula described below.

$$\mathbf{V_d = C_i/Y}$$

Where V_d = Distribution volume, and C_i = Initial labelled erythrocytes concentration.

In naïve mice calculated distribution volume was aproximately 1.19 ± 0.25 ml (n=10). In addition, basal concentration of erythrocytes in naïve mice was 7878.79×10^6 ± 752.75 erythrocytes/ml (n=10) in peripheral blood. At day 13 after

starting engraftment with daily i.p. injections of 1 ml of human blood (50% hematocrit), distribution volume calculated was 3.5 ± 0.83 ml (n=10), triplicating the basal distribution volume. Erythrocytes concentration in engraftment phase also suffered an increment, reaching the value of $11814.48x10^6$ ± 1358.83 (n=10) in mice peripheral blood. Taking into account the hematocrit and the erythrocytes concentration, the mean corpuscular volume (MCV) of erythrocytes can be estimated by dividing the hematocrit of these mice (around 80%) by the quantity of erythrocytes per microliter. The value obtained in the division was 68 fL, which it is found between the range of MCV of mice (45-55 fL) and human (80-100 fL).

At the beginning of the inftection phase (day 1 after infection), the distribution volume calculated was similar to that found in the engraftment phase, 3.44 ± 0.81 ml (n=8). The concentration of erythrocytes in mice at day 3 after infection was also similar to that found in the engraftment phase, $10457.04x10^6$ ± 378.68 erythrocytes/ml (n=5). However the distribution volume was slightly lower, 2.79 ± 0.44 ml (n=13), when comparing with the value obtained at day 1 after infection.

During the anaemia phase, where human erythrocytes were massively cleared, the concentration of eythrocytes in mice peripheral blood was reduced to the half of concentration found in naïve mice, $4532.41x10^6$ ± 702.4 erythrocytes/ml (n=5). The distribution volume calculated in this phase was similar to the value obtained in naïve mice, 1.69 ± 0.64 ml (n=10).

To conclude, distribution volume in IL2 mice depend on the phases of the model. The concentration of erythrocytes in mice peripheral blood also depend on the phases of the model and it was closely related to the distribution volume, as shown in figure 23.

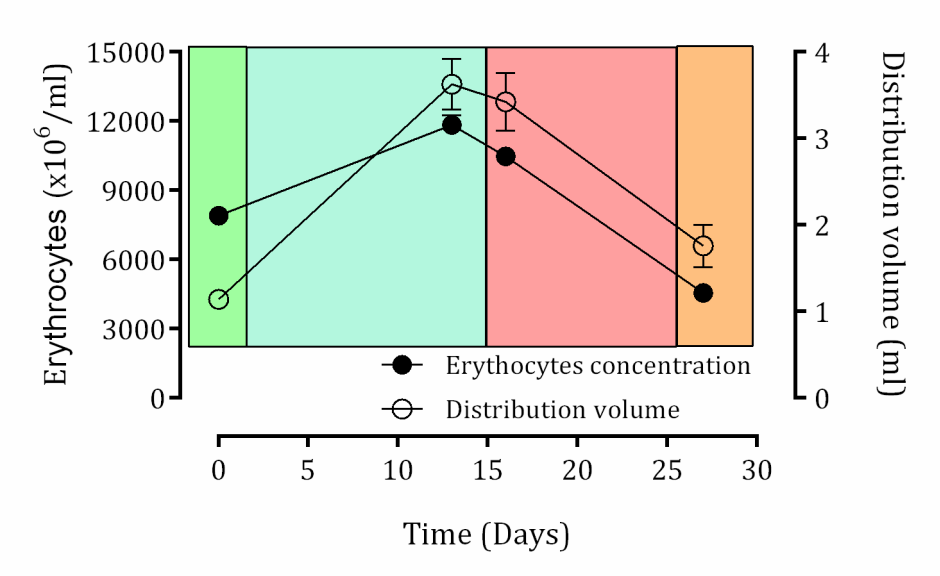

Figure 23. Comparison between distribution volume (open circles) and erythrocytes concentration (close circles) in all the phases of the GSKPfHu mouse model: i) naïve (green), ii) engraftment (blue), iii) infection (pink) and iv) anaemia (orange).

Study of cytokines involved in all the phases of the GSKPfHu mouse model

The GSK*Pf*Hu mouse model has been developed in immunodeficient mice (lacking T and B lymphocytes, and non functional NK cells), without myelodepletion of macrophages. However, IL2 mice used in this model can have active macrophages that are involved in the clearance of human erythrocytes at the beginning of the engrafment and in the anaemia phase, as seen in the previous experiments. Therefore, these mice are able to show a kind of innate response mediated by activated monocytes and macrophages in the different phases of the model. To explore the role that these active macrophages could play, some inflammatory cytokines have been studied in the different phases of the GSK*Pf*Hu mouse model to elucitate the mechanisms involved in the clearance of human erythrocytes: i) engraftment, ii) infection, and iii) anaemia. Levels of cytokines were also measured before starting engraftment with human erythrocytes. In addition, results obtained were compared with the parental mice strain for IL2 mice, NODscid mice, that also lacks T and B lymphocytes, but still have functional NK cells. NODscid mice were also engrafted and infected with the *P. falciparum* parasite.

Inflammatory cytokines studied in mice were: i) TNF-α, ii) IL-12p70, iii) IFNγ, iv) MCP-1, v) IL-10 and vi) IL-6. Using the BD CBA mouse inflamatory kit, cytokines were studied in mice plasma and were quantified by flow cytometry.

Levels of TNF-α in naïve mice were less than 10 pg/ml, these levels remains more or less stable throughout the engraftment of mice within 34 days of blood injection (figure 24A). Nevertheless, levels of TNF-α increased above 25 pg/ml, reaching one peak during infection (at day 16 of blood injection), and another peak in anaemia phase (at day 30 after blood injection), as shown in figure 24B.

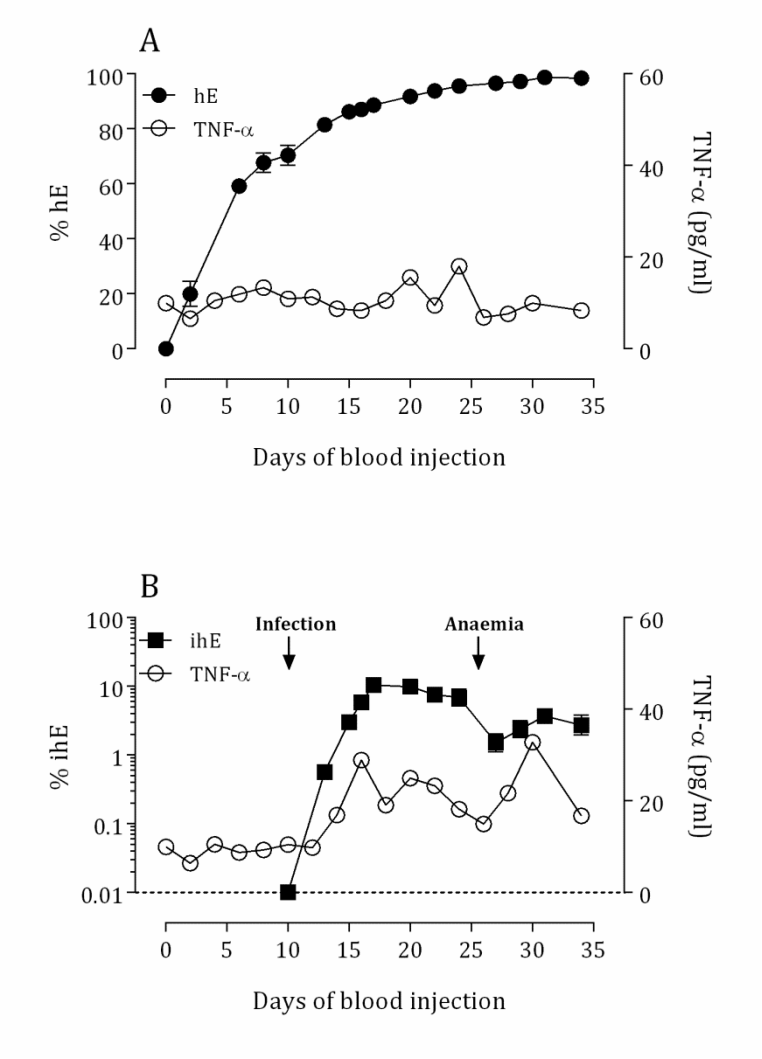

Figure 24. Levels of TNF-α in engrafted mice (A) and infected mice (B). Data are the mean ± SEM of five mice per data point in the case of percentage of human erythrocytes (hE) and infected human erythrocytes (ihE). Only errors bars that extend beyond the symbols are shown. TNF-α levels are data from an unique pool of of serum from five mice per data point.

When measuring levels of IL-12p70 in naïve mice, it was also less than 10 pg/ml, these levels were mantained throughout engraftment phase (figure 25A). However, levels of IL-12p70 increased during infection phase and reached a peak during anaemia phase, above 100 pg/ml at day 28 after starting blood injection, as shown in figure 25B.

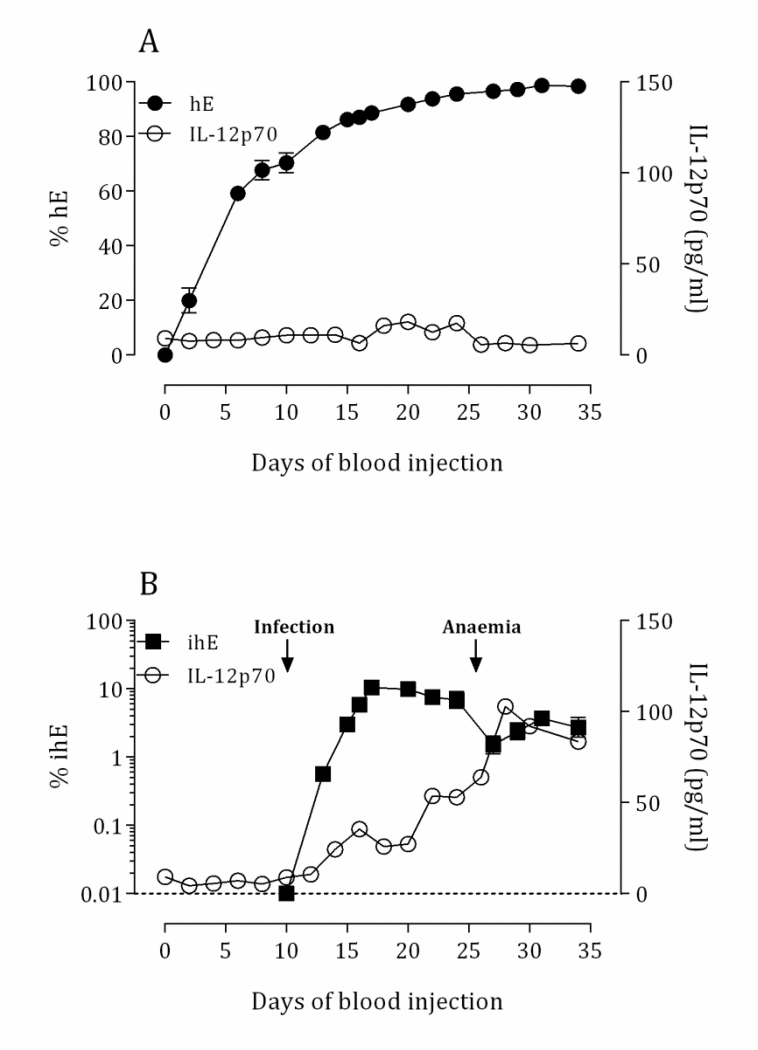

Figure 25. Levels of IL-12p70 in engrafted mice (A) and infected mice (B). Data are the mean ± SEM of five mice per data point in the case of percentage of human erythrocytes (hE) and infected human erythrocytes (ihE). Only errors bars that extend beyond the symbols are shown. IL-12p70 levels are data from an unique pool of serum from five mice per data point.

Levels of IFNγ in naïve mice before starting engrafting process were less than 3 pg/ml, these levels were mantained more or less stable throughout engraftment phase (figure 26A). In addition, levels of IFNγ were also stable during infection and anaemia phase (figure 26B).

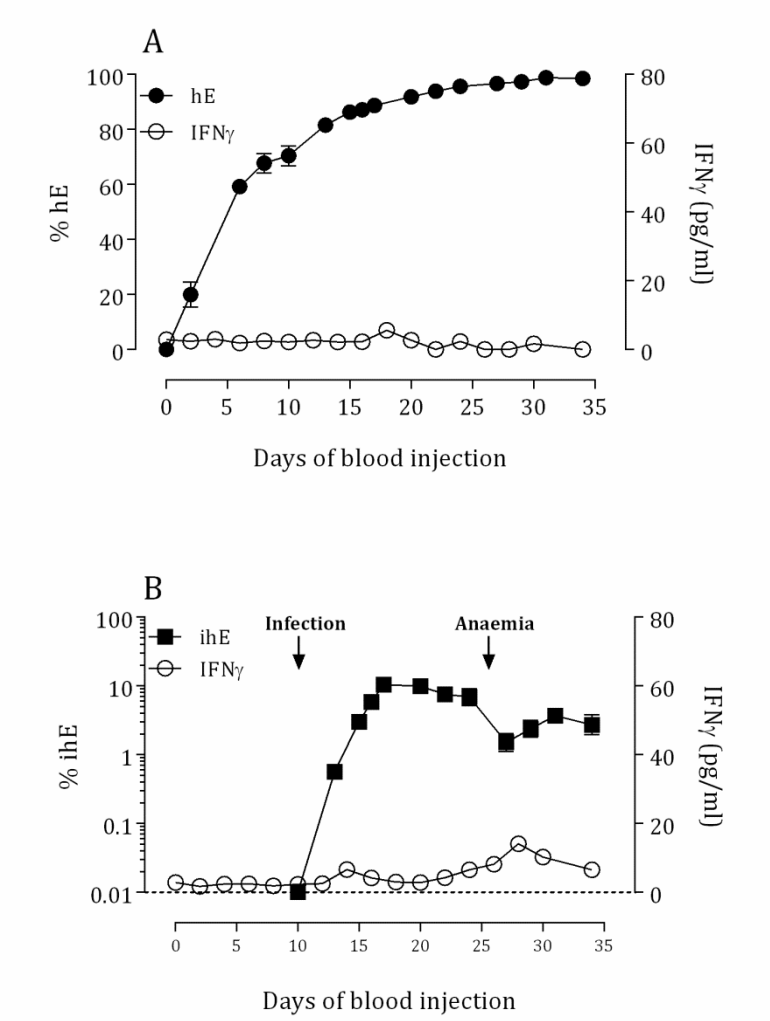

Figure 26. Levels of IFNγ in engrafted mice (A) and infected mice (B). Data are the mean ± SEM of five mice per data point in the case of percentage of human erythrocytes (hE) and infected human erythrocytes (ihE). Only errors bars that extend beyond the symbols are shown. IFNγ levels are data from an unique pool of serum from five mice per data point.

In naïve mice, measured levels of MCP-1 were approximately 80 pg/ml. During engraftment phase, these levels were mantained more or less around 100 pg/ml (figure 27A). Nonetheless, levels of MCP-1 increased during infection phase reaching a peak at around 400 pg/ml, other peaks around 200 pg/ml were reached during infection and anaemia phase, as shown in figure 27B.

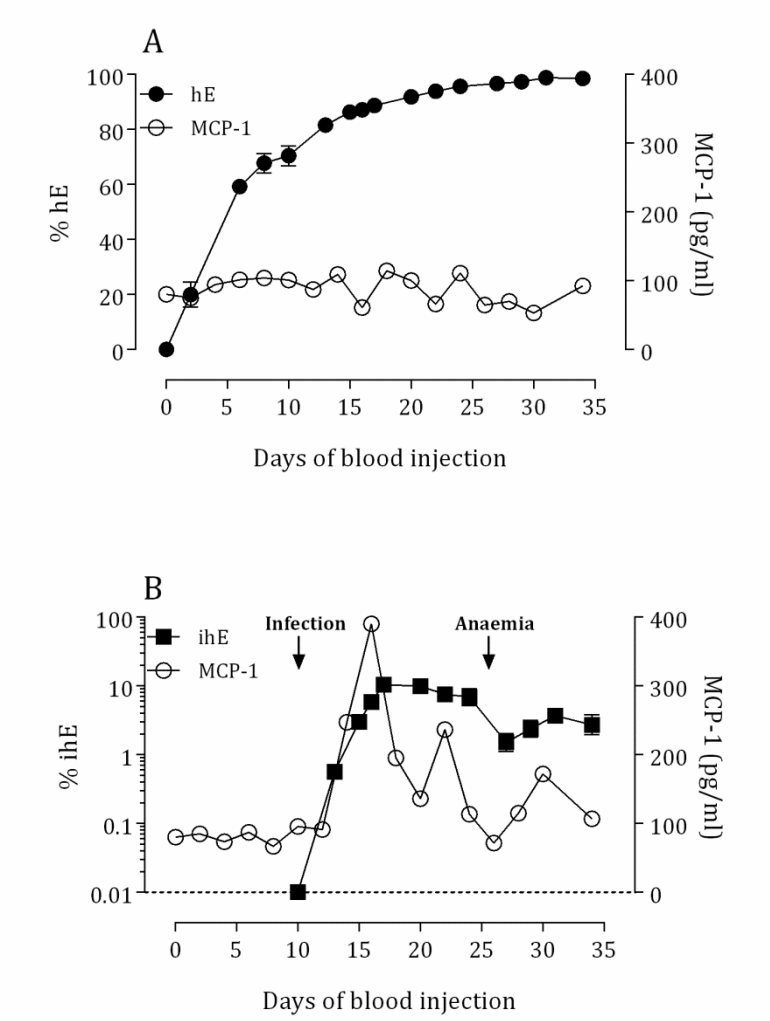

Figure 27. Levels of MCP-1 in engrafted mice (A) and infected mice (B). Data are the mean ± SEM of five mice per data point in the case of percentage of human erythrocytes (hE) and infected human erythrocytes (ihE). Only errors bars that extend beyond the symbols are shown. MCP-1 levels are data from an unique pool of serum from five mice per data point.

Levels of IL-10 in naïve mice were determined at around 35 pg/ml. During engraftment phase, levels did not shown a specific pattern, reaching some peaks with a maximum of 110 pg/ml (figure 28A). In the infection phase, the maximum peak reached was lower than engraftment phase (85 pg/ml), as shown in figure 28B.

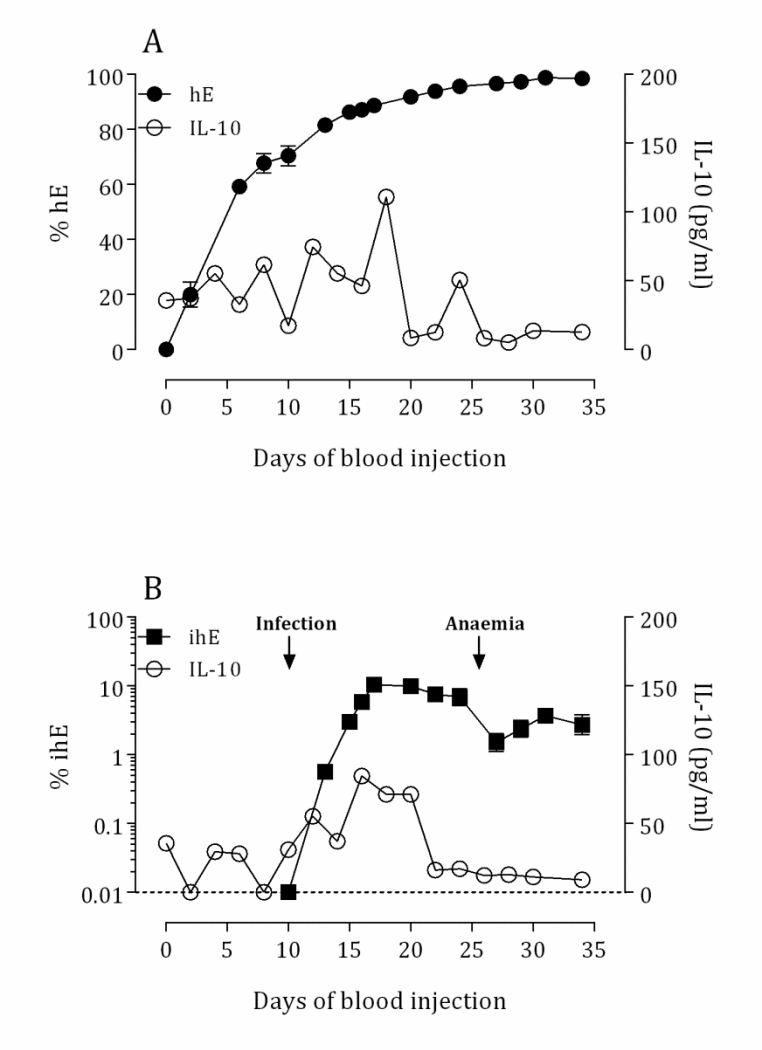

Figure 28. Levels of IL-10 in engrafted mice (A) and infected mice (B). Data are the mean ± SEM of five mice per data point in the case of percentage of human erythrocytes (hE) and infected human erythrocytes (ihE). Only errors bars that extend beyond the symbols are shown. IL-10 levels are data from an unique pool of serum from five mice per data point.

Measured levels of IL-6 in naïve mice were less than 5 pg/ml, these levels did not suffer much variation throughout engraftment phase (figure 29A). Nevertheless, levels of IL-6 showed a peak during infection phase, around 100 pg/ml at day 14 after starting blood injection, as shown in figure 29B.

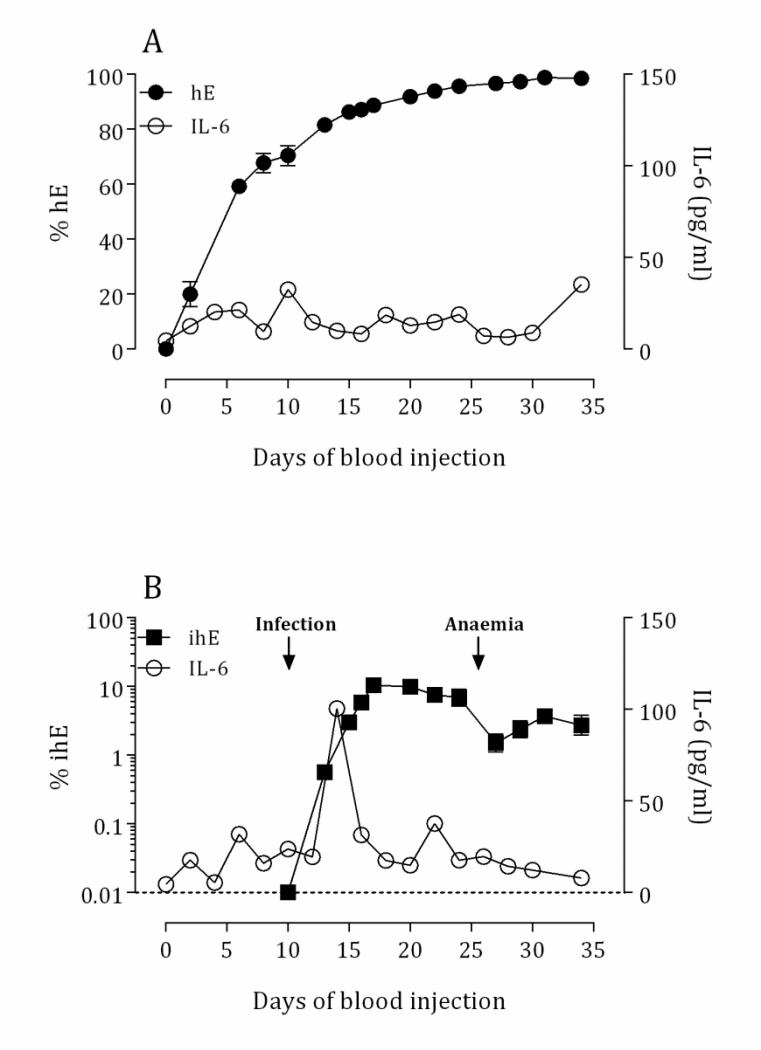

Figure 29. Levels of IL-6 in engrafted mice (A) and infected mice (B). Data are the mean ± SEM of five mice per data point in the case of percentage of human erythrocytes (hE) and infected human erythrocytes (ihE). Only errors bars that extend beyond the symbols are shown. IL-6 levels are data from an unique pool of serum from five mice per data point.

To summarize, inflammatory cytokines studied in the different phases of the GSK*Pf*Hu mouse model showed different expression throughout the experiment, where IFNγ was absent during all the phases of the model. In addition, the only cytokine detected during the engraftment phase was IL-10. However, during the infection phase most of the inflmmatory cytokines studied were involved: TNFα, IL-12p70, MCP-1, IL-6 and IL-10. Whereas cytokines expressed during the anaemia phase were reduced and only TNFα, IL-12p70 and MCP-1 were expressed. A determination of the AUCs for the different cytokines studies was assessed to have a better understanding of the cytokines expression in the GSK*Pf*Hu mouse model, AUCs of cytokines values obtained througout the experiment were compared with the expression of the same cytokines obtained in parental mice strain

(NODscid) and in the same conditions of engraftment with hE and infection with *P. falciparum* 3D7 strain (figure 30).

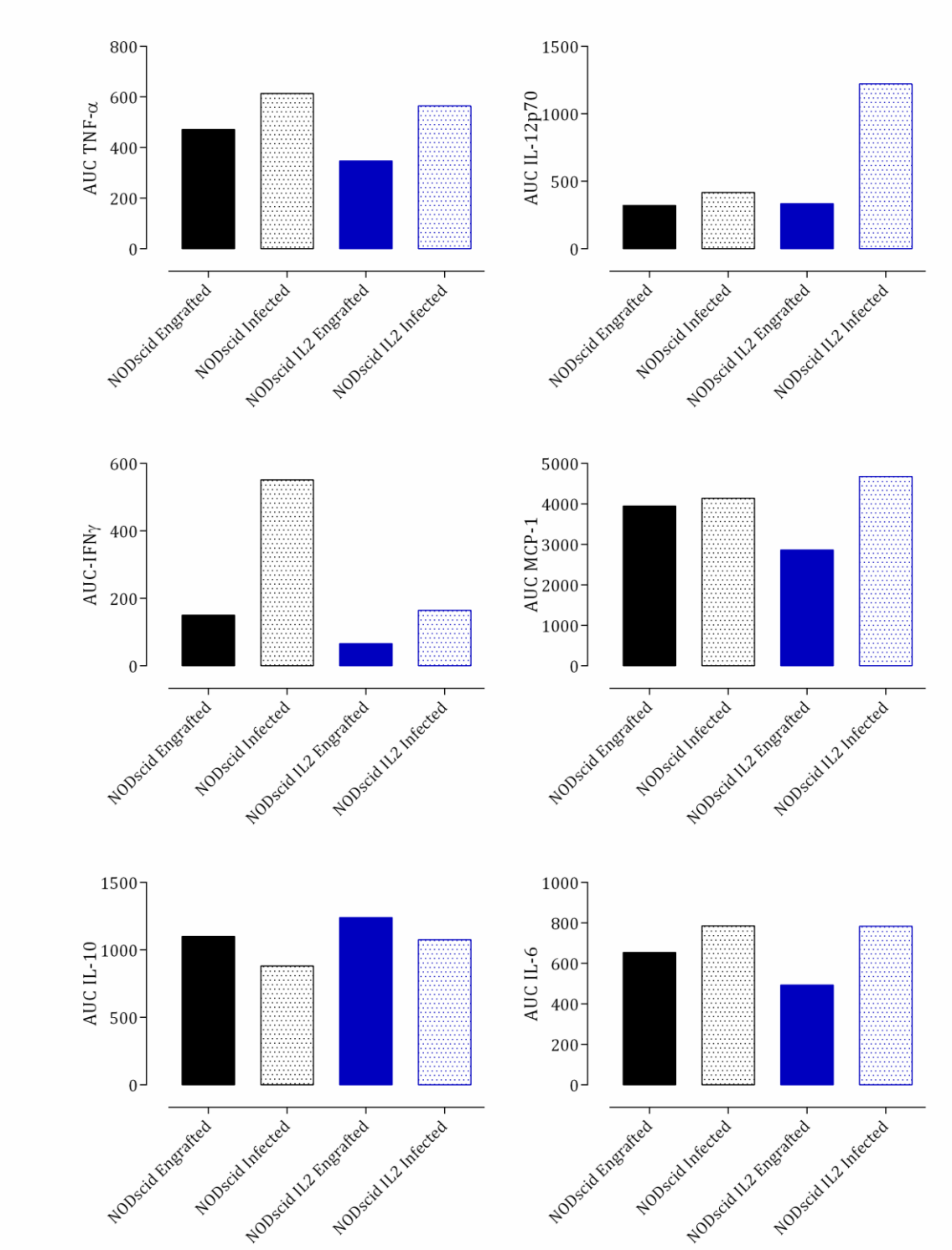

Figure 30. AUC comparison of inflammatory cytokines expression between NODscid and IL2 mice under the conditions of GSKPfHu mouse model (engraftment with the daily i.p. injection

of 1 ml of hE and infection with 20x10^6 Pf 3D7 infected erythrocytes after 10 days of engraftment). AUC is calculated from levels of cytokines obtained from an unique pool of serum from five mice per data point. Note that Y axis scale are different in each graphic.

When comparing AUCs of cytokines expression of IL2 mice with their parental mice strain, it can be observed that the expression MCP-1 and IL-10 cytokines stayed more or less the same in both mice strain with no significant difference during the engrafment and infection procedure. However, TNF-α and IL-6 maintained similar expression in the two mice strain but it is slightly higher during the infection. In addition, expression of IL-12p70 was only activated throughout infection and by consequence anaemia phase in IL2 mice. Nevertheless, expression of IFN-γ is lower in IL2 infected mice comparing with the parental NODscid.

Study of erythrophagocytosis in the GSKPfHu mouse model

In vivo erythrophagocytosis

It is described that in malaria most of the erythrophagocytosis takes place in the spleen [119]. Massive clearance of human erythrocytes in the GSK*Pf*Hu mouse model takes place mostly in two phases of the GSK*Pf*Hu mouse model: naïve and anaemia phase. *In vivo* erythrophagocytosis of hEry in the spleen was studied in these two phases. Two different mice strains were used to address erythrophagocytosis, CD1 mice as control of high clearance of human erythrocytes. Whereas, IL2 mice engrafted with human erythrocytes were used as control of low clearance of human erythrocytes.

To study erythrophagocytosis naïve IL2 and CD1 mice were injected with 2.2x10^8 CFSE-labelled hEry, mice peripheal blood was collected at different timepoints to quantify CFSE labelled hEry, when a significative decrease in this number was detected (more than a half of the labelled hEry detected after the injection), spleens were excised. In addition, IL2 engrafted mouse was injected with the same number of CFSE labelled erythrocytes at day 14 after starting with the blood injections, spleen was removed 15 hours after injection of labelled erythrocytes. Finally, in anaemia phase mice were injected with the same number of CFSE labelled hEry by i.v. route at day 10 after *P. falciparum* infection, then spleens were excised at different time points to assess erythrophagocytosis: 7, 14, 15, 24, 32 and 48 hours after injection.

Once the spleens were excised, they were desintegrated and cells obtained were used to study the erythrophagocytosis by flow cytometry using different monoclonal antibodies: CD45, F4/80 or GR-1.

Cells from disintegrated macrophages stained with the different monoclonal antibodies at the same time using different fluorocromes conjugations. Macrophages that were phagocytosing erythrocytes were considered as populations positive for CFSE staining and positive for CD45, F4/80 or GR-1 macrophage membrane protein markers in dot plots graphics.

Results obtained showed that in the control CD1 mice, 10% of leukocytes ($CD45^+$ population) were phagocytosing CFSE-labelled erythrocytes. From the total leukocytes population, the erythrophagocytosis was performed by $F4/80^+$ and $GR\text{-}1^+$ active macrophages populations, as shown in figure 31A. Accordingly, erythrophagocytosis in IL2 naïve mice (non-engrafted) was also achieved by the 10% of $CD45^+$ leukocytes. The $F4/80^+$ macrophage population and the $GR\text{-}1^+$ population were also responsible of this erythrophagocytosis, as shown in figure 31B. During engraftment phase there was also erythrophagocytosis of CFSE labelled hEry ascertained in the spleen, although calculated half life of human erythrocytes was 253.56 hours. In engrafted mice, 9% of $CD45^+$ leukocytes were phagocytosing CFSE-labelled hE. In addition, in engrafted mice the percentage of phagocytosis on $F4/80^+$ macrophages was higher than $GR\text{-}1^+$ population, as shown in figure 31C.

Erythropagocytosis in anemia phase was studied at different time points in order to cover the massive clearance of human erythrocytes. The phagocytosis of CFSE-labelled hE was detected in all the time points that have been explored. A representative time point in which erythrophagocytosis was present was selected to be shown in figure 31D. At 14 hours after the injection of CFSE labelled erythrocytes, around 5% of $CD45^+$ leukocytes were phagocytosing CFSE-hEry. Furthermore, mostly of phagocytosis was performed by $F4/80^+$ population.

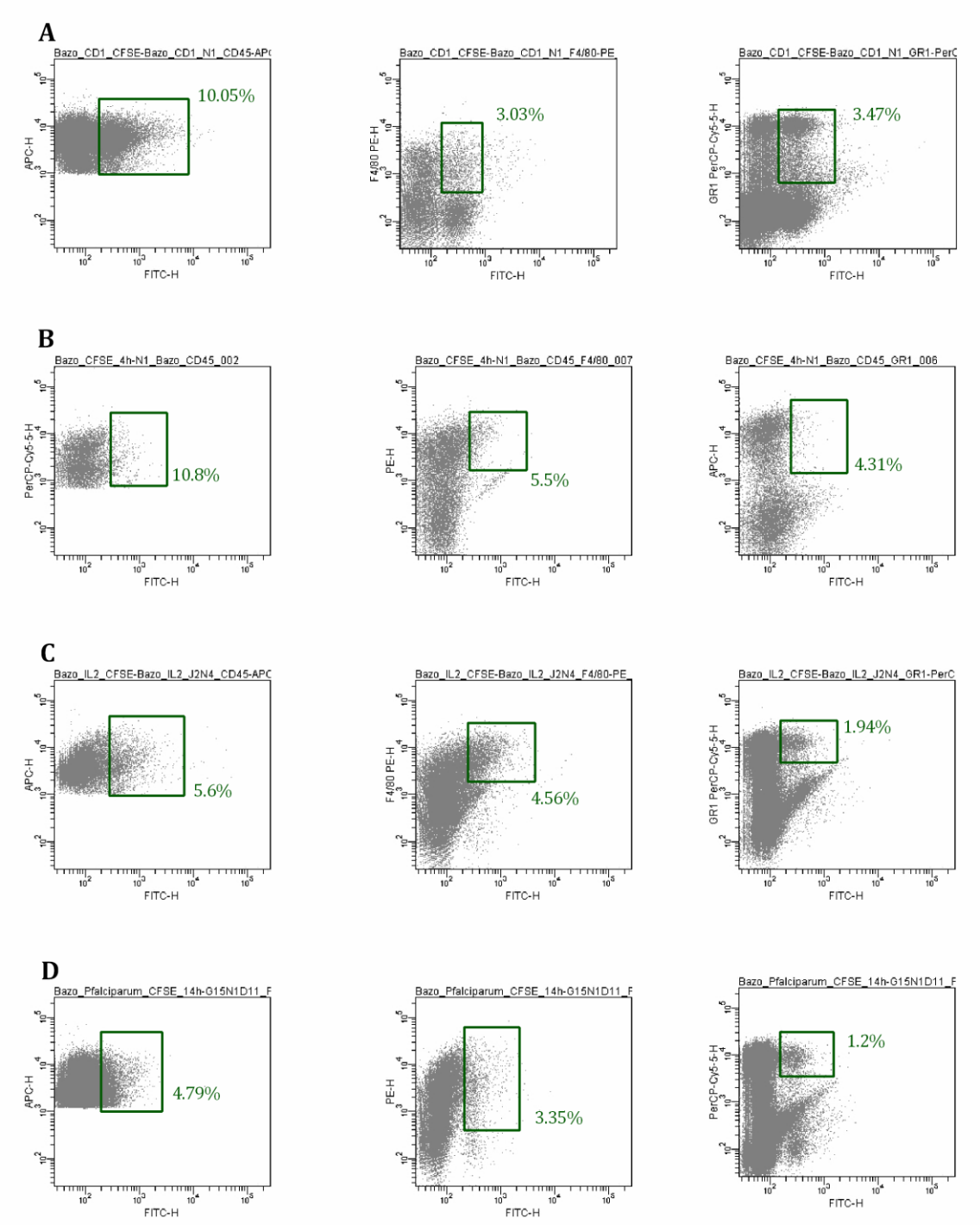

Figure 31. Dot plot graphics from LSRII flow cytometer from erythrophagocytosis study in spleen at different phases of the GSKPfHu mouse model. Erythrophagocytosis was studied in CD45, F4/80 or GR-1 leukocytes populations (from left to right), and was studied in CD1, IL2 naïve, IL2 engrafted and IL2 anemic mice (A, B, C and C, respectively).

In conclusion, erythrophagocytosis in spleen is present in all the phases of the GSK*Pf*Hu mouse model. Cells populations involved in the phagocytosis of human erythrocytes in IL2 mice spleen are positive for CD45 (marker for leukocytes), F4/80 (marker for spleen red

pulp macrophages) and GR-1 (marker for inflammatory monocytes) membrane proteins. In the case of engrafted and anemic mice the erythrophagocytosis was mostly mediated by $F4/80^+$ macrophages. By contrast, in naïve mice, the phagocytosis is assessed equally by $F4/80^+$ and $GR\text{-}1^+$.

Optimization of the GSK*Pf*Hu mouse model

Kinetics of human erythrocytes after intraperitoneal injection

The results of the erythrokinetics obtained after i.v. injection revealed that in naïve mice the clearance of human erythrocytes was very fast, this massive removal of hE can be caused by the rejection of the xenotransplant. The xenotransplant with hE in the GSK*Pf*Hu mouse model was done by i.p. injections of 1 ml of human blood (50% hematocrit). To study the kinetics of human erythrocytes after i.p. injection of 1 ml of human blood 50% hematocrit in IL2 mice, several samples from mice peripheral blood were taken at different time points after a unique i.p. injection. These samples were analyzed by flow cytometry to calculate the concentration of human erythrocytes in mice peripheral blood.

The analysis of the kinetic revealed the presence of different peaks of absorption of human erythrocytes. The first peak was around 6 hours after injection, followed by a small drop in the total of human erythrocytes in mice peripheral blood (figure 32). Each mouse received $3961.68x10^6$ human erythrocytes in the mililiter of human blood injected. The maximum peak of human erythrocytes found in mice peripheral blood was $1369.5x10^6$. In conclussion, only around the 35% of human erythrocytes injected went through the peritoneum to the peripheral blood.

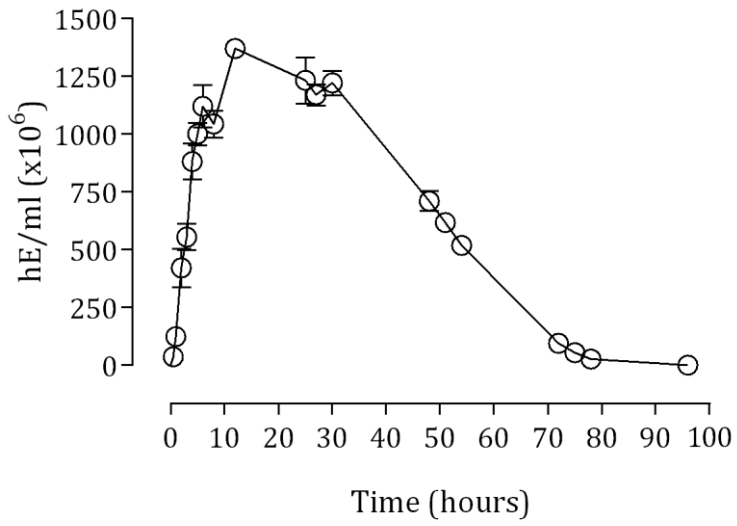

Figure 32. Kinetic of human erythrocytes after i.p. injection of 1 ml of human blood (50% hematocrit) in IL2 naïve mice. Data are the the mean ± standard error of the mean of a cohort of five mice sampled at different time points. Only errors bars that extend beyond the symbols are shown. Quantification of human erythrocytes (TER119-PE- events) was done by flow cytometry using Trucount™ tubes.

The maximum peak of absorption was reached 12 hours after the intraperitoneal injection. This data reveals that exists a rejection of the xenotransplant of human erythrocytes in IL2 mice so far as the clearance of human erythrocytes starts as soon as the maximum peak of abosorption was reached. This speed of clearance is slower than the calculated after i.v. injection of human erythrocytes (5.42 hours), in this case the half life of human erythrocytes is around 32 hours. Thus, the injection of 1 ml of human blood at 50% hematocrit every 24 hours may be a suboptimal regime for engraftment of IL2 and there is still room for improvement of the protocol in terms of engraftment.

Study of erythrophagocytosis in the GSKPfHu mouse model

In vitro

The engraftment of IL2 mice is done with intraperitoneal injections of human blood, and the recruitment of monocytes in the peritoneum is common in inflammatory processess [133]. For this reason, the ability of IL2 peritoneum cells to perform phagocytosis of hEry was assessed. Peritoneal cells were obtained from the peritoneal cavity of IL2 mice and the they were icubated *in vitro* overnight to allow adhesion to the plate for the erythrophagocytosis study.

Human erythrocytes were labelled with PKH26 membrane staining, and then $3x10^9$ of labelled hEry were added to the peritoneum cells culture plate and incubated during 2 hours at 37ºC in a CO_2 incubator. After the incubation, excess of erythrocytes were washed and lysed, and peritoneum cells were detached from the bottom of the plate to observe the phagocytosis by flow cytometry.

The, peritoneum cells were incubated with CD45-APC monoclonal antibody (leukocyte membrane antibody), during 20 minutes at 4ºC to avoid phagocytosis. Then, cells were fixed with 1% paraformaldehyde and acquired in LSR II flow cytometer. Peritoneum cells were positive for the CD45 antibody, this means that these cells are leukocytes. Unstained hEry were used for phagocytosis control in absence of PKH26 fluorescence (figure 33A). Whereas, figure 33B shows peritoneum cells ($CD45^+$) put in culture in the presence of PKH26 labelled erythrocytes.

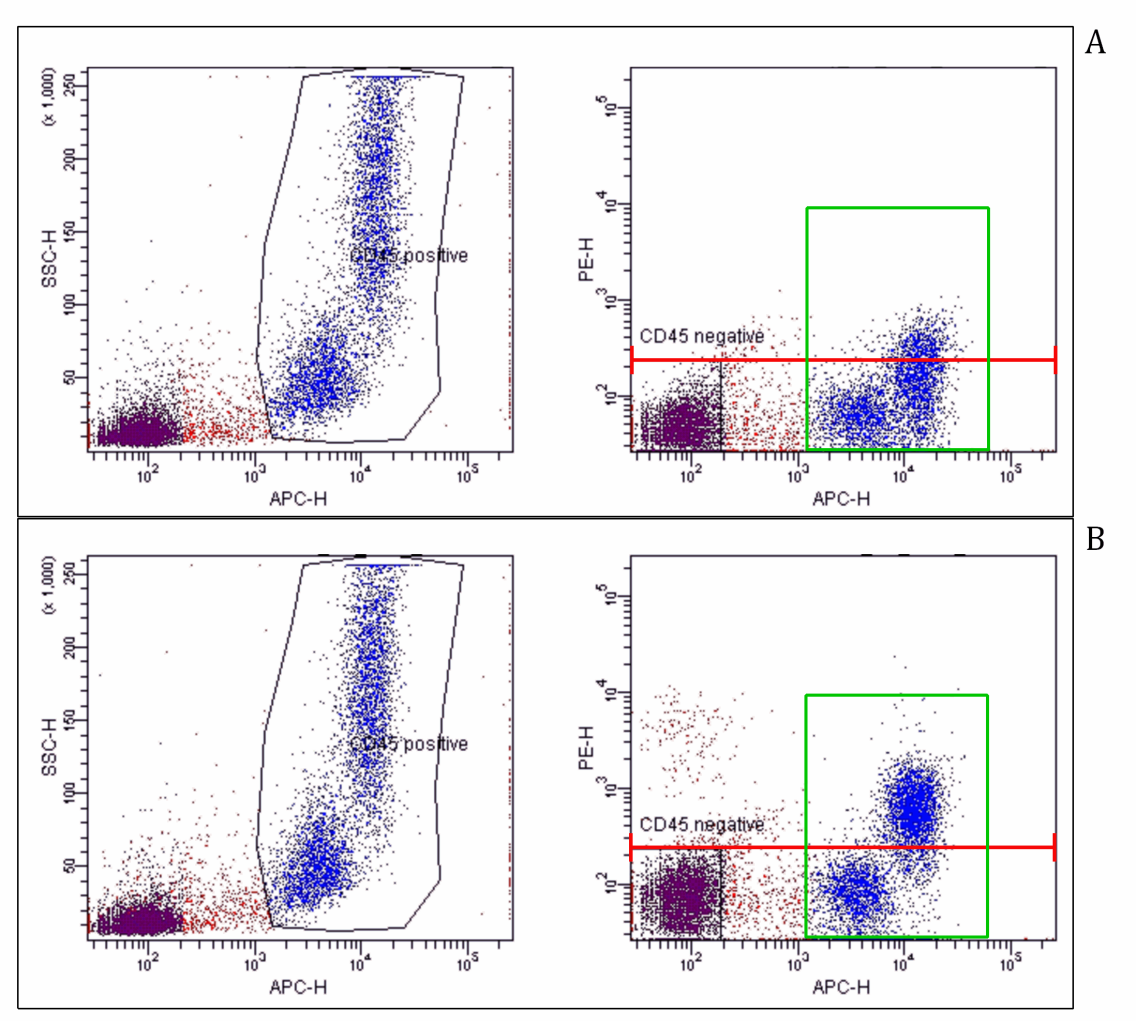

Figure 33. Flow cytometry dot plots from in vitro erythrophagocytosis study. Upper dot plots (A) shows culture of peritoneal cells in which non-labelled human erythrocytes have been added. CD45⁺ cells are selected on upper-left dot plot, upper-right dot plot represents erythrophagocytosis of non-labelled hEry (CD45⁺-PE⁻ cells). Lower dot plots (B) culture of peritoneal cells with PKH26-labelled human erythrocytes added. CD45⁺ cells are selected on lower-left dot plot, lower-right dot plot represents erythrophagocytosis of PKH26-labelled hEry (CD45⁺-PE⁺cells. Green square shows CD45⁺cells and red line divides Y axis in negative (below the line) and positive (above the line) for PE (PKH26) fluorescence.

Population included in green box corresponds to CD45 positive cells. This population was selected in a SSC-H/APC dot plot, by the selection of cells that express CD45 antibody, which is tagged with a APC fluorocrome. To select macrophages that were phagocytosing hEry, it was used a PE-H/APC-H dot plot, in which in the X axis (APC) there was selected a population positive for the CD45 antibody, and in the Y axis was selected those CD45⁺ cells that were also positive for PE (PKH26 expression). When the Mean Fluorescence Intensity in Y axis (PE-H) of the CD45⁺ population on the lower right dot plot (figure 33B) was

compared with that MFI in the control dot plot (figure 33A), it can be observed that there is an increase of these MFI in the Y axis for these $CD45^+$ cells. This increase means that this $CD45^+$ population is showing fluorescence in the PE channel, which correspond to the PKH26 expression of labelled human erythrocytes that have been internalized inside the $CD45^+$ cells (hEry that had been phagocytosed).

Fluorescence microscopy was used to confirm that the erythrophagocytosis observed by flow cytometry correspond to erythrocytes that have been internalized by the macrophages. Fluorescence of the culture plate was observed in an inverted flouorescence microscopy, in three different channels: i) UVA to detect DNA of the macrophages stained with DAPI; ii) PE for the detection of PKH26 labelled human erythrocytes; and iii) bright field to observe the structure of the macrophages. Microphotographies in these different channels are shown in figure 34, and exhibit internalized PKH26 hE by macrophages.

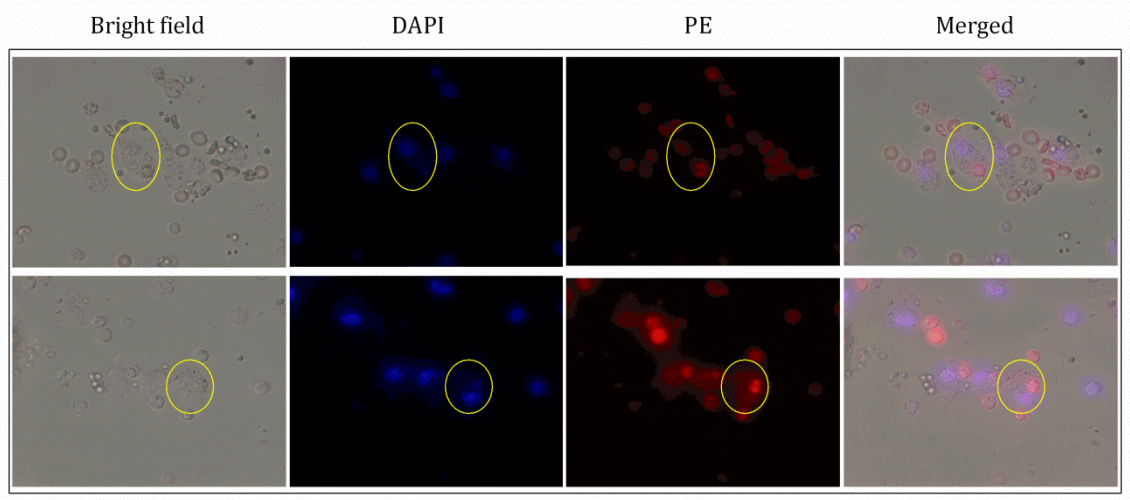

Figure 34. Microphotographies of the erythrophagocytosis of labelled PKH26 erythrocytes by macrophages. Yellow circles show where the erythrophagocytosis is taking place. From left to right: Bright field, DAPI to label macrophages DNA, PE that detects PKH26 erythrocytes and the merge of the three fields.

To conclude, peritoneum cells isolated from IL2 mice are active and are able to phagocytose human erythrocytes as it has been checked in an *in vitro* erythrophagocytosis assay. These results supports the hypothesis that hEry are being phagocytosed after the intraperitoneal injection and as result only 35% of hEry reach mice pheripheral blood after the injection.

Optimization of the dosing regime of blood in the GSKPfHu mouse model

Following empirical protocols previously published, the engraftment of β2 with hEry, used in the first implementation of the GSK*Pf*Hu mouse model, was achieved by daily intraperitoneal injection of 1 ml of hE suspension (50% hematocrit) [5]. This procedure led to ~50% hE in mice peripheral blood in 10 days, which requires an average of 4 ml of hE concentrate per mouse and week for engraftment.

In previous experiments, it has been hypotethized that the intraperitoneal injection of 1 ml of hEry (50% hematocrit) every 24 hours may be a suboptimal engraftment protocol, and blood dosing regime for engraftment could be reduced using alternative regimes of intraperitoneal injections of hEry.

In order to optimize the use of hEry concentrates in the standard GSK*Pf*Hu mouse model, different regimes of intraperitoneal injection and volumes of suspension were tested in IL2 mice. Briefly, mice were randomly divided in groups of 4 mice each and assigned to one of the 9 combinations of 3 different frequency of injection (24, 48 and 72 hours) and 3 different volumes of hEry suspension for each frequency (0.5, 1 and 1.5 ml) at a 50% hematocrit.

Under these experimental conditions, the best engraftment protocol should be the one that achieve ~50% hEry in mice peripheral blood in 10 days or less without deleterious effects in mice welfare, measured as negative weight increment throughout the experiment.

Results obtained in this study lead to the conclussion that the regime used for the engraftment of β2 and IL2 mice previosuly published [5, 63], is suitable for engraftment without causing damage to mice welfare ($AUC_{0\text{-}19}$=1015.45 ± 131.17). This means, i.p. injection of 1 ml of human blood every 24 hours lead to achieve ~50% hEry in mice peripheral blood in 10 days, as shown in figure 35. In addition, the injection of 1.5 ml of human blood every 48 hours also led to ~50% hEry in mice peripheral blood in 10 days without deleterious effects in mice with similar $AUC_{0\text{-}19}$ (898.45 ± 41.72) (figure 35 and 36B). However, besides being one of the best regime for IL2 mice engraftment with hE ($AUC_{0\text{-}19}$= 925.72 ± 342.66), the regime of 1.5 ml every 24 hours was discarded due to loss of weight in mice (figure 36A). No significant differences were observed among these three regimes of blood injection after two-way ANOVA test of AUCs.

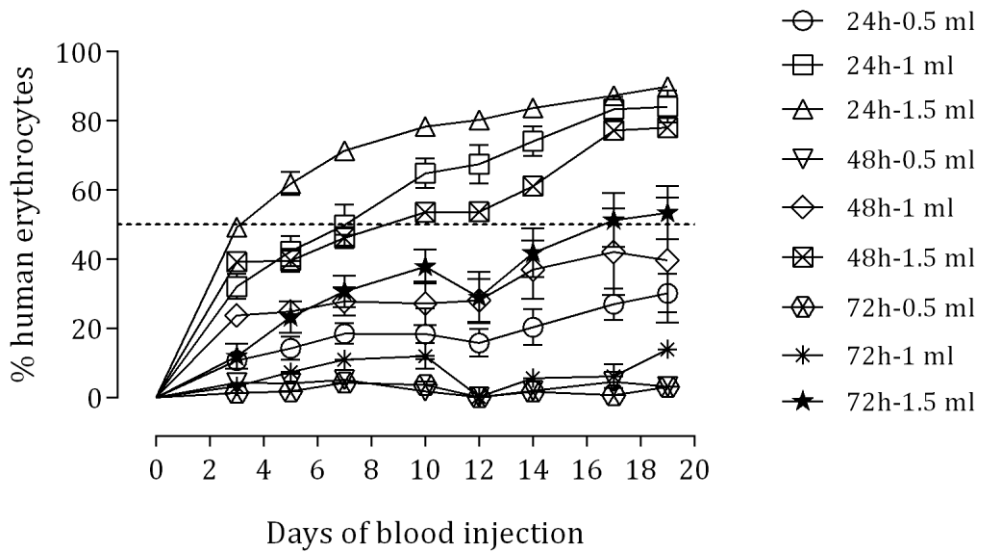

Figure 35. Kinetics of engraftment with hEry in the dosing regimes in terms of volume and time of blood i.p. injection. The percentage of human erythrocytes was calculated by flow cytometry as TER119-PE- events. Data are the mean ± standard error of the mean of four mice per group. Only errors bars that extend beyond the symbols are shown.

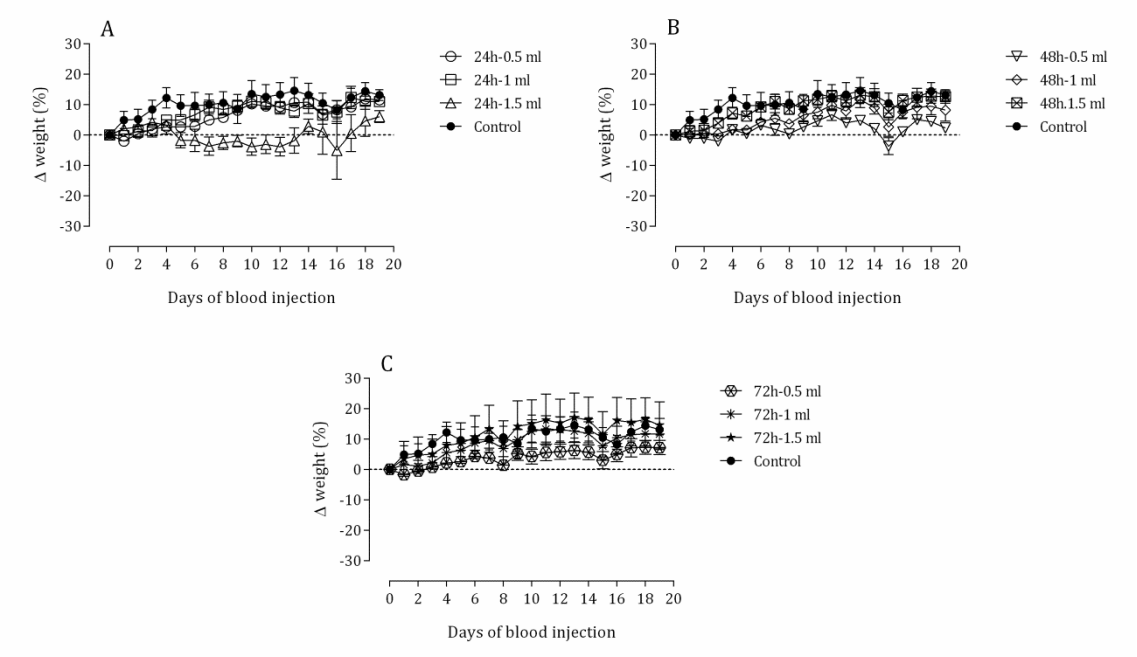

Figure 36. Increment in the body weight of mice injected with different volumes of i.p. hEry injections at 24, 48 and 72 hours (A, B and C, respectively). Data are the mean ± standard error of the mean of four mice per group. Only errors bars that extend beyond the symbols are shown.

In conclusion, in terms of human blood consumption, with the regime of intraperitoneal injection of 1.5 ml of erythrocytes suspension (50% hematocrit) every 48 hours, approximately 1 ml of human blood can be saved per mouse and week.

Other regimes of human blood injection for the optimization of blood consumption in the GSKPfHu mouse model

In order to optimize the blood consumption, other protocols for mice engraftment with human erythrocytes were explored. One of these protocols it is based on the injection of an extra dose of human erythrocytes within 12 hours (time observed before human erythrocytes clearance starts after intraperitoneal injection), this regime of blood injections may lead to a faster engraftment of mice with human erythrocytes and a reduction in the human blood consumption.

To prove this hypothesis, IL2 mice were randomly divided in groups of 5 mice each and assigned to one of the 3 groups tested: i) control group (i.p. injections every 24 hours with 1 ml of hEry), ii) 1x12h (i.p. injections of 1 ml of hEry every 12 hours until 24 hours, then injections every 24 hours) and iii) 2x12h (i.p. injections of 1 ml of hEry every 12 hours until 48 hours, then injections every 24 hours). Mice were injected only four days, and negative weight increment was used as control of deleterious effect on mice welfare throughout experiment.

Results obtained in this experiment, revealed that mice injected with human erythrocytes from groups ii) and iii) (1x12h and 2x12h, respectively), led to ~40-50% of hEry in peripheral blood in 4 days (figure 37A). Mice welfare was not affected by the increment of i.p. injections at the beginning of the experiment (figure 37B). When comparing AUC of % human erythrocytes increment from day 0 to 4, control group showed an AUC_{0-4}=1605 ± 276.4. Meanwhile, 1x12h had an AUC_{0-4}=2203 ± 835.6 and 2x12h group an AUC_{0-4}=3669 ± 368, only significant differences were found when comparing control and 1x12h group with 2x12h.

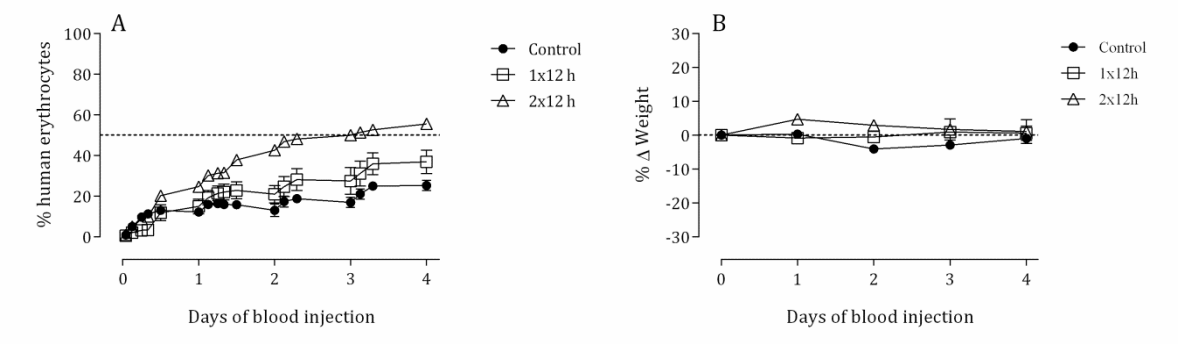

Figure 37. Kinetics of engraftment with hEry in the different groups tested, compared with control group (A). The percentage of human erythrocytes was calculated by flow cytometry as TER119-PE- events. Increment in the body weight of the mice in the experimental groups throughout the experiment (B). Data are the mean ± standard error of the mean of five mice per group. Only errors bars that extend beyond the symbols are shown.

As conclusion, with these new protocols of engraftment, there is a saving in human blood consumption. When using 1x12h protocol, 1 ml of human blood can be saved per mouse and week. However, with the 2x12h protocol, only 0.5 ml of human blood can be saved.

Test different P. falciparum strains to study parasite kinetics and anaemia phase

During the anaemia phase in the GSK*Pf*Hu mouse model, there is a massively destruction of human erythrocytes, as shown previously. This fast clearance of the human erythrocytes could be due to the consumption of the hEry during the exponential growth of the *P. falciparum* $^{0087/N9}$ parasite. Different *P. falciparum* strains were studied in the GSK*Pf*Hu mouse model to test the capacity of these strains to provoke the anaemia phase in mice after infection.

Various *P. falciparum* strains of different genetic background have shown a different rate of growth. Seven different *Pf* strains have been selected to perform this experiment based on different characteristics: i) V1/S, which is derived from a human isolate in Vietnam, resistant to chloroquine, sulfadoxine, pyrimethamine and cycloguanil [26, 116]; ii) NF54, that comes from a patient isolate and is the parental of 3D7 strain [24, 118]; iii) D10, this strain was collected in Papua New Guinea [21, 32]; iv) Rap I, which is the D10 strain but with a truncation by transfection of the Ropthry protein 1 and 2 [16, 25]; v) K1, this strain has the same resistances as V1/S, but it was derived from a human isolate in Thailand [23, 31]; vi) FCR3, that show resistance to chloroquine, atovaquone and cycloguanil [22, 60] and vii) 3D7, used as the control of the experiment, and it is a clone from NF54 isolate by limiting dilution [20, 50]. *P. falciparum* strains used in this experiment were expanded in a in vitro culture prior to the adaptation *in vivo* in chimeric NSG mice by performing passages from mice to mice and intravenous infections until reproducible growth in all mice infected were obtained, as described before [5].

To perform the experiment, chimeric IL2 mice with at least 50% of human erythroytes in peripheral blood were injected by i.v. route with $20x10^6$ of infected erythrocytes of each strain. The percentage of parasitemia and human erythrocytes were measured by flow

cytometry at different time points from day 3 to at least day 25 after infection, to cover the anaemia phase that takes place around day 15 after infection in the 3D7 control strain.

When comparing the control strain with each of the other selected strains, we observe that the V1/S strain reaches a higher percentage of parasitemia, maximum peak at 30.85%, three times higher than the parasitemia peak in 3D7 (10.49%), as shown in figure 38A. Besides this increment of parasitemia in the V1/S, the clearance of human erythrocytes takes place at the same time and with a similar pattern that the 3D7 strain (figure 39A).

However, the Rap I parasitemia peak is two times higher the 3D7 control strain (23.15%), figure 38C. Moreover, the aneamia phase is delayed in mice infected with this strain, therefore human erythrocytes clearance begin at day 25 after infection, 39C. The anaemia phase is also delayed in the infection with the NF54 strain, figure 39B. But the parasitemia peak reached (6.08%) is almost half the parasitemia peak of the control strain (10.49%), figure 38B.

In three of the *Pf* strains studied: D10, FCR3 and K1 strains, the massive human erythrocytes clearance does not take place throughouth the experiment, figure 39C, 39E and 39F. Mice were euthanized at day 25 after infection, so there is not enough data to corfirm or reject that hEry clearance is supressed in the infection of these strains. The parasitemia peak in the D10 infection was similar to that found in the V1/S infection (29.64% and 30.85%, respectively). Whereas, the parasitemia peak for the FCR3 and D10 was lower to the peak in the control strain (3.77%, 7.3% and 10.49%, respetively), figure 38C, 38E and 38F.

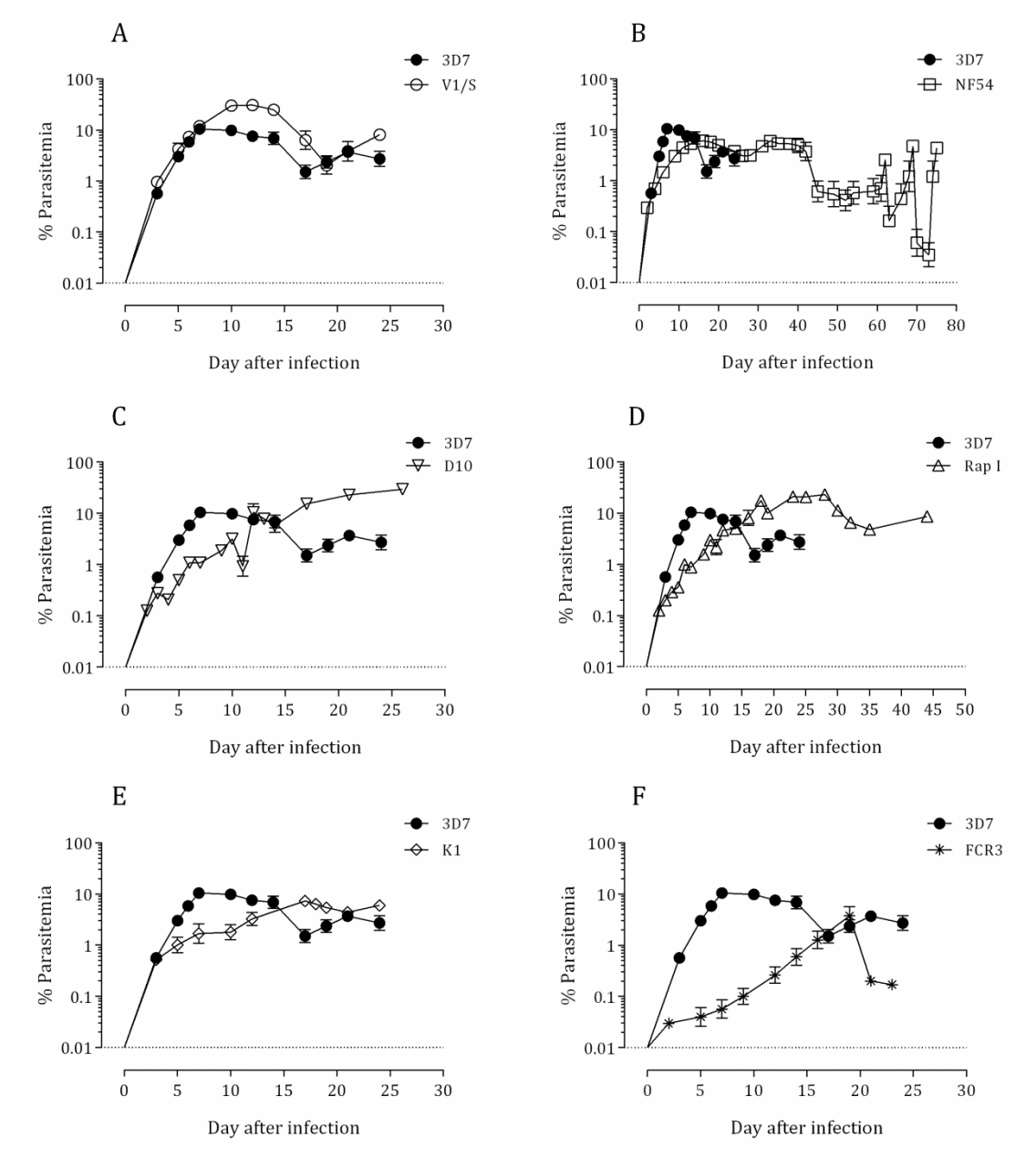

Figure 38. Parasite growth after infection in chimeric IL2 mice by i.v. with 20x10⁶ infected hEry at day 0 with different P. falciparum strains compared with the control strain 3D7 (close circles): V1/S (A), NF54 (B), D10 (C), RapI (D), K1 (E) and FCR3 (F). Data are the mean ± standard error mean of at least three mice in ecah Pf strain. Only errors bars that extend beyond the symbols are shown. The percentage of parasitemia was calculated by flow cytometry as SYTO-16⁺ and TER119-PE⁻ population.

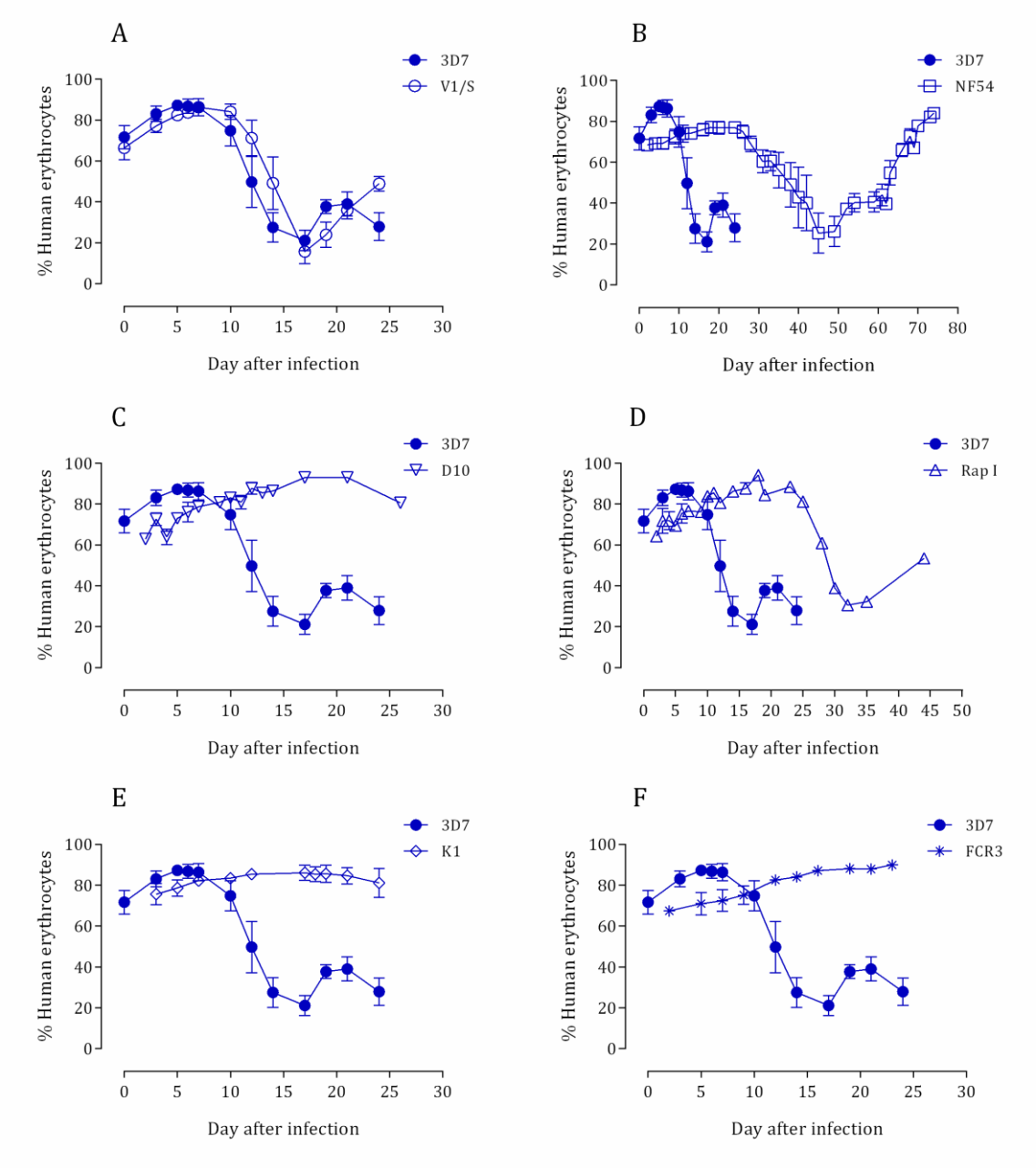

Figure 39. Dynamics of human erythrocytes after infection of chimeric IL2 mice by i.v. with 20x10⁶ infected hEry at day 0 with different P. falciparum strains compared with the control strain 3D7 (close circles): V1/S (A), NF54 (B), D10 (C), RapI (D), K1 (E) and FCR3 (F). Mice received daily i.p. injection of hEry throughout the experiment. Data are the mean ± standard error mean of at least three mice per strain. Only errors bars that extend beyond the symbols are shown. The measurement of percentage of human erythrocytes (TER119-PE⁻ events) was done by flow cytometry.

As a conclussion, three of the *Pf* strains studied also provoke the massive clearance of human erythrocytes in the GSK*Pf*Hu mouse model (anaemia phase), as the control strain 3D7. One of these strains, the V1/S resistant strain, cause the anaemia phase at the same

point as the control strain. By the contrary, the other two strains that cause anaemia showed a delay in the start of this phase when compared with the control strain (3D7). One of these strains is the NF54, which is the parental of the 3D7 strain, and the other is a modified strain that has a truncation in the ropthry protein (RapI).

Additionaly, for three of the strains studied (D10, FCR3 and K1) there are not enough data to jump to a conclusion about the presence or absence of the anaemia phase in infected mice.

Treatment with antiinflammatory drugs and macrophage depletors to reduce the human blood consumption

It has been shown that in the GSK*Pf*Hu mouse model there is an activation of macrophages in the different phases of the model, detected by the presence of inflammatory cytokines and by the study of the erythrophagocytosis in the spleen and peritoneum. To test if the GSK*Pf*Hu mouse model could be modulated through the inflammatory answer, different classes of anti inflammatory drugs were administered to mice in the different phases of the GSK*Pf*Hu mouse model (engraftment, infection and anaemia phase).

The drugs selected for this study were: i) Acetylsalicylic acid (Non-steroideal anti inflammatory drug); ii) Dexamethasone (Steroideal anti inflammatory drug); iii) Anti-GR1 (antibody that blocks granulated differentiation antigen-1). Based on the pharmacokinetics properties of the drugs, different doses regimes were chosen. ASA and Dexamethasone were administered daily by oral administration, whereas Anti-GR1 was administered every 48 hours by i.p. injection.

During the engrafment phase, IL2 mice received the anti inflammatory treatment as described above, starting the same day of the first human blood injection. Mice also received daily i.p. human blood injections throughout the experiment. This engraftment phase was studied during 14 days.

In engraftment phase, after studying the acquisition of chimerism curve (figure 40), we can observe that only the engraftment curve of mice which received the treatment of Dexamethasone at 30 mg/kg is significantly different to the untreated mice (1 way ANOVA; Dunnett´s multiple comparisons test of $AUCs_{0\rightarrow14}$, $p<0.05$).

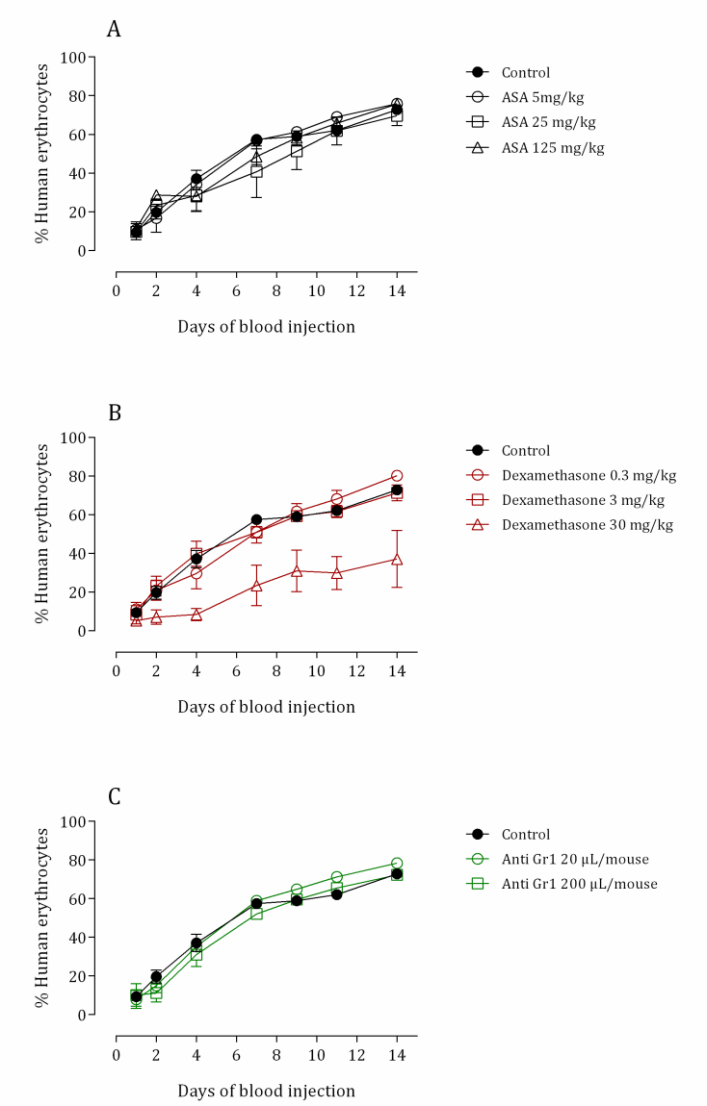

Figure 40. Comparison of kinetics of engratment with human erythrocytes in IL2 mice treated with anti inflammatory drugs: ASA, Dexamethasone and Anti GR1 (A, B and C, repectively) with the control group (no treatment). All mice were injected i.p. with hE daily throughout the experiment and were treated with the corresponding anti inflammatory drug. Data are the mean percentage ± standard error of the mean of four mice in each experimental group. Only errors bars that extend beyond the symbols are shown. Percentage of human erythrocytes was calculated by flow cytometry as TER119-PE- events.

After 14 days of engraftment, mice were infected. Parasite growth and anaemia phase were studied from day 0 to day 25 after infection (day of infection: day 0). During both phases mice received daily blood injections and were treated with anti inflammatory drugs. Comparing the engraftment curves (figure 41), it was revealed that all treatments, except Dexamethasone at 3 mg/kg, show similar parasite growth, without significant differences (1 way ANOVA; Dunnett´s multiple comparisons test of $AUCs_{0\rightarrow25}$, $p<0.05$).

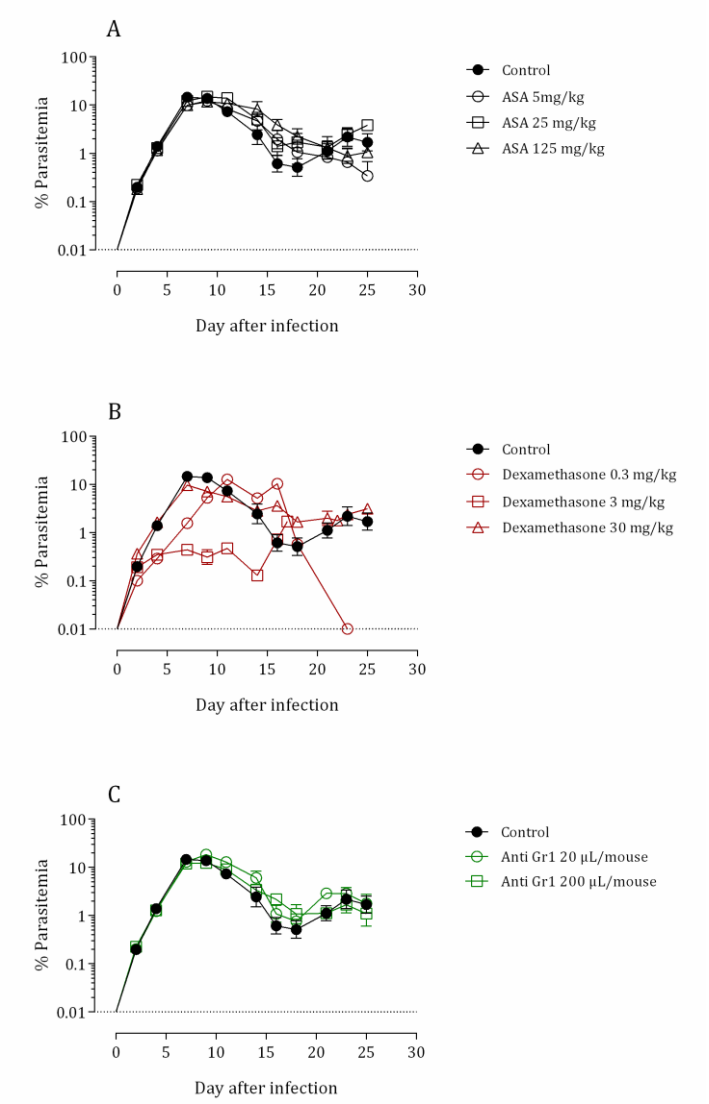

Figure 41. Comparison of parasite growth after infection by i.v. with 20x10⁶ infected hE at day 0 with P. falciparum (Pf3D7$^{0087/N9}$ strain) in IL2 mice treated with anti inflammatory drugs: ASA, Dexamethasone and Anti GR1 (A, B and C, repectively) with the control group (no treatment). All mice were injected i.p. with hE throughout the experiment and were treated with the corresponding anti inflammatory drug. Data are the mean ± standard error mean of four mice in each experimental group. Only errors bars that extend beyond the symbols are shown. The percentage of parasitemia was calculated by flow cytometry as SYTO-16⁺ and TER119-PE⁻ population.

When studying human erythrocytes clearance during infection and anaemia phase, we can observe that the massive hEry clearance is showed under all treatments with anti inflammatory drugs (figure 42). Although there are visual differences in the curves, the 1 way ANOVA test of the $AUCs_{0\rightarrow25}$ revealed that there are no significant differences among the treatments when compared with the control curve ($p<0.05$).

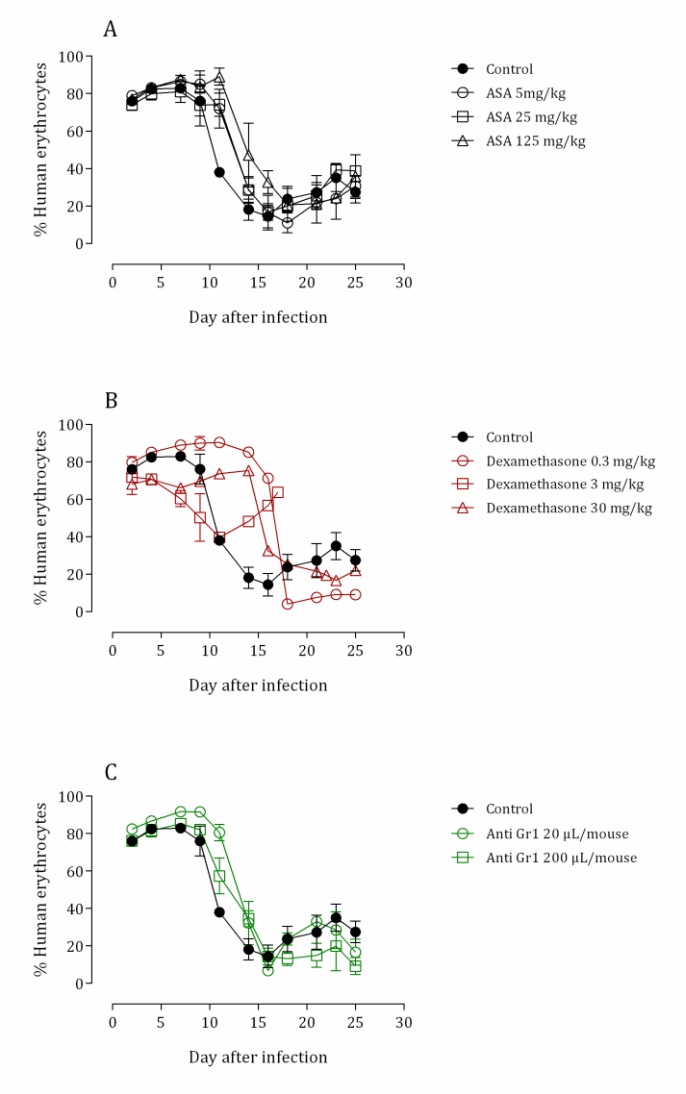

Figure 42. Comparison of the dynamics of human erythrocytes from day 0 to day 25 after infection of IL2 mice treated with anti inflammatory drugs: ASA, Dexamethasone and Anti GR1 (A, B and C, repectively) with the control group (no treatment). Mice received daily i.p. injection of hE throughout the experiment and were treated with the corresponding anti inflammatory drug. Data are the mean ± standard error mean of four mice per experimental group. Only errors bars that extend beyond the symbols are shown. Percentage of human erythrocytes was calculated by flow cytometry as TER119-PE- events.

As a conclusion, none of the treatments with anti inflammatory drugs inhibited the engrafment of IL2 mice with human erythrocytes, neither the growth of *P. falciparum* in these mice nor the massive clearance of hEry after infection with the parasite. Mice treated with Dexamethasone developed ascitis in the peritoneum, probably due to the lack of cleaning by the macrophages in the peritoneum after i.p. injections of hEry.

Figure 43. Kinetics of human erythrocytes after i.p. injection of 1 ml of human blood (50% hematocrit) in IL2 splenectomized (open cirlces) and non-splenectomized (close circles) naïve mice, within the first 24 hours (A) and complete kinetic until clearance of hE (B). Data are the the mean ± standard error of five mice sampled at different time points. Only errors bars that extend beyond the symbols are shown. Quantification of human erythrocytes (TER119-PE- events) was done by flow cytometry using Trucount™ tubes.

Test different mice strains to improve the engraftment with human erythrocytes

One of the limiting factors in the engraftment process is the human blood. In order to improve the model and avoid the anaemia phase after the infection with the parasite, different backgrounds of immunodeficient mice were selected to study the engraftment with human erythrocytes, the infection with the parasite *P. falciparum* 3D7 and the anaemia phase. Four different mouse strains were tested and compared with the IL2 control strain: i) Rag2IL2 (lack T, B, NK cells); ii) NOG (lack T and B cells, and decrease NK cells activity); iii) FRG (lack T and B cells, defect in macrophage regulation and NK activity, induced liver disease and liver was reconstituted with 80% of human hepatocytes); and iv) NRG (lack T, B, NK cells). At least 7 mice of each strain (except FRG strain, that experiment was done with only 2 mice), were injected i.p. daily with 1 ml of human blood (50% hematocrit). When mice achieved ~70% of human erythrocytes in peripheral blood, they were infected by i.v. route with $20x10^6$ infected erythrocytes. Parasite growth was studied at least until day 31 after infection to observe the presence or absence of the anaemia phase (massive hEry clearance) in the different mice strains.

During the engraftment with human erythrocytes, results show that NOG, FRG and NRG strains supports the xenotransplant with human erythocytes and can achieve~70% of hEry in mice peripheral blood in around 20 days (figure 44B, 44C and 44D). However, hEry did not reach mice peripheral blood in Rag2IL2 mice (figure 44A).

Mice splenectomy to study xenotransplant rejection

As shown previously, in the *in vivo* erythrophagocytosis study, in the spleen there are active macrophages populations that are in charge of the clearance of hEry in the different phases of the GSK*Pf*Hu mouse model. The excision of the spleen may lead to a decrease in the number of hEry clearance. To confirm this hypthesis the kinetics of hEry after an unique i.p. injection of human blood was sudied in IL2 mice without spleen (quirurgically excised), and was compared with IL2 mice with spleen.

A group of five mice were splenectomized three weeks before starting the experiment, in other to study the role of the spleen in the initial steps of the human erythrocytes xenotransplant in the GSK*Pf*Hu mouse model.

Kinetics of hEry after i.p. dosing were studied until 92 hours after injection. Results show that in the first twelve hours, in which the acquition of hEry through the peritoneum takes place, there are a slight difference between splenectomized and non-splenectomized mice (figure 43A). This difference is not statistically significative (Mann Whitney test, $p<0.05$). In addition, after hEry reaches the maximum peak in mice peripheral blood (after 12 hours, in both cases), hEry are cleared at the same speed in splenectomized and non-splenectomized mice (30.2 and 31.4 hours, respectively) as shown in figure 43B.

To conclude, kinetics of hEry after i.p. injection are very similar in splenectomized mice when compared with non-splenectomized mice. This result confirm that the spleen may not be the main organ involved in the fast clearance of hEry that occurs after the release of these erythrocytes in mice peripheral blood from a i.p. injection of human blood (50% hematocrit).

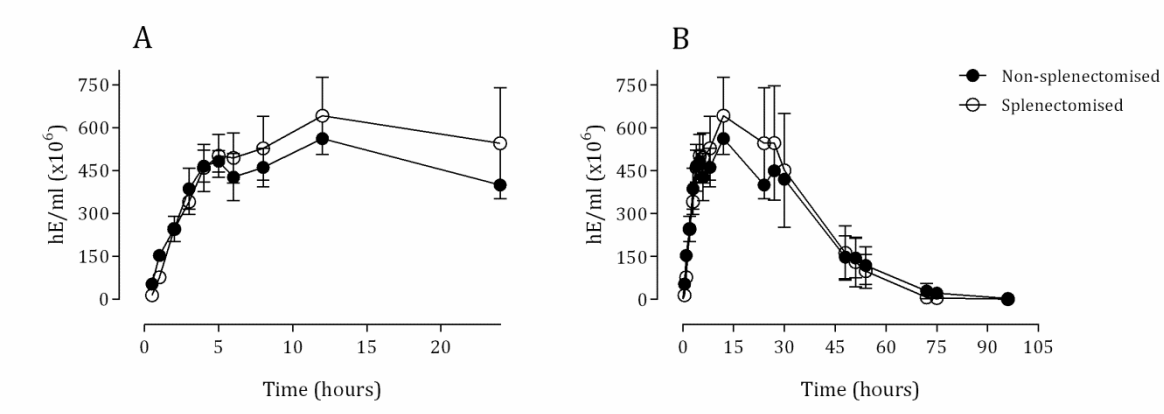

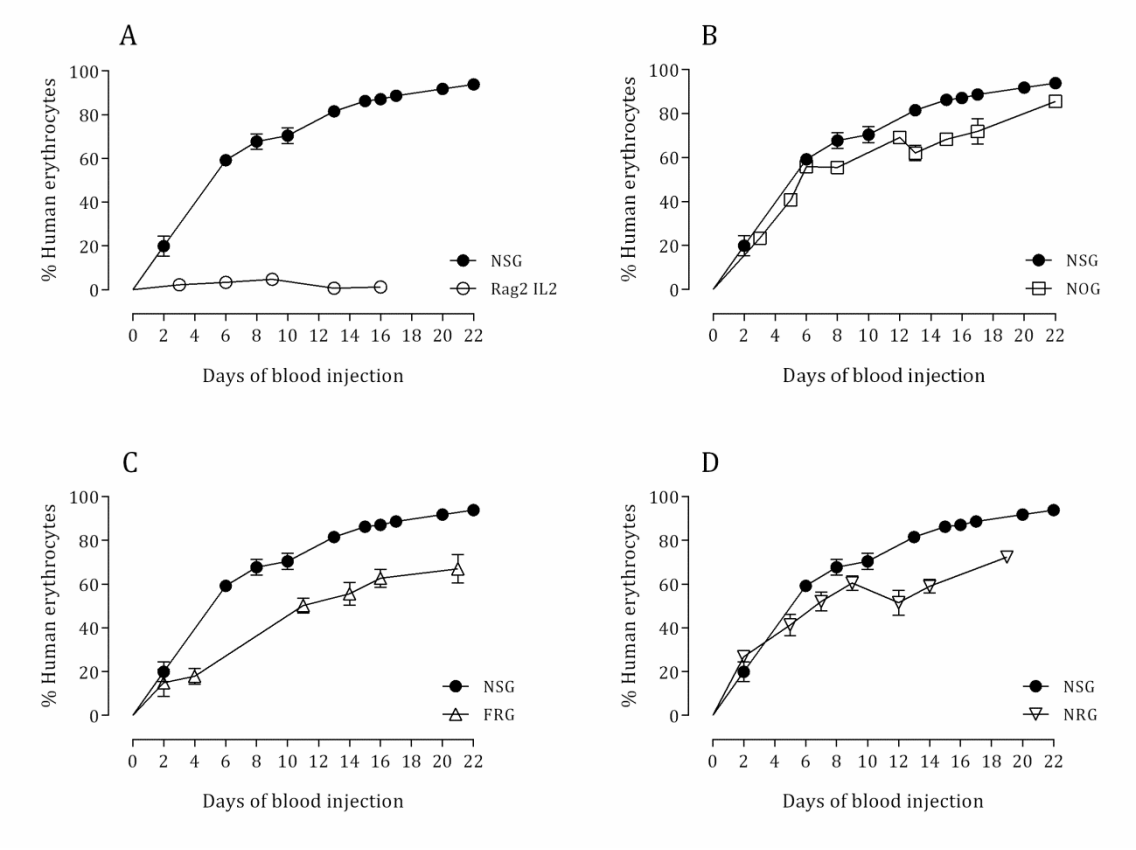

Figure 44. Kinetics of engraftment with human erythrocytes in different mice strains: Rag2 IL2 (A), NOG (B), FRG (C) and NRG (D), compared with the control IL2 mice strain (close circles). Data are the mean ± standard error mean of at least 10 mice of each strain, except FRG mice which data belong to two mice. Only errors bars that extend beyond the symbols are shown. Percentage of human erythrocytes was calculated by flow cytometry as TER119-PE- events.

Further studies were done with the Rag2 IL2 strain, to understand the absence of hEry in peripheral blood. Rag2IL2 mice received an unique i.p. and i.v. injection of hEry and kinetics of absortion and clearance was studied and compared with that obtained in IL2 mice (figure 45). Clearance of hEry after i.v. injection is slightly faster in Rag2IL2 mice, 6.97±1.11 hours (n=5) of half life, compared with IL2 mice, 10.75±1.52 hours (n=5) as shown in figure 45A. When studying the i.p. injection it was observed that Rag2 IL2 mice clearance of human erythrocyes after the release in peripheral blood is much faster than the observed in IL2 mice (half life of hEry 15.7 and 57.1 hours, respectively), figure 45B. In addition, hEry are completely cleared from mice peripheral blood 48 hours after i.p. injection in Rag2IL2 mice. Whereas in IL2 mice, this total clearance of hEry is achieved 96 hours after the i.p. injection. This results suggests that macrophage activity may be increased in Rag2IL2 strain. As a result, human erythrocytes cannot be accumulated in

mice peripheral blood, so neither engraftment with human erythrocytes nor infection with *P. falciparum* can not be achieved in this mice strain.

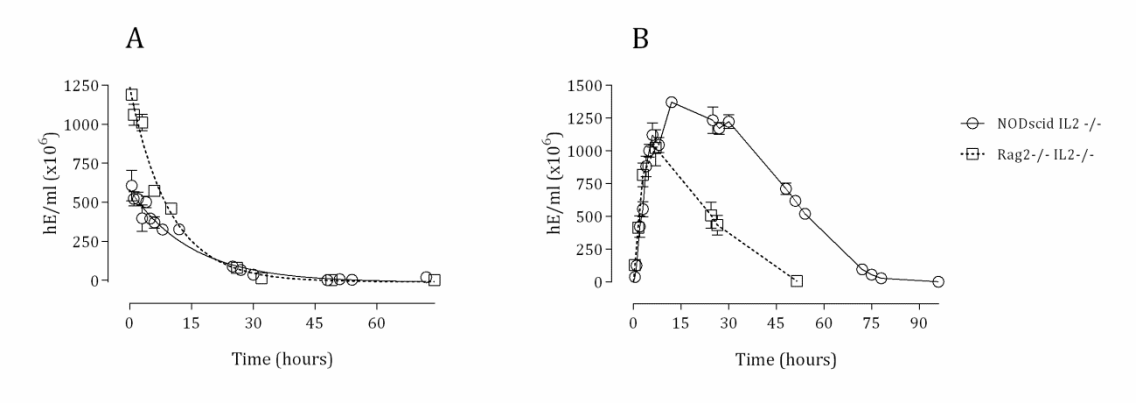

Figure 45. Kinetics of human erythrocytes after i.v. (A) and i.p. (B) injection of human erythrocytes in Rag2 IL2 (open square) and IL2 mice (open circles). Data are the mean ± standard error of five mice (except Rag2 IL2 i.p. that was done with three mice, sampled at different time points. Only errors bars that extend beyond the symbols are shown. Quantification of human erythrocytes (TER119-PE- events) was done by flow cytometry using Trucount™ tubes.

When studying parasite growth in the different mice strains infected (NOG, FRG and NRG), parasite growth can be mantained in mice peripheral blood for 31 days after infection in NRG (figure 46C), 34 days in FRG (figure 46B) and 51 days in NOG mice (figure 46A). Parasite peak of parasitemia is similar in NRG and NOG mice strains compared with the control IL2 strain, around 10%. However, FRG mice parasitemia was variable in each mouse studied, one reached 9% of parasitemia peak, but the other did not reach a parasitemia higher than 1%. No robust data could be obtained due to the size of the population studied. In addition, in this strain, parasite was almost cleared completely when the massive hEry clearance took place, around day 20 after infection.

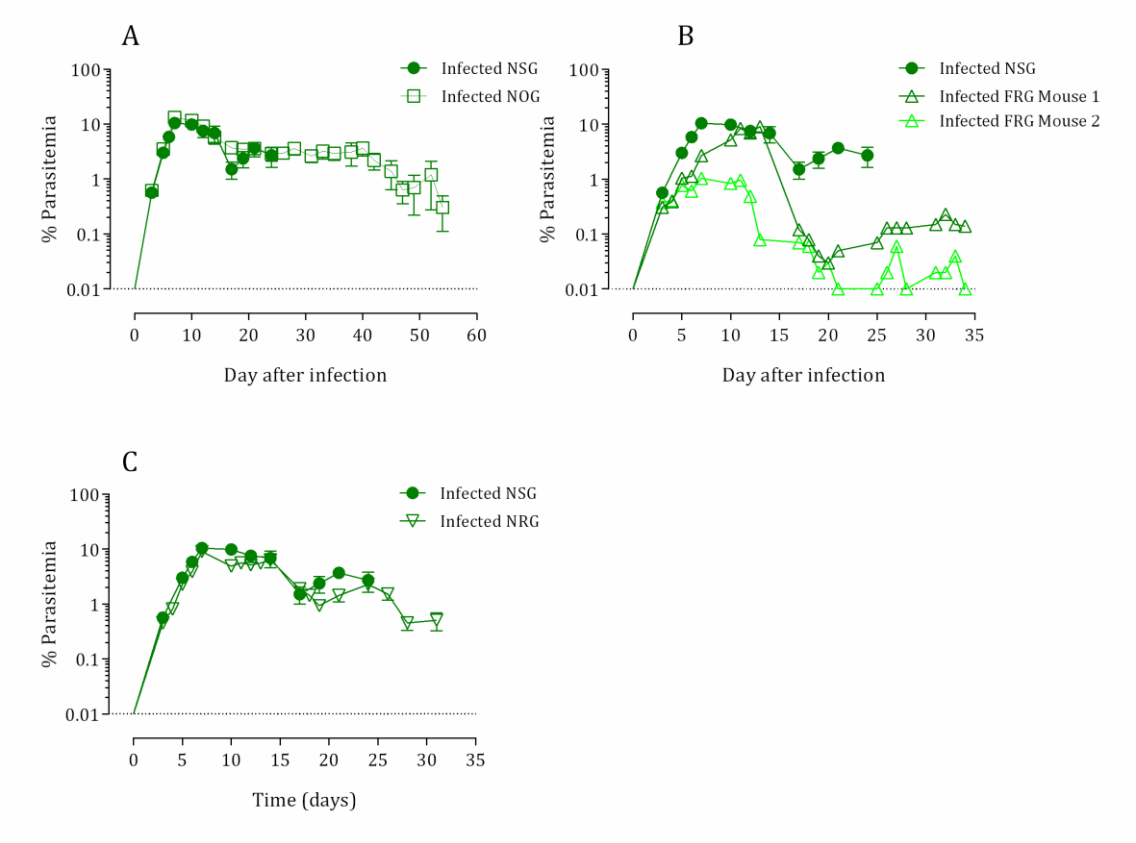

Figure 46. Parasite growth after i.v. infection of 20x10⁶ infected hEry in chimeric NOG (A), FRG (B) and NRG (C) mice strains compared with the control IL2 mice strain (close circles). Data are the mean ± standard error mean of at least 10 mice of each strain, except FRG mice which data belong to two mice. Only errors bars that extend beyond the symbols are shown. The percentage of parasitemia was calculated by flow cytometry as SYTO-16⁺ and TER119-PE⁻ population.

During the infection of *P. falciparum* parasite, around day 10 after infection, massive hE clearance took place in all mice strains studied (figure 47). The starting point of the anaemia phase was similar to that found in the IL2 control strain.

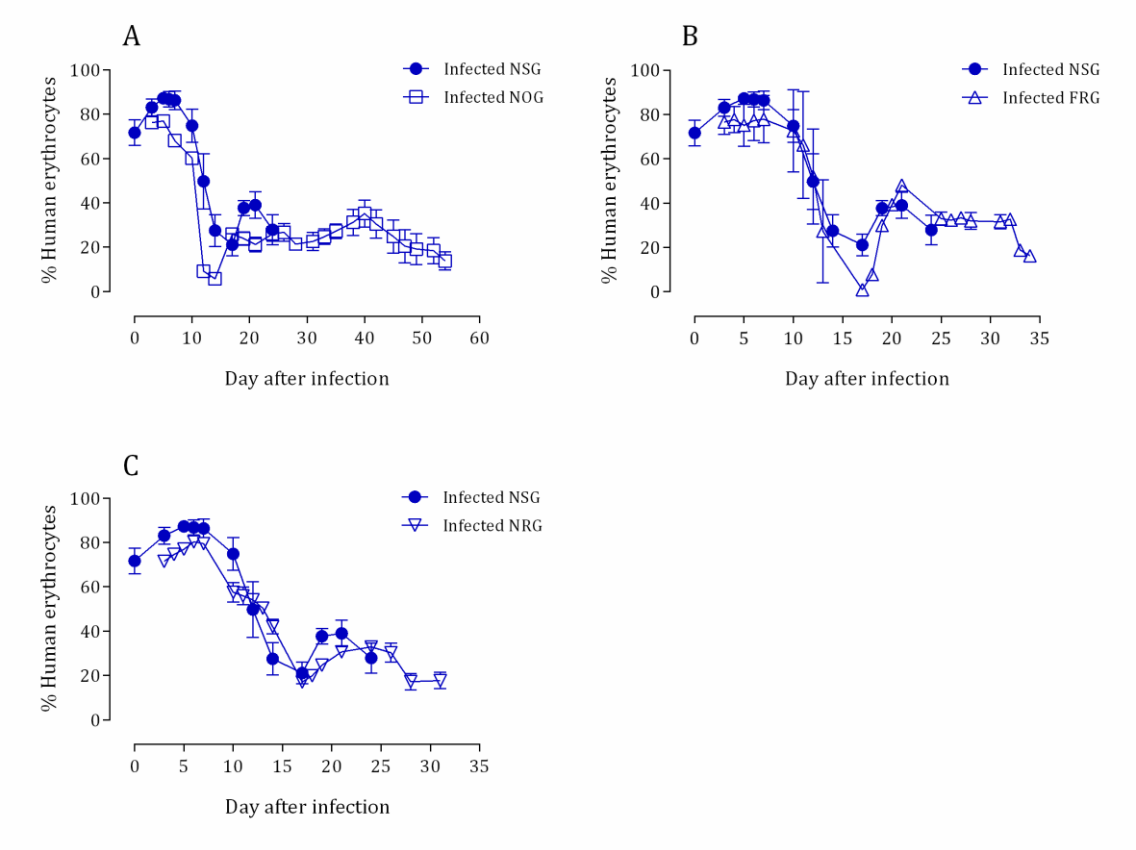

Figure 47. Dynamics of human erythrocytes after infection of chimeric NOG (A), FRG (B) and NRG (C) mice, with i.v. injection of 20x10⁶ infected hE at day 0, compared with the control IL2 mice strain (close circles). Mice received daily i.p. injection of hE throughout the experiment. Data are the mean ± standard error mean of at least 10 mice of each strain, except FRG mice which data belong to two mice. Only errors bars that extend beyond the symbols are shown. The measurement of percentage of human erythrocytes (TER119-PE⁻ events) was done by flow cytometry.

In conclusion, kinetics of hE engraftment and *P. falciparum* infection in NOG, FRG and NRG mice strain are similar to the IL2 control strain used in the GSK*Pf*Hu mouse model. Thus, these mice strains can also be used as a *P. falciparum* malaria mouse model. In addition, in the different immunodeficent genetic backgrounds studied the massive hEry clearance is also observed.

The GSK*Pf*Hu mouse model as a researching tool

A reliable humanized model for erythrocytic stages of *Plasmodium falciparum* has been developed, which shows a reproducible model of infection. The GSK*Pf*Hu mouse model share some features with the infection of the *P. falciparum* parasite in the human host such as 48 hours erythrocytic cycle and a Severe Anaemia phase, which can not explained by the parasite growth.

Due to this characteristics and the reproducibility of the infections, we can affirm that this model can be used as a valuable tool to study different aspects of the pathophisiolgy of the infection with the human parasite *P. falciparum*, for the test of new drugs against malaria disease and many other applications that need a metabolic activity of the parasite or the host.

The evaluation of drugs for malaria treatment or drug development, so as studies on transmission to the mosquito host are part of the applictions that have been explored in this work.

Drug discovery

The emergence of parasite drug resistance to currently deployed antimalarials used such as chloroquine and artemisinin containing treatments, requires the urgent development of new medicines to replace the failing ones. Also, the commitment of the WHO to eradicate this disease have made possible to fund new projects to discover and develop a new generation of antimalarials with a differentitated mode of action. In the drug discovery process the animal models have been crutial to perform the efficacy assays needed in the preclinical steps of the drug development. In the case of the malaria, the most widely model used is based in a rodent pathogen, *Plasmodium berghei*, due to the limitations in the use of primates for the test of the new drugs in a human parasite. Therefore, the development of mouse models for the infection of the human *Plasmodium* parasite has been a major breakthrough in the malaria drug discovery field.

The GSK*Pf*Hu mouse model of *P. falciparum* asexual erythrocytic stages has played a crutial role in development of new drugs against malaria.

The routinary test used for validation purposes was based on the Peters´4-day test with minor modifications [114]. Briefly, the Peters´4 day test consist in the administration of compounds starting from one to three hours after the infection, treatment is performed during 4 consecutive days once a day administration, the resulting parasitemia is measured on the fifth day after infection (24 hours after the last dose administration), and

compared to the vehicle-treated controls. The test that is performed with the GSK*Pf*Hu mouse model is denominated 4-day test and differs from the original Peters´ test in the starting parasitemia, mice are infected 3 days before treatment starts ($20x10^6$ infected erythrocytes inoculum), to obtain a parasitemia detectable at the time of the first administration dose. In addition, parasitemia is measured every day of treatment and 24 hours after finishing the treatment or day 7 after infection (figure 48). Parasitemia is measured by flow cytometry, this technique requires very small blood samples (less than 5 µl) and do not interfere with the evaluation of efficacy in vivo. At the same time that the efficacy assay is performed, blood samples for the measurement of compound levels is blood are taken from mice peripheral blood the first 24 hours of treatment at different time points, depending on the PK properties of the compounds, but a general sampling scheme is adopted (0.5, 2, 4, 6, 8 and 24 hours). The measurement of the Pharmacokinetics of the administered compounds is crutial to increase the knowledge about the efficacy of the compounds, it can give a clue if a compund do not show efficacy and it can be measure how long a compound is present in mice peripheral blood. Therefore, the 4-day test performed in the GSK*Pf*Hu mouse model is a simple assay wich allows to obtain concomitant information on pharmacokinetics (PK) and parasitological effects, pharmacocynamics (PD), of the compounds administered.

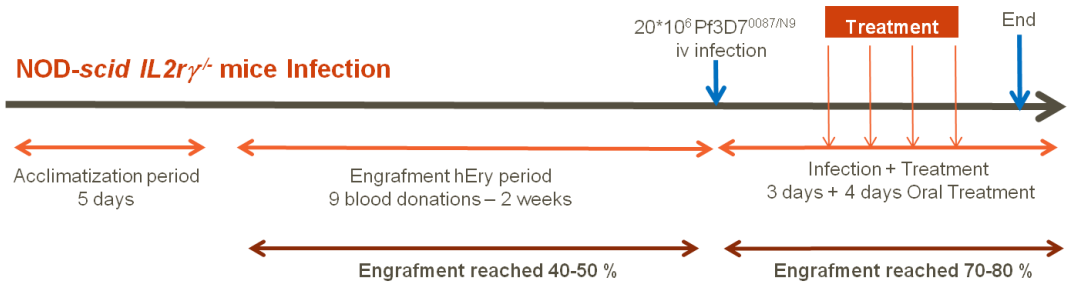

Figure 48. Schematic representation of the complete experimental process for a 4-day test assay. First mice received in the facilities are acclimatization period of 5 days, then the engraftment process starts and lasts 2 weeks until mice are infected with $20x10^6$ infected parasites. At day 3 after infection, treatment with antimalarial drugs starts and mice receive one dose for 4 consecutive days. Finally, parasitemia is measured every day and 24 hours after finishing the treatment to establish the parasite clearance curve.

The compound therapeutic efficacy can be expressed as the effective dose (mg of compound per kg of mouse body weight) that reduced parasitemia by 50% or 90% with respect to the vehicle-treated control group. Therefore, typical efficacy parameters calculated are the ED_{50}, which is the effective dose where half of the parasite population is cleared by the treatment and currently is not very used in drug discovery, and the ED_{90}, which in this case is the effective dose that clears 90% of the parasites under treatment. In addition, when the compound levels are analyzed simultaneously with the parasite clearance, another parameter can be estimated, the $AUCED_{90}$, which consist in the quantity of compound in blood per hour needed to clear the 90% of parasites in peripheral blood.

The ED_{90} and $AUCED_{90}$ parameters obtained are very useful in the critical path of drug discovery to prioritize or stop a compound development to the next step. However, the final endpoint of an efficacy assay should be the non-recrudescent dose or the cure of the animal after the treatment. Recrudescence refers to the emergence of asexual parasites belonging to the same population that gave rise to the primary infection. Recrudescence can be due to incomplete or inadequate treatment as a result of drug resistance of improper choice of drug dose. The WHO values for non-recrudescent compound in malaria is the dose at which there no detectable parasite is observed 28 days after treatement is finished. For this reason, after the 4-day test against *P. falciparum* is performed, those doses that have been enough efficacious (parasite not detectable or less than 0.3%) are kept for a recrudescence period of 28 days after finishing the treatment, in which mice receive alternative human blood injections due to the low clearance of hEry observed in the absence of parasite. This non-recrudescent dose obtained after the assay is a valuable data for the human dose predictions before the clinical assays take place.

Two examples for a 4-day test with a recrudescence study of drugs in clinical use have been detailed in this work for a better understanding of the efficacy assay. The first compound selected is Atovaquone, which is a selective inhibitor of cytochorme bc_1 from the electron transport chain present in *P. falciparum* mithocondria [15]. Briefly, IL2 engrafted mice were infected with $20x10^6$ infected erythrocytes at day 0 of the assay. Then, treatment with different doses of Atovaquone started at day 3 after infection (0.01, 0.05, 0.1, 1 and 10 mg/kg), mice received 4 oral doses once a day according to their body weight (20 ml/kg). Samples from mice peripheral blood were taken every day from day 3 to 7 after infection to measure parasitemia by flow cytometry (SYTO-16/TER119-PE). In addition, blood samples for the measurement of atovaquone concentrations were collected over the first 24 hours after dosing to establish the pharmacokinetics/pharmacodynamics (PK/PD) relationship. Chloroquine was used as a

reference drug and was used orally at 10 mg/kg, with the same treatment schedule. Mice were also dosed orally with 1% Methylcellulose as a control of parasite growth. Finally, at day 7 (24 hours after finishing treatment), mice which received efficacious doses were left for a recrudescence study.

The therapeutic efficacy of Atovaquone against P. falciparum is shown in figure 49A. The parasite clearance by Atovaquone treatment is low, at day 7 parasite is still detectable by flow cytometry (limit of detection: 0.01%). The parasites grow exponentially in infected control animals and the same level of growth was observed in the experimental group of 0.01 mg/kg/day. However, maximum parasite clearance occurred at or slightly above a dose of 0.1 mg/kg/day (figure 49A). Regarding to the drug exposures, there was a dose dependent behaviour with a half life of Atovaquone longer than the 23 hours duration of observation (figure 49B). Nevertheless, the drug exposure for the lowest dose (0.01 mg/kg) was under the limit of detection of the technique (2.5 ng/ml).

The parameters of efficacy estimated in the study are the ED_{90} and the $AUCED_{90}$. The ED_{90} is calculated by a non-linear fiting to sigmoid dose-response curve of log10 of percentage of parasitemia at day 7 after infection versus the dose (figure 49C). The $AUCED_{90}$ is used to estimate the potency and it is determined by non-linear fiting to a sigmoid dose-response curve of log10 of percentage of parasitemia at day 7 after infection versus the area under the curve of levels of compound obtained during the first 23 hours after the first administration, it is assumed that the accumulation during the treatment has not significant effect (figure 49D).

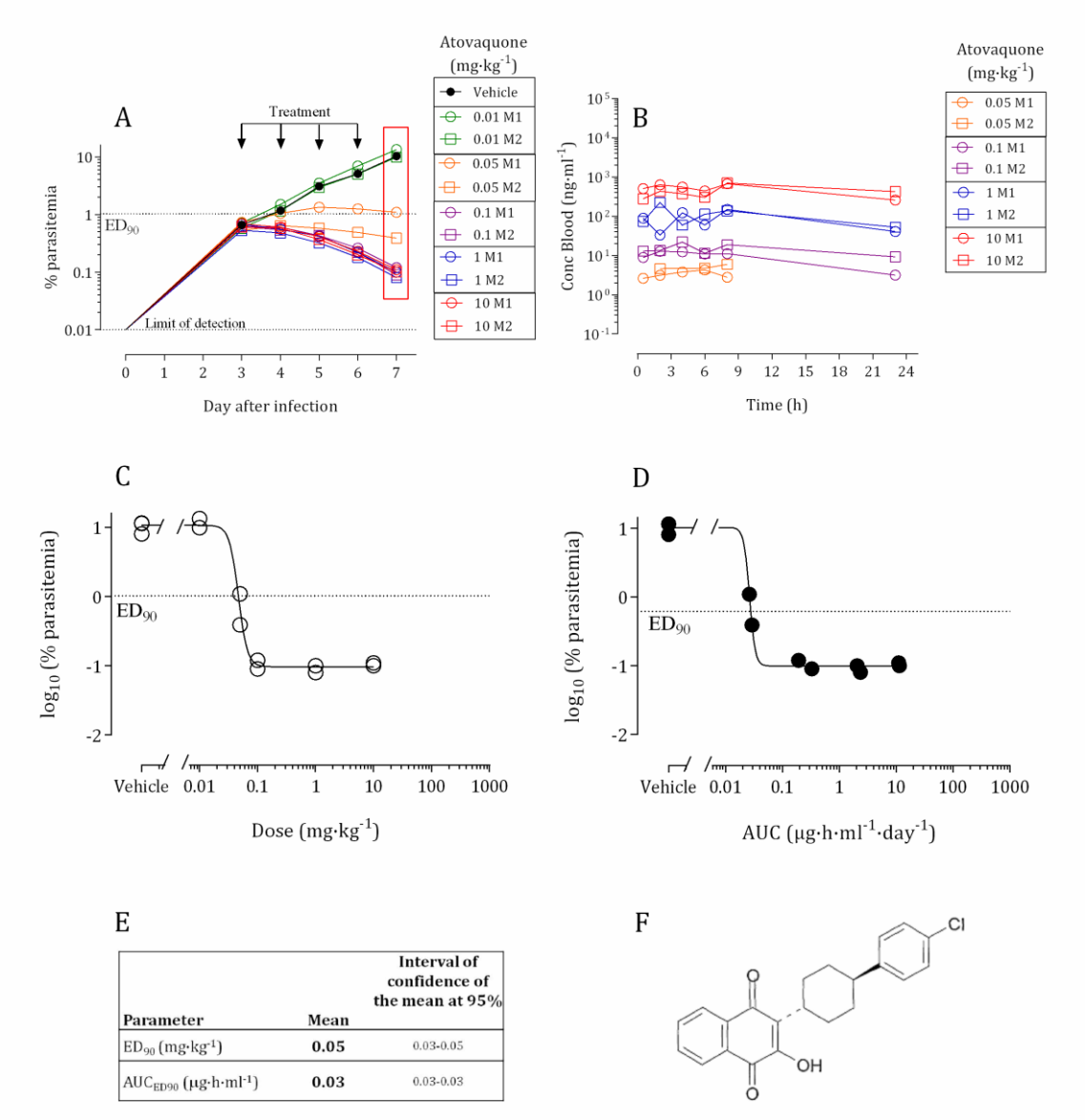

Figure 49. Therapeutic efficacy of Atovaquone in a 4-day test against P. falciparum 3D7$^{0087/N9}$ in GSKPfHu mouse model. In A it is represented the evolution of the percentage of parasitemia throughout the experiment, from day 3 (starting treatment) to day 7 (24 hours after finishing the treatment), data inside the red rectangle are used for the estimation of efficacy parameters. In B it is represented the levels of compound measured in mice blood during the first 23 hours of treatment. In C it is represented a sigmoideal dose-response used for the calculation of the efficacy parameter ED_{90} (log of %parasitemia at day 7 against log of doses administered to mice). In D it is represented a sigmoideal dose-response used for the estimation of the efficacy parameter $AUCED_{90}$ (log of %parasitemia at day 7 against log of AUC of the levels measured for compounds at the different doses). In E it is resumed the results of the efficacy parameters calculated for Atovaquone (F). Data represented are

individual data for two mice for each dose and the mean±SEM of three mice in the case of the vehicle treated group.

The efficacy parameters estimated for the Atovaquone are: ED_{90} = 0.05 mg/kg and $AUCED_{90}$ = 0.03 mg·h/ml, which means that for killing the 90% of the parasite in mice blood it is needed a four day dose treatment of 0.05 mg/kg or a mantained drug level in blood of 0.03 μg/ml every hour and day of treatment (figure 49E).

These results mean that around 10% of parasite is still alive after the treatment, for instance, 0.05 mg/kg is not a curative dose. To determine a curative dose in a 4-day test, it is needed a complementary recrudescence assay. The recrudescence is the final endpoint of an efficacy assay in which it is calculated the non-recrudescent dose or cure. To obtain this value, mice treated with the doses that reduced the parasitemia below 0.3% at day 7, were monitored for up to 28 days after finishing the 4-day treatment to observe the emergence of parasites in mice peripheral blood. The recrudescence period has been considered based on the assumption that if only one parasite is left in mice blood after finishing the treatment, 28 days are enough to observe growth by flow cytometry. In the case of the Atovaquone, parasite was detected in all doses before 28 days after treatment was acomplished, in the highest dose (10 mg/kg) parasite was detected at day 17 after finishing treatment (figure 50). However, although the clearance of the parasite during the treatment was the same from at the three highest doses (0.1, 1 and 10 mg/kg), differences are observed in the recrudescence period. Indeed the dose of 0.1 mg/kg did not cleared the parasite below the limit of detection at day 10 after infection, whereas the doses of 1 and 10 mg/kg completed the clearance of the parasite and entered into the recrudescence study. Finally, at the dose of 1 mg/kg the parasite growth was detected earlier than the dose of 10 mg/kg (figure 50). In conclusion, among the regime of doses used in the efficacy study of the Atovaquone: 0.01, 0.05, 0.1, 1 and 10 mg/kg there is no a curative dose.

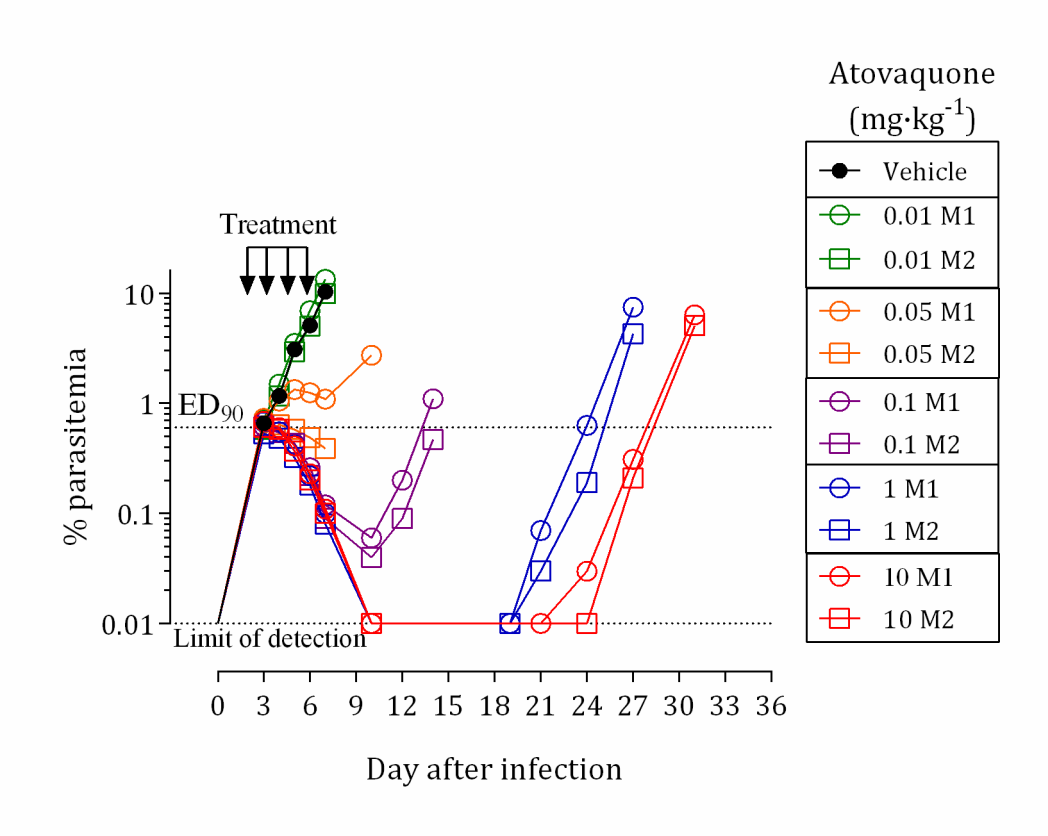

Figure 50. Recrudescence study for Atovaquone. Data represented is the percentage of parasitemia measured by flow cytometry from day 3 to day 34 after infection, when recrudescence study is concluded (day 27 after finishing treatment). Data are the individual parasitemia data for two mice for each dose and the mean±SEM of three mice in the case of the vehicle treated group.

The effect of drugs on the parasite population can be characterized by a detailed analysis of flow cytometry results.. The SYTO-16/TER119-PE staining can be used for a phenotypical study of the parasite populations affected by the treatment. The flow cytometry data suggest that the intracellular parasite can develop to a late-stage parasite after Atovaquone treatment but fails to form daughter merozoites and to propagate to the next generation (figure 51). This drug response is consistent with the primary activity of Atovaquone, which inhibits electron transport in the mithocondria but ultimately kills *Plasmodium* through downstream effects on pyrimidine synthesis. These studies have important implications for further understanding the mechanism of action of antimalarials.

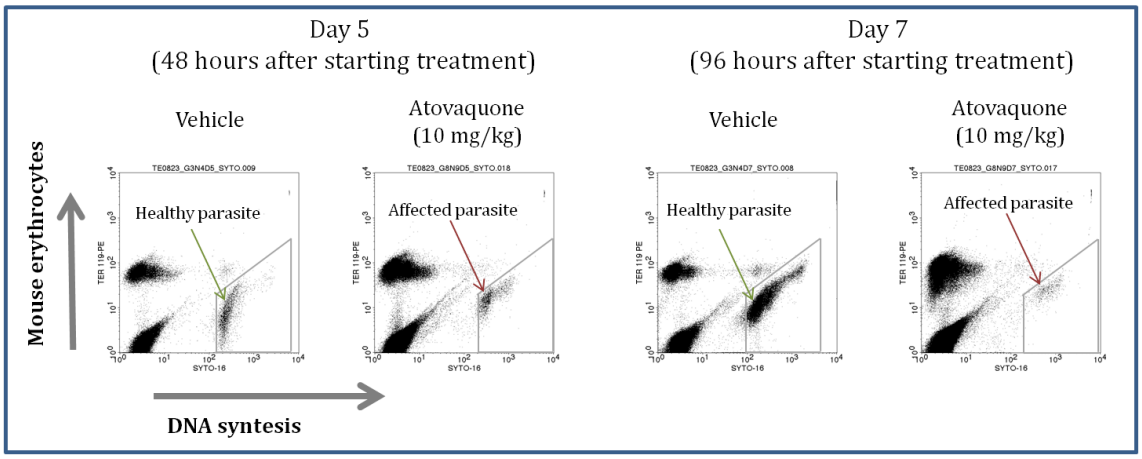

Figure 51. Atovaquone 4-day test flow cytometry dot plots. In the X axis of the dot plots it is represented the fluorenscence of the DNA dye SYTO-16, more fluorescence intensity means more quantity of DNA. In the Y axis it is represented the monoclonal antibody TER119-PE which detects mouse erythrocytes.

The second compound selected is Piperaquine, which is a compound that belongs to the aminoquinolone family which mecanism of action is based on the interference with the digestion of the hemoglobine by the parasite and targets the food vacuole of the trophozoite stage [127]. The therapeutic efficacy assay was performed as described for Atovaquone. Mice were dosed orally at 1, 5, 10, 25, 50 and 100 mg/kg for four consecutive days.

In this case, the Piperaquine parasite clearance is fast, at the highest doses tested (25, 50 and 100 mg/kg) parasitemia is under the limit of detection of the flow cytometry technique (0.01%) at day 5 after infection. However, the doses of 5 and 10 mg/kg obtained a parasite clearance at day 6 and 7, respectively. In addition, the parasitemia increased in a exponential manner at the lowest dose tested (1 mg/kg), comparable to the same growth in the infected vehicle-control mice. Of note, a dose dependent response was observed in treated mice (figure 52A). Regarding to the blood levels, it was observed a dose dependent behaviour with a half life longer than the 23 hours duration of observation (figure 52B). The ED_{90} and the $AUCED_{90}$ were estimated (figure 52C and D).

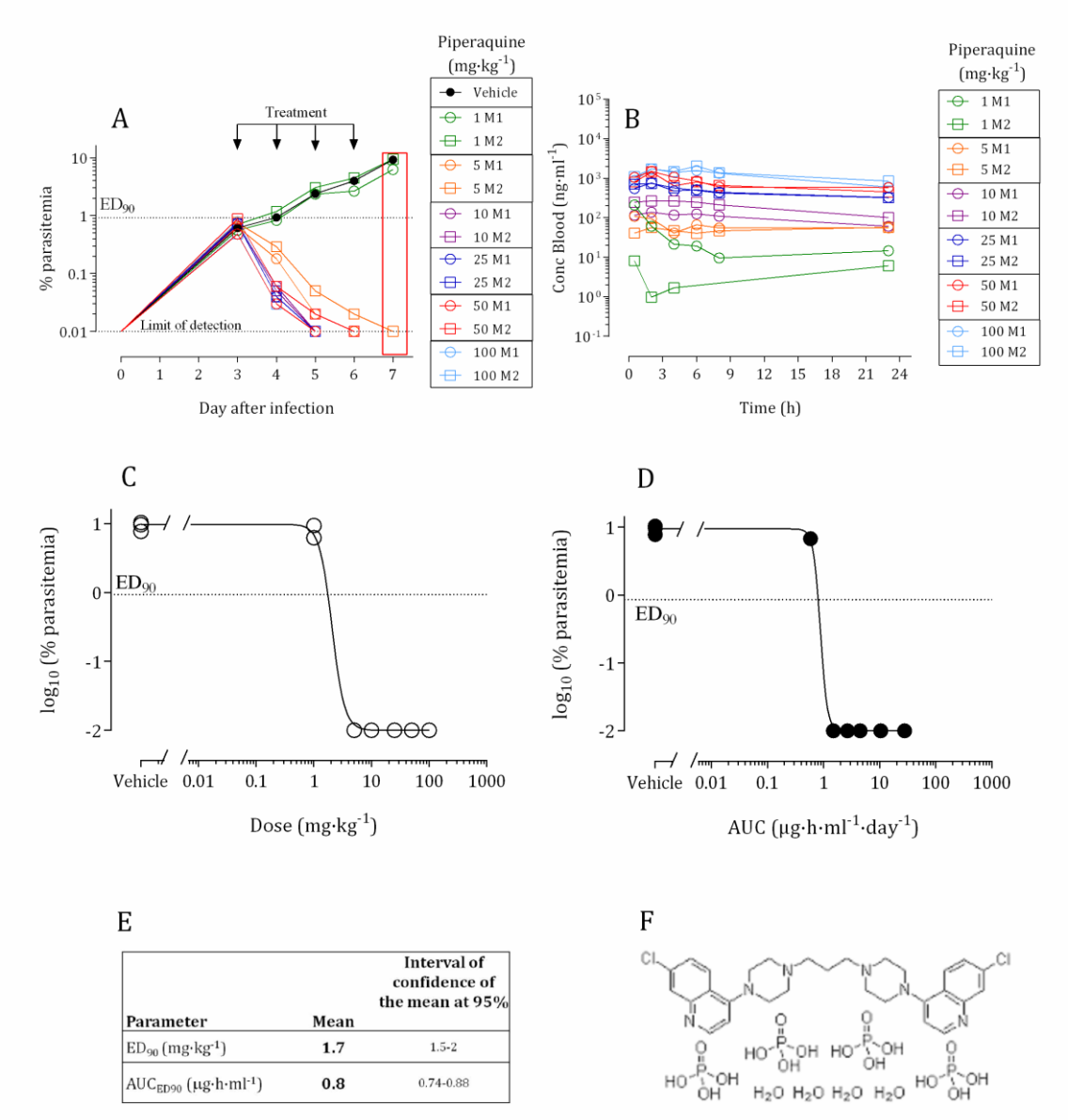

Figure 52. Therapeutic efficacy of Piperaquine in a 4-day test against P. falciparum 3D7$^{0087/N9}$ in GSKPfHu mouse model In A it is represented the evolution of the percentage of parasitemia throughout the experiment, from day 3 (starting treatment) to day 7 (24 hours after finishing the treatment), data inside the red rectangle are used for the estimation of efficacy parameters. In B it is represented the levels of compound measured in mice blood during the first 23 hours of treatment. In C it is represented a sigmoideal dose-response used for the calculation of the efficacy parameter ED_{90} (log of %parasitemia at day 7 against log of doses administered to mice). In D it is represented a sigmoideal dose-response used for the estimation of the efficacy parameter $AUCED_{90}$ (log of %parasitemia at day 7 against log of AUC of the levels measured for compounds at the different doses). In E it is resumed the results of the efficacy parameters calculated for Piperaquine (F). Data represented are

individual data for two mice for each dose and the mean±SEM of three mice in the case of the vehicle treated group.

The efficacy parameters estimated for the Piperaquine are: ED_{90} = 1.7 mg/kg and $AUCED_{90}$ = 0.8 μg·h/ml, which means that for killing the 90% of the parasite in mice peripheral blood it is needed a four day dose treatment of 1.7 mg/kg or a mantained drug level in blood of 0.8 μg/ml every hour and day of treatment (figure 52E).

To determine a curative dose for the Piperaquine in a 4-day test, a recrudescence assay was done. Mice treated with the doses that reduced the parasitemia below 0.3% at day 7, were monitored for up to 28 days after finishing the treatment to observe the recurrence of parasite in mice blood. Five doses were studied in the recrudescence assay for Piperaquine, and only one mice treated with 5 mg/kg showed recrudescence within the 28 days after treatment experiment time. Hence, four doses showed curation after a 4-day Piperaquine treatment: 10, 25, 50 and 100 mg/kg in mice infected with the huma parasite *Plasmodium falciparum* (figure 53).

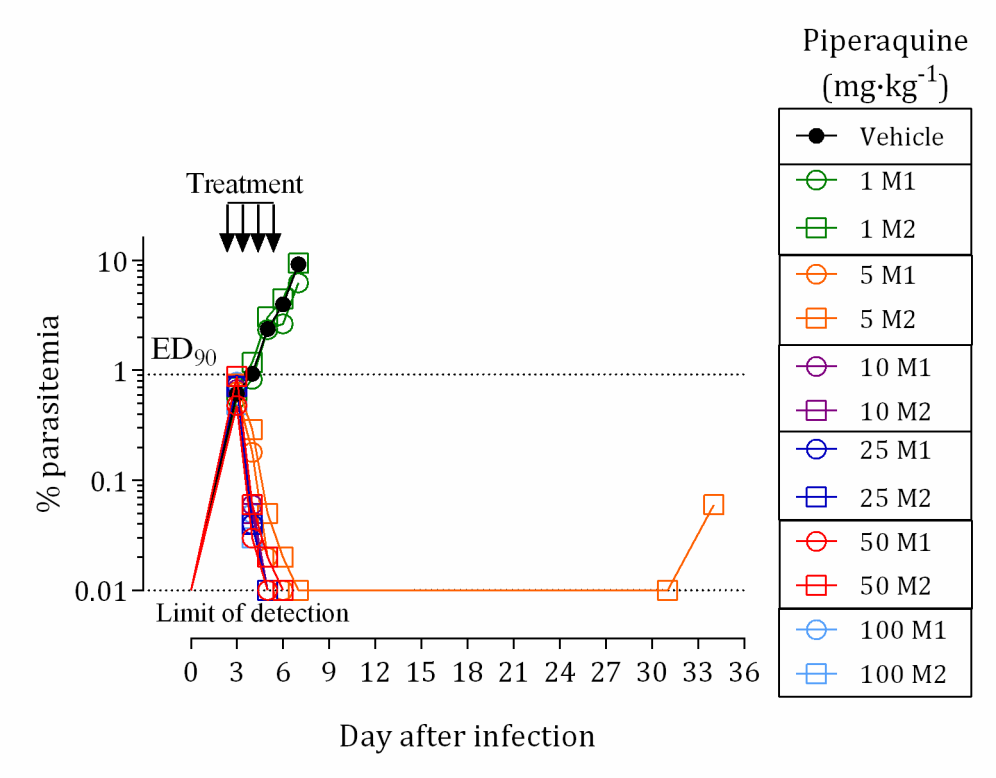

Figure 53. Recrudescence study for Piperaquine. Data represented is the percentage of parasitemia measured by flow cytometry from day 3 to day 35 after infection. Data are the individual parasitemia data for two mice for each dose and the mean±SEM of three mice in the case of the vehicle treated group.

In the phenotypic study for Piperaquine when comparing treated mice with the vehicle control, it can be observed that treated mice show a population of low quantity of DNA that is out of the region of "healthy parasite", this type of parasite is known as pyknotic form and it is known to be a condensed parasite which still contains DNA (figure 54). The aminoquinolone-related compound, Piperaquine showed an expected drug response response, parasite death during the trophozoite stage and no effect on schizont rupture. Piperaquine can inhibit the development of ring stages to pigmented trophozoites producing pyknotic cells.

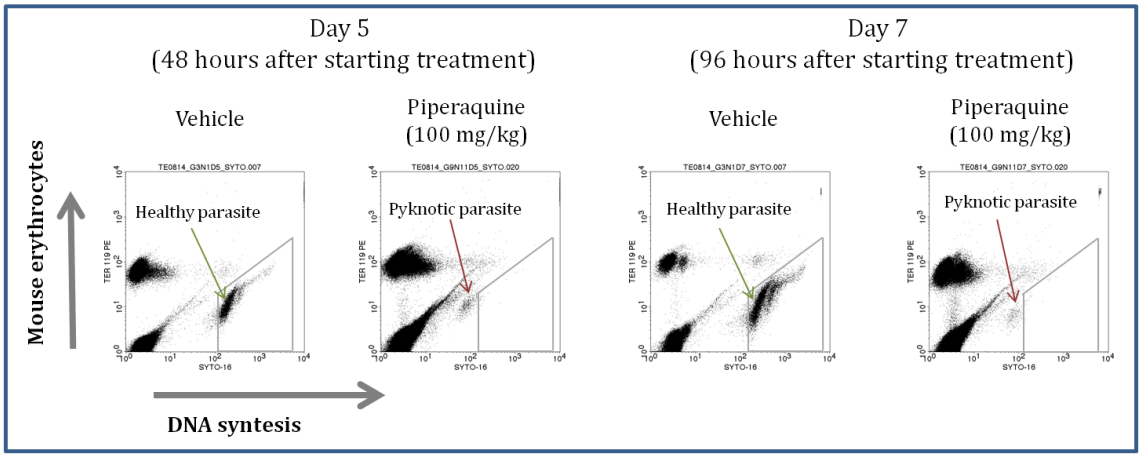

Figure 54. Piperaquine 4-day test flow cytometry dot plots. In the X axis of the dot plots it is represented the fluorenscence of the DNA dye SYTO-16, more fluorescence intensity means more quantity of DNA. In the Y axis it is represented the monoclonal antibody TER119-PE which detects mouse erythrocytes.

The potential efficacy of new antimalarial drugs can be assessed by the 4-day test. A comparison among different drugs under development can be determined. Sigmoideal dose-response curves of the log10 of parasitemia against AUC can be compared and differences in terms of potency and speed of clearance can be observed (figure 55). In the case of the Atovaquone and Piperaquine, although the Piperaquine is a fastest comopound in terms of speed of clearance, it is worse than Atovaquone in terms of potency, this means that more concentration in blood is needed for Piperaquine to kill the 90% of parasite (1.8 µg·h/ml), when for Atovaquone it is needed 10 times less compound in blood (0.03 µg·h/ml). However, in the recrudescence study it is observed that for the Atovaquone, besides being more potent thant Piperaquine, the minimum quantity of compound in peripheral blood needed to cure has to be higher than the needed for Piperaquine.

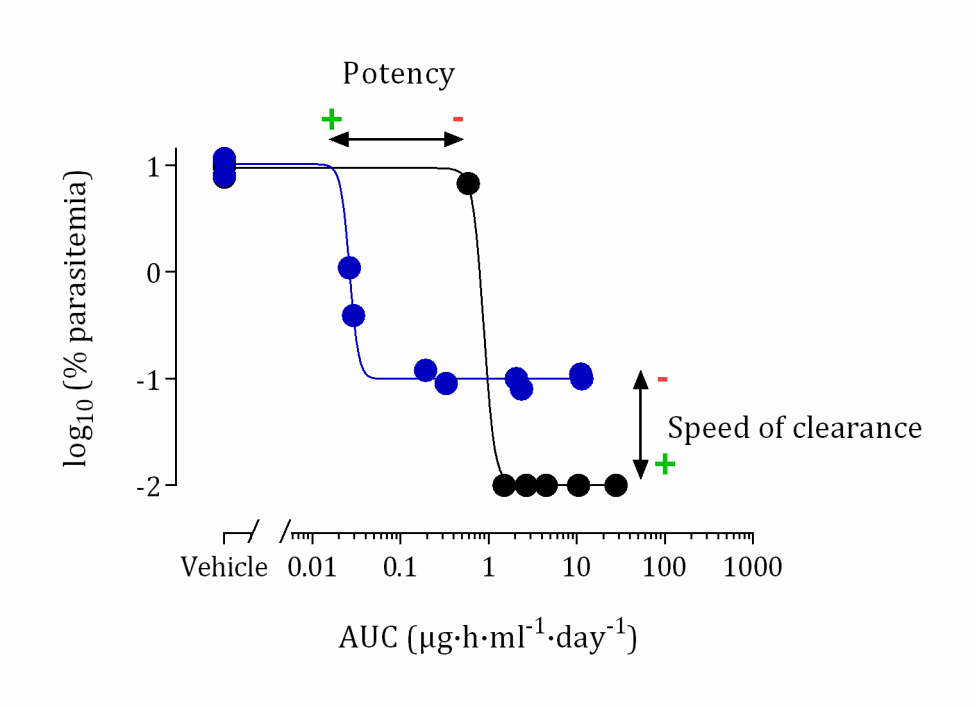

Figure 55. Sigmoideal dose response representation. In the X axis it is represented the AUC of the levels measurement in peripheral blood. In the Y axis it is represented the log of the percentage of parasitemia at day 7 after infection. Data are individual mouse, two mice per each dose and three for the vehicle treated mice.

Phenotypic assay

The reproducibility growth of the *P. falciparum* parasite in the GSK*Pf*Hu mouse model makes easy the study of the effect in parasite growth of potential antimalarial drugs. The combination of this reproducibility with the advantage of using flow cytometry techniques to quantify the percentage of parasitemia, makes possible the use of the GSK*Pf*Hu mouse model as a powerful tool for the experimental testing of antimalarials *in vivo* in a dose-response assay.

To study the effect of potential antimalarial drugs, it is important be able to detect parasite clearance under treatment with these compounds. To attempt this issue, IL2 mice engrafted with human erythrocytes, are infected with $20x10^6$ infected erythrocytes. At day 3 after infection, when parasite in mice peripheral blood is around 0.3-0.5% treatment with compounds starts. Mice receive a daily oral dose during 4 days of the compounds to be tested at efficacious doses previously defined (data not shown). Parasitemia is measured by flow cytometry (SYTO-16 and TER119-PE staining) during the treatment and 24 hours after finishing the last dose, to observe parasite clearance under treatment. Flow

cytometry technique used has a limit of detection of 0.01%, so we are able to measure one-log parasite decrease if parasite starts to decrease since the first dose received.

Different drugs has been tested in the model and depending on the speed of parasite reduction, these drugs can be divided in four different categories: i) fast: parasite clearance is achieved 24-48 hours after starting treatment; ii) medium: parasite clearance is reached 72 hours after starting treatment; iii) slow: parasite is cleared 96 hours, and iv) very slow: parasite that do not reach the limit of detection at 96 hours after starting treatment (figure 56).

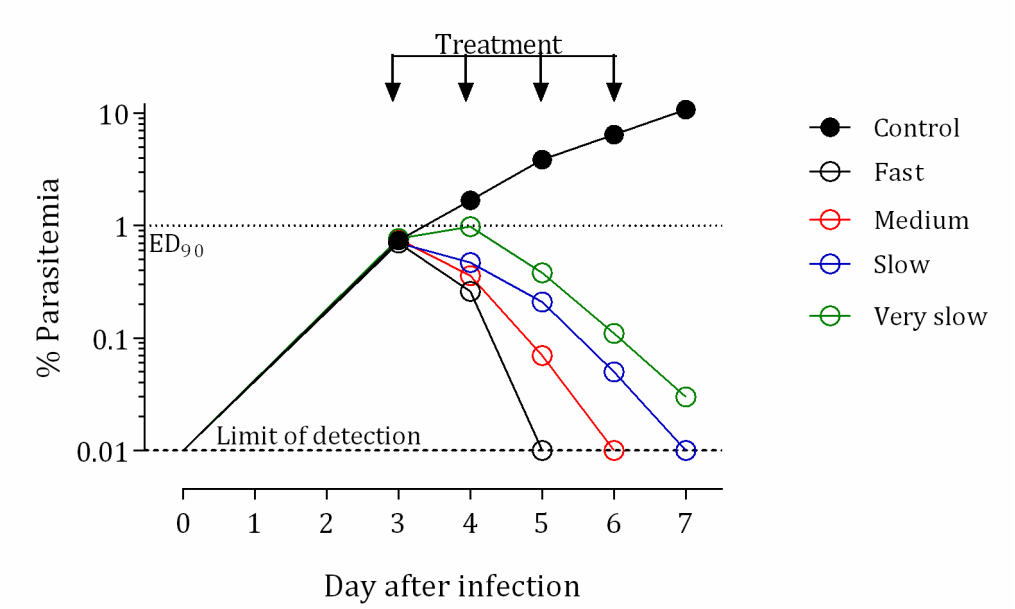

Figure 56. Schematic representation of the percentage of parasitemia of infected mice treated orally during four consecutive days, once a day with 4 different standard antimalarials that show different parasite clearance speed. Parasitemia was measured by flow cytometry as SYTO-16^{+} and TER119-PE^{-} population. The limit of detection of the technique is 0.01%.

The use of flow cytometry techniques in drug discovery studies can give more information about the drugs tested. Different monoclonal antibodies and DNA staining used can give different information about the different stages of parasite and populations of erythrocytes infected.

By using the DNA dye YOYO-1, a phenotypical study of the effect on parasite after treatment with several standard antimalarial drugs has been done. The combination of the YOYO-1 dye with the monoclonal antibody TER119-PE and the bidimensional analysis of

the dot plots can define different patterns on parasite effect of the different drugs tested in *P. falciparum* infected IL2 mice.

IL2 mice engrafted with human erythrocytes were infected with $20x10^6$ infected erythrocytes. Then, at day 3 after infection, fourteen anti-malarial drugs with different mechanism of action and belonging to different chemical families, were administered to *P. falciparum* infected IL2 mice per oral route at efficacious doses (based on previous experiment performed and in bibliography search in the case of proguanil and sulfadoxine), once a day during four consecutive days, as described previously. Blood samples were obtained 24 hours after the last dose (2 asexual cycles of the parasite), and stained with YOYO-1 and TER119-PE as described in material and methods, and analyzed using a bidimensional analysis in FL2/FL1 dot plots (figure 57).

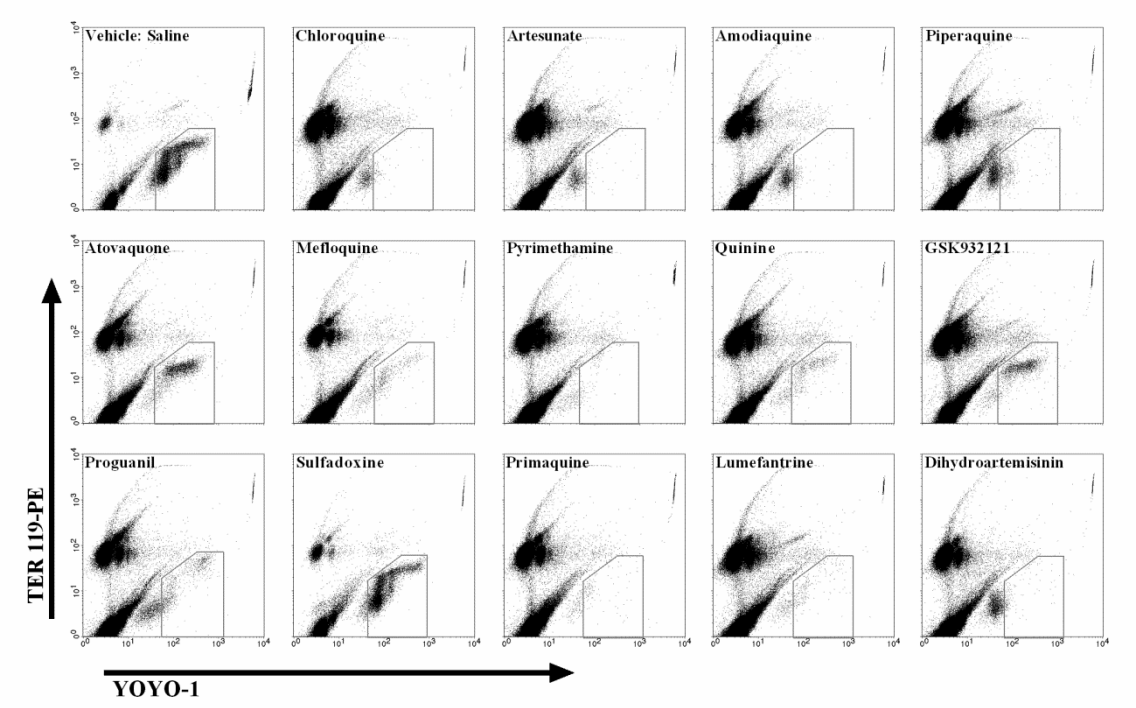

Figure 57. Flow cytometry patterns of affected parasite at day 7 after infection. Mice received an oral treatment once a day during four consecutive days with 13 standard antimalarial compounds and GSK932121 compound. Patterns are compared with healthy parasite shown on the vehicle treated dot plot. Patterns are determined using the YOYO-1 /TER119-PE flow cytometry analysis.

The fast parasite clearance of Chloroquine, Artesunate, Amodiaquine, Piperaquine and Dihydroartemisinin (figure 58) showed patterns of event distribution of lower intensity at YOYO-1 (X axis) than healthy rings obtained from vehicle-treated mice. Parasites were pyknotic and vacuolated shrinked trophozoites in giemsa smears (figure 59). Conversely,

Atovaquone, Pyrimethamine, Primaquine, Proguanil and GSK932121 rendered YOYO-$1_{FL2/FL1}$ showed patterns with most infected events mapping to the trophozoite region, with a parasite clearance very slow or slow in the case of Pyrimethamine and Primaquine (figure 58). However, in the case of Pyrimethamine and Proguanil events showed in the trophozoite region are closer to the schizont region than those found in Atovaquone/GSK932121 pattern (figure 57). By contrast, in the case of Primaquine the altered trophozites are closer to the younger stages region, this means that the effect is concentrated in young trophozoites. Consistent with this observation, blood smears unveiled vacuolated trophozoites as the main phenotype remaining in circulation of mice treated with Atovaquone or GSK932121. However, trophozoites found in blood smears of mice treated with Proguanil or Pyrimethamine were swollen and morphologically different to that found in Atovaquone/GSK932121 treatment, in addition Primaquine blood smears showed shrinked trophozoites (figure 59), which confirm the differences in the cytometry patterns. Noteworthy, Mefloquine, Quinine and Lumefantrine treatment showed also altered trophozoites, but there were still some DNA synthesis and re-infection, shown as envents in the schizont and ring stage region of the cytometry dot plots, and confirmed with the microscopy blood smear. In the case of Sulfadoxine, it showed no effect in the 4-day treatment assay against *P. falciparum* in the mouse model at the given dose of 100 mg/kg.

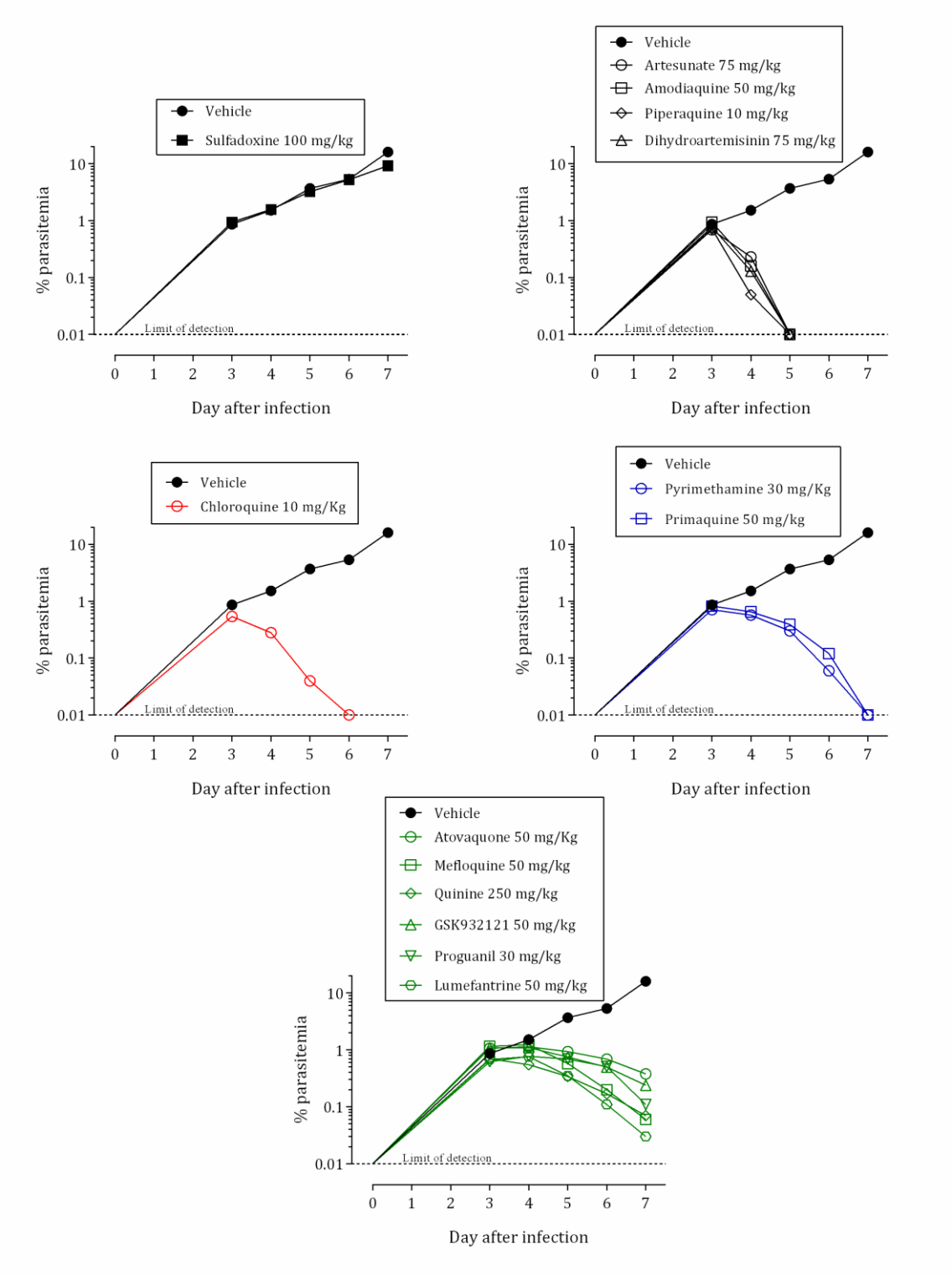

Figure 58. Parasitemia clearance after 4-day treatment with 14 different standard antimalarials. There were found different parasite clearance rate: in open black it is represented fast, in red medium, in blue slow and in green very slow parasite clearance. Filled black graphics correspond to vehicle and non efficacious treatment. Parasitemia was measured by flow cytometry as SYTO-16⁺ and TER119-PE⁻ population. The limit of detection of the technique is 0.01%.

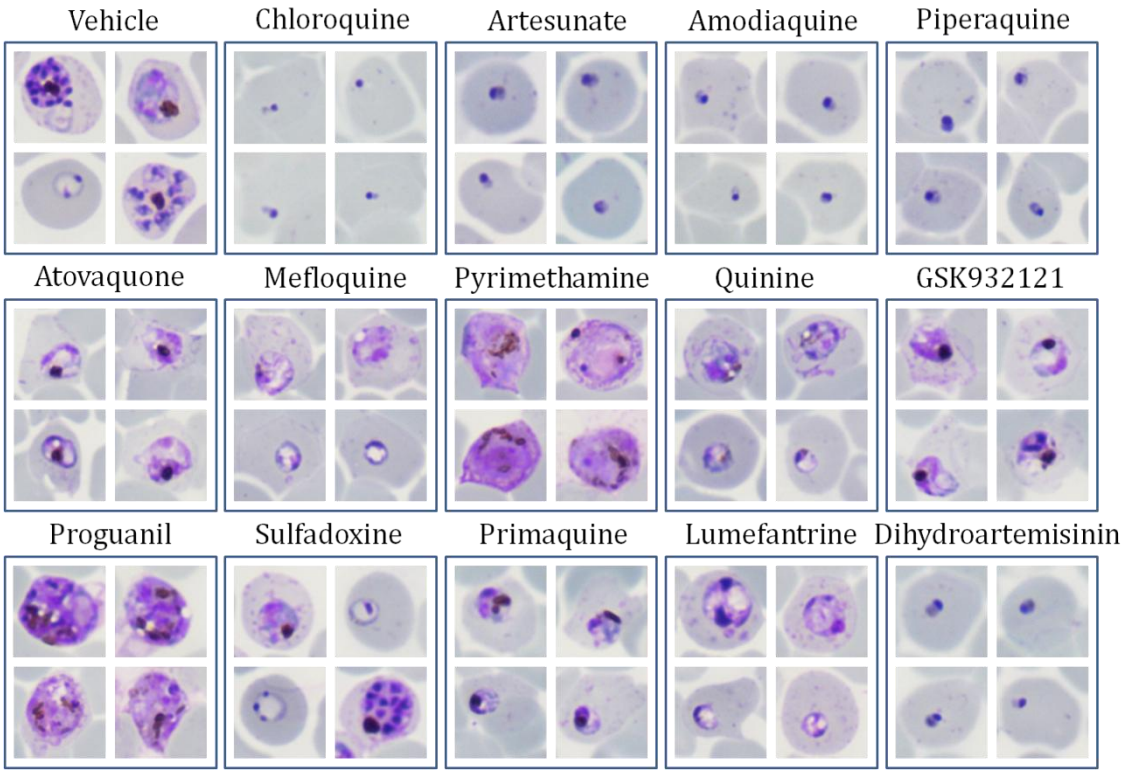

Figure 59. Microscopic photographies of P. falciparum infected mice blood smears stained with Giemsa. It is shown 4 representative photographies of each smear taken at day 7, 24 hours after finishing treatment with 14 different antimalarial drugs.

Transmission studies

The GSK*Pf*Hu mouse model is able to sustain the intraerythrocytic phase of the *P. falciparum* parasite. In the human host, during this asexual infection inside the erythrocytes, some of the parasites develop into the sexual stages of parasite (gametocytes). These sexual stages are the responsible of the transmission of the malaria parasite to the mosquito host, where the parasite sexual reproduction takes place and new parasites are formed and are ready to infect new human hosts.

The objective of the transmission studies is to evaluate the suitability of the GSK*Pf*Hu mouse model to be used to study the transmission of the human parasite to *Anopheles* mosquitoes. Two different aproaches has been evaluated: i) Natural transmission, where it is studied the ability of the *P. falciparum in vivo* adapted strain NF54$^{0230/N3}$ to develop to gametocytes in humanized mice peripheral blood and the infectivity of these gametocytes in Anopheles mosquitoes; ii) *in vitro/in vivo* transmission, where it is studied the ability of the GSK*Pf*Hu mouse model to sustain the engraftment with *in vitro* cultured Stage V gametocytes, then the infectivity of these gametocytes are studied in Anopheles mosquitoes.

Natural transmission

IL2 mice were engrafted with daily i.p. injections of 1 ml of human erythrocytes (50% hematocrit). When these mice achieved around 50% of human erythrocytes in peripheral blood, mice are injected with $20x10^6$ infected erythrocytes of *Pf* $NF54^{0230/N3}$ strain.

Firstly, it is studied the ability of this strain to generate stage V gametocytes and fertile male gametes in humanized mice peripheral blood. To attempt this issue, mice infected with *Pf* $NF54^{0230/N3}$ were monitored from day 5 to day 26 after infections. Mice blood was collected from the lateral tail vein for flow cytometry study of the parasitemia (2 µl), for Giemsa staining to study the presence of the different stages of gametocytes (2 µl) and for the exflagellation assay to study the presence of fertile male gametes (2 µl).

Gametocytes at different stages were detected from day 12 to day 26 (figure 60). In addittion, the exflagellation is first detected at day 14 after infection, obtaining the peak at day 16 (figure 61A). The exflagellation peak does not match with the peak of parasitemia (figure 61B). However, the exflagellation takes place during the anaemia phase where the erythrocytes are massively cleared (figure 61C).

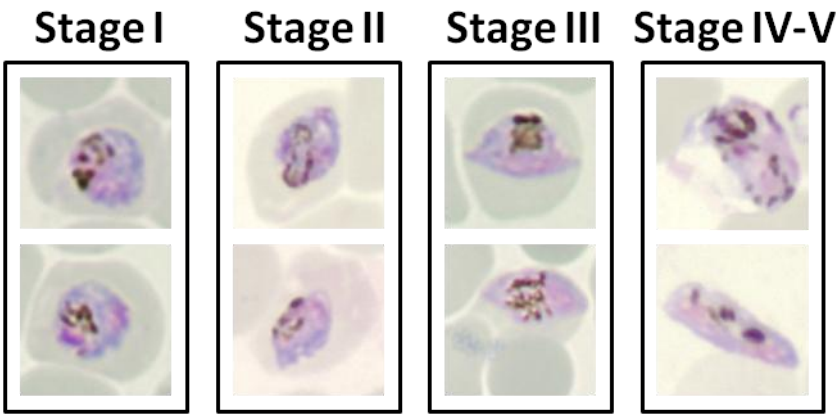

Figure 60. Photographies from giemsa stained smears of mouse number 1 peripheral blood from day 12 to day 26 after infection. Stages I to V gametocytes are observed.

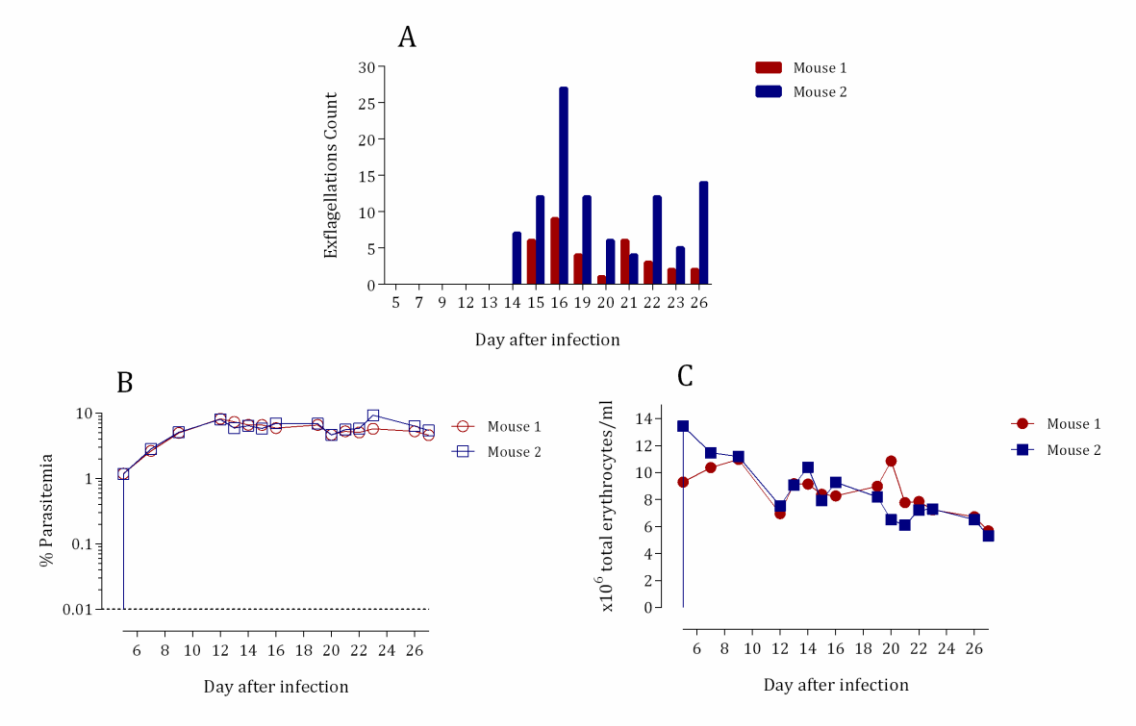

Figure 61. Graphic representations of the exflagellation counts (A), percentage of parasitemia (B) and total erythrocytes count (C) during infection with the P. falciparum NF54 strain. The exflagellation is checked under a light microscope using the 100X objective during a maximum of 10 minutes. *The percentage of parasitemia was calculated by flow cytometry as SYTO-16⁺ and TER119-PE⁻ population. The quantification of erythrocytes was done by flow cytometry, using Trucount™ tubes. Data represented shows the results of two individual mice from the experiment.*

The presence of exflagellation in mice peripheral blood suggests that the gametocytes generated by the *Pf* NF54$^{0230/N3}$ in the GSK*Pf*Hu mouse model strain may be fertile.

To test the infectivity of *Pf* NF54$^{0230/N3}$ strain gametocytes, IL2 infected mice were put for mosquito feeding at different days after infection: 6, 10, 13, 15, 17, 20, 34 and 48. Briefly, mice were anesthetized before mosquito feeding. Then, mice were put on the mesh of the mosquito container, with 30 female mosquitoes each, to allow biting. Mosquito feeding was performed during 30 minutes in dark and at 26.5 ºC. After feeding, mosquitoes were incubated during 7 or 10 days in an incubator (12 hours of dark/light cycle, 26.5±1ºC and 75-80% humidity).

At day 7 or 10 after feeding, mosquitoes were disected to obtain the midgut for oocysts counting after staining with 0.1% mercurochrome solution. Oocsyts were found at

different days after infection: 6, 10, 13, 20, 34 and 48 (figure 62). In all cases only 1 oocyst was found in each midgut. The prevalence of mosquito infection obtained was around 5%.

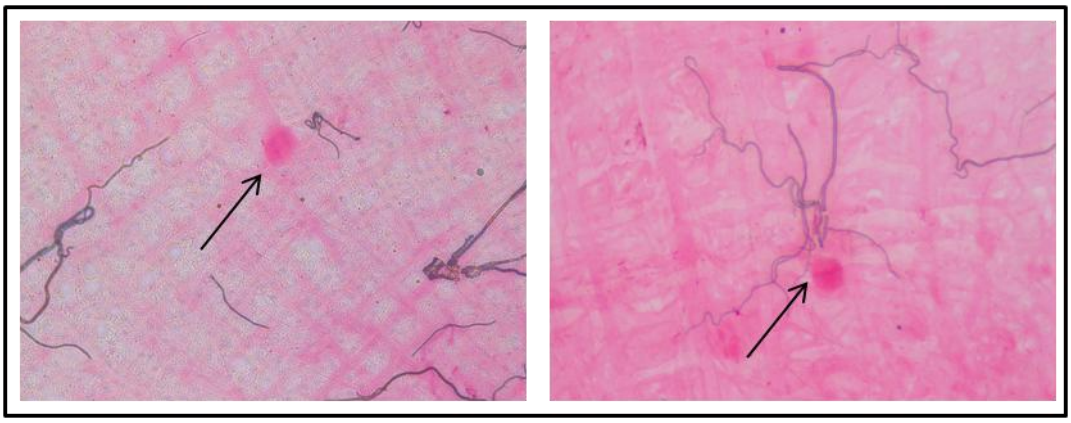

Figure 62. Photographies from mercurochrome stained midguts from mosquitoes used for mice feeding. Oocysts (black arrows) are observed in mosquitoes fed with mice infected with the Pf NF54 strain at different days after infection.

In conclussion, the gametocytes generated by the *P. falciparum* NF54 strain able to grow in the GSK*Pf*Hu mouse model, are able to infect mosquitoes by natural transmission after mosquito biting. These results confirm that the GSK*Pf*Hu mouse model can be an apropiate tool to study the biology of mosquito infection and can be the starting point to develop transmission assays.

In vitro/in vivo gametocytes engraftment

In this aproach, IL2 engrafted mice, with at least 50% human erythrocytes in peripheral blood, are used for the xenotransplant of stage V gametocytes (*Pf* NF54 strain) from *in vitro* culture. Briefly, around $40x10^6$ stage V gametocytes were injected by i.v. route in IL2 mice engrafted with human erythrocytes. Mice did not receive daily injections of human erythrocytes after the injection of gametocytes and were monitorized until gametocytes were cleared from blood (day 7 after injection). Mosquito feeding with xenotransplanted mice was done at day 2 after gametocyte injection.

After the injection, stage V gametocytes can remain in mice peripheral blood for at least 7 days (figure 63A). Gametocytes are quantified by flow cytometry every day after the injection using the SYTO-16/TER119-PE staining (figure 63B). Stage V gametocytes can be quantified until day 7 after injection. However, the clearance of these gametocytes starts at day 1 after the injection. Half of the gametocytes are cleared from day 0 to 1. Nevertheless, clearance decreases after day 1. In addition, the morphology of stage V gametocytes in mice peripheral blood is normal (figure 63C).

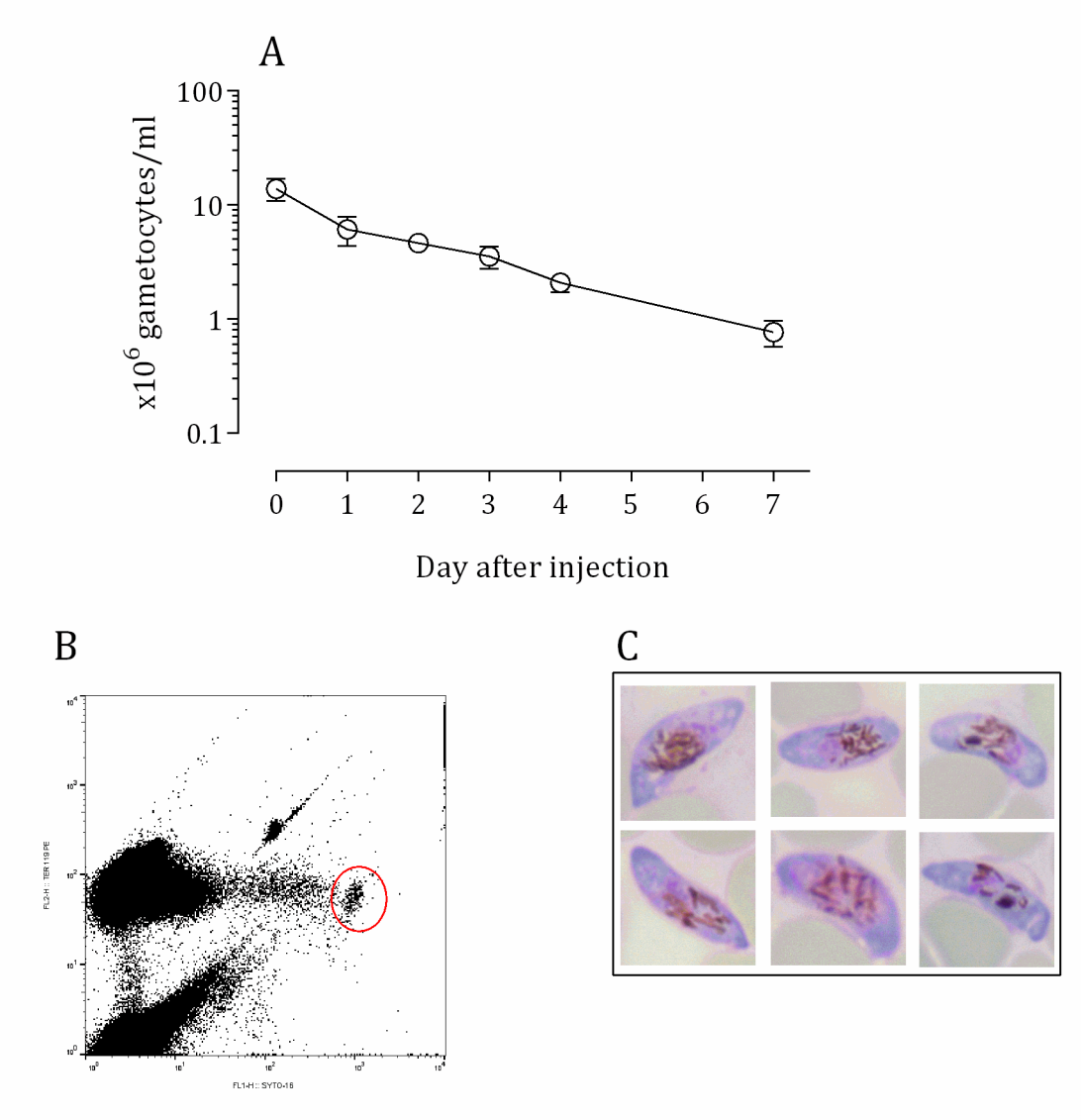

Figure 63. Stage V gametocytes injection in engrafted IL2 mice. In A is represented a graphic of the count of stage V gametocytes in mice peripheral blood after injection. The quantification is done by flow cytometry by using Trucount™ tubes. Data are the mean±standard error of the mean of five mice. In B it is shown a dot plot graphic of the SYTO-16/TER119-PE staining and detection of stage V gametocytes. The detection of gametocytes by flow cytometry was defined as SYTO-16⁺ (high fluorescence intensity in FL1), and autofluorescence (high fluorescence intensity in FL2 in the SYTO-16⁺ region), the gametocyte population is marked with a red circle. In C it is exhibited a photographies from Giemsa smears of stage V gametocytes found in mice peripheral blood after the injection.

The relative low clearance of stage V gametocytes found in engrafted IL2 mice peripheral blood, and the healthy morphology that they show, suggests that these gametocytes are fertile, also the presence of exflagellation is also confirmed.

At day 2 after injection and in order to test the infectivity of *Pf* NF54 stage V gametocytes, five IL2 injected mice were put for mosquito feeding, as it was described before.

At day 7 after feeding, mosquitoes were dissected to obtain the midguts to confirm the presence of oocysts after staining with 0.1% mercurochrome solution. Oocysts were found in mosquitoes from all the containers (figure 64). In all cases 1 oocyst was found in each midgut. The prevalence of infection was around 6%, similar to that found in the natural transmission.

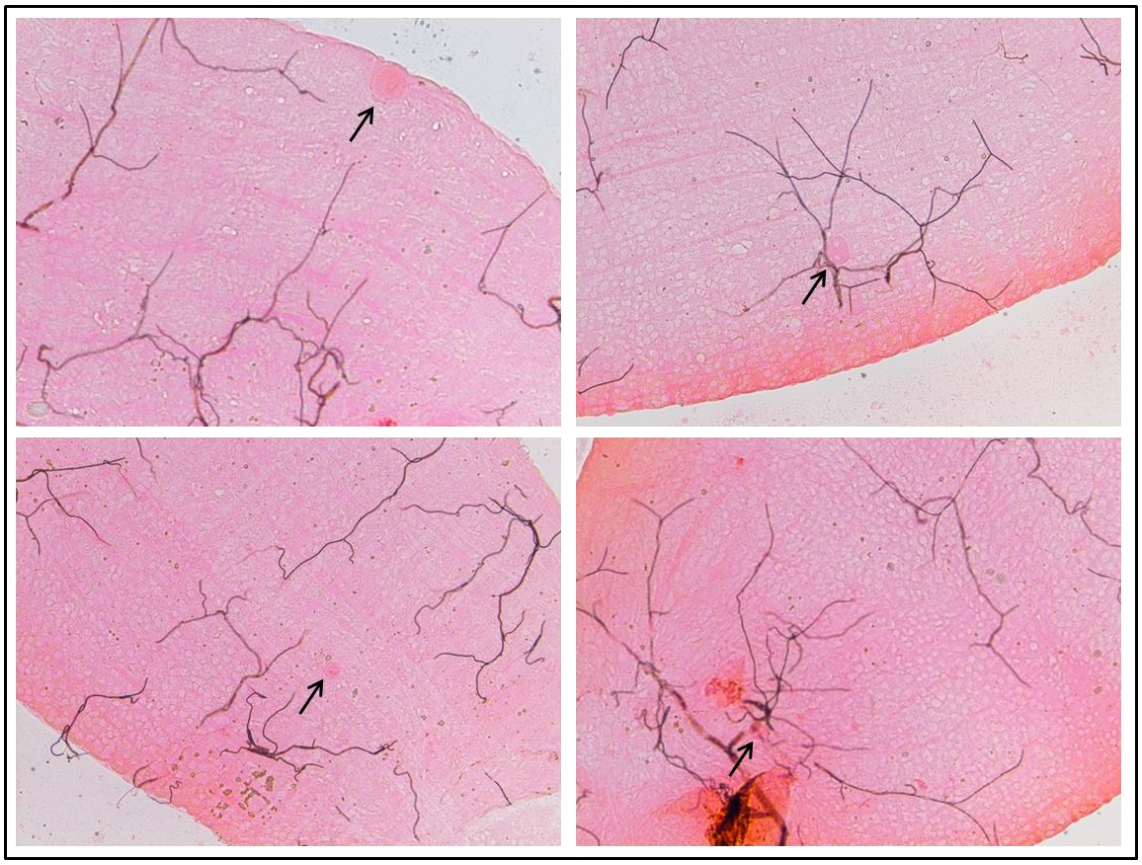

Figure 64. Photographies from mercurochrome stained midguts from mosquitoes used for mice feeding. Oocysts (black arrows) are observed in mosquitoes fed with mice injected with the stage V gametocytes (Pf NF54 strain) from an in vitro culture.

To conclude, IL2 engrafted mice are able to support the xenotransplant of stage V gametocytes. These gametocytes while in mice peripheral blood are fertile and are able to infect mosquitoes after mosquito biting of mice. These results confirm that the GSK*Pf*Hu mouse can be used in studies that combine *in vitro/in vivo* techniques for the study of the transmission of the *P. falciparum* parasite to mosquitoes.

Discussion

Characterization of the GSK*Pf*Hu mouse model

The parasite *P. falciparum* infects almost excusively human erythrocytes. The specificity of *P. falciparum* for its human host is the major limitation for the development of *in vivo* models to study the erythrocytics stages. The ability of the *P. falciparum* parasite to infect New World monkeys eythrocytes [51], made possible the use of these monkeys as an *in vivo* model to test new antimalarial drugs [67]. The use of non primate monkeys to study diseases has been drastically reduced in the last 30 years due to economic/ethical restrictions and a limited supply, and they are only used in research when there are no suitable alternative methods or species. For this reason, the development of mouse models able to support the study of many human diseases has become a crucial tool for researching. In the malaria field, the development of different types of immnudeficent mice opened the possibility to use these mice to study the parasite human host throughout its life cycle. There has been a huge advance in this field in the past 20 years [34, 131].

The election of the immunodeficent mice strain is crucial for the development of the correct mouse model for the study of the disease. The first attempts for the study of the *P. falciparum* erythrocytic stages used immunodeficent mice lacking both T and B cells (*scid* and NOD*scid* mice). In these models, an additional depletion of host macrophages using liposomes containing clodronate was needed to obtain the correct engraftment with human erythrocytes [13, 97, 146]. Afterwards, new immunodeficent mice strains were developed that also lack a complete NK cells function were used for the engrafment with human erythrocytes without the addition of immunomodulators [5, 71]. With this new mice strain, the NOD*scid* $\beta2m^{-/-}$ (abreviated β2), the engraftment with human erythrocytes had a reproducibilty that reached the 100%. The major limitation of this model is that the β2 mice develop in a high rate spontaneous lymphomas and thymomas at a certain age, so the possibility to perform long lasting experiments with these mice is reduced.

In this study it is described the use of a new immunodeficent strain, the NOD.Cg-Prkdc^{scid} IL2rg^{tm1Wjl}/SzJ mice (abreviated IL2) for the development of a new *P. falciparum* murine model without the use of immunomodulators [63]. The IL2 mice strain has a longer life span, compared to β2 mice, and lacks functional T, B and mature NK cells, and also has additional deficiencies in the innate immune system that makes these mice able to sustain different xenotransplants with human cells [58].

To study the suitability of the IL2 mice to be used as *P. falciparum* mouse model, these mice were engrafted with human erythrocytes and infected with the *in vivo* adapted *P. falciparum* $3D7^{0087/N9}$ strain following the protocol previously described for the β2 mice

[5]. The engrafment with human erythrocytes were done by the daily intraperitoneal injection of 1 ml of human erythrocytes at 50% hematocrit (RPMI 1640, 25% decomplemented AB human serum, 3.1 mM hypoxanthine). The kinetics for the acquisition of the engraftment in IL2 mice was similar to the one obtained in the β2 mice. The time required for the achievement of 50% of hEry was also found to be in the same range (6.8 ± 0.1 days for IL2 and 6.9 ± 0.4 days for β2). These results confirm that IL2 mice are able to sustain the engrafment with human erythrocytes and could be susceptible for the infection with the *P. falciparum* parasite.

Once a mouse strain is confirmed to accepts xenogenic grafts of human erythrocytes, the next step is to study the susceptibility of these mice to be infected by the human *P. falciparum* parasites. To succeed in the infection the first attempts included the use of immunomodulators to suppress the innate immune system of immunodeficient splenectomized mice in combination of intraperitoneal infections with *P. falciparum* parasites previously adapted to *in vitro* growth in presence of ascites fluid from mice. In these studies, the frequency of successful infections was about 25%, the infected mice displayed a variable kinetics of parasitemia and the parasite was only detectable until day 7 after infection. Further improvements in the immunosupresion protocol with the addition of a monoclonal antibody NIMP-R14, or the addition of inosine to the blood injection for mice lead to the obtaining of an increase in the reproducibility of the infection and long lasting parasitemias [7, 100]. However, the use of a more immunocompromised mice (β2 mice) in addition to the use of intravenous infections with a *P. falciparum* strain that was adapted to grow in immunodeficent mice from an *in vitro* culture succeeded in the achievement of a high reproducible infection with the human parasite in mice [5].

In this work, the susceptibility of the NODscidIL2Rγ^{null} mice to the infection by competent *P. falciparum* strain (*Pf*3D7$^{0087/N9}$) was studied. The infection was done with 20x10^{6} parasite infected erythrocytes by intravenous route in mice with at least an engraftment of 50% of human erythrocytes in mice peripheral blood. The IL2 mice strain was able to sustain the infection with *P. falciparum*. In addition, several improvements, compared with β2, were observed during the infection. Firstly, the *Pf*3D7$^{0087/N9}$ infectious burden in engrafted IL2 mice was 10-fold higher than that in engrafted β2 mice. This increment makes the IL2 *Pf* mouse model more suitable for drug discovery studies in which it is necessary to have a marked difference in the parasitemias between untreated and treated mice to evaluate the effect of different doses of drugs on parasitemia. Secondly, during the massive human erythrocytes clearance, the parasitemia is reduced but still detectable by flow cytometry. In β2 mice during this phase, the parasitemia is not detectable by flow

cytometry. This means, that long lasting experiments in which a minimum parastemia is needed can be performed with the IL2 *P. falciparum* model.

Once the engraftment and the infection by competent *P. falciparum* strain with the new IL2 mice was confirmed, the IL2 mice was selected as the new model for the testing of new chemical drug classes developed in GSK providing a precise analysis of the parasitological response to different exposure levels of drugs *in vivo*.

The GSK*Pf*Hu mouse model has been widely used to test new antimalarial drugs. The new model represented an improved standard for preclinical *in vivo* studies of blood-stage antimalarial drugs. It has also been implemented as a crutial tool in preclinical phases for the selection and prioritization of new drug families to be developed in the fight against the malaria [64]. However, to the best of my knowledge, little is known about the behaviour of the parasite inside the mouse host, or how the mouse respond to the xenotransplant and infection with the human parasite. To gain further insights into the GSK*Pf*Hu mouse model, one of the main objectives was to characterize this *P. falciparum* mouse model, and determine critical points for its improvement.

When the GSK*Pf*Hu mouse model was developed, the main priority was to assess a mouse model to test the activity of drugs against multiple stages of the *P. falciparum* parasite asexual life cycle. All the stages of the eythrocytic cycle (rings, trophozoites and schizonts) are present at the same time in mice peripheral blood with no signs of sequestration in tissues, as it is observed in humans or the rodent *P. berghei* infection [5]. The *P. falciparum* growth observed in the mice is different from the described in the human host. In the natural infection *P. falciparum* shows a synchronic growth, in which only young stages (rings) are present in peripheral blood, trophozoites and schizonts are sequestered in different organs and tissues, mainly spleen, liver and brain. This sequestration has been long studied but the exact mechanism responsible of this phenomena is still unkown. However, it is widely accepted that the interaction between some parasite proteins and host proteins during infection of red blood cells are implicated in the process of sequestration [48, 132]. For this reason, it is not strange to understand that the sequestration does not take place in the GSK*Pf*Hu mouse model. The absence of human host proteins in these immunodeficent mice may suspect that the parasite can not be recognized by the organism for the sequestration process.

The asynchronous development of the parasite in the animal model makes difficult the study of the intraerythrocytic cycle length in mice, it is not easy to track the parasite from ring stage to squizont stage when all the stages of parasite are present at the same time. To

overcome this issue, the parasite was synchronized to obtain a higher percentage of the same parasite stage, in this work we focus on the synchronization of mature stages. For the synchronization of the malaria parasite several methods have been developed and used for *in vitro* cultures in the last years, these methods include the use of reagents like sorbitol, plasmion or density gradient methods have been used throghout the last years [42, 122, 123, 125]. In this work, the synchronization of the parasite was perfomed by the use of the magnetic separation, firstly to avoid the use of chemical reagents that could be injected accidentaly in mice or density gradients that makes difficult to separate parasitized erythrocytes from host white blood cells [3], and secondly to obtain the highest grade of synchronicity with less manipulation, only one step is needed to obtain the synchronic parasite [1].

The magnetic separation is based in the magnetic properties that present the haemozoin which is the result of haemoglobin metabolism by the parasite. After the magnetic separation, the fraction selected for the study of the intraerythrocytic cycle was the positive fraction, which is enriched with late thropozoites and schizonts, which are the stages that perform the most active metabolism. In previous experiments, this fraction was the one that showed the shortest window of synchronization (not shown). After the infection with this fraction, the ring infection length was observed from 7 to 21 hours after infection, the thropozoite stage is observed from 21 to 42 hours and the schizont stage is observed between 42 to 49 hours, these data of stages length are slightly longer than previously observed for *in vitro* cultures [122, 149]. The total length of the intraerythrocytic cycle in the *Pf* mouse model is 49 hours, also slightly longer than what it has been observed in natural *Plasmodium falciparum* infection in human beings, but the same length in other *in vitro* experiments performed with magnetic separation synchronization [1].

Little efforts have been done to understand what is the host answer inside the mouse recipient in the humanized mice models during the engraftment and infection process. Both processes take place mainly in the peripheral blood. However, it is in some way easy to study what is happening in a model that everything occurs in the peripheral blood. The peripheral blood can be easily obtained for study, and erythrocytes can be easily marked and monitored. In this work the measurement of red cells life-span (half life) and the distribution volume (red blood cells volume) are the parameters calculated for the study of the erythrokinetics in the GSK*Pf*Hu mouse model. In the Malaria field little has been studied regarding erythrokinetics neither in the natural *P. falciparum* infection nor in animal models of this infection.

The half life is a pharmacology parameter that can be used for the estimation of the speed of clearance of erythrocytes in live animals. In the GSK*Pf*Hu mouse model there are two kind of erythrocytes at the same time, human and mouse. On the other hand, the distribution volumen, in pharmacological terms, is used for the quantification of the distribution of a drug after administration. In the GSK*Pf*Hu mouse model it is assumed that the blood volume is the same as the distribution volume. In order to study this parameter, the erythrocytes are injected intravenously, these cells are distributed equally just after the injection in the peripheral blood with no retention or sequestration by the tissues or organs.

In order to study these parameters, it is needed the tracking of erythrocytes insice mice, this has been investigated by labelling erythrocytes *in vitro* with subsequent reinjection of labeled cells into animals and tracking their distribution in peripheral blood while the animal is still alive. To determine the volume of distribution several methods are available which include radioactive iron or chrome labelled erythrocytes [19, 124]. However, in these methods it is needed the complete bleed of the animals for the estimation of the parameter, for this reason these methods are not suitable for long tracking of labelled cells in alive animals. Throughout the years, several cell tracking methods had been developed to study the cell division, proliferation or cell-based therapies in live organisms. However, most of these methods include the genetic manipulation of the cells to introduce in the genome a protein tagging system for signal amplification in gene expression and fluorescence imaging [70]. Nevertheless, these methods can not be used for the tracking of erythrocytes that lack DNA. In addition, there are other labelling methods that are based on fluorescence membrane labelling that can be more suitable for erythrocytes labelling. This type of labelling include reagents such us PKH26, DiOC6, Dextran, CFSE or Biotin-X-NHS, that have been widely used for different applications in cell tracking [9, 79, 84, 110, 121]. All these reagents were tested for erythrocyte labelling and posterior *in vivo* injection into the GSK*Pf*Hu mouse model. The best results based in fluorescence intensity, with non-toxicity and life span of labelled erythrocytes were obtained with CFSE and Biotin-X-NHS dyes. In addition, only a small sampling of peripheral blood from mice is needed for the monitoring and quantification of labelled erythrocytes and the measurement of distribution volume and half life, this allows to conduct long lasting experiments using the same mice.

In terms of blood volume, the normal values for a CD1 mouse is around 1.45 ml on average [152], 60% of this volume is plasma. The blood volume measured in IL2 naïve mice using the CFSE/Biotin method is 1.2 ml. However, with the daily injections of human

blood (50% hematocrit), the blood volume in IL2 mice increases 3 times higher (3.5 ml) compared with the naïve mice, and part of the plasma volume is mostly occupied by cells being reduced to 5-10% of the total volume. As a consequence, these mice showed an enlarged spleen and liver, and high irrigated tissues, similar to that found in the β2 GSK*Pf*Hu mouse model in engrafted mice and in transgenic polycytemic mice that overexpress erythropoietin [5, 27]. Finally, when the blood volume is determined in the anaemia phase where erythrocytes are massively cleared, the value obtained is similar to naïve mice, 1.7 ml. Though the increment in organs size still present.

Regarding to the estimation of erythrocytes half life in the GSK*Pf*Hu mouse model it has to be taken into account that in the same peripheral blood cohexist erythrocytes from human donors and mice host. The life span measured for human erythocytes is 120 days, and the half life in healthy people usually is around 50 days [37]. On the contrary, the life span determined for mouse erythrocytes is less than half of human, 50 days, this difference can be explained due to the more active metabolism showed by mice. The life span in mouse erythrocytes can be from 12 to 24 days depending on the method of calculation and the age of mice [54, 85]. When the half life is determined using the CFSE/Biotin method in GSK*Pf*Hu mouse model strong differences can be found depending of which phase of the mouse model is studied.

When estimating the half life of mouse erythrocytes in naïve mice (IL2 mice before engraftment with human blood), it is observed that the value obtained, 15 days, is included in the range previosuly described for common mice. However, when human eythrocytes are injected in naïve mice the half life obtained is 5.4 hours after injection. This low value can be explained by a rejection of the xenotransplant that leads to the removal of these erythrocytes by spleen and peripheral blood macrophages. Nevertheless, when IL2 mice have been engrafted with human erythrocytes during 13 days the half life of human erythrocytes determined in this phase increases up to 10 days. In addition, mouse erythrocytes half life in this phase decreased and is similar to the one determined for human erythrocytes. These results suggest that the initial mechanism in the engraftment phase to recognize erythrocytes for removal, is saturated and reconigzes indiscriminately both human and mouse erythrocytes for the clearance. Consistently, the enhacement of the erythrophagocytosis and the decrease in the half life of mouse erythrocytes are factors described in mouse models of polycythemia, as a response of the increased level of red blood cells in peripheral blood [27].

After the infection, mouse and human erythrocytes half life decreased more than in the engraftment phase. Of note, human erythrocytes half life is slightly slower to the one determined for mouse erythrocytes (5 and 7 days, respectively). Presumably this enhancement of human erythrocytes removal might be due to the increment in the phagocytosis by spleen macrophages provoked by the presence of the parasite [72].

Finally, the parasite infection ends with the anaemia phase. At this point, human erythtrocytes are massively cleared, and the half life of these erythrocytes is slightly higher to that found in naïve mice. Also the kinetics of clearance of hEry is exponential, the same obtained in naïve mice. On the contrary, half life of mouse erythrocytes is similar to the estimated in the infection phase, 7 days. These results suggests that the clearance of human erythrocytes, at this phase is specific and it not performed randomly.

In human beings, during the natural *P. falciparum* infection a severe anaemia is induced by the parasite. However, this phenomena does not seem to be strictely related to the levels of parasitemia in blood, it has also been observed in cases of low parasitemia burden [46]. This phenomena has been well studied and it is widely acepted that in part is caused by the alteration of the innate imflammatory mediators that lead to a massive phagocytosis of infected and uninfected erythrocytes [113]. Although multiple mechanisms have been proposed to produce the severe malaria anaemia (SMA) a detailed molecular mechanism has not been yet elucidated. Thus, what has been widely accepted is the fact that in the SMA clearance of uninfected erythrocytes is higher than the infected. Mathematical modeling of hematological data from human *P. falciparum* infections has suggested that up to 8.5 uninfected erythrocytes are cleared for every infected erythrocyte [59]. In addition, in rodent model of severe anemia with low parasite burden, the rate of uninfected/infected erythrocytes clearance obtained is much higher, 30:1 [46]. Nevertheless, under our experimental conditions in the GSK*Pf*Hu mouse model during the anaemia phase the quantity of uninfected erythrocytes cleared for every infected erythrocyte is 192. This increase in the rate of uninfected erythrocytes clearance in these mice is not strange taking into account that in the GSK*Pf*Hu mouse model the concentration of total erythrocytes is $12x10^6$ per microlitre, when in a human the normal values are around $5x10^6$ erythrocytes per microliter. Of note, the addition of fresh human erythrocytes do not avoid the anaemia, these new erythrocytes are also selected for the massive clearance.

Of importance, the presence of the SMA in the GSK*Pf*Hu mouse model has revealed that the infection with *P. falciparum* in the mouse model has similarities to the natural infection

observed in the human host. These results suggest than the GSK*Pf*Hu mouse model can be a crucial tool for further studies of the mechanisms that involve this severe anaemia phenomena. Some authors suggest that these mechanisms may be driven by an immunological response to the parasite infection driven by the response to the RSP2 protein of the parasite that is transferred to the erythrocyte or a disregulation of the innate imflammatory mediators such as IFNγ, IL12 or TNFα [113, 156].

In the human host, the immune response to the *P. falciparum* infection is driven by the release of cytokines which leads to complex downstream metabolic changes. Recent evidences suggest that the immunological response may be implied in the pathophysiology of the disease [87]. By contrast, the immune response in the *P. falciparum* mouse models has been poorly studied, only the cytokines IFNγ and IL6 have been confirmed to be expresed in the presence on the human parasite in NODscid and IL2 mice [7]. In this work, several inflammatory cytokines (TNFα, IL12p70, IFNγ, MCP-1, IL10 and IL6) have been evaluated to gain insights into the inflammatory process in the different phases of the GSK*Pf*Hu mouse model.

In the natural *P. falciparum* infection TNFα is the molecule typically associated with pathology in malaria. It is critical for parasite kiling and preventing parasite replication. IFNγ has also a protective role during early stages of *P. falciparum* infection, so as IL6. However, IL12 and IL10 role is the protection against the development of malarial anaemia. Whereas MCP-1 is involved in the immune activation.

The secretion of TNFα in the human host is induced in macrophages by the infected erythrocytes and this cytokine can enhance the phagocytosis by the increase of expression of Fc in monocytes [87]. It is raised in those patients with severe malaria and has been implicated in the pathogenesis of murine cerebral malaria. TNFα is also raised in placental malaria and is assodicated with low birth weight. Accordingly, the concentration of TNFα in the serum of GSK*Pf*Hu mice increases in the phases where the parasite is present and the phagocytosis is enhanced, the infection and anaemia phase.

The IFNγ in the human infection, plays an important role in the protection to blood stage malaria [87]. This cytokine is secreted by CD4+, CD8+ T lymphocytes and NK cells. By contrast, the IL2 mice lack T, B and NK cells, as a consequence, INFγ is not released in response to the infection in the GSK*Pf*Hu mouse model. However, this cytokine is detected in serum from *P. falciparum* infected NODscid mice, the parental strain of the IL2 mice that have functional NK cells.

The interleukine 12 is a immunomodulatory cytokine secreted from dendritic cells, monocytes and splenic macrophages, among other cells. The IL12 has been demostrated to be very important in malaria in the protection against blood stages [128]. The presence of IL12 modulates the macrophage activity and mediates the development of malarial anaemia [82, 113]. In the GSK*Pf*Hu mouse model it is observed that the IL2 levels increases from infection and reaches the peak in the anaemia phase. Of note, the levels of IL2 are higher in the phases of the model where the phagocytosis of human erythrocytes is enhanced, infection and anaemia. This behaviour correlates with what it is described about the stimulation of the IL12 secretion by the phagocytosis process [87].

Interleukine 10 is an antinflammatory molecule and it is associated to provide protection against SMA by preventing the massive production of pro-inflammatory mediators. It has been shown that decreased levels of IL10 is associated to severe anaemia in African children [74]. Accordingly, in the GSK*Pf*Hu mouse model where the severe anaemia is observed, IL10 levels in mice serum can not be detected. Interestingly, this cytokine is the only one that is detected during the engraftment phase, probably as an inflammatory response to the daily intraperitoneal injections.

Elevated levels of IL6 has been observed in patients with severe malaria. However, lower levels of this citokine have been associated to hyperparasitemia in children with falciparum malaria [6, 83]. Therefore, lack of control of the parasitemia might be the reason why in the severe pathophysiology is observed with increased levels of IL6. In the GSK*Pf*Hu mouse model the maximum peak of IL6 is reached during the infection, but this peak is only an isolated point in the different phases of the model and do not show a specific pattern.

The monocyte chemotactic protein (MCP-1) is a chemokine involved in the inflammatory process and its effect is to organize the migration of leukocytes. In the malaria disease it has been found in children with *P. falciparum* infection [30]. Correspondingly, in the GSK*Pf*Hu mouse model, highest levels of MCP-1 are detected in infection and anaemia phase, the phases where more phagocytic cells are recruited.

Most of the cytokines studied are present in the phases of infection and anaemia, and are related to the massive erythrocytes clearance. In murine malaria, parasitized and unparasitized red blood cells clearance are associated in some cases to induced apoptosis and posterior phagocytosis [144]. The recruitment of monocytes and macrophages in malaria infection is crutial to overcome the infection. In this study we have focused in the role of the spleen macrophages in the different phases of the GSK*Pf*Hu mouse model. We

have found that the macrophages phagocytosis of erythrocytes is active in all phases and is perfomed by F4/80 or GR1 positive cells, being the F4/80$^+$ population more active in the phases where human erythrocytes are massively destroyed, infection and anaemia. The F4/80 is one of the most specific cell-surface markers for murine macrophages and is highly expressed in resident tissue macrophages, including spleen red pulp. In murine *Plasmodium chabaudi* infection it has been described an increment in the number of F4/80$^+$ cells in the spleen red pulp [76]. In addition, it has been studied the role of F4/80 macrophages in *P. yoelii* infection in a model of CD47-/- mice, the CD47 is a marker of self present in red blood cells that it is related to age-dependent phagocytosis. As a consequence, CD47-/- has an accelerated clearance of young erythrocytes, and this clearance is mainly performed by F4/80 macrophages in the spleen [17]. Accordingly, the clearance of human red blood cells in the *Pf* mouse model might be done as the result of the recognition as strange cells in the mouse spleen by F4/80 cells.

On the other hand, the GR1 (Ly6C) molecule in mice is expresed mostly in neutrophils and monocytes. The role of this population in the spleen during the malaria infection is the clearance of infected erythrocytes in *P. chabaudi* infection [137]. In the GSK*Pf*Hu mouse model the phagocytosis of GR1$^+$ cells is lower than F4/80$^+$ macrophages, this difference might be due to GR1$^+$ cells are only phagocytosing infected cells which are cleared during anaemia and infection phase, which are cleared in a lower number than uninfected erythrocytes. Consitently, the spleen in the malaria infection in the human host plays an important role in the clearance of infected erythrocytes so as the modulation of the expression of parasite antigens on the surface of infected red blood cells [119].

Optimization of the GSK*Pf*Hu mouse model

In previous *Pf* mouse models described before, the route selected for the injection of red blood cells is the intraorbital plexus in mice previously treated with clodronate encapsulated liposeomes for the depletion of macrophages [12, 13, 98-101]. In our model for drug discovery purposes, the use of clodronate due to potential toxic effects and the possible intereference with tested drugs, needs to be excluded. Therefore, the injection of human red blood cells, in the GSK*Pf*Hu mouse model, is done mainly by intraperitoneal route. In addition, the intraperitoneal route for the daily human blood injections increases the reproducibility in the acquisition of chimerism [5]. Nevertheless, little is known about what happens with the erythrocytes after the injection in the intraperitoneal cavity. For this reason, in this work it has been studied the kinetics of the intraperitoneal injection, and it has been observed that less than 40% of human erythrocytes injected reached mice peripheral blood. In addition, the perfusion of the erythrocytes is slow and it takes 12

hours to reach the maximum peak of human red blood cells in mice peripheral blood after the injection. In addition, a secondary peak of human erythrocytes is found a 5 hours followed by a decrease in the number of hEry in the peripheral blood, this peak might be due to a sequestration in organs, as probably the spleen. In addition, the half life of human erythrocytes, after reaching tha maximun peak of absorption, was 6 times higher than the calculated after the i.v. injection in the erythrokinetics. This results may suggest that, although the erythrocytes are being cleared in a high proportion, there might be still erythrocytes that are being perfused to the blood stream from the peritoneal cavity. Therefore, it was hypothesized that the regime of injections every 24 hours, for the engraftment of mice, was suboptimal, human erythrocytes are being cleared from peripheral blood before the next injection is performed. Thus, new blood dosing regimes needed to be explored in further experiments to overcome this issue.

One of reasons for the low prevalence of human erythrocytes after the intraperitoneal injection, might be due to the enhanced phagocytosis of the human erythrocytes in the peritoneal cavity before their perfusion to the peripheral blood takes place. IL2 mice have a reduced phagocytic activity due to their deficiencies in the cytokines signaling transduction due to the absence of the receptor γ chain of the IL2 receptor [58]. Therefore, the erythrophagocytosis of peritoneum resident macrophages was determined in the GSK*Pf*Hu mouse model to confirm the activity of these macrophages. Peritoneal macrophages from naïve IL2 mice were extracted and put in a culture plate to study the ability of these cells to phagocytose human erythrocytes. It was found that IL2 peritoneal macrophages were active and performed the erythrophagocytosis, as well as splenic macrophages. Of note, in mice peritoneal cavity occurs erythropagocytosis, and this action is considered a rejection of the xenotransplant of human red blood cells by IL2 mice, as other authors have previously observed [55]. In addition, this rejection was also observed after the intravenous injection in naïve mice during the study of the erythrokinetic in the GSK*Pf*Hu mouse model where human erythrocytes half life in peripheral blood was only 6 hours. Consequently, the function of the phagocytic system is active and responsible for the rejection of the xenotransplant with human erythrocytes, but this system can be saturated as observed before in the erythrokinetics studies.

To overcome the rejection of the human erythrocytes after the injection, different human blood injections regimes were explored based on the results obtained in the kinetic of the intraperitoneal injection. For instance, the objective for these injections regimes was the saturation of the rejection mechanism to obtain an engraftment period lower than the 10 days needed in the actual GSK*Pf*Hu mouse model [63]. These new regimes were based on

the change on the volume of blood injected testing 0.5, 1 and 1.5 ml and the frequency of these injections, 24, 48 and 72 hours. Other regimes tested were based in the injection of human red blood cells in reduced periods of time, every 12 hours instead 24 hours, to saturate the peritoneal erythrophagocytosis and accelerate the perfusion of the human erythrocytes through the peripheral blood.

Regarding the volume of injection, 1.5 ml daily injections of human red blood cells decreased the time for engrafment to the half, in only 5 days 50-60% of human erythrocytes were in mice peripheral blood. However, these daily injections lead to a decrease in the body weight of mice, used as a measurement for animal welfare, for these reason this regime was discarded.

In terms of reducing the period of time of human blood injections needed to obtain 50-60% of human erythrocytes in mice peripheral blood, the best results were obtained in mice injected every twelve hours for two consecutive days. The engraftment period was reduced to four days, without altering the body weight of mice. These results suggest that the clearance system can be saturated only in two days, and the human erythrocytes can be accepted by the mouse immune system as a self erythrocyte.

Further studies were done for the optimization of the GSK*Pf*Hu mouse model, one of these studies included the characterization of the growth of different *P. falciparum* strains, to overcome the anaemia phase and the massive clearance of human erythrocytes. Several studies have been done to elucidate the molecular mechanisms involved in the selection for elimination of uninfected erytrhocytes, one of the most accepted causes of this clearance is that these erythrocytes have been in contact with merozoites and marked by the transference of the protein RSP-2 present in the ropthry of the merozoite to the erythrocyte surface. The presence of this protein in the eythrocyte membrane lead to the recognition of the erythrocytes by the spleen macrophages for their elimination [138].

Different strains were selected based on their characteristics: the parental strain NF54, resistant strains as V1/S, FCR3 and K1, and the transgenic strain Rap I which lacks the Rophtry proteins 1 and 2, which have been described as the responsibles of the clearance of non infected erythrocytes during the *P. falciparum* infection [75, 138], and its parental strain D10. The growth of these strains was compared with the 3D7 in the GSK*Pf*Hu mouse model and it was observed that the resistant strain V1/S in the same way than the 3D7, regarding to the anaemia phase, it was provoked at the same day after infection, although the peak of parasitemia found in the V1/S strain was 3 times higher than the control strain 3D7. However, the RapI and NF54 strain caused a delay of the aneamia phase starting 20

or 15 days later than the anaemia phase in 3D7 that occurs at day 10 after infection. The parasitemia peak found in these strains is similar to the one observed in the 3D7 strain. These results suggest that the anaemia phase may be not related to the amount of parasite found in mice peripheral blood. In human SMA is proportional not to circulating parasitemia but total parasite mass (sequestered) in the organs. The delay in the anaemia phase found with the RapI strain might be due to the absence of the ropthry proteins, but although the lack of these proteins, the anaemia phase takes place in the GSK*Pf*Hu mouse model. Presumably, this anaemia mechanism is crutial for the parasite life cycle and there might be redundant routes that lead to the massive clearance of uninfected erythrocytes provoking the anaemia. Despite the health importance, all the immunological mechanisms involved in the induction of the malaria anaemia remain incompletely understood although some efforts in the field has been done [41, 59, 75].

During the massive erythrocytes clearance and throghout the different phases of the GSK*Pf*Hu mouse model there is an activation of the inflammatory process leading to the release of different anti inflammatory cytokines and the activation of the phagocytosis by different populations of macrophages. To study the effect of the inflammatory response throughout the different phases of the model, IL2 mice were treated with different anti inflammatory drugs. Therefore, three different anti inflammatory drugs were used: i) Dexamethasone, which is a synthetic glucocorticoid that inhibits multiple immunocompetent cell types such as monocytes and macrophages, that are active in the *GSKPf* mouse model; ii) Acetylsalycilic Acid, which is a non-steroideal antiinflammatory drug that inhibits the production of prostaglandine that is secreted during an infection or an inflammatory process; iii) Anti GR-1, which is used for the depletion of GR-1 positive cells that include monocytes and macrophages. Mice were treated with different doses of these drugs, neither a massive growth of the parasite, nor the decrease of the massive erythrocytes clearance was found under the treatment that inhibits partially the activation of the phagocytic cells.

One of the main organs implied in the activation of the inflammatory response is the spleen. The spleen also serves as a filter that can remove red blood cells from circulation because of either physiological senescence or pathological alterations. When studying the structure and morphology of the spleen it can be found that the specialized structure of the venous system of the red pulp is responsible of the clearance of abnormal and senescent erythrocytes, so as the innate immune response by the presence of granulocytes and macrophages. Although the spleen has a crutial role in the malaria infection [119], it is not clear it is is involved in the rejection of the xenotransplant. Therefore, the engraftment

of human erythrocytes by intraperitoneal injections have been studied in IL2 splenectomized mice. Though the relevance of the spleen, no effect of the splenectomy was observed, IL2 splenectomized mice presented the same degree of rejection of the xenotransplant with human erythrocytes after the intraperitoneal injection as the non-splenectomized mice. Therefore, other organs could be involved in the clearance of the human erythrocytes in the absence of the spleen, this organ might be the liver, which is implied in the clerance of erythrocytes in the cases of polycythemia (incresed number of erythrocytes in peripheral blood) [27]. As a consequence, the absence of the spleen it does not seem crucial in the rejection of the xenotransplant with human erythrocytes in IL2 mice.

It is clear that the rejection of the xenotransplant of human erythrocytes in the IL2 mice is mainly driven by the innate immune system, that is the only immune response still present in this mice strain. There are several mutations that provoke serious immunodeficiency in mice. The most common mutation used is the Prkdc^{scid}, which are characteristic for the absence of B and T lymphocytes caused by arresting the lymphocyte development [29]. This mutation is present in the IL2 mice strain used in the GSK*Pf*Hu mouse model. However, the Rag2 and Rag1 mutations prevent the genetic recombination required for functional B and T cells receptors, resulting in a similar immune defects. These mutations confere increased resistence to radiation, making these mice strain more suitable for the study of tumors [89, 95, 134]. The generation of IL2 receptor gamma chain knockout produces the absence of NK cell activity in the scid or Rag background, increasing the immunodeficiency of the mice.

Different immunodeficent background were tested to evaluate the ability to sustain the xenotransplant with human erythrocytes and the infection with the *P. falciparum* parasite. The mice strains tested were: Rag2 IL2, NOG, NRG and FRG. All the different genetic background explored lead to the absence of T and B cells, in addition to NK deficent cells. Although the immunodeficency are similar in all strains tested, different results were obtained with one strain, the Rag2 IL2. The engraftment with human erythrocytes was not possible due to the fast clearance of the erythrocytes after the release of human erythrocytes in peripheral blood after the intraperitoneal injection, 24 hours earlier than in IL2 mice. However, the rest of the strains studied behaved in the same way as the IL2 strain, sustaining the *P. falciparum* infection but being unable to avoid the massive clearance of human erytrocytes.

Although different efforts have been done for the optimization of the GSK*Pf* mouse model regarding to avoid the massive clearance of human erythrocytes none of the efforts explored had a positive outcome. Further studies must be done in this field to establish the mechanisms that induce the severe anemia associated with the infection caused by human parasite *P. falciparum*. However, in spite of these difficculties the GSK*Pf*Hu mouse model is able to sustain the growth of the human *P. falciparum* parasite and the innate immune response found in mice in addition to the severe malarial anaemia are similar to the found in human beings during the infection with the *falciparum* parasite. These evidences support the fact that the GSK*Pf*Hu model can be considered as a powerful tool of research on malaria disease progression.

The GSK*Pf*Hu mouse model as a researching tool

The establishment of mice with genetic immune deficiencies, such as loss of T and B lymphocytes and carrying *null* mutations in the IL2 receptor common *gamma* chain has allowed the efficient engraftment of different types of human cells [112]. The humanized mouse models are crucial for the study of human infectious diseases, cancer biology an more recently, regenerative medicine. In the case of malaria , the development of a reliable mouse model for the human parasite *P. falciparum* has been a major breakthrough and has circumvented the ethical concerns for the use of non-human primates, that were the only alternative for malaria *in vivo* studies several years ago. Indeed, the establishment of a reproducible *P. falciparum* mouse model have changed the drug discovery panorama in the malaria field over the past 10 years. Several compounds that actually are in clinical phases of drug development have been tested in the GSK*Pf*Hu mouse model [61, 103, 117].

The main advantages of the GSK*Pf*Hu mouse model are based on the feasibility, it is needed immunodeficent mice and human blood, and the reproducibility of the *P. falciparum* growth without the addition of immunomodulators that can interfere with other drugs when the model is used for drug discovery assays. The use of IL2 mice has been crucial for the malaria drug discovery. These mice do not develop thymic lymphomas, as the β2 mice used in the first *Pf* mouse model developed in GSK facilities [5], allowing the performance of long term experiments. Besides, these mice are unable to clear *P. falciparum* infection without therapeutic interventions. These characteristics have made the GSK*Pf*Hu mouse model a reference tool in the development of new antimalarial drugs.

The use of this model can provide estimates of the efficacy therapeutic parameters in terms of efficacy dose and drug exposure by the use of a modified Peters´ 4-day test. The main modifications consist on the treatment starting point, in which mice are treated during 4 days starting when parasites are detectable in mice blood by flow cytometry. Whereas in the original 4-day test mice treatment starts from one to three hours after the infection, so parasite growht is not exponential. During the treatment, parasitemia is measured everyday to quantify the effects of the drugs on the parasite growth which allows to obtain parasite clearance curve. However, in the Peters´ 4-day test parasitemia is measured only 24 hours after finishing the treatment. Finally and in addition to the Peters´ assay, within the first 24 hours samples of the measurement of the drug levels in blood are obtained for each mouse included in the assay. The measurement of parasitemia and drug levels in blood is done for each individual mouse included in the assay to explore the individual differences.

The parameters of efficacy obtained from the 4-day test are essentially measurements of potency to achieve a biological endpoint. The usual biological endpoins estimated are the reduction in parasitemia with respect to the vehicle treated mice, the ED_{90}, which is the effective dose that reduce parasitemia by 90%. Additionally, the measurement of the drug levels in mice blood can be used for the estimation of another efficacy parameter can be estimated, the $AUCED_{90}$, which is the quantity of compound per hour in blood needed every 24 hours of treatment to reduce the parasitemia by 90%. However, the final biological endpoint in the efficacy assay and the one that usually is used in the human dose prediction and modelling, is the curative dose or the dose that do not have recrudescence of parasite up to 28 days after finishing treatment with the drug.

In this work, two complete efficacy studies are included. Compounds exhibit a different inhibition profile. However, although the effect of the Atovaquone is slower, the quantity of compound needed to kill the 90% of the parasite (ED_{90}) is less than the needed for a fast compound as the Piperaquine (0.05 mg/kg for Atovaquone *versus* 0.8 mg/kg for Piperaquine). Moreover, the quantity of drug in blood needed to kill the 90% of the parasitemia ($AUCED_{90}$) in the case of Atovaquone is also less (0.03 mg·h/kg) than the needed for Piperaquine to kill the same percentage of parasite (0.8 mg·h/kg). These results suggests that the speed of clearance of parasite is not the main driver for the estimation of the potency of the compound. In this case, the biological endpoint used is the ED_{90} or $AUCED_{90}$ and do not take into account the parasite clearance rate, but the final parasitemia obtained 24 hours after finishing the treatment. For this reason, the

Atovaquone, in spite of being considered a slow acting drug is more potent that Piperaquine.

Among the doses tested for the Atovaquone in the 4-day test (0.01, 0.05, 0.1, 1 and 10 mg/kg), the maximal biological effect or parasite clearance curve is reached at the dose of 0.1 mg/kg. As a result, the following doses obtain the same biological effect. Paradoxically, when the recrudescence study is performed to find the curative dose for Atovaquone it is found that the doses of 0.1, 1 and 10 are not curative doses and show different time to recrudescence response although having reached the maximal biological effect. Consequently, within the development of Atovaquone, when used as a single monotherapy agent in the treatment of *P. falciparum*, was probed to be highly effective, but it was associated to high recrudescence rates, and the emergence of resistances were observed 6 months after treatment [15, 81], concuring with what it has been shown in the 4-day efficacy assay in the GSK*Pf*Hu mouse model. These results prevented Atovaquone to be marketed alone and actually is used in combination usually with Proguanil, which synergized with Atovaquoen and provides better results in terms of parasite relapse [80].

When Piperaquine was administered to the infected mice, the maximal biological effect is found at the dose of 10 mg/kg, among the doses tested (1, 5, 10, 25, 50 and 100 mg/kg). In addition, at this dose it is reached the curative dose, none of the mice at this dose and higher showed recrudescence up to 28 days after finishing the treatment. The Piperaquine treatment in human beings also lead to a fast clearance of parasite, with up to 5 hours of parasite clearance half life after starting treatment in patients. In addition, the rates of parasite recrudescence are lower compared to Atovaquone, with 100% of cure in the patients that received the highest dose of Piperaquine alone in a recently clinical study performed [111]. Although Piperaquine is a very effective marketed antimalarial compound, it is administered in combination (usually Dihydroartemisinin) to avoid the emergence of resistant parasites after treatment [45].

The GSK*Pf*Hu mouse model has become an unique tool to analyze the properties of drugs as future medicines. The use of human pathogen in the model has been crucial to explore the translational use of the model for malaria disease [4], and it has been used in multiple projects during the discovery and development of new antimalarial drugs inside and outside GSK facilities [28, 69].

In human beings the efficacy of a drug is measured by the rate at which the parasite are cleared from peripheral blood and the rate of cure after treatment [154]. In the 4-day test performed with the *Pf* mouse model, the parasite clearance rate is not used as a

measurement of efficacy, but the differences in parasitemia at a given time of the assay with respect to the vehicle-treated controls, the daily sampling for parasitemia measurement and the non-recrudescence dose (cure after treatment), can be used for the modelling of parasite clearance rate in human with different potent softwares used by modellers. In addition, the microsampling of mice employed in efficacy studies for the measurement of drug levels in blood, can be used for the estimation of the PK/PD relationships that drive the efficacy, and parameters such as the quantity of drug needed every 24 hours to kill the 90% of parasite ($AUCED_{90}$) or needed to obtain the maximun parasite clearance (MCP) can be estimated and used for human dose predictions in the clinical study designs in the first time in human phase [90].

The 4-day test with drug levels measurement have been designed to obtain the maximun information of a potential antimalarial compound such as potency, speed of parasite clearance and time to recrudescence in only one assay. This information can be increased depending on the readout technique used for the parasitemia measurement. Several years ago, the gold standard for parasitemia assessment was microscopy with Giemsa stained smears, and nowadays is usually used in areas in which malaria is endemic. In countries where the first time in human clinical trials with healthy volunteers are done, the qPCR is an alternative method used for the parasitemia readout [90, 111]. However, the introduction of flow cytometry for the detection of the *Plasmodium* parasite has implied a huge breakthrough in the malaria field in pre-clinical phases of drug discovery. Thus, previous methodology as microscopy is a very time consuming technique and it is needed specialized personnel to obtain a reliable result, and for qPCR usually is needed higher content of blood sampling (from 50 to 70 µl), that makes difficult the daily sampling of mice without provoking an anaemia. However, the flow cytometry technique provides higher throughput, statistical power, accuracy in the counting of low parasitemias and it is less time consuming, and it is only needed 2 µl of blood per sampling point [62]. Consequently, the flow cytometry technique for the detection of parasite have been implemented in the pre-clinical stages of drug development and has started to be implemented for malaria diagnosis in malaria endemic areas in the last 5 years [35].

The use of flow cytometry parasite detection can be crucial to obtain more information about the drug tested in the 4-day efficacy assay providing further insights regarding the mode of action. The incorporation of high-content experimental designs might increase the decision-making and translational value of GSK*Pf*Hu mouse model. Indeed, a phenotypic study of the dying profile and parasite speed of clearance for treated

falciparum parasite can be done. This study might give a clue about the mode of action of the drugs tested.

In this work it is described how the YOYO-1 bidimensional analysis combined with the monoclonal antibody TER119-PE improve the sensitivity of the flow cytometry technique making suitable the characterization of all *P. falciparum* erythrocytic stages. Once it has been validated that the YOYO-1/TER119-PE technique is susceptible for the detection of slight differences in terms of complexity and DNA quantity in the different parasiste stages, it can be taken a step forward considering the possibility of usign YOYO-1 to monitor the morphological changes that parasite suffers under treatment with potential antimalarial drugs in the 4-day efficacy assay. Thus, it is proposed that the use of YOYO-1 technique can elucidate the most likely vulnerable erythrocytic stages to the treatment.

The addition of phenotypic effect to the *in vivo* 4-day assay may increase the information obtained in this assay. The validation of the phenotypic effect observation was assesed using standard commercial antimalarial drugs. There, mice received 4-day treatment and samples from peripheral blood were stained with the YOYO-1/TER119-PE technique. The used antimalarial drugs belong to different chemical families with different mechanism of action to validate our hypothesis, but not all of them are well known. According to the results obtained, it has been defined five different dying profiles based on the patterns shown in the YOYO-1/TER119-PE patterns found, and four different speed of parasite clearance (fast, medium, slow, very slow) depending on the time that parasite takes to be cleared from peripheral blood after starting treatment (24-48 hours for fast, 72 hours for medium, 96 hours for slow and more for verly slow clearance), which could be accountable of mode of actions with a defined delayed phenotype.

Regarding to the speed of clearance, this phenotypic characteristic might be crutial when in early stages of drug discovery it is needed a filter to discriminate different type of drugs to target a single dose treatment in clinical studies or slow acting drug to be developed as a partner of a fast acting compound in drug combination therapies [104, 130]. In the last years, the only study to discriminate this characteristic has been in vitro studies of parasite reduction rate [79]. However, in the 4-day assay with the daily parasitemia sampling is posible to obtain a complete curve of parasite clearance in a alive host, where the pharmacokinetics properties of the drug and metabolism of the host may play a crutial role to define the final effect of the drug in the parasite, characteristics that actually can not be simulated in *in vitro* cultures.

According to the results obtained, it has been able to define five different patterns of dying profile when analyzing YOYO-1/TER119-PE samples from treated mice. For instance, in the pyknotic pattern it has been englobed those compounds that produced shrinked parasites at the end of the treatment, this pattern is common in compounds that show a fast-medium parasite clearance. Compounds enclosed in this group such as Chloroquine, Amodiaquine and Piperaquine belong to the same antimalarial class, the 4-aminoquinolines. By addition, these compounds share the same mechanism of action, which is the prevention of biocrystallization of the haeme group in the food vacuole [108]. The haeme group is generated from the digestion of hemoglobin in the food vacuole by the parasite, it is toxic to the parasite and must be detoxified through polymerization to form hemozoin (malaria pigment). Other compounds are included in the pyknotic group but neither belong to the same antimalarial class nor have the same mechanism of action of the aforementioned compounds. Indeed, Artesunate and Dihydroartemisinin belong to the endoperoxide class and their proposed mechanism of action is the production of free oxidative radicals, reactive metabolites that can react with free hemin present in hemozoin and hemoglobin forming haeme adducts, and the disruption of membrane transport [107]. Although the compounds included in the pyknotic dying profile do not share the specific mechanism of action, flow cytometry pattern suggest that they have the same global final effect on parasite population and the most sensitive parasite stage to treatment is the young stages (rings and early trophozoites), due to the fact that there is not shown a parasite maturation YOYO-1 pattern at the end of treatment. Whereas, the low intensity population showed by YOYO-1 dot plots, suggests apoptotic form of parasite, confirmed by microscopy. This fact may reflect a final step in the parasite intoxication as a consequence of the treatment with the different compounds that lead to the same final fate.

By contrast, Primaquine belongs to the 8-aminoquinolines chemical class which is derived from the 4-aminoquinolines series, but differs in the mechanism of action, that is still not completely understood but it is thought to cause an interference with the cellular respiration and a dysregulation of the electron transport in the mitochondria [47], showed a dying profile that can be defined as shrinked trophozoites, that lead to parasite death in a different way as Chloroquine and Piperaquine. Although Primaquine belong to a similar chemical class as Chloroquine, it differs in its mechanism of action, these differences may explain the discrepancy observed in parasite dying profile and in parasite clearance speed, in which Primaquine induces a slow parasite clearance.

In the same way, compounds included in another dying profile, the vacuolated, belong to different chemical families although they share similar mechanism of action. In this profile it is included Atovaquone, that belong to the Hydroxy-1,4-naphthoquinone family, a GSK compound, the GSK932121 that is included in the 4(1H)-pyridone chemical family, and Primaquine which is a 8-aminoquinolines. When compound GSK932121 was developed, little was known about its mechanism of action. However, when this chemical family was selected for the progression to clinical phases further studies were performed and concluded than shared the same mechanism of action and Atovaquone but it showed efficacy against Atovaquone resistant strains [96]. Both compounds block the electron transfer chain by binding to parasite cytochrome bc_1 at different sites, and prevent the transport of H^+ to the intermembrane space and block the pyrimidine synthesis needed for the replication of DNA required before the schizontal phase [15, 36]. Indeed, treatment with these compounds lead to the blockage of parasite replication, as shown in YOYO-1 pattern, in which parasite is retained in trophozoite stages but showing an altered pattern when comparing with the vehicle treated mice. Both compounds, also share a very slow parasite clearance profile. In this case, parasite death is caused to an avoidance of replication, instead of a direct death provoked by an oxidative stress or loss of the metabolism. For this reason, it is needed that parasite reach the trophozoite stage to be affected by the treatment. In addition, affected parasite is probably retained in the same stage and can still be alive, in some way, until it is cleared by the host immune system, this may explain the slower parasite clearance profile.

Pyrimethamine and Proguanil also affect the trophozoite stage but it a slightly different way as Atovaquone and GSK932121. These compounds belong to the type-2 antifolate chemical family, which mechanism of action is the inhibition of the dihydrofolate reductase enzime (DHFR), leading to the inhibition of the biosynthesis of pyrimidines and purines, needed for DNA synthesis, and some aminoacids essential for the parasite survival [159]. Consequently, the effect found in flow cytometry pattern is very similar to that found for Atovaquone and GSK932121, that also inhibited the pyrimidine synthesis. In this case, the parasite dying pattern can be defined as swollen profile. However, the parasite stage affected for the treatment is also the trophozoite. However, Pyrimethamine and Proguanil parasite clearance is medium-slow, medium for Pyrimethamine and slow for Proguanil. This different parasite clearance speed in comparison to Atovaquone might be due to Pyrimethamine and Proguanil inhibits other biosynthesis pathways in addition to the pyrimidines synthesis, that provokes a faster parasite death. Of note, the differences between the Pyrimethamine and Proguanil in the speed of parasite clearance may be due to the fact that Proguanil need to be metabolized by the hepatic cytochrome P145 to

cycloguanil, that is the dihydrofolate reductase inhibitor [150]. This delay until the obtaining of the active metabolite might be the caus of the delay in the parasite clearance.

Sulfadoxine is another antifolate antimalarial, but belongs to the type-1 subfamily, which mechanism of action is the inhibition of the dihydropteroate synthase enzyme (DHPS), which is also a enzyme belonging to the parasite folate pathway previous to the DHFR that is inhibited by Pyrimethamine and Proguanil [57]. However, in this case the Sulfadoxine treatment led to no effect in the parasite reduction. This result might be due to an insuficient dose administered to mice (100 mg/kg), nevertheless little is known about the monotherapy treatment of Sulfadoxine *in vitro* or in clinical studies in human beings that support the fact that the dose used was inadequate.

Finally, there is another dying pattern obtained in this phenotypic study, that show swollen young stages (young trophozoites) in YOYO-1 staining, but this incovenience is not able to stop parasite maturation and parasite reinfection under treatment is possible in some way, as a result, parasite clearance is slow. Compounds that cause this pattern belong to the same chemical family, the aryl amino alcohol, and compounds tested included in this family are Quinine, Mefloquine and Lumefantrine. Although its mechanism of action has to been yet well elucidated, they show the same pattern in YOYO-1 staining. However, it is said that the mechanism of action is based on preventing the detoxification of the haeme group, as a result the toxic haeme and free radicals that are released induce parasite death [10, 127]. These mechanism of action can be similar to the 4-aminoquinolines family (pyknotic profile), but the aryl amino alcohol compounds seem to have lower affinity to the haeme group and may prevent the haeme polymerization by antagonism instead of clumping. Among the aryl amino alcohol compounds tested, the one that showed more effect is the lumefantrine (at the end of the treatment parasite clearance is better). Consequently, lumefantrine is metabolized by the cytochrome P450 to desbutyl-lumefantrine, that have been described to have from 5 to 8 fold higher antiparasitic effect than lumefantrine itself [10].

Phenotypic studies used in early stages of drug development, when little is known about the compounds, can be crutial in the decision making process in terms of compound priorization. In addition, this assay that can elucidate the most likely vulnerable erythrocytic stage, in addition to a specific dying profile, when added to *in vivo* screening assays may transform this type of assay in High-content High-throughput *in vivo* screening without neither the addition of extra sampling nor the performance of an extra assay. These data have important implications for understanding or predicting the clinical

efficacy of drug treatment, design of drugs, or combinations with broad activity across different developmental stages and for measuring the development of mechanisms of drug resistance [65, 148].

The fight against malaria includes the search for drugs that can affect the parasite in the different stages during the infection of the human host: liver and erythrocytes that include asexual and sexual stages. In the recent years the efforts to eradicate the malaria in the world has been focus on the asexual erythrocytic stages, that are responsible of the pathology of the disease, and the gametocytes (sexual stages), that is the only stage within the life cycle of malaria parasite that are able to mediate the transtition from the human host to the insect host. The advances in the generation of *P. falciparum* mouse models have been crutial for the development of new potential antimalarials against erythrocytic stages. However, actually it is not available a reliable *in vivo* model to study the efficacy of this compounds against sexual stages.

Gametocytes can be successfully produced in *in vitro* cultures, and there are available assays that can be used to evaluate the efficacy of compounds against the different gametocytes stages and also male and female gamete formation, that are the reproductive stages of parasite [44, 77, 92]. The current "gold standard" test of the ability of a compound to prevent transmission to mosquito is the standard membrane feeding assay (SMFA), which permits the feeding of stage V gametocytes in the absence or presence of compounds to mosquitoes in a experimentaly controlled manner [78].

In vitro studies are very important for the discovery of new antimalarials, but the final effect of the compound has to be tested not only in the parasite but also evaluate the physiological consequences on the host or the effect of the host metabolism in the drugs tested. The lack of small animal models to study the transmission blocking potential of drugs is a barrier for the conduction of essential preclinical researching. For this reason, it has been studied the ability of the GSK*Pf*Hu mouse model to be used as an *in vivo* tool for the study of the transmission blocking potential of new compounds. However, first of all it is needed to study the ability of the GSK*Pf*Hu mouse model to support the sexual stages of the *P. falciparum* parasite.

For this purpose, it is studied the instrinsic ability of the *P. falciparum* NF54 *in vivo* adapted strain to produce gametocytes without the addition of any reactive for the induction. It has been described before the presence of gametocytes in other *P. falciparum* humanized mouse models. However, these models are based in the direct injection of a *P. falciparum* parasite grown in an *in vitro* culture or that comes from a human volunteer to

the engrafted mice without previous adaptation to the mouse host [7, 97]. For this reason, it is not well known neither the gametocytes detected in mice peripheral blood have been developed in the previous recipent nor the induction of gametocytes have been done in the humanized mice. Gametocytes need up to 15 days to develop from stage I to stage V, which is the one that is infective to mosquitoes [73]. However, in the GSK*Pf*Hu mouse model it has been studied the gametocytogenesis in a *Pf* strain adapted to grow in humanized mice after several *in vivo* passages until obtain a reproducible growth, up to 21 passages were done, with at least 1 passage per week [5]. For this reason, in this case there is no doubt that the presence of gametocytes in this mouse model is the result of the natural induction and production in the mouse host.

The gametocytogenesis in the GSK*Pf*Hu mouse model was monitored up to 26 days after infection. Gametocytes in all stages (form I to V) were detected in giemsa smears. In addition, an exflagellation assay was performed to assess the viability of stage V gametocytes and it was revealed that the peak of exflagellation is about day 16 that is close to the 15 days required in the human host to reach the stage V gametocytes [73]. Consequently, a transmission study to mosquitoes was done as a confirmation of the viability of gametocytes, it was found that mosquitoes were infected with a prevalence of 5%, that is much lower to that found in other *Pf* humanized mouse model, 38% [97]. However, it is tha same value as the prevalence obtained in the natural *P. falciparum* infection in the human host [43].

Although this value confirms that the GSK*Pf*Hu mouse model can mimic what is happening in the nature, for the development of a transmission blocking assay it is needed an increase in the mosquito prevalence and number of oocysts per mosquito to be able to observe the effect in the reduction of this prevalence after the treatment with new drugs. For this reason, a new approach was considered to overcome the deficiencies of the natural transmission approximation.

In this new approach, a combination of *in vitro/in vivo* assay was designed. Stage V gametocytes were cultured and purificated, then injected to IL2 engrafted mice, with at least 50% of human erythrocytes to avoid the rejection of the gametocytes. At this percentage of human erythrocytes no additional blood injections are required throughout the experiment, due to the fact that hEry half life is more than 10 days and the experiment is designed to last 4 days. Half live of stage V gametocytes in the human host is 2.4 days [141], and consequently in the GSK*Pf*Hu mouse model the half life of the injected stage V gametocytes was measured in 3 days. These results confirms that there is no rejection of

stage V gametocytes in the mouse host. The viability of the gametocyes was also studied and confirmed by the exflagellation assay. Therefore, a transmission study to mosquitoes was assessed to confirm the viability of these gametocytes. It was found that although the concentration of gametocytes was higher than in the natural transmission study, the prevalence of mosquito infection was similar, 6%.

These results suggest that the GSK*Pf*Hu mouse model can be used to test the ability of compounds to block transmission of *P. falciparum* gametocytes from humanized mice to mosquitoes. However, further efforts have to be done in order to set up a reliable and reproducible *in vivo* transmission blocking assay. These efforts may include either to find and adapt new *P. falciparum* strains with a reproducible higher yield of late-stage gametoyces and focus the adaptation on the reinforcement of the sexual stages by using passages through mosquitoes to mice with human liver (FRG mice) and viceversa if the natural transmission strategy is aborded, or to identify the issues that are provoking the low prevalence in mosquito infection as may be the high hematocrit that humanized mice show or the purification step previous to the injection of the stage V gametocytes, if the *in vitro/in vivo* approach is selected. Actually, these efforts are being done and in few months new data will be obtained.

.

Conclusions/Conclusiones

Conclusions

1.- IL2 mice has allowed the establishment of an efficient and robust *P. falciparum* humanized mouse model in which the xenotransplant of human erythrocytes is reproducible and can be optimized by changing the regimes of human blood injections to mice.

2.- The *P. falciparum* growth is reproducible and the GSK*Pf*Hu mouse model can sustain the infection with different *P. falciparum* strains. The *P. falciparum* erythrocytic cycle length in the GSK*Pf*Hu mouse model have been demonstrated to be the same as in the human host, 48±1 hour. These results suggest that the GSK*Pf* Hu mouse model can be used as a good surrogate for the *P. falciparum* erythrocytic stage.

3.- The characterization in the GSK*Pf* Hu mouse model of the erythrokinetics of human and mouse erythrocytes makes possible the discrimination of three different phases in the model: engraftment, infection and anaemia. The anaemia phase is characteristic for the massive clearance of infected and uninfected eythrocytes. This pathology has been previously described in the *P. falciparum* infection in the human host and is one of the causes of the high mortality of the malaria disease, the severe malarial anaemia.

4.- The innate immune response to the xenotransplant of human erythrocytes and infection with *P. falciparum* in the GSK*Pf*Hu mouse model are mediated by the release of inflammatory cytokines by phagocytic cells. The cytokines secretion pattern is similar to that found in the natural *P. falciparum* infection in the human host.

5.- The GSK*Pf*Hu mouse model has been validated for the test of antimalarial drugs and the obtaining of the efficacy parameters in the model are crucial for the decission making for different drug development projects in preclinical stages.

6.- The GSK*Pf*Hu mouse model can sustain the sexual development of parasite, and the transmission to mosquitoes have been demonstrated. These results lay the groundwork for the development of a transmission blocking assay to test the abitily of new drugs to block the transmission to mosquitoes.

Conclusiones

1.- Los ratones IL2 permiten el establecimiento de un modelo de ratón humanizado eficiente y robusto en el que el xenotransplante con eritrocitos humanos es reproducible y es susceptible de ser mejorado mediante cambios en la pauta de inyecciones de sangre humana a los ratones.

2.- El crecimiento de *P. falciparum* es reproducible y el modelo murino GSK*Pf*Hu es capaz de soportar la infección con diferentes cepas de *P. falciparum*. Además, se ha demostrado que la duración del ciclo eritrocítico en el modelo murino GSK*Pf*Hu es la misma que en el hospedador humano, 48±1 horas. Estos resultados sugieren que el modelo murino GSK*Pf*Hu puede ser usado como sustituto para estudiar la fase eritrocítica de *P. falciparum*.

3.- La caracterización de las eritrocinéticas de los eritrocitos humanos y de ratón en el modelo murino GSK*Pf*Hu hace posible la discriminación de tres fases diferentes en el modelo: quimerización, infección y anemia. La fase de anemia se caracteriza por la eliminación masiva de eritrocitos infectados y no infectados. Este patología ha sido descrito en la infección de *P. falciparum* en el hospedador humano y es una de las causas de la alta mortalidad de la malaria, la anemia severa.

4.- La respuesta inmune innata al xenotransplante de eritrocitos humanos y la infección con *P. falciparum* en el modelo murino GSK*Pf*Hu está mediada por la secreción de citoquinas inflamatorias por las células fagocíticas. El patrón de secreción de citoquinas es similar al encontrado durante la infección de *P. falciparum* en el hospedador humano.

5.- El modelo murino GSK*Pf*Hu ha sido validado para testar fármacos antimaláricos y la obtención de parámetros de la eficacia de estos fármacos en el modelo son cruciales para la toma de decisiones en los diferentes proyectos de desarrollo farmacéutico en fases preclínicas.

6.- El modelo murino GSK*Pf*Hu es capaz de soportar el desarrollo de las formas sexuales del parásito, y la transmisión a mosquitos ha sido demostrada. Esos resultados sientan las bases para el desarrollo de un ensayo para evaluar la capacidad de bloquear la transmisión a mosquitos de nuevos fármacos.

Bibliography

1. Ahn, S.Y., M.Y. Shin, Y.A. Kim, J.A. Yoo, D.H. Kwak, Y.J. Jung, G. Jun, S.H. Ryu, J.S. Yeom, J.Y. Ahn, J.Y. Chai, and J.W. Park, *Magnetic separation: a highly effective method for synchronization of cultured erythrocytic Plasmodium falciparum.* Parasitology Research, 2008. **102**(6): p. 1195–1200.

2. Alano, P., *The sound of sexual commitment breaks the silencing of malaria parasites.* Trends in Parasitology, 2014. **30**(11): p. 509–510.

3. Andrysiak, P., W. Collins, and G. Campbell, *Concentration of Plasmodium ovale- and Plasmodium vivax-infected erythrocytes from nonhuman primate blood using Percoll gradients.* American Journal of Tropical Medicine and Hygiene, 1986. **35**(2): p. 251-254.

4. Angulo-Barturen, I. and S. Ferrer, *Humanised models of infection in the evaluation of anti-malarial drugs.* Drug Discovery Today: Technologies, 2013. **10**(3): p. e351–e357.

5. Angulo-Barturen, I., M.B. Jiménez-Díaz, T. Mulet, J. Rullas, E. Herreros, S. Ferrer, E. Jiménez, A. Mendoza, J. Regadera, P. Rosenthal, I. Bathurst, D. Pompliano, F. Gómez de las Heras, and D. Gargallo-Viola, *A murine model of falciparum-malaria by in vivo selection of competent strains in non-myelodepleted mice engrafted with human erythrocytes.* PLoS ONE, 2008. **3**(5): p. e2252.

6. Angulo, I. and M. Fresno, *Cytokines in the Pathogenesis of and Protection against Malaria.* Clinical and Diagnostic Laboratory Immunology, 2002. **9**(6): p. 1145–1152.

7. Arnold, L., R.K. Tyagi, P. Meija, C. Swetman, J. Gleeson, J.-L. Pe´rignon, and P. Druilhe, *Further Improvements of the P. falciparum Humanized Mouse Model.* PLoS ONE, 2011. **6**(3): p. e18045.

8. Arnold, L., R.K. Tyagi, P. Mejia, N.V. Rooijen, J.-L. Pérignon, and P. Druilhe, *Analysis of innate defences against Plasmodium falciparum in immunodeficient mice.* Malaria Journal, 2010. **9**(197).

9. Ault, K.A. and C. Knowles, *In vivo Biotinylation for Cell Tracking and Survival/lifespan Measurements*, in *In Living Color*. 2000. p. 284-290.

10. Aweeka, F.T. and P.I. German, *Clinical Pharmacology of Artemisinin-Based Combination Therapies.* Clinical Pharmacokinetics, 2008. **47**(2): p. 91–102.

11. Azuma, H., N. Paulk, A. Ranade, C. Dorrell, M. Al-Dhalimy, E. Ellis, S. Strom, M.A. Kay, M. Finegold, and M. Grompe, *Robust expansion of human hepatocytes in Fah−/−/Rag2−/−/Il2rg −/− mice.* Natural Biotechnology, 2012. **25**(8): p. 903–910.

12. Badell, E., C. Oeuvray, A. Moreno, S. Soe, N.v. Rooijen, A. Bouzidi, and P. Druilhe, *Human Malaria in Immunocompromised Mice. An in Vivo Model to Study Defense Mechanisms against Plasmodium falciparum.* Journal of Experimental Medicine, 2000. **192**(11): p. 1653-1660.

13. Badell, E., V. Pasqueto, N. Van Rooijen, and P. Druilhe, *A mouse model for human malaria erythrocytic stages.* Parasitology Today, 1995. **11**: p. 235-237.

14. Baer, K., C. Klotz, S.H.I. Kappe, T. Schnieder, and U. Frevert, *Release of Hepatic Plasmodium yoelii Merozoites into the Pulmonary Microvasculature.* PLOS Pathogens, 2007. **3**(11): p. e171.

15. Baggish, A.L. and D.R. Hill, *Antiparasitic Agent Atovaquone.* Antimicrobial Agents and Chemotherapy, 2002. **46**(5): p. 1163–1173.

16. Baldi, D.L., K.T. Andrews, R.F. Waller, D.S. Roos, R.F. Howard, B.S. Crabb, and A.F. Cowman, *RAP1 controls rhoptry targeting of RAP2 in the malaria parasite Plasmodium falciparum.* The EMBO Journal, 2000. **19**: p. 2435-2443.

17. Banerjeea, R., S. Khandelwalb, Y. Kozakaia, B. Sahua, and S. Kumara, *CD47 regulates the phagocytic clearance and replication of the Plasmodium yoelii malaria parasite.* PNAS, 2015. **112**(10): p. 3062–3067.

18. Bannister, L.H., J.M. Hopkins, R.E. Fowler, S. Krishna, and G.H. Mitchell, *A Brief Illustrated Guide to the Ultrastructure of Plasmodium falciparum Asexual Blood Stages.* Parasitology Today, 2000. **16**(10): p. 427–433.

19. Barbee, R., B. Perry, R.N. Re, and J.P. Murgo, *Microsphere and dilution techniques for the determination of blood flows and volumes in conscious mice.* Am. J. Physiol. Regulatory Integrative Comp. Physiol., 1992. **263**: p. 728-733.

20. BeiResources. *3D7*. Available from: https://www.beiresources.org/Catalog/BEIParasiticProtozoa/MRA-102.aspx.

21. BeiResources. *D10*. Available from: https://www.beiresources.org/Catalog/BEIParasiticProtozoa/MRA-201.aspx.

22. BeiResources. *FCR3*. Available from: https://www.beiresources.org/Catalog/BEIParasiticProtozoa/MRA-736.aspx.

23. BeiResources. *K1*. Available from: https://www.beiresources.org/Catalog/BEIParasiticProtozoa/MRA-159.aspx.

24. BeiResources. *NF54*. Available from: https://www.beiresources.org/Catalog/BEIParasiticProtozoa/MRA-1000.aspx.

25. BeiResources. *Rap I*. Available from: https://www.beiresources.org/Catalog/BEIParasiticProtozoa/MRA-572.aspx.

26. BeiResources. *V1/S*. Available from: https://www.beiresources.org/Catalog/BEIParasiticProtozoa/MRA-176.aspx.

27. Bogdanova, A., D. Mihov, H. Lutz, B. Saam, M. Gassmann, and J. Vogel, *Enhanced erythro-phagocytosis in polycythemic mice overexpressing erythropoietin.* Blood, 2007. **110**(2): p. 762-769.

28. Booker, M.L., C.M. Bastos, M.L. Kramer, J. Robert H. Barker, R. Skerlj, A.B. Sidhu, X. Deng, C. Celatka, J.F. Cortese, J.E.G. Bravo, K.N.C. Llado, A.E. Serrano, I. Angulo-Barturen, M.B. Jiménez-Díaz, S. Viera, H. Garuti, S. Wittlin, P. Papastogiannidis, J.-w. Lin, C.J. Janse, S.M. Khan, M. Duraisingh, B. Coleman, E.J. Goldsmith, M.A. Phillips, B. Munoz, D.F. Wirth, J.D. Klinger, R. Wiegand, and E. Sybertz, *Novel Inhibitors of Plasmodium falciparum Dihydroorotate Dehydrogenase with Anti-malarial Activity in the Mouse Model.* The Journal of Biological Chemistry, 2010. **285**(43): p. 33054–33064.

29. Bosma, M.J. and A.M. Carroll, *The SCID Mouse Mutant: Definition, Characterization, and Potential Uses.* Annual Review Immunology, 1991. **9**: p. 323-350.

30. Boström, S., P. Giusti, C. Arama, J.-O. Persson, V. Dara, B. Traore, A. Dolo, O. Doumbo, and M. Troye-Blomberg, *Changes in the levels of cytokines, chemokines and malaria-specific antibodies in response to Plasmodium falciparum infection in children living in sympatry in Mali.* Malaria Journal, 2012. **11:109**.

31. Brockman, A., R.N. Price, M.v. Vugt, D.G. Heppner, D. Walsh, P. Sookto, T. Wimonwattrawatee, S. Looareesuwan, N.J. White, and F. Nosten, *Plasmodium falciparum antimalarial drug susceptibility on the north-western border of Thailand during five years of extensive use of artesunate–mefloquine.* Transactions of the Royal Society of Tropical Medicine and Hygiene, 2000. **94**(5): p. 537–544.

32. Brown, G.V., R.F. Anders, and G. Knowles, *Differential effect of immunoglobulin on the in vitro growth of several isolates of Plasmodium falciparum.* Infection and Immunity, 1983. **39**(3): p. 1228-35.

33. Bruce, M.C., P. Alano, S. Duthie, and R. Carter, *Commitment of the malaria parasite Plasmodium falciparum to sexual and asexual development.* Parasitology, 1990. **100**(2): p. 191-200.

34. Butcher, G.A., A.F. Couchman, J.F.V. Pelt, S.L. Fleck, and R.E. Sinden, *The SCID mouse as a laboratory model for development of the exoerythrocytic stages of human and rodent malaria.* Experimental Parasitology, 1993. **77**: p. 257-260.

35. Campo, J.J., J.J. Aponte, A.J. Nhabomba, J. Sacarlal, I. Angulo-Barturen, M.B. Jiménez-Díaz, P.L. Alonso, and C. Dobaño, *Feasibility of Flow Cytometry for Measurements of Plasmodium falciparum Parasite Burden in Studies in Areas of Malaria Endemicity by Use of Bidimensional Assessment of YOYO-1 and Autofluorescence.* Journal of Clinical Microbiology, 2011. **49**(3): p. 968–974.

36. Capper, M.J., P.M. O'Neill, N. Fisher, R.W. Strange, D. Moss, S.A. Ward, N.G. Berry, A.S. Lawrenson, S.S. Hasnain, G.A. Biagini, and S.V. Antonyuka, *Antimalarial 4(1H)-pyridones bind to the Qi site of cytochrome bc1.* PNAS, 2015. **112**(3): p. 755–760.

37. Cohen, R.M., R.S. Franco, P.K. Khera, E.P. Smith, C.J. Lindsell, P.J. Ciraolo, M.B. Palascak, and C.H. Joiner, *Red cell life span heterogeneity in hematologically normal people is sufficient to alter HbA1c.* Blood, 2008. **112**(10): p. 4284–4291.

38. Corneo, B., D. Moshous, T. Güngör, N. Wulffraat, P. Philippet, F.L. Deist, A. Fischer, and J.-P. de Villartay, *Identical mutations in RAG1 or RAG2 genes leading to defective V(D)J recombinase activity can cause either T-B–severe combined immune deficiency or Omenn syndrome.* Blood, 2001. **97**(9): p. 2772-2776.

39. Coslédan, F., L. Fraisse, A. Pellet, F. Guillou, B. Mordmüller, P. Kremsner, A. Moreno, D. Mazier, J. Maffrand, and B. Meunier, *Selection of a trioxaquine as an antimalarial drug candidate.* Proceedings of the National Academy of Sciences, 2008. **105**: p. 17579-17584.

40. Coteron, J.M., M. Marco, J. Esquivias, X. Deng, K.L. White, J. White, M. Koltun, F. El Mazouni, S. Kokkonda, K. Katneni, R. Bhamidipati, D.M. Shackleford, I. Angulo-Barturen, S.B. Ferrer, M.B. Jiménez-Díaz, F.-J. Gamo, E.J. Goldsmith, W.N. Charman, I. Bathurst, D. Floyd, D. Matthews, J.N. Burrows, P.K. Rathod, S.A. Charman, and M.A. Phillips, *Structure-Guided Lead Optimization of Triazolopyrimidine-Ring Substituents Identifies Potent Plasmodium falciparum Dihydroorotate Dehydrogenase Inhibitors with Clinical Candidate Potential.* Journal of Medicinal Chemistry, 2011. **54**(15): p. 5540-5561.

41. Chang, K.-H. and M.M. Stevenson, *Malarial anaemia: mechanisms and implications of insufficient erythropoiesis during blood-stage malaria.* International Journal of Parasitology, 2004. **34**(13-14): p. 1501–1516.

42. Childs, R.A., J. Miao, C. Gowda, and L. Cui, *An alternative protocol for Plasmodium falciparum culture synchronization and a new method for synchrony confirmation.* Malaria Journal, 2013. **12:386**.

43. Churcher, T.S., J.-F. Trape, and A. Cohuet, *Human-to-mosquito transmission efficiency increases as malaria is controlled.* Nature Communications, 2015. **6**: p. Article number: 6054 (2015).

44. Delves, M.J., A. Ruecker, U. Straschil, J. Lelièvre, S. Marques, M.J. López-Barragán, E. Herreros, and R.E. Sinden, *Male and Female Plasmodium falciparum Mature Gametocytes Show Different Responses to Antimalarial Drugs.* Antimicrobial Agents And Chemotherapy, 2013. **57**(7): p. 3268–3274.

45. Denis, M.B., T.M.E. Davis, S. Hewitt, S. Incardona, K. Nimol, T. Fandeur, Y. Poravuth, C. Lim, and D. Socheat, *Efficacy and Safety of Dihydroartemisinin-Piperaquine (Artekin) in Cambodian Children and Adults with Uncomplicated Falciparum Malaria.* Clinical Infectious Diseases, 2012. **35**(12): p. 1469-1476.

46. Evans, K.J., D.S. Hansen, N. Van Rooijen, L.A. Buckingham, and L. Schofield, *Severe malarial anemia of low parasite burden in rodent models results from accelerated clearance of uninfected erythrocytes.* Blood, 2006. **107**(3): p. 1192-1199.

47. Fernando, D., C. Rodrigo, and S. Rajapakse, *Primaquine in vivax malaria: an update and review on management issues.* Malaria Journal, 2011. **10**(351).

48. Franke-Fayard, B., J. Fonager, A. Braks, S.M. Khan, and C.J. Janse, *Sequestration and Tissue Accumulation of Human Malaria Parasites: Can We Learn Anything from Rodent Models of Malaria?* Plos Pathogens, 2010. **6**(9): p. e1001032.

49. Frosch, T., S. Koncarevic, L. Zedler, M. Schmitt, K. Schenzel, K. Becker, and J. Popp, *In Situ Localization and Structural Analysis of the Malaria Pigment Hemozoin.* The Journal of Physical Chemistry, 2007. **111**(37): p. 11047–11056.

50. Gardner, M.J., N. Hall, E. Fung, O. White, M. Berriman, R.W. Hyman, J.M. Carlton, A. Pain, K.E. Nelson, S. Bowman, I.T. Paulsen, K. James, J.A. Eisen, K. Rutherford, S.L. Salzberg, A. Craig, S. Kyes, M.-S. Chan, V. Nene, S.J. Shallom, B. Suh, J. Peterson, S. Angiuoli, M. Pertea, J. Allen, J. Selengut, D. Haft, M.W. Mather, A.B. Vaidya, D.M.A. Martin, A.H. Fairlamb, M.J. Fraunholz, D.S. Roos, S.A. Ralph, G.I. McFadden, L.M. Cummings, G.M. Subramanian, C. Mungall, J.C. Venter, D.J. Carucci, S.L. Hoffman, C. Newbold, R.W. Davis, C.M. Fraser, and B. Barrell, *Genome sequence of the human malaria parasite Plasmodium falciparum.* Nature, 2002. **419**: p. 498-511.

51. Geiman, Q.M. and M.J. Meagher, *Susceptibility of a New World Monkey to Plasmodium falciparum from Man.* Nature, 1967. **215**: p. 437-439.

52. Gilson, P.R. and B.S. Crabb, *Morphology and kinetics of the three distinct phases of red blood cell invasion by Plasmodium falciparum merozoites.* International Journal of Parasitology, 2009. **39**(1): p. 91–96.

53. Hasegawa, M., K. Kawai, T. Mitsui, K. Taniguchi, M. Monnai, M. Wakui, M. Ito, M. Suematsu, G. Peltzi, M. Nakamura, and H. Suemizu, *The reconstituted 'humanized liver' in TK-NOG mice is mature and functional.* Biochemical and Biophysical Research Communications, 2011. **405**(3): p. 405–410.

54. Hoffman-Fezer, G., J. Mysliwietz, W. Mörtlbauer, H. Zeitler, E. Eberle, U. Hönle, and S. Thierfelder, *Biotin labeling as an alternative nonradioactive approach to determination of red cell survival.* Annals of Hematology, 1993. **67**: p. 81-87.

55. Hu, Z., N.V. Rooijen, and Y.-G. Yang, *Macrophages prevent human red blood cell reconstitution in immunodeficient mice.* Blood, 2011. **118**(22): p. 5938–5946.

56. Hulden, L. and L. Hulden, *Activation of the hypnozoite: a part of Plasmodium vivax life cycle and survival.* Malaria Journal, 2011. **10**(90).

57. Hyde, J.E., *Exploring the folate pathway in Plasmodium falciparum.* Acta Tropica, 2005. **94**(3): p. 191-206.

58. Ishikawa, F., M. Yasukawa, B. Lyons, S. Yoshida, Y. Miyamoto, G. Yoshimoto, T. Watanabe, K. Akashi, L. Shultz, and M. Harada, *Development of functional human blood and immune systems in NOD/SCID/IL2 receptor gamma chain-null mice.* Blood, 2005. **106**(5): p. 1565-1573.

59. Jakeman, G., A. Saul, W. Hogarth, and W. Collins, *Anaemia of acute malaria infections in non-immune patients primarily results from destruction of uninfected erythrocytes.* Parasitology, 1999. **119**: p. 127-33.

60. Jensen, J.B., T.C. Capps, and J.M. Carlin, *Clinical Drug-Resistant Falciparum Malaria Acquired From Cultured Parasites.* American Journal of Tropical Medicine and Hygiene, 1981. **30**(3): p. 523-525.

61. Jiménez-Díaz, M.B., D. Ebert, Y. Salinas, A. Pradhan, A.M. Lehane, M.-E. Myrand-Lapierre, K.G. O'Loughlin, D.M. Shackleford, M.J.d. Almeida, A.K. Carrillo, J.A. Clark, A.S.M. Dennis, J. Diep, X. Deng, S. Duffy, A.N. Endsley, G. Fedewa, W.A. Guiguemde, M.G. Gómez, G. Holbrook, J. Horst, C.C. Kim, J. Liu, M.C.S. Lee, A. Matheny, M.S. Martínez, G. Miller, A. Rodríguez-Alejandre, L. Sanz, M. Sigal, N.J. Spillman, P.D. Stein, Z. Wang, F. Zhu, D. Waterson, S. Knapp, A. Shelat, V.M. Avery, D.A. Fidock, F.-J. Gamo, S.A. Charman, J.C. Mirsalis, H. Ma, S. Ferrer, K. Kirk, I. Angulo-Barturen, D.E. Kyle, J.L. DeRisi, D.M. Floyd, and R.K. Guy, *(+)-SJ733, a clinical candidate for malaria that acts through ATP4 to induce rapid host-mediated clearance of Plasmodium.* PNAS, 2014. **111**(50): p. E5455–E5462.

62. Jiménez-Díaz, M.B., T. Mulet, V. Gómez, S. Viera, A. Alvarez, H. Garuti, Y. Vázquez, A. Fernández, J. Ibañez, M. Jiménez, D. Gargallo-Viola, and I. Angulo-Barturen, *Quantitative measurement of Plasmodium-infected erythrocytes in murine models of malaria by flow cytometry using bidimensional assessment of SYTO-16 fluorescence.* Cytometry Part A, 2009. **75A**: p. 225-235.

63. Jiménez-Díaz, M.B., T. Mulet, S. Viera, V. Gómez, H. Garuti, J. Ibañez, A. Alvarez-Doval, L. Shultz, A. Martínez, D. Gargallo-Viola, and I. Angulo-Barturen, *Improved murine model of falciparum-malaria using non-myelodepleted NOD-scid IL2R gamma-null mice engrafted with human erythrocytes.* Antimicrobial Agents and Chemotherapy, 2009. **53**(10): p. 4533–4536.

64. Jiménez-Díaz, M.B., S. Viera, E. Fernández-Álvaro, and I. Angulo-Barturen, *Animal models of efficacy to accelerate drug discovery in malaria.* Parasitology, 2014. **141**: p. 93-103.

65. Jiménez-Díaz, M.B., S. Viera, J. Ibáñez, T. Mulet, N. Magán-Marchal, H. Garuti, V. Gómez, L. Cortés-Gil, A. Martínez, S. Ferrer, M.T. Fraile, F. Calderón, E. Fernández, L.D. Shultz, D. Leroy, D.M. Wilson, J.F. García-Bustos, F.J. Gamo, and I. Angulo-Barturen, *A New In Vivo Screening Paradigm to Accelerate Antimalarial Drug Discovery.* PLoS ONE, 2013. **8**(6): p. e66967.

66. Josling, G.A. and M. Llinas, *Sexual development in Plasmodium parasites: knowing when it's time to commit.* Nat Rev Micro, 2015. **13**(9): p. 573-587.

67. Katakai, Y., S. Suzuki, Y. Tanioka, S. Hattori, Y. Matsumoto, M. Aikawa, and M. Ito, *The suppressive effect of dexamethasone on the proliferation of Plasmodium falciparum in squirrel monkeys.* Parasitology Research, 2002. **88**(1): p. 53-57.

68. Kats, L.M., B.M. Cooke, R.L. Coppel, and C.G. Black, *Protein Trafficking to Apical Organelles of Malaria Parasites – Building an Invasion Machine.* Traffic, 2008. **9**(2): p. 176-186.

69. Keurulainen, L., M. Vahermo, M. Puente-Felipe, E. Sandoval-Izquierdo, B. Crespo-Fernández, L. Guijarro-López, L. Huertas-Valentín, L.d.l. Heras-Dueña, T.O. Leino, A. Siiskonen, L. Ballell-Pages, L.M. Sanz, P. Castañeda-Casado, M.B. Jiménez-Díaz, M.S. Martínez-Martínez, S. Viera, P. Kiuru, F. Calderón, and J. Yli-Kauhaluoma, *A Developability-Focused Optimization Approach Allows Identification of in Vivo Fast-Acting Antimalarials: N-[3-[(Benzimidazol-2-yl)amino]propyl]amides.* Journal of Medicinal Chemistry, 2015. **58**(11): p. 4573–4580.

70. Kircher, M., S. Gambhir, and J. Grimm, *Noninvasive cell-tracking methods.* Nature Reviews Clinical Oncology, 2011. **8**(11): p. 677-88.

71. Kollet, O., A. Peled, T. Byk, H. Ben-Hur, D. Greiner, L. Shultz, and T. Lapidot, *b2 Microglobulin-deficient (B2mnull) NOD/SCID mice are excellent recipients for studying human stem cell function.* Blood, 2000. **95**(10): p. 3102-3105.

72. Krücken, J., L.I. Mehnert, M.A. Dkhil, M. El-Khadrady, W.P.M. Benten, H. Mossmann, and F. Wunderlich, *Massive destruction of malaria-parasitized red blood cells despite spleen closure.* Infection and Immunity, 2005. **73**(10): p. 6390-6398.

73. Kuehn, A. and G. Pradel, *The Coming-Out of Malaria Gametocytes.* Journal of Biomedicine and Biotechnology, 2010. **2010**(Article ID 976827): p. 11.

74. Kurtzhals, J.A., V. Adabayeri, B.Q. Goka, B.D. Akanmori, J.O. Oliver-Commey, F.K. Nkrumah, C. Behr, and L. Hviid, *Low plasma concentrations of interleukin 10 in severe malarial anaemia compared with cerebral and uncomplicated malaria.* The Lancet, 1998. **351**: p. 1768–1772.

75. Layez, C., P. Nogueira, V. Combes, F.T. Costa, I. Juhan-Vague, L. Pereira da Silva, and J. Gysin, *Plasmodium falciparum rhoptry protein RSP2 triggers destruction of the erythroid lineage.* Blood, 2005. **106**(10): p. 3632-3638.

76. Leisewitz, A.L., K.A. Rockett, B. Gumede, M. Jones, B. Urban, and D.P. Kwiatkowski, *Response of the Splenic Dendritic Cell Population to Malaria Infection.* Infection and Immunity, 2004. **72**(7): p. 4233–4239.

77. Lelièvre, J., M.J. Almela, S. Lozano, C. Miguel, V. Franco, D. Leroy, and E. Herreros, *Activity of Clinically Relevant Antimalarial Drugs on Plasmodium falciparum Mature Gametocytes in an ATP Bioluminescence "Transmission Blocking" Assay.* PLoS ONE, 2012. **7**(4): p. e35019.

78. Li, T., A.G. Eappen, A.M. Richman, P.F. Billingsley, Y. Abebe, M. Li, D. Padilla, I. Rodriguez-Barraquer, B.K.L. Sim, and S.L. Hoffman, *Robust, reproducible, industrialized, standard membrane feeding assay for assessing the transmission blocking activity of vaccines and drugs against Plasmodium falciparum.* Malaria Journal, 2015. **14**(1): p. 150.

79. Linares, M., S. Viera, B. Crespo, V. Franco, M.G. Gómez-Lorenzo, M.B. Jiménez-Díaz, Í. Angulo-Barturen, L.M. Sanz, and F.-J. Gamo, *Identifying rapidly parasiticidal anti-malarial drugs using a simple and reliable in vitro parasite viability fast assay.* Malaria Journal, 2015. **14:441**.

80. Looareesuwan, S., J.D. Chulay, C.J. Canfield, and D.B.A. Hutchinson, *Malarone (Atovaquone and Proguanil Hydrochloride): A Review Of Its Clinical Development For Treatment Of Malaria.* American Journal of Tropical Medicine and Hygiene, 1999. **60**(4): p. 533–541.

81. Looareesuwan, S., C. Viravan, H.K. Webster, D.E. Kyle, D.B. Hutchinson, and C.J. Canfield, *Clinical Studies Of Atovaquone, Alone Or In Combination With Other Antimalarial Drugs, For Treatment Of Acute Uncomplicated Malaria In Thailand.* American Journal of Tropical Medicine and Hygiene, 1996. **54**(1): p. 62-66.

82. Luty, A.J.F., D.J. Perkins, B. Lell, R. Schmidt-Ott, L.G. Lehman, D. Luckner, B. Greve, P. Matousek, K. Herbich, D. Schmid, J.B. Weinberg, and P.G. Kremsner, *Low Interleukin-12 Activity in Severe Plasmodium falciparum Malaria.* Infection and Immunity, 2000. **68**(7): p. 3909–3915.

83. Lyke, K.E., R. Burges, Y. Cissoko, L. Sangare, M. Dao, I. Diarra, A. Kone, R. Harley, C.V. Plowe, O.K. Doumbo, and M.B. Sztein, *Serum Levels of the Proinflammatory Cytokines Interleukin-1 Beta (IL-1), IL-6, IL-8, IL-10, Tumor Necrosis Factor Alpha, and IL-12(p70) in Malian Children with Severe Plasmodium falciparum Malaria and Matched Uncomplicated Malaria or Healthy Controls.* Infection and Immunity, 2004. **72**(10): p. 5630-5637.

84. Lyons, A.B., S.J. Blake, and K.V. Doherty, *Flow cytometric analysis of cell division by dilution of CFSE and related dyes*, in *Current Protocols in Flow Cytometry*. 2013. p. 9.11.1-9.11.12.

85. Magnani, M., L. Rossi, V. Stocchi, L. Cucchiarini, G. Piacentini, and G. Fornaini, *Effect of age on some properties of mice erythrocytes.* Mechanisms of Ageing and Development, 1987. **42**: p. 37-47.

86. Maier, A.G., B.M. Cooke, A.F. Cowman, and L. Tilley, *Malaria parasite proteins that remodel the host erythrocyte.* Nature Reviews Microbiology, 2009. **7**: p. 341-354

87. Malaguarnera, L. and S. Musumeci, *The immune response to Plasmodium falciparum malaria.* The Lancet Infectious Diseases, 2002. **2**(8): p. 472-478.

88. Manach, C.L., C. Scheurer, S. Sax, S. Schleiferböck, D.G. Cabrera, Y. Younis, T. Paquet, L. Street, P. Smith, X.C. Ding, D. Waterson, M.J. Witty, D. Leroy, K. Chibale, and S. Wittlin, *Fast in vitro methods to determine the speed of action and the stage-specificity of anti-malarials in Plasmodium falciparum.* Malaria Journal, 2013. **13**(424).

89. Maykel, J., J.H. Liu, H. Li, L.D. Shultz, D.L. Greiner, and J. Houghton, *NOD-scidIl2rg (tm1Wjl) and NOD-Rag1 (null) Il2rg (tm1Wjl) : a model for stromal cell-tumor cell*

interaction for human colon cancer. Digestive Diseases and Sciences, 2014. **59**(6): p. 1169–1179.

90. McCarthy, J.S., L. Marquart, S. Sekuloski, K. Trenholme, S. Elliott, P. Griffin, R. Rockett, P. O'Rourke, T. Sloots, I. Angulo-Barturen, S. Ferrer, M.B. Jiménez-Díaz, M.S. Martínez, R.H.v. Huijsduijnen, S. Duparc, D. Leroy, T.N.C. Wells, M. Baker, and J.J. Möhrle, *Linking Murine and Human Plasmodium falciparum Challenge Models in a Translational Path for Antimalarial Drug Development.* Antimicrobial Agents and Chemotherapy, 2016. **60**(6): p. 3669–3675.

91. Mercer, D.F., D.E. Schiller, J.F. Elliott, D.N. Douglas, C. Hao, A. Rinfret, W.R. Addison, K.P. Fischer, T.A. Churchill, J.R.T. Lakey, D.L.J. Tyrrell, and N.M. Kneteman, *Hepatitis C virus replication in mice with chimeric human livers.* Nat Med, 2001. **7**(8): p. 927-933.

92. Miguel-Blanco, C., J. Lelièvre, M.J. Delves, A.I. Bardera, J.L. Presa, M.J. López-Barragán, A. Ruecker, S. Marques, R.E. Sinden, and E. Herreros, *Imaging-Based High-Throughput Screening Assay To Identify New Molecules with Transmission-Blocking Potential against Plasmodium falciparum Female Gamete Formation* Antimicrobial Agents And Chemotherapy, 2015. **59**(6): p. 3298-3305.

93. Mikolajczak, S.A., J. John B. Sacci, P.D.L. Vega, N. Camargo, K. VanBuskirk, U. Krzych, J. Cao, M. Jacobs-Lorena, A.F. Cowman, and S.H.I. Kappe, *Disruption of the Plasmodium falciparum liver-stage antigen-1 locus causes a differentiation defect in late liver-stage parasites.* Cell Microbiology, 2011. **13**(8): p. 1250–1260.

94. Mikolajczak, S.A., A.M. Vaughan, N. Kangwanrangsan, W. Roobsoong, M. Fishbaugher, N. Yimamnuaychok, N. Rezakhani, V. Lakshmanan, N. Singh, A. Kaushansky, N. Camargo, M. Baldwin, S.E. Lindner, J.H. Adams, J. Sattabongkot, and S.H.I. Kappe, *Plasmodium vivax Liver Stage Development and Hypnozoite Persistence in Human Liver-Chimeric Mice.* Cell Host & Microbe, 2015. **17**(4): p. 526–535.

95. Mombaerts, P., J. Iacomini, R.S. Johnson, K. Herrup, S. Tonegawa, and V.E. Papaioannou, *RAG-1-deficient mice have no mature B and T lymphocytes.* Cell, 1992. **68**(5): p. 869–877.

96. Monastyrskyi, A., D.E. Kyle, and R. Manetsch, *4(1H)-Pyridone and 4(1H)-Quinolone Derivatives as Antimalarials with Erythrocytic, Exoerythrocytic, and Transmission Blocking Activities.* Current Tropical Medicine Chemistry, 2014. **14**(14): p. 1693–1705.

97. Moore, J.M., N. Kumar, L.D. Shultz, and T.V. Rajah, *Maintenance of the Human Malarial Parasite, Plasmodium falciparum, in scid Mice and Transmission of Gametocytes to Mosquitoes.* J. Exp. Med, 1995. **181**: p. 2265-2270.

98. Moreno, A., E. Badell, N. Van Rooijen, and P. Druilhe, *Human Malaria in Immunocompromised Mice: New In Vivo Model for Chemotherapy Studies.* Antimicrobial Agents and Chemotherapy, 2001. **45**(6).

99. Moreno, A., E. Ferrer, S. Arahuetes, C. Eguiluz, N.V. Rooijen, and A. Benito, *The course of infections and pathology in immunomodulated NOD/LtSz-SCID mice inoculated with Plasmodium falciparum laboratory lines and clinical isolates.* International Journal of Parasitology, 2006. **36**(3): p. 361–369.

100. Moreno, A., M. Moreno, F.J. Moreno, C. Eguiluz, N. Van Rooijen, and A. Benito, *Experimental infection of immunomodulated NOD/LtSz-SCID mice as a new model of Plasmodium falciparum erythrocytic stages.* Parasitology Research, 2005. **95**: p. 97-105.

101. Moreno, A., J.L. Pérignon, S. Morosan, D. Mazier, and A. Benito, *Plasmodium falciparum-infected mice: more than a tour de force.* Trends in Parasitology, 2007. **23**(6): p. 254–259.

102. Ngwa, C.J., T.F.d.A. Rosa, and G. Pradel, *The Biology of Malaria Gametocytes*, in *Current Topics in Malaria*, A.J. Rodriguez-Morales, Editor. 2016.

103. Nilsen, A., A.N. LaCrue, K.L. White, I.P. Forquer, R.M. Cross, J. Marfurt, M.W. Mather, M.J. Delves, D.M. Shackleford, F.E. Saenz, J.M. Morrisey, J. Steuten, T. Mutka, Y. Li, G. Wirjanata, E. Ryan, S. Duffy, J.X. Kelly, B.F. Sebayang, A.-M. Zeeman, R. Noviyanti, R.E. Sinden, C.H.M. Kocken, R.N. Price, V.M. Avery, I. Angulo-Barturen, M.B. Jiménez-Díaz, S. Ferrer, E. Herreros, L.M. Sanz, F.-J. Gamo, I. Bathurst, J.N. Burrows, P. Siegl, R.K. Guy, R.W. Winter, A.B. Vaidya, S.A. Charman, D.E. Kyle, R. Manetsch, and M.K. Riscoe, *Quinolone-3-Diarylethers: A new class of drugs for a new era of malaria eradication.* Science Translational Medicine, 2013. **5**(177): p. 177ra37.

104. Noedl, H., S. Krudsood, K. Chalermratana, U. Silachamroon, W. Leowattana, N. Tangpukdee, S. Looareesuwan, R.S. Miller, M. Fukuda, K. Jongsakul, S. Sriwichai, J. Rowan, H. Bhattacharyya, C. Ohrt, and C. Knirsch, *Azithromycin Combination Therapy with Artesunate or Quinine for the Treatment of Uncomplicated Plasmodium falciparum Malaria in Adults: A Randomized, Phase 2 Clinical Trial in Thailand* Clinical Infectious Diseases, 2006. **43**(10): p. 1264-1271.

105. O'Brien, B.A., Y. Huang, X. Geng, J.P. Dutz, and D.T. Finegood, *Phagocytosis of Apoptotic Cells by Macrophages From NOD Mice Is Reduced.* Diabetes, 2002. **51**(8): p. 2481-2488.

106. O'Brien, C., Henrich, P. P., N. Passi, and D.A. Fidock, *Recent clinical and molecular insights into emerging artemisinin resistance in Plasmodium falciparum.* Current Opinion in Infectious Diseases, 2011. **24**(6): p. 570–577.

107. O'Neill, P.M., V.E. Barton, and S.A. Ward, *The Molecular Mechanism of Action of Artemisinin—The Debate Continues.* Molecules, 2010. **15**: p. 1705-1721.

108. O'Neill, P.M., V.E. Barton, S.A. Ward, and J. Chadwick, *4-Aminoquinolines: Chloroquine, Amodiaquine and Next-Generation Analogues*, in *Treatment and Prevention of Malaria*. 2011, Springer. p. 19-44.

109. Ogasawara, K., J.A. Hamerman, H. Hsin, S. Chikuma, H. Bour-Jordan, T. Chen, T. Pertel, C. Carnaud, J.A. Bluestone, and L.L. Lanier, *Impairment of NK Cell Function by NKG2D Modulation in NOD Mice.* Immunity, 2003. **18**(1): p. 41–51.

110. Parish, C.R., *Fluorescent dyes for lymphocyte migration and proliferation studies.* Immunology and Cell Biology, 1999. **77**: p. 499–508.

111. Pasay, C.J., R. Rockett, S. Sekuloski, P. Griffin, L. Marquart, C. Peatey, C.Y.T. Wang, P. O'Rourke, S. Elliott, M. Baker, J.J. Möhrle, and J.S. McCarthy, *Piperaquine Monotherapy of Drug-Susceptible Plasmodium falciparum Infection Results in Rapid Clearance of Parasitemia but Is Followed by the Appearance of Gametocytemia.* The Journal of Infection Diseases, 2016. **214**(1): p. 105–113.

112. Pearson, T., D. Greiner, and L. Shultz, *Creation of "Humanized" mice to study human immunity.* Currents Protocols in Immunology, 2008. **81**: p. 15.21.1-15.21.21.

113. Perkins, D.J., T. Were, G.C. Davenport, P. Kempaiah, J.B. Hittner, and J.M. Ong'echa, *Severe Malarial Anemia: Innate Immunity and Pathogenesis.* International Journal of Biological Science, 2011. **7**(9): p. 1427–1442.

114. Peters, W. and B.L. Robinson, in *Handbook of Animal Models of Infection*, O. Zak and M.A. Sande, Editors. 1999, Academic Press London. p. 757–773.

115. Peters, W. and B.L. Robinson, *The chemotherapy of rodent malaria. LVI. Studies on the development of resistance to natural and synthetic endoperoxides.* Annals of Tropical Medicine Parasitology, 1999. **93**(4): p. 325-9.

116. Peterson, D.S., W.K. Milhous, and T.E. Wellems, *Molecular basis of differential resistance to cycloguanil and pyrimethamine in Plasmodium falciparum malaria.* PNAS, 1990. **87**: p. 3018-3022.

117. Phillips, M.A., J. Lotharius, K. Marsh, J. White, A. Dayan, K.L. White, J.W. Njoroge, F.E. Mazouni, Y. Lao, S. Kokkonda, D.R. Tomchick, X. Deng, T. Laird, S.N. Bhatia, S. March, C.L. Ng, D.A. Fidock, S. Wittlin, M. Lafuente-Monasterio, F.J.G. Benito, L.M.S. Alonso, M.S. Martinez, M.B. Jimenez-Diaz, S.F. Bazaga, I. Angulo-Barturen, J.N. Haselden, J. Louttit, Y. Cui, A. Sridhar, A.-M. Zeeman, C. Kocken, R. Sauerwein, K. Dechering, V.M. Avery, S. Duffy, M. Delves, R. Sinden, A. Ruecker, K.S. Wickham, R. Rochford, J. Gahagen, L. Iyer, E. Riccio, J. Mirsalis, I. Bathhurst, T. Rueckle, X. Ding, B. Campo, D. Leroy, M.J. Rogers, P.K. Rathod, J.N. Burrows, and S.A. Charman, *A long-duration dihydroorotate dehydrogenase inhibitor (DSM265) for prevention and treatment of malaria.* Science Translational Medicine, 2015. **7**(296): p. 296ra111.

118. Ponnudurai, T., A. Leeuwenberg, and J. Meuwissen, *Chloroquine sensitivity of isolates of Plasmodium falciparum adapted to in vitro culture.* Tropical and Geographical Medicine, 1981. **33**(1): p. 50-54.

119. Portillo, H.A.d., M. Ferrer, T. Brugat, L. Martin-Jaular, J. Langhorne, and M.V.G. Lacerda, *The role of the spleen in malaria.* Cellular Microbiology, 2012. **14**(3): p. 343–355.

120. Prudêncio, M., A. Rodriguez, and M.M. Mota, *The silent path to thousands of merozoites: the Plasmodium liver stage.* Nature Reviews Microbiology, 2006. **4**: p. 849-856.

121. Quah, B.J.C., H.S. Warren, and C.R. Parish, *Monitoring lymphocyte proliferation in vitro and in vivo with the intracellular fluorescent dye carboxyfluorescein diacetate succinimidyl ester.* Nature Protocols, 2007. **2**: p. 2049 - 2056.

122. Radfar, A., D. Méndez, C. Moneriz, M. Linares, P. Marín-García, A. Puyet, A. Diez, and J.M. Bautista, *Synchronous culture of Plasmodium falciparum at high parasitemia levels.* Nature Protocols, 2009. **4**: p. 1899 - 1915

123. Ranford-Cartwright, L.C., A. Sinha, G.S. Humphreys, and J.M. Mwangi, *New synchronization method for Plasmodium falciparum.* Malaria Journal, 2010. **9:170**.

124. Riches, A., J. Sharp, D. Brynmor Thomas, and S. Vaughan Smith, *Blood volume determination in the mouse.* Journal of Physiology, 1973. **228**: p. 279-284.

125. Roncalés, M., J. Vidal, P.A. Torres, and E. Herreros, *In Vitro Culture of Plasmodium falciparum: Obtention of Synchronous Asexual Erythrocytic Stages.* Open Journal of Epidemiology, 2015. **5**: p. 71-80.

126. Sabbatani, S., S. Fiorino, and R. Manfredi, *The emerging of the fifth malaria parasite (Plasmodium knowlesi): a public health concern?* Brazilian Journal of Infectious Diseases, 2010. **14**(3): p. 299-309.

127. Saifi, M.A., T. Beg, A.H. Harrath, F. Suleman, H. Altayalan, and S.A. Quraishy, *Antimalarial drugs: Mode of action and status of resistance.* African Jounal of Pharmacy and Pharmacology, 2013. **7**(5): p. 148-156.

128. Sam, H. and M.M. Stevenson, *Early IL-12 p70, but not p40, production by splenic macrophages correlates with host resistance to blood-stage Plasmodium chabaudi AS malaria.* Clinical and Experimental Immunology, 1999. **117**(2): p. 343–349.

129. Sanni, L.A., L.F. Fonseca, and J. Langhorne, *Mouse Models for Erythrocytic-Stage Malaria.* Methods in Molecular Medicine, 2002. **72**: p. 57-76.

130. Sanz, L.M., B. Crespo, C. De-Cózar, X.C. Ding, J.L. Llergo, J.N. Burrows, J.F. García-Bustos, and F.-J. Gamo, *P. falciparum In Vitro Killing Rates Allow to Discriminate between Different Antimalarial Mode-of-Action.* PLoS ONE, 2012. **7**(2): p. e30949.

131. Seydel, K.B. and S.L.J. Stanley, *SCID Mice and the Study of Parasitic Disease.* Clinical Microbiology Reviews, 1996. **9**(2): p. 126–134.

132. Sherman, I.W., S. Eda, and E. Winograd, *Cytoadherence and sequestration in Plasmodium falciparum: defining the ties that bind.* Microbes and Infection, 2003. **5**(10): p. 897–909.

133. Shi, C. and E.G. Pamer, *Monocyte recruitment during infection and inflammation.* Nat Rev Immunol, 2011. **11**(11): p. 762-774.

134. Shinkai, Y., G. Rathbun, K.-P. Lam, E.M. Oltz, V. Stewart, M. Mendelsohn, J. Charron, M. Datta, F. Young, A.M. Stall, and F.W. Alt, *RAG-2-deficient mice lack mature lymphocytes owing to inability to initiate V(D)J rearrangement.* Cell, 1992. **68**(5): p. 855–867.

135. Sinden, R.E., *Plasmodium differentiation in the mosquito.* Parassitologia, 1999. **41**(1-3): p. 139-48.

136. Soulard, V., H. Bosson-Vanga, A. Lorthiois, C.m. Roucher, J.-F. Franetich, G. Zanghi, M. Bordessoulles, M. Tefit, M. Thellier, S. Morosan, G.L. Naour, F. Capron, H. Suemizu, G. Snounou, A. Moreno-Sabater, and D. Mazier, *Plasmodium falciparum full life cycle and Plasmodium ovale liver stages in humanized mice.* Nature Communications, 2015. **6**.

137. Sponaas, A.-M., A.P.F.d. Rosario, C. Voisine, B. Mastelic, J. Thompson, S. Koernig, W. Jarra, L. Renia, M. Mauduit, A.J. Potocnik, and J. Langhorne, *Migrating monocytes recruited to the spleen play an important role in control of blood stage malaria.* Blood, 2009. **114**: p. 5522-5531.

138. Sterkers, Y., C. Scheidig, M. da Rocha, C. Leopolard, J. Gysin, and A. Scherf, *Members of the low-molecular-mass rhoptry protein complex of Plasmodium falciparum bind to the surface of normal erythrocytes.* Journal of Infectious Diseases, 2006. **196**: p. 617-621.

139. Stowers, A.W., V. Cioce, R.L. Shimp, M. Lawson, G. Hui, O. Muratova, D.C. Kaslow, R. Robinson, C.A. Long, and L.H. Miller, *Efficacy of Two Alternate Vaccines Based on Plasmodium falciparum Merozoite Surface Protein 1 in anAotus Challenge Trial.* Infection and Immunity, 2001. **69**(3): p. 1536-1546.

140. Sturm, A., R. Amino, C.v.d. Sand, T. Regen, S. Retzlaff, A. Rennenberg, A. Krueger, J.-M. Pollok, R. Menard, and V.T. Heussler, *Manipulation of Host Hepatocytes by the Malaria Parasite for Delivery into Liver Sinusoids.* Science, 2006. **313**(5791): p. 1287-1290.

141. Talman, A.M., O. Domarle, F.E. McKenzie, F. Ariey, and V. Robert, *Gametocytogenesis : the puberty of Plasmodium falciparum.* Malaria Journal, 2004. **3**(1): p. 24.

142. The RTS, S.C.T.P., *First Results of Phase 3 Trial of RTS,S/AS01 Malaria Vaccine in African Children.* New England Journal of Medicine, 2011. **365**(20): p. 1863-1875.

143. Thompson, P.E. and L.M. Werbel, *Antimalarial agents. Chemistry and Pharmacology.* Academic Press, 1972.

144. Totino, P.R., A.D. Magalhães, L.A. Silva, D.M. Banic, C.T. Daniel-Ribeiro, and M.d.F. Ferreira-da-Cruz, *Apoptosis of non-parasitized red blood cells in malaria: a putative mechanism involved in the pathogenesis of anaemia.* Malaria Journal, 2010. **9:350**.

145. Trager, W. and J. Jensen, *Human malaria parasites in continuous culture.* Science, 1976. **193**(4254): p. 673-675.

146. Tsuji, M., C. Ishihara, S. Arai, R. Hiratai, and I. Azuma, *Establishment of a SCID mouse model having circulating human red blood cells and a possible growth of Plasmodium falciparum in the mouse.* Vaccine, 1995. **13**(15): p. 1369-1392.

147. Vaughan, A.M., S.A. Mikolajczak, E.M. Wilson, M. Grompe, A. Kaushansky, N. Camargo, J. Bial, A. Ploss, and S.H.I. Kappe, *Complete Plasmodium falciparum liver-stage development in liver-chimeric mice.* The Journal of Clinical Investigation, 2012. **122**(10): p. 3618–3628.

148. Viera, S., J. Ibáñez, N. Magán-Marchal, H. Garuti, V. Gómez, L. Cortés-Gil, T. Mulet, and M.B. Jiménez-Díaz, *In vivo Assessment of the Mode of Action of New Antimalarials by Flow Cytometry.* unpublished.

149. Vivas, L., A. Easton, H. Kendricka, A. Cameron, J.-L. Lavandera, D. Barros, F.G.d.l. Heras, R.L. Brady, and S.L. Croft, *Plasmodium falciparum: Stage specific effects of a selective inhibitor of lactate dehydrogenase.* Experimental Parasitology, 2005. **111**(2): p. 105–114.

150. Ward, S.A., W.M. Watkins, E. Mberu, J.E. Saunders, D.K. Koech, H.M. Gilles, R.E. Howells, and A.M. Breckenridge, *Inter-subject variability in the metabolism of proguanil to the active metabolite cycloguanil in man.* British Journal of Clinical Pharmacology, 1989. **27**(6): p. 781-787.

151. Warrell, D.A. and H.M. Gilles, *Essential Malariology, 4Ed*. 2002: CRC Press.

152. WebPage. *National Centre for the Replacement Refinement and Reduction of Animals in Research*. Available from: https://www.nc3rs.org.uk/mouse-decision-tree-blood-sampling.

153. White, N.J., *Not much progress in treatment of cerebral malaria.* The Lancet, 1998. **352**(9128): p. 594–595.

154. White, N.J., *The parasite clearance curve.* Malaria Journal, 2011. **10:278**.

155. WHO. *Malaria Report*. 2016; Available from: http://apps.who.int/iris/bitstream/10665/252038/1/9789241511711-eng.pdf?ua=1.

156. Winter, G. and M. Wahlgren, *Severe anemia in malaria: defense gone wrong?* Blood, 2005. **106**: p. 3337-3338.

157. Wongsrichanalai, C., A.L. Pickard, W.H. Wernsdorfer, and S.R. Meshnick, *Epidemiology of drug-resistant malaria.* The Lancet Infectious Diseases, 2002. **2**(4): p. 209–218.

158. Yeates, C.L., J.F. Batchelor, E.C. Capon, N.J. Cheesman, M. Fry, A.T. Hudson, M. Pudney, H. Trimming, J. Woolven, J.M. Bueno, J. Chicharro, E. Fernández, J.M. Fiandor, D. Gargallo-Viola, F. Gómez de las Heras, E. Herreros, and M.L. León, *Synthesis and Structure–Activity Relationships of 4-Pyridones as Potential Antimalarials.* Journal of Medicinal Chemistry, 2008. **51**(9): p. 2845-2852.

159. Yuthavong, Y., *Basis for antifolate action and resistance in malaria.* Microbes and Infection, 2002. **4**(2): p. 175–182.